Endocytosis Redesigned:

Host–Parasite Coevolution Drives Adaptation of the *Giardia lamblia* Endocytic System

---

Dissertation

zur

Erlangung der naturwissenschaftlichen Doktorwürde
(Dr. sc. nat.)

vorgelegt der

Mathematisch-naturwissenschaftlichen Fakultät

der

Universität Zürich

von

Jon Paulin Zumthor

von

Haldenstein GR

Promotionskomitee

Prof. Dr. Adrian B. Hehl
(Vorsitz und Leitung der Dissertation)

Prof. Dr. Urs Greber
Prof. Dr. Lloyd Vaughan

Zürich, 2016

Table of Contents

PART I SUMMARY

1. Summary

Giardia lamblia (syn. *G. intestinalis* and *G. duodenalis*) is a protozoan enteroparasite and a major cause for non-bacterial diarrhea worldwide. The disease, called Giardiasis, spreads worldwide from the Arctic [11] to the Tropics [12] and the WHO estimates that 270 million people are symptomatic, with more than 0.5 Mio new cases reported each year [10]. The simple life cycle of *Giardia lamblia* alternates between a flagellated trophozoite stage which proliferates in the small intestine of mammalian hosts and a cyst stage which survives in the environment and is responsible for transmission. Although giardiasis occurs most frequently in developing countries, the number of yearly endemic cases in Europe and the USA cause significant hospitalizations costs. Aside from its role as a human pathogen, *Giardia* has received growing attention in biology research. Phylogenetically, *G. lamblia* had been thought of as an ancient organism that could represent the missing evolutionary link between prokaryotes and eukaryotes. To date, the current hypothesis favors *Giardia's* simplified cellular organization as the result of reductive evolution, a process that is thought to be driven by the extreme adaptation to a given ecological niche, as experienced by parasitic organisms. During host-parasite co-evolution *G. lamblia* has minimized cellular complexity and adapted morphologically to the intestinal environment. In addition, *Giardia* is amenable to *in vitro* culture and has therefore become an attractive eukaryotic model for the study of complex cell biological and phylogenetic aspects in a "bare-bones" eukaryotic cellular system.

One of the most striking morphological adaptations in *G. lamblia* to the host's environment was the evolution of the ventral disc (VD). The VD mediates attachment of the trophozoite to the gut epithelium and prevents extrusion by peristalsis. Consequently, *Giardia*'s flat ventral domain is in close contact with the epithelium whilst the dome-shaped dorsal domain is exposed to the intestinal lumen. This dorso-ventral polarization is reflected in the distribution of *Giardia*'s endocytic organelles, the peripheral vacuoles (PVs). PVs underly the entire dorsal plasma membrane (PM) but are excluded from the area occupied by the VD. Traces of reductive evolution are also seen in PVs, in that they present some similarities and many differences compared to canonical endocytic compartments. In line with classical endosomes PVs are the initial recipients of endocytosed material and associate with the conserved endocytic key factors clathrin (*Gl*CHC), dynamin (*Gl*DRP) and adaptor protein 2 (*Gl*AP2). Although their molecular functions are not very well understood, it appears that they are not involved in the formation of highly dynamic clathrin coated vesicles (CCVs) as such PM derived transport intermediates have never been observed. In contrast to most eukaryotic endocytic systems, PVs have a fixed position in close proximity to the PM and are of a non-fusogenic nature. Moreover they seem to undergo a regulated organelle cycle for indiscriminate

uptake of fluid phase material. Taken together, PV organelles maintain endocytic and lysosomal properties in parallel and can directly communicate with the extracellular environment by temporary membrane fusions to the PM.

In the main part of my thesis we tested the hypothesis that the formation of short lived endocytic transport intermediates has become obsolete due to the minimal distance between PVs and PM and that clathrin was therefore coopted towards a new, yet undefined role in *G. lamblia* endocytosis. To do so, we used an array of state-of-the-art imaging techniques to characterize *Gl*CHC on a subcellular level and to investigate the morphological aspects of material uptake through the PM into PVs. Furthermore we developed a customized co-immunoprecipitation (co-IP) protocol to define a network of proteins that interact with *Gl*CHC, *Gl*DRP and *Gl*AP2. Our results indicate that *Gl*CHC likely fulfils a structural role and, aside from *Gl*DRP and *Gl*AP2, mainly interacts with lineage specific protein factors in the endocytic system of *G. lamblia* including proteins interacting with phosphoinositdes (PIs), key signaling molecules in the endocytic systems of higher eukaryotes. Furthermore we showed that PVs are up to three times larger than previously thought and that they gain access to the extracellular environment by fusing with membrane invaginations occurring at the PM. Taken together, our data support a model where clathrin provides a static scaffold for the regulated fusion of the invaginating PM with PVs in a "kiss and flush" manner that functions independently of CCVs. The *Gl*CHC interactome presented in this thesis includes two PX domain-containing proteins (*Gl*PXDs). Moreover the giardial genome encodes the necessary enzymes for the generation of differentially phosphorylated PIs. This is in line with the role for PIs in canonical endocytic systems whose regulation can depend on the recruitment of PX domain-containing proteins. In total six *Gl*PXDs can be identified in the giardial genome and the interaction with clathrin for two of them suggests that PI signaling may be involved in the regulation of the giardial endocytic pathway, raising questions about subcellular localization, PI binding preferences and interacting partner proteins for the members of PXD family. The data presented here demonstrate differential PI binding affinities for all six PX domains and distinct patterns of sub-organellar distributions on the limiting PV membranes for all family members. Our results support a role for both PIs and their *Gl*PXD effector proteins and suggest that PI mediated regulation is a conserved feature of endocytic pathways in this highly diverged parasite.

2. Zusammenfassung

Der zu den Protozoen gehöhrende Dünndarmparasit *Giardia lamblia* (syn. *G. intestinalis* und *G. duodenalis)* ist einer der Hauptverursacher von nicht-bakteriellen Durchfallerkrankungen. Die „Giardiose" genannte Erkrankung tritt weltweit, von der Arktis bis zu den Tropen, auf. Die WHO

schätzt, dass bis zu 270 Millionen Menschen an symptomatischer Giardiose leiden und jährlich werden mehr als eine halbe Million neue Fälle gemeldet. *Giardia* durchläuft einen sehr einfachen Lebenszyklus mit zwei Stadien: das des begeisselten Trophozoiten, der sich im Dünndarm seines Wirts vermehren und jenes der Cyste, welches ausserhalb des Wirts überleben kann und für die Übertragung des Parasiten verantwortlich ist. Obwohl die Giardiose hauptsächlich in Entwicklungsländern stark verbreitet ist, zeichnen sich die endemischen Fälle in Europa und den USA für signifikante Hospitalisationskosten verantwortlich. Neben der Wichtigkeit als Krankheitserreger fand *Giardia* über die letzten Jahre vermehrt Beachtung in der zellbiologischen Grundlagenforschung. Bis vor wenigen Jahren war die Wissenschaft der Ansicht, *Giardia* sei ein sehr ursprünglicher Organismus, der sich phylogenetisch zwischen Prokaryoten und Eukaryoten ansiedelt und ein Übergangsstadium zwischen diesen beiden Lebensformen darstelle. Die aktuellste Hypothese hingegen geht davon aus, dass es nicht fehlende Evolutionsschritte seien, die eine vereinfachte Zellorganisation bedingen, sondern dass dies das Resultat einer reduktiven Evolution sei. Die reduktive Evolution zeichnet sich durch eine ausgeprägte Anpassung eines Organismus an eine gegebene ökologische Nische aus, z.B. die eines Parasiten an seinen Wirt. Während der Koevolution zwischen Parasit und Wirt haben sich sowohl die morphologischen als auch die zellbiologischen Aspekte von *Giardia* in ausserordentlicher Weise an ein Leben im Dünndarm angepasst. Trotz der aussergewöhnlichen zellbiologischen Charakteristika lässt sich *Giardia* im Labor relativ einfach vermehren, weshalb sich dieser Parasit zu einem attraktiven Modell für das Studium von komplexen zellbiologischen und phylogenetischen Fragestellungen vor einem vereinfachtem euykariotischen Hintergrund entwickelt hat.

Eine der auffälligsten morphologischen Anpassungen von *Giardia* ist die evolutionäre Entwicklung der ventralen Saugplatte (SP). Die SP vermittelt die Adhäsion der Trophozoiten an das Darmepithel, um ihre Elimination durch die Darmperistaltik zu verhindern. Folglich liegt der ventrale Teil des Parasiten eng an den Epithelzellen an, während der kuppelartige dorsale Teil zum Darmlumen hin orientiert ist. Diese dorso-ventrale Zellpolarisation ist in der Verteilung der endozytischen Organellen ersichtlich, die Peripheral Vacuoles (PVs) genannt werden. PVs befinden sich, abgesehen vom Bereich der SP, direkt unterhalb der gesamten Plasmamembran (PM) und sind damit mehrheitlich zum Darmlumen hin orientiert. Hinweise auf eine reduktive Evolution sind auch an den PVs selbst erkennbar, die nur wenige Charakteristika mit kanonischen Endozytose-Kompartimenten teilen, sich aber in den meisten von diesen unterscheiden. Wie klassische Endosome sind auch PVs die ersten Empfänger von endozytärem Material und stehen in enger Verbindung mit den konservierten und wichtigsten Endocytoseproteinen Clathrin (*Gl*CHC), Dynamin (*Gl*DRP) und Adapter Protein 2 (*Gl*AP2). Obwohl die molekulare Funktion dieser drei Faktoren in *Giardia* nicht genau verstanden wird, hat

sich herausgestellt, dass sie nicht an der Entstehung von Clathrin-ummantelten Vesikeln (CCVs) beteiligt sind, da solche, an der PM entstandene, Vesikel in *Giardia* noch nie beobachtet wurden. Im Gegensatz zu den meisten Endocytose-Systemen von eukaryotischen Zellen sind PVs in einer festen Position, direkt unterhalb der PM fixiert und fusionieren nicht untereinander. Des Weiteren scheint es, als dass diese Organellen einem regulierten Zyklus zur willkürlichen Aufnahme von flüssigen Komponenten unterliegen. Letztendlich kombinieren PVs endosomale und lysosomale Eigenschaften und etablieren durch kurzlebige und reversible Fusionen mit der PM eine unmittelbare Kommunikation mit dem extrazellulärem Raum. Im Hauptteil meiner Dissertation haben wir die Hypothese, dass die Bildung von kurzlebigen, endozytären Transport-Zwischenprodukten durch die kurze Distanz zwischen den PVs und der PM überflüssig wurde und sich Clathrin im Zuge dessen in eine neue, noch nicht definierte Rolle im endozytose Prozess in *Giardia* kooptierte, getestet. Um *Gl*CHC auf subzellulärer Ebene zu charakterisieren und die morphologischen Aspekte der Materialaufnahme durch die PM in PVs zu untersuchen, haben wir eine ganze Palette von modernen bildgebenden Verfahren benutzt. Zusätzlich wurde ein individuell angepasstes Protokoll zur Durchführung einer co-Immunopräzipitation (co-IP) entwickelt, um ein Netzwerk an Proteinen zu definieren, die mit *Gl*CHC, *Gl*DRP und *Gl*AP2 interagieren. Unsere Resultate deuten darauf hin, dass *Gl*CHC in der Endozytose von *Giardia* eine strukturelle Rolle einnimmt und, abgesehen von *Gl*DRP und *Gl*AP2, hauptsächlich mit *Giardia*-spezifischen Proteinen interagiert. Darunter befinden sich Proteine, die mit Phosphoinositiden (PIs) interagieren, welche wichtige Signalmoleküle in endozytären Systemen von höheren Eukaryoten sind. Ausserdem ist es uns gelungen zu zeigen, dass PVs bis zu drei Mal grösser sind als bisher beschrieben und sich durch Fusionen mit der sich einstülpenden PM einen Zugang zum extrazellulärem Raum verschaffen. Unsere Daten stimmen mit einem Modell überein, in welchem *Gl*CHC ein statisches Gerüst für die regulierten Fusionen zwischen PVs und der sich einstülpenden PM bereitstellt, ein Prozess, der in einer „Kiss and Flush"-Weise funktioniert und komplett unabhängig von CCVs ist.

Die in dieser Arbeit gezeigten *Gl*CHC-Proteininteraktionen beinhalten zwei Proteine, die eine PX-Domäne besitzen (*Gl*PXDs). Darüber hinaus sind die für die Synthese von phosphorylierten PIs nötigen Enzyme im Genom von *Giardia* enthalten. Dies stimmt mit der Rolle von PIs in klassischer Endozytose überein, deren Regulation von der Rekrutierung von PX-Proteinen abhängig sein kann. Im Ganzen sind sechs *Gl*PXDs im Genom von Giardia identifizierbar. Die hier gezeigte Interaktion von zwei davon mit *Gl*CHC legen eine mögliche Beteiligung an der Regulation der Endozytose in *Giardia* nahe, was die Frage nach der genauen subzellulären Lokalisation, den Protein-Protein-Interaktionen und den PI-Bindungspräferenzen dieser Proteine nach sich zieht. Die in dieser Arbeit präsentierten Ergebinsse zeigen unterschiedliche PI-Bindungspräferenzen für alle sechs (isolierten) PX-Domänen

und eindeutige suborganelle Verteilungsmuster innerhalb der begrenzten Membranen von PVs für vier der sechs *Gl*PXDs. Unsere Resultate deuten auf eine Rolle für PIs und für *Gl*PXDs im Endozytose-System von *Giardia* hin und lassen vermuten, dass die PI-bedingte Regulation ein konserviertes Merkmal der Endozytose in diesem divergenten Parasiten ist.

PART II Aim of the Thesis

Giardia lamblia is a unicellular, intestinal parasite that has undergone strong adaptation in the course of host-parasite co-evolution. This process often referred to as reductive or secondary evolution has resulted in a maximally reduced and compact pathogen and is evident on a genomic and subcellular level. *G. lamblia*'s highly diverged genome encodes for about 5000 single proteins but more than 50% of them show no similarity with any proteins sequences in public protein databases. On a subcellular level the high degree of adaptation has led to a minimized endomembrane system lacking several eukaryotic hallmark organelles (e.g. Golgi or distinct endo- and lysosomal compartments).

In the case of the giardial endocytic system, reduction entails a completely different distribution and morphology of endocytic organelles, termed peripheral vacuoles (PVs), compared to mammalian systems. Current data suggest a unique mode of operation for PV organelles regulated by molecular machineries that share some similarity with canonical endocytic pathways. PV organelles comprise the entire endocytic system in this parasite and function as both sorting and digestive compartments. There is mounting evidence that PVs function as sorting stations at the crossroads of endo- and exo -cytic pathways and are therefore at the forefront of host parasite interactions.

The main aim of my thesis was to investigate the peculiar endocytic system in *Giardia* on a morphological and molecular level and to address questions about the mode of material uptake and the role of the conserved major coat protein clathrin. Furthermore, we developed a second research line aimed at characterizing a family of phosphoinositide- (PI) binding PX domain-containing proteins to investigate the role of PIs in the giardial endocytic system.

The study of endocytosis in *Giardia* has proven challenging. This is mainly due to the massive degree of reductive evolution which occurred in this parasite. The consequences of this phenomenon are, amongst others, limitations in the availability of suitable and effective research tools. The remarkable divergence of the genome prevents the use of most commercial markers or antibodies and makes homology-based protein identification in most cases impossible. Furthermore, the tetraploid status of vegetative trophozoites has hampered all attempts to obtain functional gene knockouts whilst knockdown strategies (RNAi or morpholinos) were shown to be very inconsistent in their efficacy. Overcoming these biological limitations in *G. lamblia* research means that scholars are constantly forced to adapt and implement new research tools and strategies. In my opinion this process is inescapable and constitutes a substantial and exciting part of every PhD thesis pursued in the *Giardia* research field.

PART III Introduction

1. Giardia lamblia

1.1. Giardiasis and the life cycle of Giardia lamblia

The intestinal protozoan parasite *Giardia lamblia* (syn. *G. intestinalis* and *G. duodenalis*) is the major cause of protozoa induced diarrhea in humans and animals [10]. The WHO estimates that 270 million people have symptomatic giardiasis with more than 0.5 Mio new cases reported each year [11] and is therefore considered to be a neglected disease that spreads worldwide from the Arctic [12] to the Tropics [13]. Although most of the cases occur in developing countries, recent publications estimate 1.2 Mio cases of giardiasis in the United States, causing 34 Mio dollars in hospitalization costs [14, 15]. Giardiasis' potential as a zoonotic disease is not yet completely understood, but at least some genetic assemblages are thought to be transmitted from animals to humans and vice versa [16]. In young farm animals *Giardia* infection can lead to loss in productivity [17]. Together with the need to control waterborne transmission due to the low infection dose (2 – 10 cysts) [18], the impact of this parasitic disease is economically important [17]. An infection with *Giardia* does not necessarily lead to an apparent disease; therefore the clinical manifestations vary from asymptomatic cases to acute or chronic infections. When manifest, giardiasis leads to symptoms such as nausea, weight loss, bloating, abdominal pain, and diarrhea [19]. Treatment of infection is usually based on imidazoles such as metronidazole or albendazol. Even though effective in most cases, treatment failures may occur due to drug resistance, requiring combinatorial treatments (e.g. metronidazole and albendazol) [20].

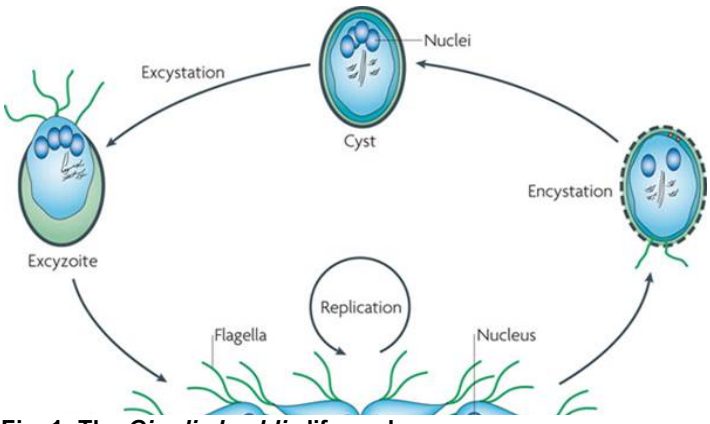

Fig. 1: The *Giardia lamblia* life cycle
Attached to the intestinal epithelium with the adhesive/ventral disc, trophozoites replicate with a generation time of 6-12 hours. Encystation occurs when trophozoites migrate to the distal duodenum where the extracellular milieu changes. Environmentally resistant and metabolically dormant cysts contain four tetraploid nuclei, resulting in a ploidy of 16*n*. Taken up by a new host, excystation occurs and liberates the 16*n* -excyzoite which divides twice, giving rise to 4 4*n* -trophozoites. Adapted from [1]

Giardia has a simple lifecycle comprising of only two developmental stages (Fig. 1); the vegetative trophozoite stage colonizes the host's upper small intestine while the metabolically reduced cyst stage ensures transmission by surviving in the environment. In the host, the flagellated trophozoite proliferates attached to the epithelium of the small intestine. In response to certain external triggers (e.g. high concentrations of bile and/or changes in pH) some trophozoites undergo

stage-conversion to the infective cyst, a process known as encystation. Once differentiated and protected by a cyst wall, the cysts are shed in the feces. Subsequent oral uptake and stomach passage of cysts by a susceptible host initiates a process known as excystation, through which the excyzoite is formed and gives rise to four motile trophozoites after two rapid cell divisions [1].

1.2. Evolutionary background

In 1989, Thomas Cavalier-Smith formulated the Archezoa hypothesis, proposing a new kingdom comprising eukaryotic organisms that diverged before the endosymbiotic acquisition of mitochondria [21, 22]. In this "elitist", rRNA analysis-based model, many protozoan parasites including lineages such as *Giardia*, *Trichomonas, Entamoeba* and *Trypanosoma* were placed into the Archezoa group, suggesting they emerged from the basal trunk of the eukaryotic tree of life [1, 3] (Fig. 2A). In particular *Giardia* was described as a "biological fossil" and part of the missing link between prokaryotes and eukaryotes [1] as it had retained some bacterial/archeaal features and possessed several unusual characteristic (e.g. the absence of aerobic mitochondria, the Golgi complex and peroxisomes) [3, 10]. However, this model was soon put into question as many "mitochondria lacking" organisms, including *Giardia* and *Entamoeba*, were studied in more detail and revealed to possess nuclear-encoded mitochondria related genes [23-26] and, in all cases, mitochondria related organelles [27, 28]. It is now thought that Giardia's bacterial characteristics are rather a consequence of lateral gene transfer than of close phylogenetic relationship and/or eukaryotic primitivity [29, 30]. Furthermore, a combination of molecular and morphological studies [3], the increasing amount of available genomic data and advances in phylogenetics in the past years have allowed the development of a new model forthe tree of life. This "egalitarian" approach predicts 5 eukaryotic super groups containing the majority of eukaryotes [31-33] (Fig. 1B). Within

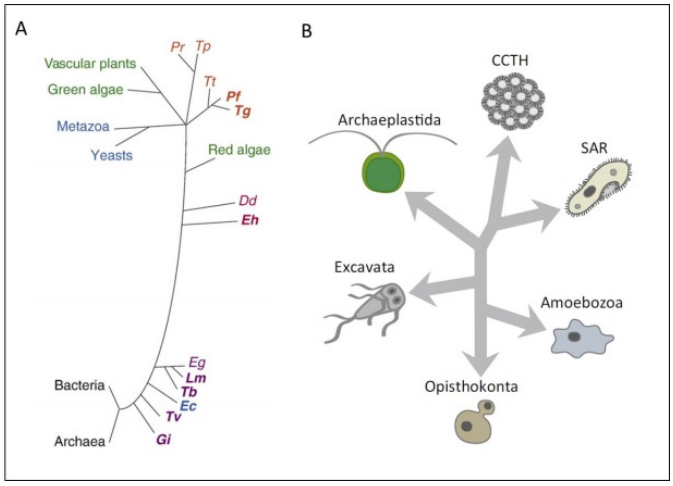

Fig. 2 Rooted elitist compared to unrooted egalitarian tree of life

(A) The "elitist" model is organized in a time line with mammals being placed at the apex (modern organisms). In contrast, lineages placed at the trunk were considered to have speciated early in evolution (ancient organisms). (B) In the "egalistic" model all lineages are equally ancient or modern, assuming rapid formation of all eukaryotic supergroups in a time un-resolved event. Note: the CCTH supergroup is only tentative. *SAR: **s**tramenopiles; **a**lveolates and **r**hizaria. CCTH: **c**ryptomonads, **c**entrohelids, **t**elonemids, and **h**aptophytes. Dd: Dictyostelium discoideum*; *Eh: Entamoeba histolytica*, *Gi: Giardia intestinalis syn. lamblia*; *Lm: Leishmania major*; *Pf: Plasmodium falciparum*; *Tg: Toxoplasma gondii*; *Tv: Trichomonas vaginalis*; *Tb: Trypanosoma brucei*. Adapted from: [3, 4]

these new eukaryotic systematics, protozoan parasites are distributed in the super groups Amoebozoa, Excavata and SAR [4, 33]. According to the previous elitist approach, Giardia spp. served as models to study very early eukaryotic evolution. This dogma has now been abandoned and, in line with the unrooted egalistic tree of life, Giardia is now thought to have undergone a process termed "secondary reduction" or "reductive evolution" [9] i.e. evolution of simplified cellular and molecular systems from more complex ancestors. In the case of *Giardia* spp. reductive evolution is most likely been driven by host-parasite interactions and includes strong adaption to the narrow ecological niche of the small intestine. This likely resulted in high degrees of genome divergence, the lack of eukaryotic hallmark organelles like a Golgi apparatus or proper mitochondria and morphological adaptations e.g. the presence of flagella.

1.3. The Endomembrane System in Giardia lamblia

In line with the proposed of model of reductive evolution due to a parasitic lifestyle [28], *G. lamblia* has a rather simple subcellular compartmentation. Whilst eukaryotic key organelles like the Golgi, peroxisomes or proper mitochondria are absent, the trophozoite harbors, in addition to the nuclei, 3 distinct endomembrane systems [9, 29, 34, 35].

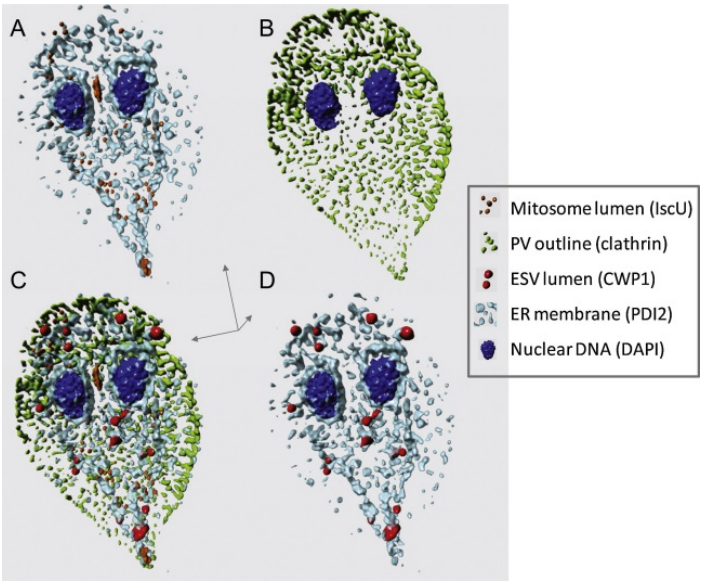

Fig. 3: 3D reconstruction of *Giardia* subcellular compartments as seen by confocal microscopy.
(A&D) Stage specific ESVs and mitosomes are shown together with the ER. (B) Clathrin is used as a reporter for PV organelles in the cell cortex. (C) Composite image of all 5 labels. Nuclear DNA is stained with DAPI. IscU: iron-sulfur cluster assembly enzyme. CWP1: cyst wall protein 1. PDI2: Protein disulfide isomerase 2. DAPI: 4′,6-Diamidin-2-phenylindol. Adapted from [9].

The endoplasmic reticulum (ER), which is the largest intracellular compartment, spans most of the cell body. For endocytic uptake the cell harbors an array of elongated organelles termed peripheral vacuoles (PVs). Mitosomes, mitochondria relic organelles, are the only other organelles identified in vegetative trophozoites. In trophozoites undergoing encystation a new set of organelles is formed *de novo* called encystation specific vesicles (ESVs). These are key organelles participating in the formation of the cyst wall.

The Nuclei

The presence of two nuclei is the most intriguing cellular feature in trophozoites that is common to all diplomonads. Each nucleus is about 1um in diameter and they are located in the anterior half of

the cell [36]. Both nuclei contain the diploid genome in five chromosome-like bodies [37] making this parasite a tetraploid organism [38]. Both nuclei are transcriptionally active but some data indicate that there are differences between them due to the observation of aneuploidy occurring in certain isolates [39], of unequal numbers and distribution of nuclear pores [36] and of asymmetric gene expression [40]. During the semi-open giardial mitosis the spindle microtubules penetrate the nuclei through openings in the nuclear envelopes which are never disassembled completely [1]. Trophozoite proliferation cycles between a ploidy of 4*n* and 8*n* as both nuclei replicate during cell division [41]. During encystation the nuclear DNA replicates twice and divides once, giving rise to four tetraploid nuclei in cysts [41]. One theory for the presence of two nuclei in *G. lamblia* is that the asymmetric gene expression offers unique possibilities for the regulation of gene expression [1].

Endoplasmic reticulum

The existence of the ER in *G. lamblia* was recognized only in 1996 when it was identified simultaneously by two groups using antibodies against the giardial homologue of Hsp70/BiP [42, 43]. The giardial ER extends from the nuclear envelope almost throughout the whole cell and appears as a bilateral symmetrical structure when visualized in fluorescence microscopy [9, 44-46]. Factors for co-translational import and protein folding in the secretory pathway (e.g. chaperons, protein disulfide-isomerase and translocation machinery [29, 45, 47]) are conserved in the giardial ER [9]. In contrast a calnexin-calreticulin machinery for quality control of N-glycosylated proteins has not been identified so far [48-50]. Additionally, *G. lamblia* and also *P. falciparum* miss most Alg genes coding for enzymes that generate N-glycan precursors and are therefore limited in protein glycosylation, with short precursor stumps that contain just N-acetyl-D-glucosamine$_{1-2}$ (GlcNAC$_{1-2}$)[9, 50, 51]. Nevertheless, G. lamblia possesses a considerable repertoire of N-glycosylated proteins that differs in size and composition between trophozoites and cysts [52]. Moreover, the giardial ER is implicated in a dual function that includes, aside from protein synthesis, a catabolic function in the PV-dominated endocytic pathway. This is based on data showing that some endocytosed substances are transported beyond the endocytic system into the ER, most likely via transient PV-ER contact points [44].

Mitosomes

The tiny (< 0.2um [28]) double membrane bound mitosomes found in Giardia represent the simplest form of mitochondria and are the product of reductive evolution [53]. In *Giardia*, two distinct populations of mitosomes can be found. Whilst the peripheral mitosomes are distributed throughout the cell, the central mitosome complex comprises of a cluster of individual organelles situated between the two nuclei (Rout et. al. 2016 in preparation).

However, a difference in function between the two populations has not been described so far. Mitosomes have lost their organellar genome and the capability to produce ATP. Hence the only metabolic pathway assigned to mitosomes is the biogenesis and maturation of iron-sulfur clusters [54]. In line with its reduced functions, mitosomes harbor only very few conserved proteins. A case in point is the translocon of the outer membrane (Tom40). Tom40 is the only conserved component of the translocase of the outer membrane (Tom) complex identified in *Giardia* and all of the recently found Tom40 interacting proteins are of unknown function and could not be assigned to known factors from canonical mitochondria (Rout et. al. 2016 in preparation). Similarly, the first component of the translocase of the inner membrane (TIM) complex, a putative Tim44, that was identified only recently seems to interact only species specific proteins [55].

Encystation specific vesicles (ESVs)

To survive outside of the host the lumen dwelling trophozoite undergoes stage conversion to become an environmentally resistant cyst during encystation. This conversion requires the formation of a rigid and protective cyst wall that is made out of only three cyst wall proteins (CWP1-3) and the homopolymer β1-3 *N*-Acetylgalactosamine (GalNAc) [56, 57]. Encystation is triggered by several environmental factors (e.g. changes in pH and bile concentration) and can be performed *in vitro* over 14-20h [58, 59]. During encystation, large amounts of CWP1-3 are produced in the ER before being sorted via ER exit sites into ESVs [60]. The stage specific transport of CWPs by ER exit sites-derived ESVs is the only known regulated secretion pathway in this parasite. However, ESVs are not just simple vesicles carrying proteins from the ER to the PM. There is growing evidence that ESVs represent stage specific Golgi-analogues that are formed *do novo* during encystation [9]. In fact, after ESV formation is completed, vesicular transport to the PM is delayed for several hours, most likely to allow for posttranslational maturation and sequential partitioning of the CWP1-3 before secretion to the cell surface [61]. In addition, ESVs are transiently associated with the coat protein 1 (COP1) [34], a known Golgi marker, and they are sensitive to brefeldin A (a fungal antibiotic causing Golgi disassembly by blocking COP1-dependent transport pathways) [62, 63]. Moreover, correct ESV formation and maturation depends on small GTPases such as Rab1, Arf1 and Sar1 [64] and the large GTPase dynamin [5]. Despite the listed Golgi-like characteristics of ESVs, these organelles lack some molecular and morphological hallmarks of Golgi organelles such as golgins and conserved Golgi matrix proteins.

Peripheral vacuoles

The PVs constitute the endocytic system in *G. lamblia* with a defined subcellular distribution. The PV organelle system populates the entire cell cortex in very close proximity to the PM and is excluded only from the PM domain associated to the ventral disc (VD), the structure that mediates attachment of the parasite to the intestinal epithelium [65]. These endocytic organelles represent the only known site of endocytosis in *G. lamblia* and are within the main scope of my thesis. Hence, they will be discussed in more detail in chapter 3, dedicated to endocytosis in *G. lamblia*.

1.4. Constitutive and regulated protein secretion

In canonical eukaryotic systems, secretory proteins are translated in the ER, quality controlled and modified in the Golgi from where they are sorted to their final destination. In G. lamblia two distinct protein secretion pathways are described so far. On the one hand proteins can be secreted constitutively in trophozoites; on the other hand the formation of the cyst wall during encystation is achieved by a tightly controlled and regulated protein trafficking pathway [9]. Constitutive protein secretion in proliferating trophozoites is best observed with the secretion of the variant surface proteins (VSPs) and cysteine-rich, non-variable proteins [9, 66]. VSPs mediate immune evasion by antigenic variation [67, 68] and are therefore considered as one of the major virulence factors of Giardia spp. [1]. About 200 genes encoding for individual VSPs are found in the genome [29] with only one variant expressed at a time and coating the entire parasitic surface [69, 70]. Antigenic switching i.e. exposure of a novel VSP, occurs every 6 – 13 generations and depends on environmental factors [71]. In contrast to organisms that contain a Golgi apparatus, secreted giardial VSPs and other constitutively expressed proteins are not delayed for protein processing and are most likely trafficked directly from the ER to the PM [62, 72, 73]. Even though many aspects of constitutive protein secretion remain unclear (e.g. the effect of brefeldin A on VSP trafficking despite the absence of a COPI associated membrane compartment in non-encysting trophozoites [63]), some conserved secretory and sorting motifs have been characterized. VSPs carry a sorting signal (CRGKA) (Cys-Arg-Gly- Lys-Ala) located in the conserved C-terminal domain that was shown to be essential for correct protein targeting [74]. Another example is sorting of the encystation specific protease (ESCP) from the ER to PVs which depends on a YXXφ (a tyrosine residue followed by any 2 aminoacids and a bulky hydrophobic amino acid side chain) targeting signal [73]. However, the exact route of ESCP trafficking to PVs remains unclear. In the absence of a central sorting organelle such as the Golgi, one explanation is that proteins targeted to PVs are by default sorted to the PM and subsequently taken up into PVs via the YXXφ internalization signal. Alternatively, proteins may reach the PV system via direct contacts points with the ER [44]. For several proteins found in the Giardia secretome, including the immuno-modulating enzymes arginine deaminase and ornithine carbamoyl transferase, no

secretory signal or sorting motif could be identified, suggesting the existence of non-conventional protein export routes. Interestingly, many secreted proteins are also found in the PV lumen [73, 75-77], leading to the hypothesis that PVs may function as a site for protein modification and /or activation. However, the exact mode of endocytosis is not defined yet in this parasite. Therefore the possibility remains that at least some of the secreted proteins detected in the PV lumen were simply endocytosed after being released in the extracellular environment.

The key structure for *Giardia* cysts to survive in the environment is the cyst wall. The differentiation process from trophozoites into cysts entails orchestration of a finely regulated secretion of the three CWPs to the cell surface where they most likely polymerize to form the cyst wall. In the first 7h after induction of encystation, large amounts of CWP1-3 are produced in the ER [78, 79]. Already 2h post induction synthesized CWPs are sorted to post ER/Golgi-like compartments i.e. nascent ESVs emerging from ER-exit sites [60, 61]. The synthesis of CWPs peaks 7h post induction [60] and their export from the ER to ESVs is complete after 8-10h [80]. Following ESV neogenesis, CWPs undergo post-translational maturation and sorting before being secreted [9, 61]. CWP deposition onto the cell surface occurs over several hours and is defined by the fast secretion of a first layer, providing a structural matrix, and the slow secretion of the second layer, leading to complete environmental resistance of the cysts [61].

2. Canonical clathrin-mediated endocytosis

The plasma membrane defines the unity of a eukaryotic cell. It is therefore the only cellular compartment that is in constant and simultaneous exposure both to the cell inside and to the outside. Hence the communication with the extracellular environment of any given cell has to occur via the outer and inner leaflets of the PM. To achieve this, eukaryotic cells have evolved varying mechanisms that allow internalization of extracellular material and PM components via the *de novo* production of internal membranes from the PM, a process called endocytosis. The morphological counterpart of the endocytic process, called exocytosis, includes fusion of internal membranes with the plasma membrane to deliver proteins and lipids to the PM and to release material to the extracellular space. Endocytosis however is a broad term defined in 1963 by the Nobel prize winner Christian de Duve [81]. It includes several different modes of uptake (Fig. 4), some of which were discovered only very recently (e.g. entosis, a process that occurs in cancer cells and involves invasion of a live cell into another, was discovered in 2007, [82]), whilst clathrin-mediated endocytosis (CME) was described already in the 1970s [83]. Endocytic processes are not only involved in the uptake of nutrients or the regulation of receptors at the cell surface. Endocytic malfunctions play pivotal roles

in diseases such as hemochromatosis [84] or diabetes [85]. Moreover endocytic pathways are often exploited by pathogens to enter host cells [86].

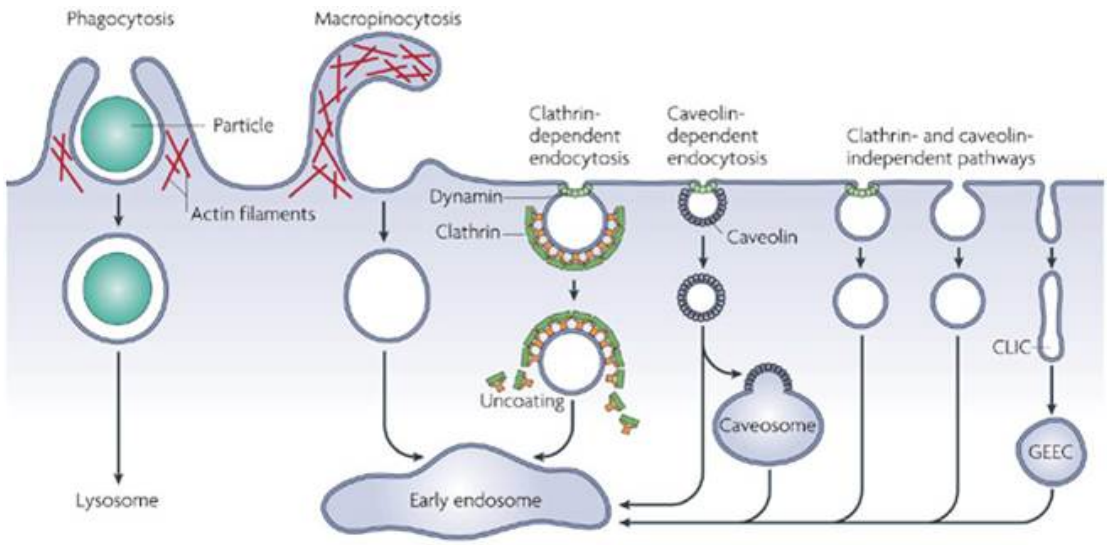

Fig. 4: Overview of endocytic pathways
In mammalian cells, the internalization of membrane components and extracellular material is facilitated by several independent endocytic pathways. CLIC = Clathrin- (and dynamin) Independent Carriers; GEEC = GPI-Enriched Endocytic Compartment. Adapted from [7].

Not all internalization pathways have received equal attention in the past years. CME is the most investigated and therefore best understood endocytic pathway by far. This may be due to its early discovery associated to the intriguing and characteristic structure of clathrin coated vesicles in electron microscopy [83]. CME mediates the highly selective uptake of hormones, metabolites or proteins. These cargo molecules bind to receptors which confer selectivity and specificity to this process which is also known as receptor-mediated endocytosis (RME). In this particular pathway, clathrin complexes, triskelion-shaped scaffolding proteins consisting of 3 heavy and 3 light chains, play a key role as they support membrane bending and define the size of the emerging vesicle called a clathrin coated vesicle (CCV) [87]. Besides clathrin, *ca.* 50 proteins involved in the formation of these transport intermediates have been identified. CCV formation is initiated by the assembly of a nucleation module at the plasma membrane with a preference for phosphatidylinositol-4,5-bisphosphate [88]. Further recognition of receptor/ligand-complexes on the cytoplasmic leaflet of the PM by adaptor protein complex 2 (AP2) recruits clathrin and accessory proteins to promote, increase and stabilize membrane curvature [88]. The emerging vesicle is almost entirely coated with clathrin but remains clathrin free at the neck where the large GTPase dynamin facilitates constriction and severing of the vesicle from the PM [89]. Immediately after vesicle formation, the clathrin coat is disassembled by HSC70 and its co-factor auxillin [90, 91] (Fig.5) before it ultimately fuses with an acceptor membrane of the endosomal system. In the opposite direction, but following the same

principle, CCVs emerging from the *trans*-Golgi network incorporate and transport proteins to endo-lysosomal compartments [92].

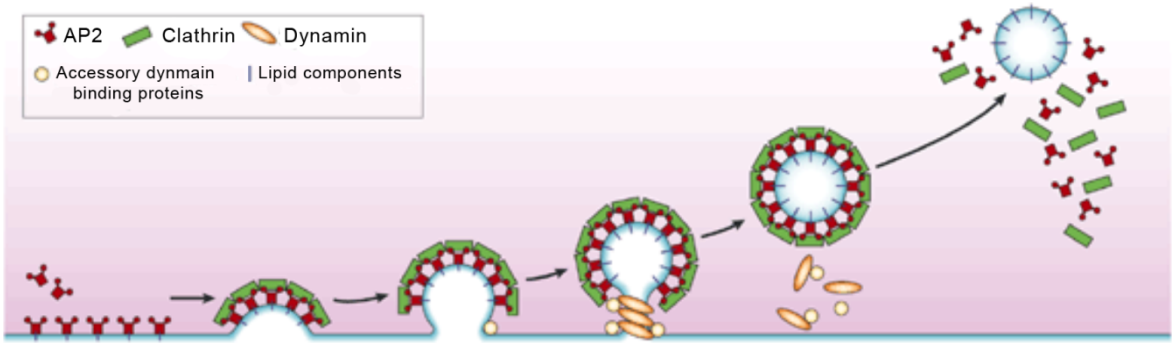

Fig. 5: Schematic representation of the molecular underpinnings of clathrin mediated endocytosis: The main steps in CME involve the recruitment of clathrin by AP2 bound to $PI4,5P_2$ and the endocytic motifs of membrane receptors or other cargo. Once recruited from the cytosol, clathrin assembles into polyhedral membrane coats. A multitude of accessory proteins drives deep membrane invagination for the formation of a constricted pit which is released from the PM into the cytosol in a dynamin dependent manner. The clathrin coat is disassembled by an uncoating ATPase prior to fusion with a target compartment. Adapted from [8].

Although CME is a tightly orchestrated process regulated by dozens of weak protein-protein interactions [88], three main components are clearly discernible (Fig. 5). Besides clathrin, these are AP2 and dynamin, all of which will be discussed in detail in the next paragraph.

2.1. Clathrin

The major scaffold protein clathrin was first described in a series of papers dating back to 1964 [93-95] but the term "clathrin" was only coined in 1975 by Barbara Pearse. She attempted to isolate microtubules from pig brains but instead found "vesicles in a basket" when analyzing her preparation at the electron microscope (EM) and named the isolated protein, due to their clathrate (lattice of bars) appearance, clathrin [83]. Only few years later the isolated 180kDa protein was shown to strongly interact with clathrin light chains to from clathrin triskelia [96]. The strength of the association is such that heavy and light chain complexes can only be disrupted using chaotropic reagents such as urea or thiocyanate [97]. Whilst the highly conserved clathrin heavy chain has been identified in all sequenced eukaryotic genomes except for *Microsporidia* [98], light chains share very low sequences similarities between species [99]. Clathrin triskelia have the capacity to self-assemble and form lattices of pentagons and hexagons on the cytoplasmic sides of membranes; these structures have been documented by electron microscopy (Fig.6). In CME, clathrin triskelia interact with a multitude of proteins but are unable to bind membranes directly [100] and depend on adaptor proteins to do so [100]. Once recruited to an endocytic nucleation site by such adaptors, clathrin governs vesicle formation by intrinsic polymerization. In contrast, clathrin disassembly is an energy-dependent process that relies on the regulated action of the ATPase-containing protein heat shock cognate 70 (HSC70) [101]. Recently, the amino acid motif, QLMLT (Gln-Leu-Met-Leu-Thr), essential

for HSC70 mediated clathrin coat disassembly has been identified at the carboxyl-terminus of the clathrin heavy chain [90]. Besides the role in endocytic vesicle formation, clathrin is involved in endosomal sorting/maturation, internal protein trafficking and also exhibits moonlighting functions e.g. at the mitotic spindle apparatus [102-105]. At endosomes, emerging into multivesicular bodies (MVBs), clathrin assembles into bilayered structures. In stark contrast to clathrin assemblies at the PM, bilayered clathrin at endosomes does not deform the membrane but is rather responsible for clustering hepatocyte growth factor-regulated tyrosine kinase substrate (HRS) [106]. In turn, HRS recognizes ubiquitinated proteins and thus facilitates protein sorting for degradation into MVB's. Interestingly, immune-labeling of bilayered clathrin coats failed to detect any of the adaptor proteins normally associated to clathrin coats [104, 107]. In anterograde intracellular protein trafficking, clathrin provides the coats for vesicular transport from the Golgi to the endo-/lysosomal system. These pathways are highly related to the CME pathway but depend on adaptor proteins 1, 3 and 4 [108, 109].

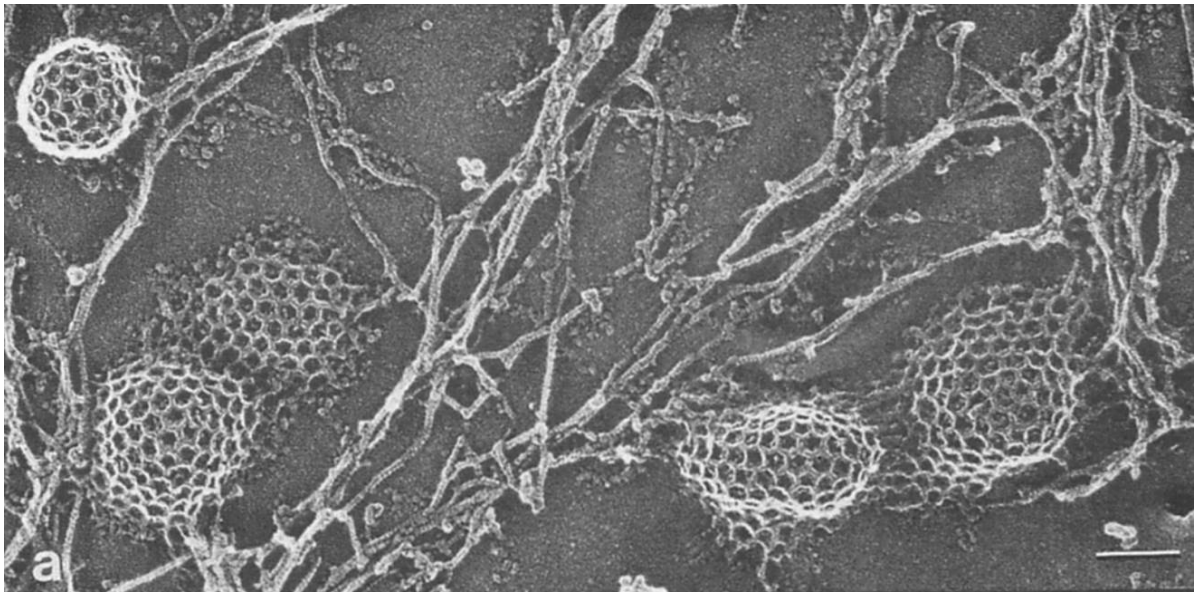

Fig. 6: Different stages of clathrin coat formation

The electron microscopy image shows clathrin assemblies on a carbon platinum replica of the cytosolic surface of a chicken fibroblast. Adapted from [110]. Scale bar 100nm.

2.2. Adaptor protein complex 2

AP2 is a heterotetramer comprising of two high molecular weight subunits, α and β, one medium sized μ subunit and the low molecular weight σ subunit [108, 111]. Five distinct APs are found in this protein family and only AP2 was found to function at the PM in CME. AP1, 3, 4 and 5 are all found at the Golgi and/or the endosomal system. AP1 is involved in membrane trafficking between the Golgi and tubular endosomes [112], AP3 between tubular endosomes and late endosomes/lysosomes and AP4 mediates trafficking between the trans Golgi network (TGN) and endosomes [113, 114]. Although, the exact role for AP5, discovered only in 2011 [114], has not been described in detail, it was implicated to regulate endosomal dynamics [115]. Phylogenetic and homology based analysis suggest that all five AP complexes were present in the latest common eukaryotic ancestor (LCEA) [116, 117] but that AP1, 2 and 4 evolved only after the evolution of the trans-Golgi network (TGN) [114]. Besides the general molecular architecture, APs also share the ability to recognize integral membrane or cargo proteins carrying exposed cytoplasmic YXXφ or dileucine based binding motifs [100].

AP2 localizes primarily to the PM; this is due to the affinity for phosphoinositide 4,5 phosphate (PtdIns4,5P_2) or PtdIns3,4,5P_3 [118, 119]. The association to phosphoinositides and to cargo at the PM most likely induces a conformational change in AP2 that enables active recruitment of clathrin triskelia to the site of endocytosis, a mechanism that at the same time prevents inappropriate clathrin recruitment by cytosolic AP2 [120]. The position of AP2 is such that it constitutes the majority of the middle layer of a clathrin coat, as it links the outer clathrin layer to the inner membrane layer with its embedded cargo proteins [121]. Thus, aside from clathrin, AP2 is the most abundant non-clathrin component of CCVs and recruits, in addition to clathrin, a great variety of CME associated proteins via the appendage domains of the two large α and β subunits [122, 123].

2.3. Dynamin

Classical dynamins function in endocytosis and are the founding members of the large family of dynamin like proteins (DLPs) [89]. The common structural features of all dynamins, which also distinguishes them from other GTPases, are the structure of the large GTPase domain, the middle domain and the GTPase effector domain (GED) [124] (Fig. 7a). Aside from the classical dynamins, the family of DLPs includes proteins such as Mitofusin or dynamin related protein 1 (DRP1), two proteins that function in mitochondrial fusion and fission, respectively [125], atlastin, a protein involved in the fusion of ER membranes [126] and “accumulation and replication of chloroplasts 5” (ARC5) which is implicated in chloroplast fission in plants [127]. Interestingly, models for CME based on molecular paleontology investigations show that dynamin was probably not involved in CME in the LCEA [128]. Moreover, classical dynamins seem to have evolved from DRPs involved in mitochondrial fission

and/or cytokinesis, following acquisition of the pleckstrin homology domain (PHD) and the proline rich domain (PRD) for PM targeting [129]. This suggests that dynamins originally evolved to function in mitochondrial homeostasis or cytokinesis and only later evolved to function in severing membranes in endocytic pathways [128]. In CME, dynamin has a distinct role in vesicle fission and recruitment of accessory proteins (e.g. BAR-domain containing proteins) as well as actin to scission events. More recently, it was assigned to function in early clathrin coated pit (CCP) formation/maturation [89, 130-132]. In line with this, a report from 2013 used customized imaging approaches to show early recruitment and constant accumulation of dynamin during CCV formation with a peak prior to vesicle fission [133]. The same study further reports that early dynamin recruitment is a prerequisite for the formation of a productive CCP, as dynamin-negative CCPs disappear from the PM dramatically faster than dynamin-positive CCPs [133]. However, the exact role for dynamin in early CCP formation remains unclear. Dynamin recruitment prior to CCV scission is in line with its mode of action, where dynamin dimers get recruited onto membranes and polymerize into helical collars. This polymerization in turn induces GTP hydrolysis and results in membrane fission [89] (Fig. 7b). The pivotal role for dynamin in CME is further highlighted by the expression of dominant negative dynamin mutants deficient in GTP hydrolysis (K44A, K44E, or S45N) which, if expressed at high enough levels, interfere with correct receptor internalization and deep membrane invagination of CCPs in mammalian cells [134-137].

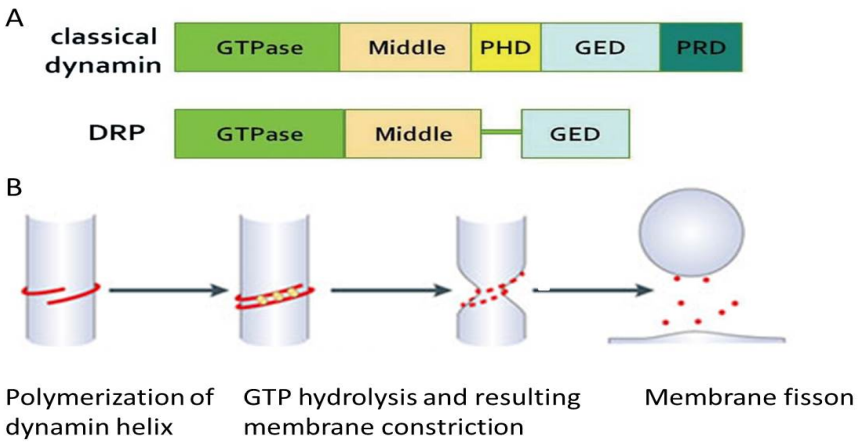

Fig. 7: Dynamin domains and mode of action

(A) Domain organization of classical dynamins and DRPs. The conserved GTPase, middle and GED domains are hallmarks of all members of the dynamin superfamily. Classical dynamins involved in CME have acquired a PHD and PRD domain to regulate targeting and protein activity. (B) Schematic representation of the different steps during dynamin mediated membrane fission. Adapted from [89, 128].

3. Endocytosis in Giardia lamblia

For a long time considered to be an ancient organism and an early branching eukaryote, the most widely-supported view describes *G. lamblia* as a likely product of reductive evolution [1]. This

hypothesis states that evolutionary pressure has led to a minimization of this parasite in terms of genome size and cellular complexity. The main force responsible for the high degree of reduction in this parasite is the narrow ecological niche in the host duodenum colonized by giardial trophozoites. One of the morphological consequences of this highly specific host-parasite interaction driven process is reflected in a strong polarization of the cell. Most strikingly, *G. lamblia* has evolved a VD, a specialized, suction-cup shaped structure covered by the PM that mediates the parasite's attachment to the gut epithelium, and defines the ventral domain of the parasite [138]. The opposite dorsal PM is dome-shaped and converges with the ventral PM into a flat and tapered tail (Fig. 8A). Subcellularly, we hypothesize that a parasitic lifestyle has led to the loss of several eukaryotic hallmark organelles such as the Golgi apparatus, proper mitochondria or peroxisomes [1]. On a metabolic level most pathways are minimized, reflected in the absence of a functional Krebs cycle or in the inability for *de novo* lipid synthesis [29]. Hence giardial trophozoites scavenge metabolites from the nutrient rich gut lumen through endocytosis. The endocytic system however does not comprise a canonical system of endosomes and lysosomes but consists of an array of endocytic organelles, the PVs [65] that define, in the absence of a cytostome, the only known endocytic sites, in this parasite [9, 139]. In line with the morphological adaptation to the host environment, PVs underly the dorsal PM and are therefore exposed to the gut lumen [99] (Fig. 8B). These oval shape 100-150nm sized organelles appear to be fixed in position as no organelle movement was identified so far [5]. The endocytic nature of PVs was recognized in several separate studies demonstrating the accumulation of fluid phase markers [5], ferritin particles [140], fluorescent lipid analogues [141] and viral particles [139] in PVs. Additionally, a study published in 2010 demonstrates AP2 dependent endocytosis of low-density lipo protein (LDL), which is abundant in the culture medium but not in the natural intestinal environment [9], as a receptor ligand complex, into PVs [2]. In addition to the established role for PVs as the initial recipients of endocytosed material, indicating a relation to canonical endosomes, these organelles, similar to mammalian lysosomes, can acidify their luminal content [142, 143] and contain hydrolytic enzymes such as proteinases, phosphatases or RNases [144, 145]. PVs are therefore recognized as organelles combining endo-/lysosomal properties [99]. These endocytic organelles have been shown to constantly sample the environment by bulk fluid phase uptake [5]. This process occurs with remarkable speed since within 15-20min the entire PV-system is saturated with fluid phase marker [5]. The same study demonstrated, that chasing the PV system saturated with a first fluid phase marker (e.g. dextran-green) with a second (e.g. dextran-red), leads to completed exchange of the former with the latter with no signs of signal overlap in individual organelles [5]. These data suggest a periodic cycle for these organelles that entails temporary and reversible communication between PVs and the extracellular space for complete exchange of old PV content with a new fluid phase sample. Moreover, analysis of endocytic markers inside PVs using fluorescence recovery after

photobleaching (FRAP), indicate no material exchange between or fusion of organelles. Interestingly, some fluid phase markers taken up into PVs seem to remain unprocessed and are expelled into the environment during the endocytic cycle [5]. In contrast, other substances such as fluorescently labelled casein, is taken up into PVs and transported further into the ER, most likely into catabolic ER-subdomains via direct luminal communication of the two organelle systems [44]. Based on these data the current model describes the PV-organelle system as a safety lock, that allows indiscriminate sampling of the extracellular space by fluid phase uptake into PVs in a "kiss and flush" manner [9]. Inside PVs however, yet unidentified mechanisms may distinguish between useful material for further digestion/processing and waste or harmful substances that are expelled to the extracellular environment [9].

Whilst the molecular machineries for the endocytic process in *G. lamblia* remain mostly undefined, the endocytic mechanisms in other protozoan parasites have been described in more molecular detail. In *Leishmania donov*ani, a kinetoplast causing visceral leishmaniosis known as "black fever", endocytosis occurs through a defined structure called the flagellar pocket and largely depends on the formation of CCVs, similar to canonical CME [146]. The endocytic system of the protozoan *Entamoeba hystolytica*, the causative agent of amoebic dysentery and amoeba-induced liver abscess, includes a conserved CME pathway to internalize ferritin particles which are essential for parasite metabolism, proliferation and virulence [147]. Likewise, in African trypanosomes, highly divergent protozoan parasites which cause "sleeping sickness" in humans, all endocytosis through the flagellar pocket is clathrin-mediated [148] and includes the formation of distinct CCPs and CCVs [149]. Interestingly, in *T. brucei* endocytosis functions in the absence of AP2 and most clathrin associated components are lineage-specific [150].

In stark contrast, a CME pathway was never described and CCVs were never observed in *G. lamblia*. This is surprising given that the giardial genome encodes for the 3 CME key players, namely clathrin heavy chain (*Gl*CHC), AP2 (*Gl*AP2) and a dynamin related protein (*Gl*DRP). Even though the presence of *Gl*CHC in the genome and its constitutive expression throughout all stages in the giardial lifecycle has been known for longer than a decade [72], only very few data are available on GlCHC. The 1871 amino acid long protein localizes in the PV-containing cell cortex (Fig. 8C) and several groups have provided evidence for its participation in the endocytic process [2, 5, 141, 151]. However, no characteristic clathrin lattices, CCPs or short lived clathrin coated transport intermediates have been observed [99]. Unlike heavy chains, clathrin light chains share very low sequence similarity between species [99]. It is therefore not surprising that in the diverged giardial genome no light chain was identified. Nonetheless, the possibility that *Giardia* harbours a clathrin light chain diverged beyond recognition by current search algorithms needs to be considered. Taken together, the scarce data on

*Gl*CHC suggest an involvement of this protein in endocytosis but do not provide functional information on its role in *G. lamblia* endocytosis. Data on *Gl*AP2 are similarly rare. *Giardial* AP2 co-distributes with *Gl*CHC in close PV proximity (Fig. 8C), has been implicated in RME and was shown to be essential for survival and stage differentiation [2]. The giardial dynamin related protein (*Gl*DRP) constitutes the third and last of the identified conserved endocytic factors in *G. lamblia*. *Gl*DRP contains all three necessary domains that define the minimal architecture of the protein superfamily of dynamin like proteins (DLP) i.e. an N-terminal GTPase domain, a middle domain and a C-terminal GED domain [89]. Additionally, *Gl*DRP contains a putative prolin rich domain (PRD), one of two domains only present in endocytosis associated classical dynamins but mostly absent in DLPs [89]. Unlike in classical dynamins, the giardial PRD domain is located upstream of the GED. In contrast to CME-associated dynamins, *Gl*DRP misses a PH domain which mediates membrane interaction via lipid binding ([5, 152] . However, giardial dynamin partially co-localizes with *Gl*CHC and *Gl*AP2 in PV proximity (Fig. 8D) [5]. The expression of dynamin mutant impaired in GTP hydrolysis and predicted to elicit a dominant-negative effect altered PV morphology and affected internalization of surface proteins but, importantly,did not affect fluid phase uptake [5].

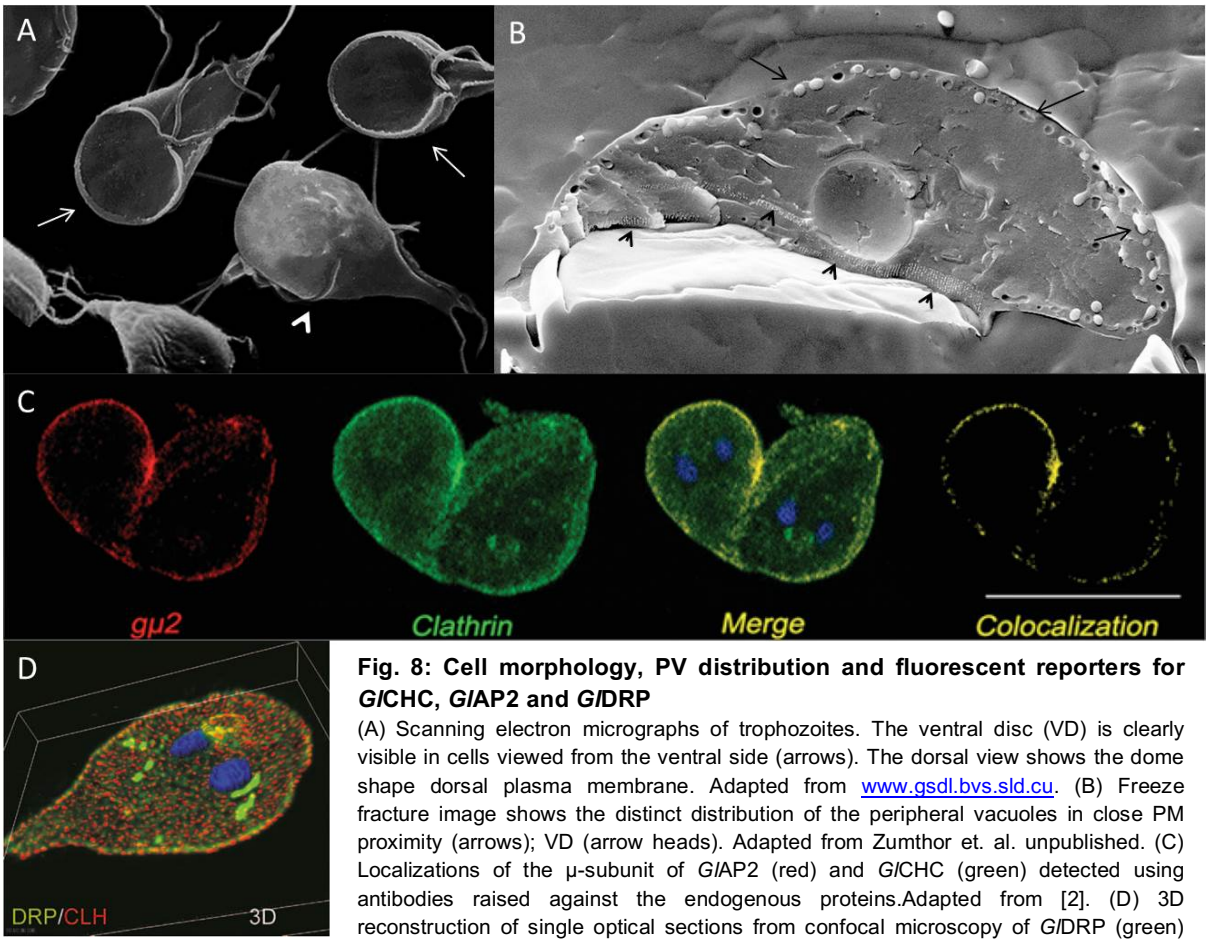

Fig. 8: Cell morphology, PV distribution and fluorescent reporters for *Gl*CHC, *Gl*AP2 and *Gl*DRP

(A) Scanning electron micrographs of trophozoites. The ventral disc (VD) is clearly visible in cells viewed from the ventral side (arrows). The dorsal view shows the dome shape dorsal plasma membrane. Adapted from www.gsdl.bvs.sld.cu. (B) Freeze fracture image shows the distinct distribution of the peripheral vacuoles in close PM proximity (arrows); VD (arrow heads). Adapted from Zumthor et. al. unpublished. (C) Localizations of the μ-subunit of *Gl*AP2 (red) and *Gl*CHC (green) detected using antibodies raised against the endogenous proteins.Adapted from [2]. (D) 3D reconstruction of single optical sections from confocal microscopy of *Gl*DRP (green) and *Gl*CHC (red). Adapted from [5].

4. PX domain-containing proteins and phosphoinositides.

Endocytic processes are one example of intracellular membrane trafficking. This broad term describes the transport of proteins and macromolecules between the endomembrane compartments and the PM through the formation of membrane-bound transport vesicles [153]. In addition to endocytic pathways, membrane trafficking includes transport events between the ER, the Golgi and the endo-/lysosomal compartments. Although often following a similar principle, each transport pathway requires the action of specific machineries. Hence these machineries need to distinguish between the corresponding membranes in order to reach their correct destination at the right time. Phosphoinositides (PIs), phosphorylated derivatives of the minor membrane lipid phosphatidylinositol (PtdIns) play a major role in this process in higher eukaryotes [154] and most likely also in *G. lamblia* [154, 155]. PIs comprise <1% of all cell lipids [6] can be reversibly phosphorylated at positions 3, 4 and 5 of their inositol ring giving rise to seven different phosphorylation derivations. The versatile nature and fast metabolic interconversions are hallmarks of these membrane lipids, regulating, aside from membrane trafficking, such diverse cellular processes as cell growth and survival [154, 155]. However, the subcellular distribution of PIs underscores their key role in intracellular membrane trafficking of higher eukaryotes (Fig.9) [156]. PIs exhibit their functions by recruiting specific effectors proteins to distinct membranes of the endomembrane system in a spatio-temporal manner [156]. Such effector proteins harbor specialized protein domains such as the FYVE domain (named after the four proteins where it was first found: Fab1, YOTB/ZK632.12, Vac1, and EEA1), the epsin N-terminal homology (ENTH) domain or the Phox (PX) domain that are capable of binding PIs [154].

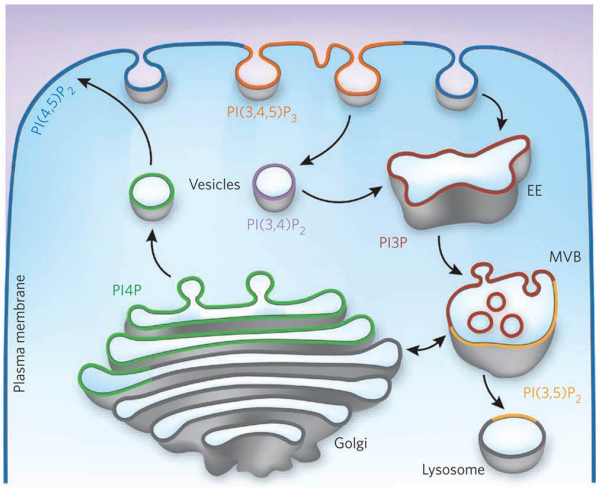

Fig. 9: Distribution of the predominant PIs on cytosolic membranes
Although most membranes are defined by a specific type of PI, heterogeneous distribution of PIs within a single membrane is also possible. EE = early endosome; MVB = multivesicular bodies. Adapted from [6].

PX domain modules for PI binding were discovered in 1996 and were named after the two phagocytic NADPH oxidase (phox) subunits, p40phox and p47phox [157]. PX domain-containing proteins (PXD) are implicated to have roles in endocytosis, membrane trafficking, protein sorting, transcription, cell polarity and signaling [158]. The largest mammalian protein group containing PX domains is the protein family of sorting nexins (SNX) which are mostly involved in endosomal sorting and recycling,

transport and lysosomal degradation of epidermal growth factor receptor, and in membrane tubulation [6]. Even though most PX domains have a preference for PtdIns phosphorylated at position 3 (PI3P) binding to other PIs, has also been described [6].

The *G. lamblia* genome harbors genes for a PX domain protein family with six members. So far, these *G. lamblia* PX domain-containing proteins (*Gl*PXD) have never been investigated on a molecular level. However, phylogenetic analysis classified the *Gl*PXDs as proteins with unknown function unrelated to mammalian SNX-proteins [159] and found that the PX domain is the only feature shared among the six *Gl*PXDs (Faso et al. unpublished). However, there is strong support for a functional PI signaling pathway in *Giardia*; sequence and phylogenetic analysis have identified several kinases and phosphatases capable of phosphorylation and dephosphorylation of PtdIns and PIs [29, 160]. These data are in line with the presence of additional proteins containing PI binding modules of the FYVE or ENTH type, for both of which PI binding has been experimentally proven [161, 162].

5. Goals of the Thesis

5.1. Main project: Structural and molecular investigation of the endocytic system in Giardia lamblia

The peripheral vacuoles (PVs) constitute the only known system capable of endocytosis in *G. lamblia*. However, data on how this system governs internalization are mainly descriptive with very few mechanistic insights. Nevertheless, the past two decades of endocytosis research in *G. lamblia* have set 3 cornerstones**:** i) PVs distribute in fixed positions at the cell cortex beneath the PM [65]; ii) PVs combine properties of endosomes and lysosomes, do not receive endocytic material from short-lived membrane carriers and undergo a regulated, yet undefined organelle cycle for the acquisition of extracellular fluid phase material [5, 44, 65, 99]; iii) *Gl*CHC, *Gl*AP2 and *Gl*DRP are the only conserved endocytic factors identified in the giardial genome and are implicated to play pivotal roles in giardial endocytosis [2, 5, 9, 72, 99, 163].

Based on these observations we formulated the following hypothesis which combines existing data with morphological and molecular aspects of host parasite co-evolution: The invention of the ventral disk (VD) for epithelial adhesion has driven redistribution of PV organelles mostly to the dorsal cell cortex where the PM is exposed to the gut lumen. As a consequence of this close proximity of the endocytic organelles to the PM, we propose that formation of clathrin-coated vesicles (CCVs) in *G. lamblia* most likely became obsolete and resulted in an alternative uptake mechanism that includes a coopted role for *Gl*CHC. Consequently, our hypothesis raised questions on the precise function of

*Gl*CHC, its interactome, its localization, and recruitment to membranes in the absence CCV formation and clearly identifiable monomeric clathrin adapters.

To address these open questions we plan to use a combination of molecular and state-of-the-art imaging techniques. In particular we aim to i) establish and apply a customized co-immunoprecipitation protocol to identify *Gl*CHC interacting proteins, and ii) implement confocal, super-resolution and electron microscopy techniques to, on one hand, define precise *Gl*CHC localizations and dynamics and, on the other hand, identify key morphological aspects of the endocytic process.

Endocytosis in *G. lamblia* is most likely highly diverged and includes only very few conserved CME factors. Given that CME was already present in the LCEA, our study will provide insights in a clathrin associated endocytic system that has undergone massive reductive evolution due to *G. lamblia*'s parasitic life style.

5.2. Subproject: Characterization of the giardial PX-domain containing protein family

This subproject is based on data generated from the main project showing that two PX-domain containing proteins were found to interact with clathrin in close vicinity to PVs. PX domains are lipid binding modules with distinct affinities for phosphorylated derivatives of phosphatidylinsositols (PtdIns) called phosphoinositides (PsI). In canonical endocytic systems PX-domains are recruited by PIs in a tightly regulated spatio-temporal manner to participate in the control of the endo-lysosomal organelle cycle [164]. Using homology-based in silico searches, we identified four additional giardial PX-domain containing proteins (*Gl*PXDs) that were not found to interact with giardial clathrin. Based on this and the endocytosis associated nature of PX domains, we hypothesized that all six *Gl*PXDs localize to PVs but with different lipid binding specificities, thus defining different membrane subdomains on the limiting PV-membrane.

To test our hypothesis, we aim to i) use lipid binding assays to determine binding preferences for each giardial PX domain; ii) define subcellular and suborganellar localization of all six members of the protein family of *Gl*PXDs using different fluorescence microscopy techniques, and iii) explore the existence of PV membrane subdomains characterized by specific PX domain-dependent protein intercatomes using co-immunoprecipitation approaches.

Very little is known about the combined endo-/lysosomal properties of endocytic organelles in *G.lamblia*. PIs play a key role in endocytic trafficking events in higher eukaryotes. Most likely this is also the case in Giardia where all molecular prerequisites for functional PI signaling pathways can be identified. Three different PI binding modules are found in giardial proteins (FYVE, ENTH and PX).

Whilst the FYVE domain and the ENTH domain containing proteins are encoded as single copies [161, 162], the *G*lPXDs comprise a family of six members. Investigating PX-domain proteins will therefore contribute substantial information on the regulation and conservation of lipid residue-dependent signaling pathways in Giardia's diverged endo-/lysosomal system.

6. Bibliography

1. Ankarklev J, Jerlstrom-Hultqvist J, Ringqvist E, Troell K, Svard SG. Behind the smile: cell biology and disease mechanisms of Giardia species. Nature reviews Microbiology. 2010;8(6):413-22. Epub 04/20. doi: 10.1038/nrmicro2317

10.1038/nrmicro2317. Epub 2010 Apr 19. PubMed PMID: 20400969.

2. Rivero MR, Vranych CV, Bisbal M, Maletto BA, Ropolo AS, Touz MC. Adaptor protein 2 regulates receptor-mediated endocytosis and cyst formation in Giardia lamblia. The Biochemical journal. 2010;428(1):33-45. Epub 03/05. doi: 10.1042/BJ20100096

10.1042/BJ20100096. PubMed PMID: 20199400.

3. Dacks JB, Walker G, Field MC. Implications of the new eukaryotic systematics for parasitologists. Parasitol Int. 2008;57(2):97-104. doi: 10.1016/j.parint.2007.11.004. PubMed PMID: 18180199.

4. Mast FD, Barlow LD, Rachubinski RA, Dacks JB. Evolutionary mechanisms for establishing eukaryotic cellular complexity. Trends Cell Biol. 2014;24(7):435-42. doi: 10.1016/j.tcb.2014.02.003. PubMed PMID: 24656655.

5. Gaechter V, Schraner E, Wild P, Hehl AB. The single dynamin family protein in the primitive protozoan Giardia lamblia is essential for stage conversion and endocytic transport. Traffic. 2007;9(1):57-71. Epub 09/26. doi: 10.1111/j.1600-0854.2007.00657.x. PubMed PMID: 17892527.

6. Kutateladze TG. Translation of the phosphoinositide code by PI effectors. Nat Chem Biol. 2010;6(7):507-13. doi: 10.1038/nchembio.390. PubMed PMID: 20559318; PubMed Central PMCID: PMCPMC3182472.

7. Mayor S, Pagano RE. Pathways of clathrin-independent endocytosis. Nat Rev Mol Cell Biol. 2007;8(8):603-12. doi: 10.1038/nrm2216. PubMed PMID: 17609668.

8. Gundelfinger ED, Kessels MM, Qualmann B. Temporal and spatial coordination of exocytosis and endocytosis. Nat Rev Mol Cell Biol. 2003;4(2):127-39. doi: 10.1038/nrm1016. PubMed PMID: 12563290.

9. Faso C, Hehl AB. Membrane trafficking and organelle biogenesis in Giardia lamblia: use it or lose it. International journal for parasitology. 2011;41(5):471-80. Epub 02/08. doi: 10.1016/j.ijpara.2010.12.014

10.1016/j.ijpara.2010.12.014. Epub 2011 Feb 4. PubMed PMID: 21296082.

10. Adam RD. Biology of Giardia lamblia. Clin Microbiol Rev. 2001;14(3):447-75. doi: 10.1128/CMR.14.3.447-475.2001. PubMed PMID: 11432808; PubMed Central PMCID: PMCPMC88984.

11. Lane S, Lloyd D. Current trends in research into the waterborne parasite Giardia. Crit Rev Microbiol. 2002;28(2):123-47. doi: 10.1080/1040-840291046713. PubMed PMID: 12109771.

12. Hotez PJ. Neglected infections of poverty among the indigenous peoples of the arctic. PLoS Negl Trop Dis. 2010;4(1):e606. doi: 10.1371/journal.pntd.0000606. PubMed PMID: 20126272; PubMed Central PMCID: PMCPMC2811175.

13. Kline K, McCarthy JS, Pearson M, Loukas A, Hotez PJ. Neglected tropical diseases of Oceania: review of their prevalence, distribution, and opportunities for control. PLoS Negl Trop Dis.

2013;7(1):e1755. doi: 10.1371/journal.pntd.0001755. PubMed PMID: 23383349; PubMed Central PMCID: PMCPMC3561157.
14. Collier SA, Stockman LJ, Hicks LA, Garrison LE, Zhou FJ, Beach MJ. Direct healthcare costs of selected diseases primarily or partially transmitted by water. 2013.
15. Scallan E, Hoekstra RM, Angulo FJ, Tauxe RV, Widdowson M-A, Roy SL, et al. Foodborne Illness Acquired in the United States—Major Pathogens. In: Centers for Disease Control and Prevention A, Georgia, USA, editor. 2011.
16. Cotton JA, Beatty JK, Buret AG. Host parasite interactions and pathophysiology in Giardia infections. Int J Parasitol. 2011;41(9):925-33. doi: 10.1016/j.ijpara.2011.05.002. PubMed PMID: 21683702.
17. O'Handley RM, Buret AG, McAllister TA, Jelinski M, Olson ME. Giardiasis in dairy calves: effects of fenbendazole treatment on intestinal structure and function. Int J Parasitol. 2001;31(1):73-9. PubMed PMID: 11165274.
18. RENDTORFF RC. The experimental transmission of human intestinal protozoan parasites. II. Giardia lamblia cysts given in capsules. Am J Hyg. 1954;59(2):209-20. PubMed PMID: 13138586.
19. Savioli L, Smith H, Thompson A. Giardia and Cryptosporidium join the 'Neglected Diseases Initiative'. Trends Parasitol. 2006;22(5):203-8. doi: 10.1016/j.pt.2006.02.015. PubMed PMID: 16545611.
20. Leitsch D. Drug Resistance in the Microaerophilic Parasite Giardia lamblia. Curr Trop Med Rep. 2015;2(3):128-35. doi: 10.1007/s40475-015-0051-1. PubMed PMID: 26258002; PubMed Central PMCID: PMCPMC4523694.
21. Cavalier-Smith T. Molecular phylogeny. Archaebacteria and Archezoa. Nature. 1989;339(6220):l00-1. doi: 10.1038/339100a0. PubMed PMID: 2497352.
22. Cavalier-Smith T. Kingdom protozoa and its 18 phyla. Microbiol Rev. 1993;57(4):953-94. PubMed PMID: 8302218; PubMed Central PMCID: PMCPMC372943.
23. Clark CG, Roger AJ. Direct evidence for secondary loss of mitochondria in Entamoeba histolytica. Proc Natl Acad Sci U S A. 1995;92(14):6518-21. PubMed PMID: 7604025; PubMed Central PMCID: PMCPMC41549.
24. Bui ET, Bradley PJ, Johnson PJ. A common evolutionary origin for mitochondria and hydrogenosomes. Proc Natl Acad Sci U S A. 1996;93(18):9651-6. PubMed PMID: 8790385; PubMed Central PMCID: PMCPMC38483.
25. Germot A, Philippe H, Le Guyader H. Evidence for loss of mitochondria in Microsporidia from a mitochondrial-type HSP70 in Nosema locustae. Mol Biochem Parasitol. 1997;87(2):159-68. PubMed PMID: 9247927.
26. Roger AJ, Svärd SG, Tovar J, Clark CG, Smith MW, Gillin FD, et al. A mitochondrial-like chaperonin 60 gene in Giardia lamblia: evidence that diplomonads once harbored an endosymbiont related to the progenitor of mitochondria. Proc Natl Acad Sci U S A. 1998;95(1):229-34. PubMed PMID: 9419358; PubMed Central PMCID: PMCPMC18184.
27. Tovar J, Fischer A, Clark CG. The mitosome, a novel organelle related to mitochondria in the amitochondrial parasite Entamoeba histolytica. Mol Microbiol. 1999;32(5):1013-21. PubMed PMID: 10361303.
28. Tovar J, León-Avila G, Sánchez LB, Sutak R, Tachezy J, van der Giezen M, et al. Mitochondrial remnant organelles of Giardia function in iron-sulphur protein maturation. Nature. 2003;426(6963):172-6. doi: 10.1038/nature01945. PubMed PMID: 14614504.
29. Morrison HG, McArthur AG, Gillin FD, Aley SB, Adam RD, Olsen GJ, et al. Genomic minimalism in the early diverging intestinal parasite Giardia lamblia. Science. 2007;317(5846):1921-6. Epub 09/29. doi: 10.1126/science.1143837. PubMed PMID: 17901334.
30. Andersson JO, Sjögren AM, Horner DS, Murphy CA, Dyal PL, Svärd SG, et al. A genomic survey of the fish parasite Spironucleus salmonicida indicates genomic plasticity among diplomonads and significant lateral gene transfer in eukaryote genome evolution. BMC Genomics. 2007;8:51. doi: 10.1186/1471-2164-8-51. PubMed PMID: 17298675; PubMed Central PMCID: PMCPMC1805757.

31. Dacks JB, Doolittle WF. Reconstructing/deconstructing the earliest eukaryotes: how comparative genomics can help. Cell. 2001;107(4):419-25. PubMed PMID: 11719183.
32. Adl SM, Simpson AG, Farmer MA, Andersen RA, Anderson OR, Barta JR, et al. The new higher level classification of eukaryotes with emphasis on the taxonomy of protists. J Eukaryot Microbiol. 2005;52(5):399-451. doi: 10.1111/j.1550-7408.2005.00053.x. PubMed PMID: 16248873.
33. Adl SM, Simpson AG, Lane CE, Lukeš J, Bass D, Bowser SS, et al. The revised classification of eukaryotes. J Eukaryot Microbiol. 2012;59(5):429-93. doi: 10.1111/j.1550-7408.2012.00644.x. PubMed PMID: 23020233; PubMed Central PMCID: PMCPMC3483872.
34. Marti M, Regos A, Li Y, Schraner EM, Wild P, Muller N, et al. An ancestral secretory apparatus in the protozoan parasite Giardia intestinalis. The Journal of biological chemistry. 2003;278(27):24837-48. Epub 04/25. doi: 10.1074/jbc.M302082200. PubMed PMID: 12711599.
35. Dacks JB, Field MC. Evolution of the eukaryotic membrane-trafficking system: origin, tempo and mode. J Cell Sci. 2007;120(Pt 17):2977-85. doi: 10.1242/jcs.013250. PubMed PMID: 17715154.
36. Benchimol M. Giardia lamblia: behavior of the nuclear envelope. Parasitol Res. 2004;94(4):254-64. doi: 10.1007/s00436-004-1211-8. PubMed PMID: 15349774.
37. Erlandsen SL, Rasch EM. The DNA content of trophozoites and cysts of Giardia lamblia by microdensitometric quantitation of Feulgen staining and examination by laser scanning confocal microscopy. J Histochem Cytochem. 1994;42(11):1413-6. PubMed PMID: 7930524.
38. Ankarklev J, Jerlström-Hultqvist J, Ringqvist E, Troell K, Svärd SG. Behind the smile: cell biology and disease mechanisms of Giardia species. Nat Rev Microbiol. 2010;8(6):413-22. doi: 10.1038/nrmicro2317. PubMed PMID: 20400969.
39. Tůmová P, Hofstetrová K, Nohýnková E, Hovorka O, Král J. Cytogenetic evidence for diversity of two nuclei within a single diplomonad cell of Giardia. Chromosoma. 2007;116(1):65-78. doi: 10.1007/s00412-006-0082-4. PubMed PMID: 17086421.
40. Saraiya AA, Wang CC. snoRNA, a novel precursor of microRNA in Giardia lamblia. PLoS Pathog. 2008;4(11):e1000224. doi: 10.1371/journal.ppat.1000224. PubMed PMID: 19043559; PubMed Central PMCID: PMCPMC2583053.
41. Bernander R, Palm JE, Svärd SG. Genome ploidy in different stages of the Giardia lamblia life cycle. Cell Microbiol. 2001;3(1):55-62. PubMed PMID: 11207620.
42. Luján HD, Mowatt MR, Conrad JT, Nash TE. Increased expression of the molecular chaperone BiP/GRP78 during the differentiation of a primitive eukaryote. Biol Cell. 1996;86(1):11-8. PubMed PMID: 8688827.
43. Soltys BJ, Falah M, Gupta RS. Identification of endoplasmic reticulum in the primitive eukaryote Giardia lamblia using cryoelectron microscopy and antibody to Bip. Journal of cell science. 1996;109 (Pt 7):1909-17. Epub 07/01. PubMed PMID: 8832413.
44. Abodeely M, DuBois KN, Hehl A, Stefanic S, Sajid M, DeSouza W, et al. A contiguous compartment functions as endoplasmic reticulum and endosome/lysosome in Giardia lamblia. Eukaryotic cell. 2009;8(11):1665-76. Epub 09/15. doi: 10.1128/EC.00123-09. PubMed PMID: 19749174.
45. Knodler LA, Noiva R, Mehta K, McCaffery JM, Aley SB, Svärd SG, et al. Novel protein-disulfide isomerases from the early-diverging protist Giardia lamblia. J Biol Chem. 1999;274(42):29805-11. PubMed PMID: 10514458.
46. Stefanic S, Palm D, Svärd SG, Hehl AB. Organelle proteomics reveals cargo maturation mechanisms associated with Golgi-like encystation vesicles in the early-diverged protozoan Giardia lamblia. J Biol Chem. 2006;281(11):7595-604. doi: 10.1074/jbc.M510940200. PubMed PMID: 16407213.
47. Svärd SG, Rafferty C, McCaffery JM, Smith MW, Reiner DS, Gillin FD. A signal recognition particle receptor gene from the early-diverging eukaryote, Giardia lamblia. Mol Biochem Parasitol. 1999;98(2):253-64. PubMed PMID: 10080393.
48. Banerjee S, Vishwanath P, Cui J, Kelleher DJ, Gilmore R, Robbins PW, et al. The evolution of N-glycan-dependent endoplasmic reticulum quality control factors for glycoprotein folding and

degradation. Proc Natl Acad Sci U S A. 2007;104(28):11676-81. doi: 10.1073/pnas.0704862104. PubMed PMID: 17606910; PubMed Central PMCID: PMCPMC1905923.
49. Banerjee S, Cui J, Robbins PW, Samuelson J. Use of Giardia, which appears to have a single nucleotide-sugar transporter for UDP-GlcNAc, to identify the UDP-Glc transporter of Entamoeba. Mol Biochem Parasitol. 2008;159(1):44-53. doi: 10.1016/j.molbiopara.2008.01.004. PubMed PMID: 18346800; PubMed Central PMCID: PMCPMC4258307.
50. Samuelson J, Banerjee S, Magnelli P, Cui J, Kelleher DJ, Gilmore R, et al. The diversity of dolichol-linked precursors to Asn-linked glycans likely results from secondary loss of sets of glycosyltransferases. Proc Natl Acad Sci U S A. 2005;102(5):1548-53. doi: 10.1073/pnas.0409460102. PubMed PMID: 15665075; PubMed Central PMCID: PMCPMC545090.
51. Samuelson J, Robbins PW. Effects of N-glycan precursor length diversity on quality control of protein folding and on protein glycosylation. Semin Cell Dev Biol. 2015;41:121-8. doi: 10.1016/j.semcdb.2014.11.008. PubMed PMID: 25475176; PubMed Central PMCID: PMCPMC4452448.
52. Ratner DM, Cui J, Steffen M, Moore LL, Robbins PW, Samuelson J. Changes in the N-glycome, glycoproteins with Asn-linked glycans, of Giardia lamblia with differentiation from trophozoites to cysts. Eukaryot Cell. 2008;7(11):1930-40. doi: 10.1128/EC.00268-08. PubMed PMID: 18820077; PubMed Central PMCID: PMCPMC2583543.
53. Embley TM, Martin W. Eukaryotic evolution, changes and challenges. Nature. 2006;440(7084):623-30. doi: 10.1038/nature04546. PubMed PMID: 16572163.
54. Lill R, Kispal G. Maturation of cellular Fe-S proteins: an essential function of mitochondria. Trends Biochem Sci. 2000;25(8):352-6. PubMed PMID: 10916152.
55. Martincová E, Voleman L, Pyrih J, Žárský V, Vondráčková P, Kolísko M, et al. Probing the Biology of Giardia intestinalis Mitosomes Using In Vivo Enzymatic Tagging. Mol Cell Biol. 2015;35(16):2864-74. doi: 10.1128/MCB.00448-15. PubMed PMID: 26055323; PubMed Central PMCID: PMCPMC4508323.
56. Gerwig GJ, van Kuik JA, Leeflang BR, Kamerling JP, Vliegenthart JF, Karr CD, et al. The Giardia intestinalis filamentous cyst wall contains a novel beta(1-3)-N-acetyl-D-galactosamine polymer: a structural and conformational study. Glycobiology. 2002;12(8):499-505. PubMed PMID: 12145190.
57. Jarroll EL, Manning P, Lindmark DG, Coggins JR, Erlandsen SL. Giardia cyst wall-specific carbohydrate: evidence for the presence of galactosamine. Mol Biochem Parasitol. 1989;32(2-3):121-31. PubMed PMID: 2927442.
58. Boucher SE, Gillin FD. Excystation of in vitro-derived Giardia lamblia cysts. Infection and immunity. 1990;58(11):3516-22. Epub 11/01. PubMed PMID: 2228222.
59. Luján HD, Mowatt MR, Byrd LG, Nash TE. Cholesterol starvation induces differentiation of the intestinal parasite Giardia lamblia. Proc Natl Acad Sci U S A. 1996;93(15):7628-33. PubMed PMID: 8755526; PubMed Central PMCID: PMCPMC38797.
60. Faso C, Konrad C, Schraner EM, Hehl AB. Export of cyst wall material and Golgi organelle neogenesis in Giardia lamblia depend on endoplasmic reticulum exit sites. Cell Microbiol. 2013;15(4):537-53. doi: 10.1111/cmi.12054. PubMed PMID: 23094658.
61. Konrad C, Spycher C, Hehl AB. Selective condensation drives partitioning and sequential secretion of cyst wall proteins in differentiating Giardia lamblia. PLoS pathogens. 2010;6(4):e1000835. Epub 04/14. doi: 10.1371/journal.ppat.1000835

10.1371/journal.ppat.1000835. PubMed PMID: 20386711.
62. Marti M, Li Y, Schraner EM, Wild P, Kohler P, Hehl AB. The secretory apparatus of an ancient eukaryote: protein sorting to separate export pathways occurs before formation of transient Golgi-like compartments. Molecular biology of the cell. 2003;14(4):1433-47. Epub 04/11. doi: 10.1091/mbc.E02-08-0467. PubMed PMID: 12686599.
63. Luján HD, Marotta A, Mowatt MR, Sciaky N, Lippincott-Schwartz J, Nash TE. Developmental induction of Golgi structure and function in the primitive eukaryote Giardia lamblia. J Biol Chem. 1995;270(9):4612-8. PubMed PMID: 7876232.

64. Stefanic S, Morf L, Kulangara C, Regos A, Sonda S, Schraner E, et al. Neogenesis and maturation of transient Golgi-like cisternae in a simple eukaryote. Journal of cell science. 2009;122(Pt 16):2846-56. Epub 07/23. doi: 10.1242/jcs.049411

10.1242/jcs.049411. Epub 2009 Jul 21. PubMed PMID: 19622633.
65. Lanfredi-Rangel A, Attias M, de Carvalho TM, Kattenbach WM, De Souza W. The peripheral vesicles of trophozoites of the primitive protozoan Giardia lamblia may correspond to early and late endosomes and to lysosomes. Journal of structural biology. 1999;123(3):225-35. Epub 01/08. doi: 10.1006/jsbi.1998.4035. PubMed PMID: 9878577.
66. Davids BJ, Reiner DS, Birkeland SR, Preheim SP, Cipriano MJ, McArthur AG, et al. A new family of giardial cysteine-rich non-VSP protein genes and a novel cyst protein. PLoS One. 2006;1:e44. doi: 10.1371/journal.pone.0000044. PubMed PMID: 17183673; PubMed Central PMCID: PMCPMC1762436.
67. Adam RD, Aggarwal A, Lal AA, de La Cruz VF, McCutchan T, Nash TE. Antigenic variation of a cysteine-rich protein in Giardia lamblia. J Exp Med. 1988;167(1):109-18. PubMed PMID: 3335828; PubMed Central PMCID: PMCPMC2188815.
68. Aggarwal A, Nash TE. Antigenic variation of Giardia lamblia in vivo. Infect Immun. 1988;56(6):1420-3. PubMed PMID: 3372015; PubMed Central PMCID: PMCPMC259415.
69. Svärd SG, Meng TC, Hetsko ML, McCaffery JM, Gillin FD. Differentiation-associated surface antigen variation in the ancient eukaryote Giardia lamblia. Mol Microbiol. 1998;30(5):979-89. PubMed PMID: 9988475.
70. Prucca CG, Lujan HD. Antigenic variation in Giardia lamblia. Cell Microbiol. 2009;11(12):1706-15. doi: 10.1111/j.1462-5822.2009.01367.x. PubMed PMID: 19709056.
71. Nash TE, Banks SM, Alling DW, Merritt JW, Conrad JT. Frequency of variant antigens in Giardia lamblia. Exp Parasitol. 1990;71(4):415-21. PubMed PMID: 1699782.
72. Hehl AB, Marti M. Secretory protein trafficking in Giardia intestinalis. Mol Microbiol. 2004;53(1):19-28. doi: 10.1111/j.1365-2958.2004.04115.x. PubMed PMID: 15225300.
73. Touz MC, Lujan HD, Hayes SF, Nash TE. Sorting of encystation-specific cysteine protease to lysosome-like peripheral vacuoles in Giardia lamblia requires a conserved tyrosine-based motif. The Journal of biological chemistry. 2002;278(8):6420-6. Epub 12/06. doi: 10.1074/jbc.M208354200. PubMed PMID: 12466276.
74. Marti M, Li Y, Köhler P, Hehl AB. Conformationally correct expression of membrane-anchored Toxoplasma gondii SAG1 in the primitive protozoan Giardia duodenalis. Infect Immun. 2002;70(2):1014-6. PubMed PMID: 11796643; PubMed Central PMCID: PMCPMC127713.
75. McCaffery JM, Faubert GM, Gillin FD. Giardia lamblia: traffic of a trophozoite variant surface protein and a major cyst wall epitope during growth, encystation, and antigenic switching. Experimental parasitology. 1994;79(3):236-49. Epub 11/01. doi: 10.1006/expr.1994.1087. PubMed PMID: 7525336.
76. Slavin I, Saura A, Carranza PG, Touz MC, Nores MJ, Lujan HD. Dephosphorylation of cyst wall proteins by a secreted lysosomal acid phosphatase is essential for excystation of Giardia lamblia. Molecular and biochemical parasitology. 2002;122(1):95-8. Epub 06/22. PubMed PMID: 12076774.
77. Ward W, Alvarado L, Rawlings ND, Engel JC, Franklin C, McKerrow JH. A primitive enzyme for a primitive cell: the protease required for excystation of Giardia. Cell. 1997;89(3):437-44. Epub 05/02. PubMed PMID: 9150143.
78. Mowatt MR, Luján HD, Cotten DB, Bowers B, Yee J, Nash TE, et al. Developmentally regulated expression of a Giardia lamblia cyst wall protein gene. Mol Microbiol. 1995;15(5):955-63. PubMed PMID: 7596296.
79. Luján HD, Mowatt MR, Conrad JT, Bowers B, Nash TE. Identification of a novel Giardia lamblia cyst wall protein with leucine-rich repeats. Implications for secretory granule formation and protein assembly into the cyst wall. J Biol Chem. 1995;270(49):29307-13. PubMed PMID: 7493963.

80. Hehl AB, Marti M, Kohler P. Stage-specific expression and targeting of cyst wall protein-green fluorescent protein chimeras in Giardia. Molecular biology of the cell. 2000;11(5):1789-800. Epub 05/04. PubMed PMID: 10793152.
81. Sabatini DD, Adesnik M. Christian de Duve: Explorer of the cell who discovered new organelles by using a centrifuge. Proc Natl Acad Sci U S A. 2013;110(33):13234-5. doi: 10.1073/pnas.1312084110. PubMed PMID: 23924611; PubMed Central PMCID: PMCPMC3746853.
82. Overholtzer M, Mailleux AA, Mouneimne G, Normand G, Schnitt SJ, King RW, et al. A nonapoptotic cell death process, entosis, that occurs by cell-in-cell invasion. Cell. 2007;131(5):966-79. doi: 10.1016/j.cell.2007.10.040. PubMed PMID: 18045538.
83. Pearse BM. Coated vesicles from pig brain: purification and biochemical characterization. J Mol Biol. 1975;97(1):93-8. PubMed PMID: 1177317.
84. Enns CA. Pumping iron: the strange partnership of the hemochromatosis protein, a class I MHC homolog, with the transferrin receptor. Traffic. 2001;2(3):167-74. PubMed PMID: 11260522.
85. Krischer J, Gilbert A, Gorden P, Carpentier JL. Endocytosis is inhibited in hepatocytes from diabetic rats. Diabetes. 1993;42(9):1303-9. PubMed PMID: 7688706.
86. Marsh M, Helenius A. Virus entry: open sesame. Cell. 2006;124(4):729-40. doi: 10.1016/j.cell.2006.02.007. PubMed PMID: 16497584.
87. Kirchhausen T, Owen D, Harrison SC. Molecular structure, function, and dynamics of clathrin-mediated membrane traffic. Cold Spring Harbor perspectives in biology. 2014;6(5):a016725. Epub 05/03. doi: 10.1101/cshperspect.a016725

10.1101/cshperspect.a016725. PubMed PMID: 24789820.
88. McMahon HT, Boucrot E. Molecular mechanism and physiological functions of clathrin-mediated endocytosis. Nature reviews Molecular cell biology. 2011;12(8):517-33. Epub 07/23. doi: 10.1038/nrm3151

10.1038/nrm3151. PubMed PMID: 21779028.
89. Ferguson SM, De Camilli P. Dynamin, a membrane-remodelling GTPase. Nat Rev Mol Cell Biol. 2012;13(2):75-88. doi: 10.1038/nrm3266. PubMed PMID: 22233676; PubMed Central PMCID: PMCPMC3519936.
90. Rapoport I, Boll W, Yu A, Bocking T, Kirchhausen T. A motif in the clathrin heavy chain required for the Hsc70/auxilin uncoating reaction. Molecular biology of the cell. 2007;19(1):405-13. Epub 11/06. doi: 10.1091/mbc.E07-09-0870. PubMed PMID: 17978091.
91. Eisenberg E, Greene LE. Multiple roles of auxilin and hsc70 in clathrin-mediated endocytosis. Traffic. 2007;8(6):640-6. doi: 10.1111/j.1600-0854.2007.00568.x. PubMed PMID: 17488288.
92. Braulke T, Bonifacino JS. Sorting of lysosomal proteins. Biochim Biophys Acta. 2009;1793(4):605-14. doi: 10.1016/j.bbamcr.2008.10.016. PubMed PMID: 19046998.
93. Kanaseki T, Kadota K. The "vesicle in a basket". A morphological study of the coated vesicle isolated from the nerve endings of the guinea pig brain, with special reference to the mechanism of membrane movements. J Cell Biol. 1969;42(1):202-20. PubMed PMID: 4182372; PubMed Central PMCID: PMCPMC2107565.
94. ROTH TF, PORTER KR. YOLK PROTEIN UPTAKE IN THE OOCYTE OF THE MOSQUITO AEDES AEGYPTI. L. J Cell Biol. 1964;20:313-32. PubMed PMID: 14126875; PubMed Central PMCID: PMCPMC2106398.
95. Heuser JE, Reese TS. Evidence for recycling of synaptic vesicle membrane during transmitter release at the frog neuromuscular junction. J Cell Biol. 1973;57(2):315-44. PubMed PMID: 4348786; PubMed Central PMCID: PMCPMC2108984.
96. Ungewickell E, Branton D. Assembly units of clathrin coats. Nature. 1981;289(5796):420-2. PubMed PMID: 7464911.
97. Hoffmann A, Dannhauser PN, Groos S, Hinrichsen L, Curth U, Ungewickell EJ. A comparison of GFP-tagged clathrin light chains with fluorochromated light chains in vivo and in vitro. Traffic. 2010;11(9):1129-40. Epub 06/16. doi: 10.1111/j.1600-0854.2010.01084.x

10.1111/j.1600-0854.2010.01084.x. Epub 2010 Jun 2. PubMed PMID: 20545906.
98. Barlow LD, Dacks JB, Wideman JG. From all to (nearly) none: Tracing adaptin evolution in Fungi. Cell Logist. 2014;4(1):e28114. doi: 10.4161/cl.28114. PubMed PMID: 24843829; PubMed Central PMCID: PMCPMC4022609.
99. Touz MC, Rivero MR, Miras SL, Bonifacino JS. Lysosomal protein trafficking in Giardia lamblia: common and distinct features. Frontiers in bioscience. 2011;4:1898-909. Epub 12/29. PubMed PMID: 22202006.
100. Popova NV, Deyev IE, Petrenko AG. Clathrin-mediated endocytosis and adaptor proteins. Acta Naturae. 2013;5(3):62-73. PubMed PMID: 24307937; PubMed Central PMCID: PMCPMC3848845.
101. Chappell TG, Welch WJ, Schlossman DM, Palter KB, Schlesinger MJ, Rothman JE. Uncoating ATPase is a member of the 70 kilodalton family of stress proteins. Cell. 1986;45(1):3-13. PubMed PMID: 2937542.
102. Royle SJ. Protein adaptation: mitotic functions for membrane trafficking proteins. Nat Rev Mol Cell Biol. 2013;14(9):592-9. doi: 10.1038/nrm3641. PubMed PMID: 23942451.
103. McMahon HT, Mills IG. COP and clathrin-coated vesicle budding: different pathways, common approaches. Curr Opin Cell Biol. 2004;16(4):379-91. doi: 10.1016/j.ceb.2004.06.009. PubMed PMID: 15261670.
104. Sachse M, Urbé S, Oorschot V, Strous GJ, Klumperman J. Bilayered clathrin coats on endosomal vacuoles are involved in protein sorting toward lysosomes. Mol Biol Cell. 2002;13(4):1313-28. doi: 10.1091/mbc.01-10-0525. PubMed PMID: 11950941; PubMed Central PMCID: PMCPMC102271.
105. Brodsky FM. Diversity of clathrin function: new tricks for an old protein. Annu Rev Cell Dev Biol. 2012;28:309-36. doi: 10.1146/annurev-cellbio-101011-155716. PubMed PMID: 22831640.
106. Raiborg C, Wesche J, Malerød L, Stenmark H. Flat clathrin coats on endosomes mediate degradative protein sorting by scaffolding Hrs in dynamic microdomains. J Cell Sci. 2006;119(Pt 12):2414-24. doi: 10.1242/jcs.02978. PubMed PMID: 16720641.
107. Clague MJ. Membrane transport: a coat for ubiquitin. Curr Biol. 2002;12(15):R529-31. PubMed PMID: 12176377.
108. Kirchhausen T. Adaptors for clathrin-mediated traffic. Annu Rev Cell Dev Biol. 1999;15:705-32. doi: 10.1146/annurev.cellbio.15.1.705. PubMed PMID: 10611976.
109. Gupta SN, Kloster MM, Rodionov DG, Bakke O. Re-routing of the invariant chain to the direct sorting pathway by introduction of an AP3-binding motif from LIMP II. Eur J Cell Biol. 2006;85(6):457-67. doi: 10.1016/j.ejcb.2006.02.001. PubMed PMID: 16542748.
110. Heuser JE, Anderson RG. Hypertonic media inhibit receptor-mediated endocytosis by blocking clathrin-coated pit formation. J Cell Biol. 1989;108(2):389-400. PubMed PMID: 2563728; PubMed Central PMCID: PMCPMC2115439.
111. Traub LM. Clathrin-associated adaptor proteins - putting it all together. Trends Cell Biol. 1997;7(2):43-6. doi: 10.1016/S0962-8924(96)20042-X. PubMed PMID: 17708899.
112. Robinson MS, Sahlender DA, Foster SD. Rapid inactivation of proteins by rapamycin-induced rerouting to mitochondria. Dev Cell. 2010;18(2):324-31. doi: 10.1016/j.devcel.2009.12.015. PubMed PMID: 20159602; PubMed Central PMCID: PMCPMC2845799.
113. Burgos PV, Mardones GA, Rojas AL, daSilva LL, Prabhu Y, Hurley JH, et al. Sorting of the Alzheimer's disease amyloid precursor protein mediated by the AP-4 complex. Dev Cell. 2010;18(3):425-36. doi: 10.1016/j.devcel.2010.01.015. PubMed PMID: 20230749; PubMed Central PMCID: PMCPMC2841041.
114. Hirst J, Barlow LD, Francisco GC, Sahlender DA, Seaman MN, Dacks JB, et al. The fifth adaptor protein complex. PLoS Biol. 2011;9(10):e1001170. doi: 10.1371/journal.pbio.1001170. PubMed PMID: 22022230; PubMed Central PMCID: PMCPMC3191125.
115. Hirst J, Irving C, Borner GH. Adaptor protein complexes AP-4 and AP-5: new players in endosomal trafficking and progressive spastic paraplegia. Traffic. 2013;14(2):153-64. doi: 10.1111/tra.12028. PubMed PMID: 23167973.

116. Field MC, Dacks JB. First and last ancestors: reconstructing evolution of the endomembrane system with ESCRTs, vesicle coat proteins, and nuclear pore complexes. Curr Opin Cell Biol. 2009;21(1):4-13. doi: 10.1016/j.ceb.2008.12.004. PubMed PMID: 19201590.
117. Dacks JB, Poon PP, Field MC. Phylogeny of endocytic components yields insight into the process of nonendosymbiotic organelle evolution. Proc Natl Acad Sci U S A. 2008;105(2):588-93. doi: 10.1073/pnas.0707318105. PubMed PMID: 18182495; PubMed Central PMCID: PMCPMC2206580.
118. Gaidarov I, Keen JH. Phosphoinositide-AP-2 interactions required for targeting to plasma membrane clathrin-coated pits. J Cell Biol. 1999;146(4):755-64. PubMed PMID: 10459011; PubMed Central PMCID: PMCPMC2156139.
119. Chang MP, Mallet WG, Mostov KE, Brodsky FM. Adaptor self-aggregation, adaptor-receptor recognition and binding of alpha-adaptin subunits to the plasma membrane contribute to recruitment of adaptor (AP2) components of clathrin-coated pits. EMBO J. 1993;12(5):2169-80. PubMed PMID: 8491205; PubMed Central PMCID: PMCPMC413438.
120. Kelly BT, Graham SC, Liska N, Dannhauser PN, Honing S, Ungewickell EJ, et al. Clathrin adaptors. AP2 controls clathrin polymerization with a membrane-activated switch. Science. 2014;345(6195):459-63. Epub 07/26. doi: 10.1126/science.1254836

10.1126/science.1254836. PubMed PMID: 25061211.
121. Brodsky FM, Chen CY, Knuehl C, Towler MC, Wakeham DE. Biological basket weaving: formation and function of clathrin-coated vesicles. Annual review of cell and developmental biology. 2001;17:517-68. Epub 11/01. doi: 10.1146/annurev.cellbio.17.1.517. PubMed PMID: 11687498.
122. Praefcke GJ, Ford MG, Schmid EM, Olesen LE, Gallop JL, Peak-Chew SY, et al. Evolving nature of the AP2 alpha-appendage hub during clathrin-coated vesicle endocytosis. The EMBO journal. 2004;23(22):4371-83. Epub 10/22. doi: 10.1038/sj.emboj.7600445. PubMed PMID: 15496985.
123. Schmid EM, McMahon HT. Integrating molecular and network biology to decode endocytosis. Nature. 2007;448(7156):883-8. Epub 08/24. doi: 10.1038/nature06031. PubMed PMID: 17713526.
124. Praefcke GJ, McMahon HT. The dynamin superfamily: universal membrane tubulation and fission molecules? Nat Rev Mol Cell Biol. 2004;5(2):133-47. doi: 10.1038/nrm1313. PubMed PMID: 15040446.
125. Hoppins S, Lackner L, Nunnari J. The machines that divide and fuse mitochondria. Annu Rev Biochem. 2007;76:751-80. doi: 10.1146/annurev.biochem.76.071905.090048. PubMed PMID: 17362197.
126. Orso G, Pendin D, Liu S, Tosetto J, Moss TJ, Faust JE, et al. Homotypic fusion of ER membranes requires the dynamin-like GTPase atlastin. Nature. 2009;460(7258):978-83. doi: 10.1038/nature08280. PubMed PMID: 19633650.
127. Gao H, Kadirjan-Kalbach D, Froehlich JE, Osteryoung KW. ARC5, a cytosolic dynamin-like protein from plants, is part of the chloroplast division machinery. Proc Natl Acad Sci U S A. 2003;100(7):4328-33. doi: 10.1073/pnas.0530206100. PubMed PMID: 12642673; PubMed Central PMCID: PMCPMC153092.
128. Liu YW, Su AI, Schmid SL. The evolution of dynamin to regulate clathrin-mediated endocytosis: speculations on the evolutionarily late appearance of dynamin relative to clathrin-mediated endocytosis. Bioessays. 2012;34(8):643-7. doi: 10.1002/bies.201200033. PubMed PMID: 22592980.
129. Miyagishima SY, Kuwayama H, Urushihara H, Nakanishi H. Evolutionary linkage between eukaryotic cytokinesis and chloroplast division by dynamin proteins. Proc Natl Acad Sci U S A. 2008;105(39):15202-7. doi: 10.1073/pnas.0802412105. PubMed PMID: 18809930; PubMed Central PMCID: PMCPMC2567515.
130. Taylor MJ, Lampe M, Merrifield CJ. A feedback loop between dynamin and actin recruitment during clathrin-mediated endocytosis. PLoS Biol. 2012;10(4):e1001302. doi: 10.1371/journal.pbio.1001302. PubMed PMID: 22505844; PubMed Central PMCID: PMCPMC3323523.

131. Conner SD, Schmid SL. Regulated portals of entry into the cell. Nature. 2003;422(6927):37-44. doi: 10.1038/nature01451. PubMed PMID: 12621426.
132. Mettlen M, Pucadyil T, Ramachandran R, Schmid SL. Dissecting dynamin's role in clathrin-mediated endocytosis. Biochem Soc Trans. 2009;37(Pt 5):1022-6. doi: 10.1042/BST0371022. PubMed PMID: 19754444; PubMed Central PMCID: PMCPMC2879887.
133. Aguet F, Antonescu CN, Mettlen M, Schmid SL, Danuser G. Advances in analysis of low signal-to-noise images link dynamin and AP2 to the functions of an endocytic checkpoint. Developmental cell. 2013;26(3):279-91. Epub 07/31. doi: 10.1016/j.devcel.2013.06.019

10.1016/j.devcel.2013.06.019. Epub 2013 Jul 25. PubMed PMID: 23891661.
134. Herskovits JS, Burgess CC, Obar RA, Vallee RB. Effects of mutant rat dynamin on endocytosis. J Cell Biol. 1993;122(3):565-78. PubMed PMID: 8335685; PubMed Central PMCID: PMCPMC2119668.
135. Damke H, Baba T, van der Bliek AM, Schmid SL. Clathrin-independent pinocytosis is induced in cells overexpressing a temperature-sensitive mutant of dynamin. J Cell Biol. 1995;131(1):69-80. PubMed PMID: 7559787; PubMed Central PMCID: PMCPMC2120592.
136. Damke H, Baba T, Warnock DE, Schmid SL. Induction of mutant dynamin specifically blocks endocytic coated vesicle formation. J Cell Biol. 1994;127(4):915-34. PubMed PMID: 7962076; PubMed Central PMCID: PMCPMC2200053.
137. van der Bliek AM, Redelmeier TE, Damke H, Tisdale EJ, Meyerowitz EM, Schmid SL. Mutations in human dynamin block an intermediate stage in coated vesicle formation. J Cell Biol. 1993;122(3):553-63. PubMed PMID: 8101525; PubMed Central PMCID: PMCPMC2119674.
138. Tumova P, Kulda J, Nohynkova E. Cell division of Giardia intestinalis: assembly and disassembly of the adhesive disc, and the cytokinesis. Cell motility and the cytoskeleton. 2007;64(4):288-98. Epub 01/06. doi: 10.1002/cm.20183. PubMed PMID: 17205565.
139. Tai JH, Ong SJ, Chang SC, Su HM. Giardiavirus enters Giardia lamblia WB trophozoite via endocytosis. Exp Parasitol. 1993;76(2):165-74. doi: 10.1006/expr.1993.1019. PubMed PMID: 8454025.
140. Bockman DE, Winborn WB. Electron microscopic localization of exogenous ferritin within vacuoles of Giardia muris. The Journal of protozoology. 1968;15(1):26-30. Epub 02/01. PubMed PMID: 5643476.
141. Hernandez Y, Castillo C, Roychowdhury S, Hehl A, Aley SB, Das S. Clathrin-dependent pathways and the cytoskeleton network are involved in ceramide endocytosis by a parasitic protozoan, Giardia lamblia. Int J Parasitol. 2007;37(1):21-32. doi: 10.1016/j.ijpara.2006.09.008. PubMed PMID: 17087963; PubMed Central PMCID: PMCPMC1831817.
142. Kattenbach WM, Pimenta PF, de Souza W, Pinto da Silva P. Giardia duodenalis: a freeze-fracture, fracture-flip and cytochemistry study. Parasitology research. 1991;77(8):651-8. Epub 01/01. PubMed PMID: 1805207.
143. Feely DE, Gardner MD, Hardin EL. Excystation of Giardia muris induced by a phosphate-bicarbonate medium: localization of acid phosphatase. J Parasitol. 1991;77(3):441-8. PubMed PMID: 2040956.
144. Feely DE, Dyer JK. Localization of acid phosphatase activity in Giardia lamblia and Giardia muris trophozoites. The Journal of protozoology. 1987;34(1):80-3. Epub 02/01. PubMed PMID: 3572844.
145. Lindmark DG. Giardia lamblia: localization of hydrolase activities in lysosome-like organelles of trophozoites. Experimental parasitology. 1988;65(1):141-7. Epub 02/01. PubMed PMID: 3276550.
146. Agarwal S, Rastogi R, Gupta D, Patel N, Raje M, Mukhopadhyay A. Clathrin-mediated hemoglobin endocytosis is essential for survival of Leishmania. Biochimica et biophysica acta. 2013;1833(5):1065-77. Epub 01/19. doi: 10.1016/j.bbamcr.2013.01.006

10.1016/j.bbamcr.2013.01.006. Epub 2013 Jan 14. PubMed PMID: 23328080.
147. López-Soto F, González-Robles A, Salazar-Villatoro L, León-Sicairos N, Piña-Vázquez C, Salazar EP, et al. Entamoeba histolytica uses ferritin as an iron source and internalises this protein by means

of clathrin-coated vesicles. Int J Parasitol. 2009;39(4):417-26. doi: 10.1016/j.ijpara.2008.08.010. PubMed PMID: 18848948.
148. Allen CL, Goulding D, Field MC. Clathrin-mediated endocytosis is essential in Trypanosoma brucei. The EMBO journal. 2003;22(19):4991-5002. Epub 10/01. doi: 10.1093/emboj/cdg481. PubMed PMID: 14517238.
149. Grünfelder CG, Engstler M, Weise F, Schwarz H, Stierhof YD, Morgan GW, et al. Endocytosis of a glycosylphosphatidylinositol-anchored protein via clathrin-coated vesicles, sorting by default in endosomes, and exocytosis via RAB11-positive carriers. Mol Biol Cell. 2003;14(5):2029-40. doi: 10.1091/mbc.E02-10-0640. PubMed PMID: 12802073; PubMed Central PMCID: PMCPMC165095.
150. Adung'a VO, Gadelha C, Field MC. Proteomic analysis of clathrin interactions in trypanosomes reveals dynamic evolution of endocytosis. Traffic. 2013;14(4):440-57. Epub 01/12. doi: 10.1111/tra.12040

10.1111/tra.12040. Epub 2013 Feb 5. PubMed PMID: 23305527.
151. Touz MC, Kulakova L, Nash TE. Adaptor protein complex 1 mediates the transport of lysosomal proteins from a Golgi-like organelle to peripheral vacuoles in the primitive eukaryote Giardia lamblia. Mol Biol Cell. 2004;15(7):3053-60. doi: 10.1091/mbc.E03-10-0744. PubMed PMID: 15107467; PubMed Central PMCID: PMCPMC452563.
152. Lemmon MA, Ferguson KM, O'Brien R, Sigler PB, Schlessinger J. Specific and high-affinity binding of inositol phosphates to an isolated pleckstrin homology domain. Proc Natl Acad Sci U S A. 1995;92(23):10472-6. PubMed PMID: 7479822; PubMed Central PMCID: PMCPMC40633.
153. Cheung AY, de Vries SC. Membrane trafficking: intracellular highways and country roads. Plant Physiol. 2008;147(4):1451-3. doi: 10.1104/pp.104.900266. PubMed PMID: 18678737; PubMed Central PMCID: PMCPMC2492619.
154. Di Paolo G, De Camilli P. Phosphoinositides in cell regulation and membrane dynamics. Nature. 2006;443(7112):651-7. Epub 10/13. doi: 10.1038/nature05185. PubMed PMID: 17035995.
155. Balla T. Phosphoinositides: tiny lipids with giant impact on cell regulation. Physiol Rev. 2013;93(3):1019-137. doi: 10.1152/physrev.00028.2012. PubMed PMID: 23899561; PubMed Central PMCID: PMCPMC3962547.
156. Vicinanza M, D'Angelo G, Di Campli A, De Matteis MA. Function and dysfunction of the PI system in membrane trafficking. EMBO J. 2008;27(19):2457-70. doi: 10.1038/emboj.2008.169. PubMed PMID: 18784754; PubMed Central PMCID: PMCPMC2536629.
157. Ponting CP. Novel domains in NADPH oxidase subunits, sorting nexins, and PtdIns 3-kinases: binding partners of SH3 domains? Protein Sci. 1996;5(11):2353-7. doi: 10.1002/pro.5560051122. PubMed PMID: 8931154; PubMed Central PMCID: PMCPMC2143296.
158. Seet LF, Hong W. The Phox (PX) domain proteins and membrane traffic. Biochimica et biophysica acta. 2006;1761(8):878-96. Epub 06/20. doi: 10.1016/j.bbalip.2006.04.011. PubMed PMID: 16782399.
159. Koumandou VL, Klute MJ, Herman EK, Nunez-Miguel R, Dacks JB, Field MC. Evolutionary reconstruction of the retromer complex and its function in Trypanosoma brucei. J Cell Sci. 2011;124(Pt 9):1496-509. doi: 10.1242/jcs.081596. PubMed PMID: 21502137; PubMed Central PMCID: PMCPMC3078816.
160. Cox SS, van der Giezen M, Tarr SJ, Crompton MR, Tovar J. Evidence from bioinformatics, expression and inhibition studies of phosphoinositide-3 kinase signalling in Giardia intestinalis. BMC microbiology. 2006;6:45. Epub 05/19. doi: 10.1186/1471-2180-6-45. PubMed PMID: 16707026.
161. Ebneter JA, Hehl AB. The single epsin homolog in Giardia lamblia localizes to the ventral disk of trophozoites and is not associated with clathrin membrane coats. Molecular and biochemical parasitology. 2014;197(1-2):24-7. Epub 10/07. doi: 10.1016/j.molbiopara.2014.09.008

10.1016/j.molbiopara.2014.09.008. Epub 2014 Oct 5. PubMed PMID: 25286382.
162. Sinha A, Mandal S, Banerjee S, Ghosh A, Ganguly S, Sil AK, et al. Identification and characterization of a FYVE domain from the early diverging eukaryote Giardia lamblia. Current microbiology. 2010;62(4):1179-84. Epub 12/18. doi: 10.1007/s00284-010-9845-5

10.1007/s00284-010-9845-5. Epub 2010 Dec 17. PubMed PMID: 21165741.
163. Rivero MR, Miras SL, Quiroga R, Ropolo AS, Touz MC. Giardia lamblia low-density lipoprotein receptor-related protein is involved in selective lipoprotein endocytosis and parasite replication. Molecular microbiology. 2011;79(5):1204-19. Epub 01/06. doi: 10.1111/j.1365-2958.2010.07512.x

10.1111/j.1365-2958.2010.07512.x. Epub 2011 Jan 5. PubMed PMID: 21205007.
164. Mayinger P. Phosphoinositides and vesicular membrane traffic. Biochimica et biophysica acta. 2012;1821(8):1104-13. Epub 01/28. doi: 10.1016/j.bbalip.2012.01.002

10.1016/j.bbalip.2012.01.002. Epub 2012 Jan 14. PubMed PMID: 22281700.

PART IV Manuscripts

1. Manuscript I

Static clathrin assemblies at the peripheral vacuole – plasma membrane interface of the parasitic protozoan *Giardia lamblia*

The work on the endocytic system in *G. lamblia* comprises the main part of my PhD, and I was awarded with the Forschungskredit (research grant) from the University of Zurich in two consecutive years (2013/14). This work resulted in the manuscript presented thereafter. My supervisior Adrian B. Hehl and Dr. Carmen Faso (Oberassistent) supported me during my whole PhD in terms of lab work, conceptual work and manuscript writing.

Electron microscopy analysis was entirely performed at the Center for Microscopy and Image Analysis at the University of Zürich in collaboration with Dr. Andres Kaech. During this time, I became an independent user of the Leica confocal and STED (stimulated emission depletion) super resolution microscopy systems. All other experiments were performed by me, except for the generation of the 3D images for the putative giardial clathrin light chain which was done by Ms. Lenka Cernikova as well as the MS-analyses that were performed at the Functional Genomics Center Zurich (FGCZ).

I substantially contributed in writing the manuscript and the compilation of all the figures in the manuscript.

Manuscript status: *published*

Static clathrin assemblies at the peripheral vacuole - plasma membrane interface of the parasitic protozoan *Giardia lamblia*

Jon Paulin Zumthor[1], Lenka Cernikova[1], Samuel Rout[1#], Andres Kaech[2], Carmen Faso[1]* and Adrian B. Hehl[1]*

[1] Institute of Parasitology, University of Zurich, Zurich, Switzerland

[2] Center for Microscopy and Image Analysis, University of Zurich, Zurich, Switzerland

[#]Current address: Department of Chemistry and Biochemistry, University of Berne, Berne, Switzerland

Keywords: Giardia; clathrin heavy chain; clathrin light chain; co-immunoprecipitation; interactome; cross-linking; tandem mass spectrometry; focused ion beam electron microscopy; APEX2 reporter for electron microscopy; FRAP; peripheral vacuoles, endocytosis; host-pathogen

Short title:

Clathrin assemblies in *Giardia lamblia*

*To whom correspondence and requests for materials should be addressed:

adrian.hehl@uzh.ch (ABH)

carmen.faso@uzh.ch (CF)

Abstract

Giardia lamblia is a parasitic protozoan that infects a wide range of vertebrate hosts including humans. Trophozoites are non-invasive but associate tightly with the enterocyte surface of the small intestine. This narrow ecological specialization entailed extensive morphological and functional adaptations during host-parasite co-evolution, including a distinctly polarized array of endocytic organelles termed peripheral vacuoles (PVs), which are confined to the dorsal cortical region exposed to the gut lumen and are in close proximity to the plasma membrane (PM). Here, we investigated the molecular consequences of these adaptations on the *Giardia* endocytic machinery and membrane coat complexes. Despite the absence of canonical clathrin coated vesicles in electron microscopy, *Giardia* possesses conserved PV-associated clathrin heavy chain (*Gl*CHC), dynamin-related protein (*Gl*DRP), and assembly polypeptide complex 2 (AP2) subunits, suggesting a novel function for *Gl*CHC and its adaptors. We found that, in contrast to GFP-tagged AP2 subunits and DRP, CHC::GFP reporters have no detectable turnover in living cells, indicating fundamental differences in recruitment to the membrane and disassembly compared to previously characterized clathrin coats. Histochemical localization in electron tomography showed that these long-lived *Gl*CHC assemblies localized at distinctive approximations between the plasma and PV membrane. A detailed protein interactome of *Gl*CHC revealed all of the conserved factors in addition to novel or highly diverged proteins, including a putative clathrin light chain and lipid-binding proteins. Taken together, our data provide strong evidence for giardial CHC as a component of highly stable assemblies at PV-PM junctions that likely have a central role in organizing continuities between the PM and PV membranes for controlled sampling of the fluid environment. This suggests a novel function for CHC in *Giardia* and the extent of molecular remodeling of endocytosis in this species.

Author summary

In canonical clathrin mediated endocytosis (CME) models, the concerted action of ca. 50 proteins mediates the uptake of extracellular components. The key player in this process is clathrin which coats transport intermediates called clathrin coated vesicles (CCV). The intestinal parasite *Giardia lamblia* has undergone extensive remodeling during colonization of the mammalian duodenum. Here, we report on unique features of this parasite's endocytic system, consisting of fixed peripheral vacuoles (PV) in close proximity to the exposed plasma membrane (PM), with no discernible CCVs. Using state-of-the-art imaging strategies, we show that the surface of *Giardia* trophozoites is pock-marked with PM invaginations reaching to the underlying PV membrane. Co-immunoprecipitation and analysis of protein dynamics reveal that, in line with the absence of CCVs, giardial clathrin assemblies have no dynamic behavior. CHC still remains associated to AP2 and dynamin, both conserved dynamic CME components, and to a newly identified putative clathrin light chain. The emerging model calls for giardial clathrin organized into static cores surrounded by dynamic interaction partners, and most likely involved in the regulation of fusion between the PM and the PVs in a "kiss-and-flush"-like mechanism. This suggests that Giardia harbors a conceptually novel function for clathrin in endocytosis, which might be a consequence of host-parasite co-evolution.

Introduction

Giardia lamblia trophozoites proliferate in a very narrow ecological niche, attached to the epithelium of the upper small intestine of vertebrate hosts [1]. This high degree of specialization required significant host-parasite co-evolution-driven morphological adaptations. Notably, *Giardia* trophozoites show a distinctive dorso-ventral polarization with a novel organelle for direct physical attachment to the gut epithelium. Within the diplomonad phylum, *Giardia* is the only known genus , to have evolved this so called ventral disc (VD), a cytoskeleton structure shaped like a suction cup underneath the PM, on the flat ventral domain [2]. The cell body proper is dome-shaped and delimited by the PM on the dorsal side. This defines the overall cell morphology and converges with the ventral PM into a flat, tapered tail at the posterior end. Trophozoites are preferentially tightly attached to the gut epithelium or to artificial supports in cell culture systems, exposing the dorsal PM to the nutrient rich lumen. This strong dorso-ventral polarization is also reflected in the subcellular arrangement of organelles. To communicate with the fluid phase environment trophozoites use a distinctive set of endocytic organelles [3]. This endocytic system consists of a fixed non-anastomosing set of organelles arrayed exclusively in a cortical region underneath the dorsal PM and at the center of the VD, termed PVs [4]. The endo/lysosomal nature of PV organelles and their ability to sample the fluid phase environment is widely recognized [3], but the exact mode of endocytic internalization and further processing/transport of endocytosed substances towards the cell interior remains elusive. Moreover, there are several examples of exocytic cargo that have been localized to PVs [5-9] whilst a constitutive secretory pathway in trophozoites has not been fully characterized yet [8]. This suggests these organelles to be at the crossroads of endo- and exocytosis and therefore a direct bidirectional interface for host parasite interaction.

Clathrin mediated endocytosis (CME) is by far the best understood pathway of internalization in eukaryotic cells. Many of the approximately 50 factors involved in the selective uptake of plasma membrane subdomains via the formation of transport intermediates called clathrin coated vesicles (CCVs) have been functionally characterized [10]. The basic concept as well as structural and functional aspects of CCV formation are conserved from mammals to early diverged protozoa such as African trypanosomes; this is also reflected in the presence of clathrin heavy chain-encoding ORFs in all sequenced eukaryotic genomes but microsporidia [10].

The formation of a CCV can be divided into distinct steps each of which is amenable to documentation by fluorescence and/or electron microscopy (EM) [11-14]. In transmission EM sections (tEM), CCVs and other clathrin assemblies are identified as a distinctly periodic pattern of the cytoplasmic membrane coat arising from clathrin-triskelion oligomerization [15-17]. In live cell

fluorescence microscopy of all cell types investigated so far, CME is characterized by the high dynamics that are observed for vesicle formation driven by clathrin triskelion oligomerization with an average life time of coats between 45-80s [18]. The dynamics of clathrin coats are further increased by constant exchange of individual triskelia throughout formation of the coated pit and the CCV to allow the reorganization from hexagons into pentagons as membrane curvature increases [14]. Active retrograde transport of PM-derived uncoated CCVs to endosomes adds a spatial dimension to the complex dynamics of CME.

In line with the endocytic nature of PV organelles, 3 protein complexes conserved in *Giardia* and associated with the endocytic machinery show a discrete localization in the cortical area of trophozoites by fluorescence microscopy: clathrin heavy chain (*Gl*CHC), subunits of the AP2 heterotetramer (*Gl*AP2) and *Giardia* dynamin related protein (*Gl*DRP) [3, 19]. These factors are key components of the clathrin-dependent endocytic machinery in higher eukaryotes and protozoa alike. However, no clathrin coated transport intermediates have been detected in *Giardia* by electron- or fluorescence microscopy. In terms of transport from the PM to PVs this is in line with the very short distances involved (~50 nm). Moreover, bulk fluid phase endocytosis into PVs has been demonstrated by time-lapse microscopy and appears to be independent of AP2 and dynamin [3, 19]. In addition, genes coding for regulatory factors involved in the dynamic formation and disassembly of coated pits and CCVs at the PM (i.e. clathrin light chain, HSC70, auxillin) cannot be identified, either because they are absent from the *Giardia* genome or because their sequence has diverged beyond recognition. Taken together, an important consequence of evolving a dedicated organelle (the ventral disk) for epithelial attachment may be remodeling of the endosomal organelle system and redistribution to the cortical region of trophozoites. In turn, given the proximity of PVs to the PM, these adaptations would have made dynamic CCV-mediated endocytic transport redundant and favored PV evolution towards fixed cortical compartments. This raises questions concerning the function of clathrin, its localization, and recruitment to membranes. To address these questions we performed a functional and structural characterization of conserved components of the giardial endocytic system. Extensive electron tomography revealed that the endocytic system of trophozoites is a network of elongated tubular compartments that may communicate with the extracellular environment by fusion at invaginations of the PM. On a molecular level, our data indicated that clathrin assemblies are small and focal clusters with no measurable turnover and exclusive cortical localization distal to PVs. To investigate the nature of these unusually static assemblies we generated an extended *Gl*CHC interactome which included conserved factors as well as new candidate adaptor proteins and a putative clathrin light chain (CLC). To our knowledge, this is the first report describing static clathrin heavy chain assemblies as a non-dynamic structural component of an endocytic

system. Since formation of CCVs is conserved in all other eukaryotes, this suggests a novel function for clathrin and associated factors in the context of ecological specialization driven by host-pathogen interaction.

Materials and Methods

Giardia cell culture, induction of encystation and transfection

G. lamblia WBC6 (ATCC catalog number 50803) trophozoites were cultured and harvested applying standard protocols [20]. Induction of encystation was done by the two-step method as previously described [21, 22]. Transgenic parasites were generated using standard protocols for the electroporation of linearized pPacV-Integ-based plasmid vectors amplified *E. coli* as described in [23]. Transgenic cells were selected for puromycin resistance. Once selected, trophozoites were cultured and analyzed without antibiotics.

Construction of expression vectors

Primer sequences of all oligonucleotides used for cloning are listed in S2 Table.

All genetically modified proteins in this manuscript were expressed under the control of the corresponding endogenous promoters except the 3 constructs for the truncation experiments of ORF4259 that were controlled by the inducible cyst wall protein 1 promoter.C-terminally hemagglutinin (HA)-tagged proteins were generated using a modified pPacV-Integ [24] with additional restrictions sites (Vector map in S2 Fig). All other cloning strategies were based on the previously described pPacV-Integ [24].

Co-immunoprecipitation with limited cross-linking

G. lamblia WBC6 and transgenic trophozoites expressing N- or C-terminally HA tagged bait proteins were harvested and correct subcellular distribution of bait proteins was confirmed by immunofluorescence assay. After harvesting parasites were washed in 50 ml of cold phosphate buffer saline solution (PBS) and adjusted to $2x10^7$ cells ml^{-1} in PBS (VWR Prolabo). A titration assay was applied to determine the appropriate concentration (0.4mM) of the cell-permeable, lysine-reactive crosslinker Dithiobis[succinimidyl propionate] (DSP, also called Lamont's Reagent). DSP is a particularly suitable crosslinking reagent to interrogate labile protein-protein interactions [25-28]. For the co-immunoprecipitation (co-IP) assays, 10^9 parasites were resuspended in 20 ml 0.4mM DSP (in PBS) and incubated for 30 minutes at room temperature (RT) in the presents of 1 mM phenylmethylsulfonyl fluoride (PMSF; SIGMA, Cat. No. P7626). Thereafter cells were washed with PBS and quenched in 20 ml 100 mM glycine in PBS for 15 minutes at RT. Cells were pelleted and

resuspended in 5ml of PBS supplemented with 2 mM PMSF and 1 x Protease Inhibitor Cocktail (PIC, Cat. No. 539131, Calbiochem USA) and sonicated twice using a Branson Sonifier with microtip (Branson Sonifier 250, Branson Ultrasonics Corporation) with the following settings: 60 pulses, 2 output control, 30% duty cycle, and 60 pulses, 4 output control, 40% duty cycle, respectively. The sonicate was centrifuged (14,000 *x g*, 10 minutes, 4 °C) before the soluble protein fraction was diluted 1:1 with PBS supplemented with 2% Triton X -100 (TX-100) (Fluka Chemicals) and 60 µl anti-HA agarose bead slurry (Pierce, product # 26181). For the binding reaction of the HA-tagged proteins and the beads, samples were incubated for 2h on a rotating wheel at 4°C. Subsequently, beads were washed 4 times with 3 ml Tris-Buffered Saline (TBS) supplemented with 0.1% TX-100 and once with 3 ml PBS by pulse-centrifugation at 4°C. Loaded beads were transferred to a spin column (Pierce spin column screw cap, product # 69705, Thermo Scientific) in 350ul PBS, centrifuged for 10s at 4°C and eluted in 30ul PBS. To reverse the crosslinking, eluted fractions were supplemented with 100mM Dithiothreitol (DTT; 100mM; Thermo Scientific, Cat. # RO861) and incubated for 30min at 37°C before boiling for 5min and centrifugation (14,000 x g, 10 minutes, RT).

Protein analysis and sample preparation for mass spectrometry-based protein identification

Analysis of input, flow-through, and eluted fractions was performed by SDS-PAGE on 10% polyacrylamide gels under reducing conditions, (molecular weight marker Cat. No. 26616, Thermo Scientific, Lithuania). Immunoblotting was done as previously described in [29]. Gels for mass spectrometry (MS) analysis were stained using Instant Blue (Expedeon, Prod. # ISB1L) and washed with ultrapure water.

Mass Spectrometry, protein identification and data storage

Stained gel lanes were cut into 8 equal sections. Each section was further diced into smaller pieces and washed twice with 100 µl of 100 mM ammonium bicarbonate/ 50 % acetonitrile for 15 min at 50 °C. The sections were dehydrated with 50 µl of acetonitrile. The gel pieces were rehydrated with 20 µl trypsin solution (5ng/µl in 10mM Tris-HCl/ 2mM $CaCl_2$ at pH8.2) and 40µl buffer (10mM Tris-HCl/ 2mM $CaCl_2$ at pH8.2). Microwave-assisted digestion was performed for 30 minutes at 60 °C with the microwave power set to 5 W (CEM Discover, CEM corp., USA). Supernatants were collected in fresh tubes and the gel pieces were extracted with 150µl of 0.1% trifluoroacetic acid/ 50% acetonitrile. Supernatants were combined, dried, and the samples were dissolved in 20µl 0.1% formic acid before being transferred to the autosampler vials for liquid chromatography-tandem MS (injection volume 7 to 9 µl). Samples were measured on a Q-exactive mass spectrometer (Thermo Scientific) equipped with a nanoAcquity UPLC (Waters Corporation). Peptides were trapped on a Symmetry C18, 5µm, 180µm x 20mm column (Waters Corporation) and separated on a BEH300 C18, 1.7µm, 75µm x

150mm column (Waters Corporation) using a gradient formed between solvent A (0.1% formic acid in water) and solvent B (0.1% formic acid in acetonitrile). The gradient started at 1% solvent B and the concentration of solvent B was increased to 40% within 60 minutes. Following peptide data acquisition, database searches were performed using the MASCOT search program against the *G. lamblia* database (http://tinyurl.com/37z5zqp) with a concatenated decoy database supplemented with commonly observed contaminants and the Swissprot database to increase database size. The identified hits were then loaded onto the Scaffold Viewer version 4 (Proteome Software, Portland, US) and filtered based on high stringency parameters (minimal mascot score of 95% for peptide probability, a protein probability of 95%, and a minimum of 2 unique peptides per protein (95_2_95) or on slightly relaxed stringency parameters (95_2_50). Access to raw MS data is provided through the ProteomeXchange Consortium on the PRIDE platform [30]. Data are freely retrievable using project accession number PXD003718 and project DOI 10.6019/PXD003718. Accession numbers for datasets derived from bait-specific and corresponding control co-IP MS analyses are the following: **62506**: truncated HA-tagged ORF4259 as bait and non-transfected cells as control; **62507**: HA-tagged ORF4259 and non-transfected cells as control; **62508**: HA-tagged ORFs 17304 and 21423 and non-transfected cells as control; **62509**: HA-tagged ORF102108 and non-transfected cells as control; **62510**: native coIP on HA-tagged ORF102108; **62511**: HA-tagged ORF16595 and non-transfected cells as control; **62512**: HA-tagged ORFs 15411 and 16653; **62513**: HA-tagged ORFs 14373 and 7723.

In silico co-immunoprecipitation dataset analysis

Analysis of primary structure and domain architecture of putative components of the giardial clathrin heavy chain protein network was performed using the following tools and databases: SMART (http://smart.embl-heidelberg.de/) for prediction of patterns and functional domains, pBLAST for protein homology detection (http://blast.ncbi.nlm.nih.gov/Blast.cgi?PAGE=Proteins), HHPred (http://toolkit.tuebingen.mpg.de/hhpred) for protein homology detection based on Hidden Markov Model (HMM-HMM) comparison, PSORTII (http://psort.hgc.jp/form2.html) for subcellular localization prediction, TMHMM (http://www.cbs.dtu.dk/services/TMHMM/) for transmembrane helix prediction, and the Giardia Genome Database (http://giardiadb.org/giardiadb/) to extract organism-specific information like protein expression levels, predicted molecular sizes and nucleotide/protein sequence. The *Gl*CHC co-IP dataset was filtered using a dedicated ctrl. co-IP dataset generated with non-transgenic WB parasites. Additional bait-specific co-IP datasets were compared to the average of four biological replicates of the ctrl.co-IP dataset.

Immunofluorescence analysis (IFA) and microscopy

Sample preparation for immunofluorescence based wide field and laser scanning confocal microscopic (LSCM) analysis of transgenic cell lines was done as described previously in [23, 29]. Nuclear DNA was labeled with 4',6-diamidino-2-phenylindole (DAPI). Proteins were detected with either the anti-HA antibody (clone 3F10, monoclonal antibody from Roche) or with monospecific antibodies raised against *Gl*CHC. Cells (≥100/sample) were generally imaged at maximum width, where the nuclei and the bare-zone are at maximum diameter. Huygens Professional (Scientific Volume Imaging) was used to deconvolve image stacks of optical sections. Three-dimensional reconstructions, isosurface models and fluorescence lifetime analysis, and signal overlap quantification (Mander's coefficient) in volume images of reconstructed stacks were performed using IMARIS x64 version 7.7.2 software suite (Bitplane AG).

Live-cell microscopy and fluorescence recovery after photobleaching (FRAP)

For live-cell imaging trophozoites (≥40/sample) expressing *Gl*CHC::GFP, *Gl*17304::GFP, *Gl*4259::GFP or GFP::*Gl*DRP were harvested, washed once in cold PBS before re-suspending in PBS supplemented with 5mM glucose (Cat. No. 49139, Fluka) and 0.1mM ascorbic acid (Cat. No. 95209, Fluka) at pH 7.1. FRAP and time-lapse series were performed as described previously [3, 29].

PV labelling using fluid-phase and membrane-associated markers

Fluid-phase uptake assays for *G. lamblia* and *S. vortens* were performed as described previously [3] using dextran 10,000Da coupled to either Texas Red (dextran-TxR) (Cat. No. D-1863, Thermo Fisher Scientific) or Oregon Green (dextran-OG) (Cat. No. D-7171, Thermo Fisher Scientific) fluorophores, both at 1mg/ml final concentration. Labelling of the plasma membrane was performed with cholera toxin b subunit coupled to Alexafluor 594 fluorophore (CTxb-594) (C22842, Thermo Fisher Scientific) at a final concentration of 10µg/ml [31].

Super resolution (gSTED) microscopy

Sample preparation was done as described for wide field microscopy and LSCM. For imaging, samples were mounted in ProLong Gold antifade reagent (Cat. No. P36934, Thermo Fisher Scientific). Super resolution microscopy was performed on a LSCM SP8 gSTED 3X Leica (Leica Microsystems). Nuclear labeling was omitted due to possible interference with the STED laser. Further data processing and three dimensional reconstructions of image stacks were done as described for LSCM.

DAB staining in APEX2 expressing cells

Transgenic trophozoites expressing *Gl*CHC-APEX2-2HA, *Gl*4259-APEX2-2HA or APEX2-2HA–*Gl*DRP were harvested and washed with PBS. Fixation was done in 2.5% EM grade glutaraldehyde in

cacodylate buffer (100mM cacodylate (Cat. No. 20838, Fluka), 2mM CaCl2 (Cat. No. 21097, Fluka) in PBS) for 1h at RT. Samples were washed twice before and after quenching for 5min in 20mM glycine/cacodylate buffer. For staining, the cells were resuspended in 500ul substrate solution containing 1.4mM DAB tetrahydrochloride (Cat. No. D5637, Sigma) with 0.3mM H2O2 (Cat. No. H1009, Sigma) in cacodylate buffer and incubated between 1 and 15min. To stop the reaction, samples were washed trice in cacodylate buffer and prepared as described for TEM imaging. The pcDNA3 APEX2-NES vector was a gift from Alice Ting (Addgene plasmid # 49386).

Preparation of chemically fixed, DAB stained cells

DAB stained cell suspensions were post-fixed with 1% aqueous OsO4 for 1 hour on ice, subsequently rinsed three times with pure water and dehydrated in a sequence of ethanol solutions (70% up to 100%), followed by incubation in 100% propylene oxide and embedding in Epon/Araldite (Sigma-Aldrich, Buchs, Switzerland). Samples were polymerized at 60°C for 24h. Thin sections were imaged without post-staining as well as after post-staining with aqueous uranyl acetate (2%) and Reynolds lead citrate.

Preparation of native cell suspensions by high-pressure freezing

For subsequent TEM and FIB-SEM analysis, 30µl of concentrated *Giardia lamblia* suspension was pipetted onto a carbon coated 6mm Sapphire discs (100µm thickness) set up in a special middle plate for high-pressure freezing of adherent cell cultures in an EM HPM 100 high-pressure freezing system (Leica Microsystems, Vienna, Austria). After an incubation time of 5 minutes letting the cells attach to the surface, the suspension was drawn off with a filter paper and the cells were covered with a 6mm aluminum specimen carrier wetted with 1-hexadecene and the 100µm cavity facing the cells. Finally, a 200µm-thick spacer ring (diameter 6mm) was added on top and the specimen immediately high-pressure frozen without using alcohol as synchronization fluid. Freeze-substitution was carried out in water-free acetone with 1% OsO4 for 8h at -90°C, 7h at -60°C, 5h at -30°C, 1h at 0°C, with transition gradients of 30°C per hour. Samples were rinsed twice with acetone water-free, stained with 1% uranyl acetate in acetone (stock solution: 20% in MeOH) for 1h at 4°C, rinsed twice with water-free acetone and embedded in Epon/Araldite: 66% in acetone overnight, 100% for 1h at RT and polymerized at 60°C for 20h. Thin sections were post-stained with Reynolds lead citrate.

All thin sections were imaged in a CM 100 transmission electron microscope (FEI, Eindhoven, The Netherlands) at an acceleration voltage of 80kV using a Gatan Orius 1000 CCD camera (Gatan, Munich, Germany).

For subsequent FIB-SEM tomography, an Epon/Araldite block containing *Giardia* cells was mounted on a regular SEM stub using conductive carbon and coated with 10 nm of carbon by electron beam

evaporation to render the sample conductive. Ion milling and image acquisition was performed simultaneously in an Auriga 40 Crossbeam system (Zeiss, Oberkochen, Germany) using the FIBICS Nanopatterning engine (Fibics Inc., Ottawa, Canada). A large trench was milled at a current of 20nA and 30kV, followed by fine milling at 600pA and 30kV during image acquisition with an advance of 5nm per image. Prior to starting the fine milling and imaging, a protective platinum layer of approximately 300nm was applied on top of the surface of the area of interest using the single gas injection system at the FIB-SEM. SEM images were acquired at 1.7kV (30µm aperture) using an in-lens energy selective backscattered electron detector (ESB) with a grid voltage of 1.4kV, and a dwell time of 40µs. The pixel size was set to 5nm and tilt-corrected to obtain isotropic voxels.

The final image stack was cropped to the area of interest using the ImageJ image processing package Alignment of the image stack was performed with the Sift plugin. For 3D reconstructions, organelle membranes and plasma membrane invaginations were traced manually in the interactive learning and segmentation toolkit (Ilastik) [32] and subsequently rendered in Imaris (Bitplane AG, Zurich, Switzerland).

For subsequent Cryo-SEM, a concentrated *Giardia* cell suspension was sandwiched between two interlocking gold specimen carriers (Leica Microsystems) and immediately high-pressure frozen using a EM HPM100 without alcohol as synchronization fluid. After freezing, the sandwich was mounted under liquid nitrogen on a designated specimen holder for freeze fracturing in the VCT 100 cryopreparation box and transferred onto the cold stage of a BAF 060 freeze-fracturing device using the VCT 100 cryotransfer system (Leica Microsystems). The specimen was fractured at -120°C by removing the top carrier with the hard metal knife supplied with the BAF 060 device. The specimen was heated to -105°C for 5 minutes for sublimation and coated with 2.5nm platinum/carbon by electron beam evaporation at an angle of 45° unidirectionally and with 2.5nm platinum/carbon at 45° using stage rotation (40rpm). The specimen was retracted into the transfer shuttle of the VCT 100 system and transferred under high vacuum onto the cryostage in the SEM (Auriga 40 Crossbeam system, Zeiss). Specimens were imaged at 115°C (the saturation water vapor pressure of the specimen corresponding to the vacuum in the chamber of $5x10^{-7}$mbar) and at an acceleration voltage of 5kV using the in-lens secondary electron detector.

Structural analysis using iTASSER

Ab initio prediction of hypothetical 3D models for CLC homologues and *Gl*4259 was done using i-TASSER (http://zhanglab.ccmb.med.umich.edu/I-TASSER/) [33-35]. Ten annotated CLC protein sequences were selected from several eukaryotic supergroups and each one subjected to pairwise alignment analysis with human clathrin light chain A isoform a. Modelled sequences were obtained by trimming at the variable N-terminus until the signature CLC motif was reached [36]. This resulted

in the following truncated sequences: *M. musculus* (NP_001073853.1; residues 27-218), *S. cerevisiae* (EDN61754.1; residues 35-233), *D. melanogaster* (NP_524178.2; residues 28-219), *T. gondii* (KFG44257.1; residues 109-323), *T. resei* (XP_006967655.1; residues 27-236), *C. reinhardtii* (XP_001697531.1; residues 40-228), *C. elegans* (NP_504999.1, residues 36-226), *H. sapiens* (NP_001824.1; residues 27-218), *T. cruzi* (XP_819466.1; residues 31-215), *G. lamblia* (XP_001707073.1; residues 47-283). The final structures were displayed using VMD. Superimpositions of solved structures were done using a VMD MultiSeq plugin [37] and structural similarities were expressed as Q_H values.

Results

PVs form a network of elongated organelles with morphologically distinct PV-PM interfaces

Despite extensive EM studies of the giardial endocytic system, a detailed morphological characterization of PVs and associated structures was not yet done. We showed previously that a fluid phase maker, fluorescently labeled dextran-TxR, is taken up in bulk by PVs and expelled again in a cycle of approximately 20 minutes [3, 38]. This reflects rapid and unselective uptake of large extracellular fluid volumes across the PM into PVs, calling for either direct *i.e*. membrane-to-membrane, or indirect *i.e.* vesicle-mediated fusion events involving the plasma and PV membranes. To characterize the morphology of PVs and structures at the PV – PM interface that might mediate continuity between these compartments, we applied tEM, SEM and FIB-SEM microscopy on chemically fixed or high-pressure-frozen (HPF) cells. The intact surface of freeze-fractured trophozoites reveals evenly distributed small surface indentations on the extracellular side of the PM (Fig. 1A, B). On the cytoplasmic side, PVs are clearly visible as oval or elongated tubular compartments just underneath the PM. To determine whether these surface indentations might correspond to PM-PV membrane contact sites we used TEM imaging. Thin lateral sections (70nm) revealed PM invaginations of up to ~50-70nm which were always associated with PVs, in line with earlier observations [4] (Fig. 1C-E). To define the architecture of the cortical PV organelle system in relation to the observed PM invaginations more precisely in three dimensions, we used FIB-SEM tomography of HPF-fixed trophozoites (Fig. 2A). Surface-rendered reconstructions revealed a distinctly tubular nature of the cortical organelle array which had not been appreciated before. We also noted that some organelles reached deep in the cytoplasm (Fig. 2A). Membrane tracing and subsequent surface rendering also showed that funnel-shaped PM invaginations always associated with one PV organelle, averaging one invagination/PV (Fig. 2B-F).

To address the question whether fusion events occur between the PM and PV membrane we first saturated PVs with dextran-Oregon Green and then labeled the PM with Alexafluor 594-conjugated

cholera toxin-B subunit (CTxb-594) to follow the fate of PM lipid components over time [31]. Within 40 min, the vast majority of CTxb-594 label re-located to fluorescently-labeled PVs (S1A and C Fig.). Translocation of CTxb-594 signal from the PM to PVs is consistent with the steady increase over time in Mander's coefficient of signal overlap (S1B Fig.). This is direct evidence for lipid exchange between PM – PV membranes most likely at specific contact sites, with similar dynamics to previously measured turnover of PV fluid phase content [3].

Taken together, this suggests a direct communication of the elongated endocytic organelles with the extracellular environment by way of PM-invaginations forming continuities with PV membranes. This raised questions about the molecular underpinnings of these membrane deformations and the nature of the electron-dense material at the PM-PV interfaces (Fig 1 C-E).

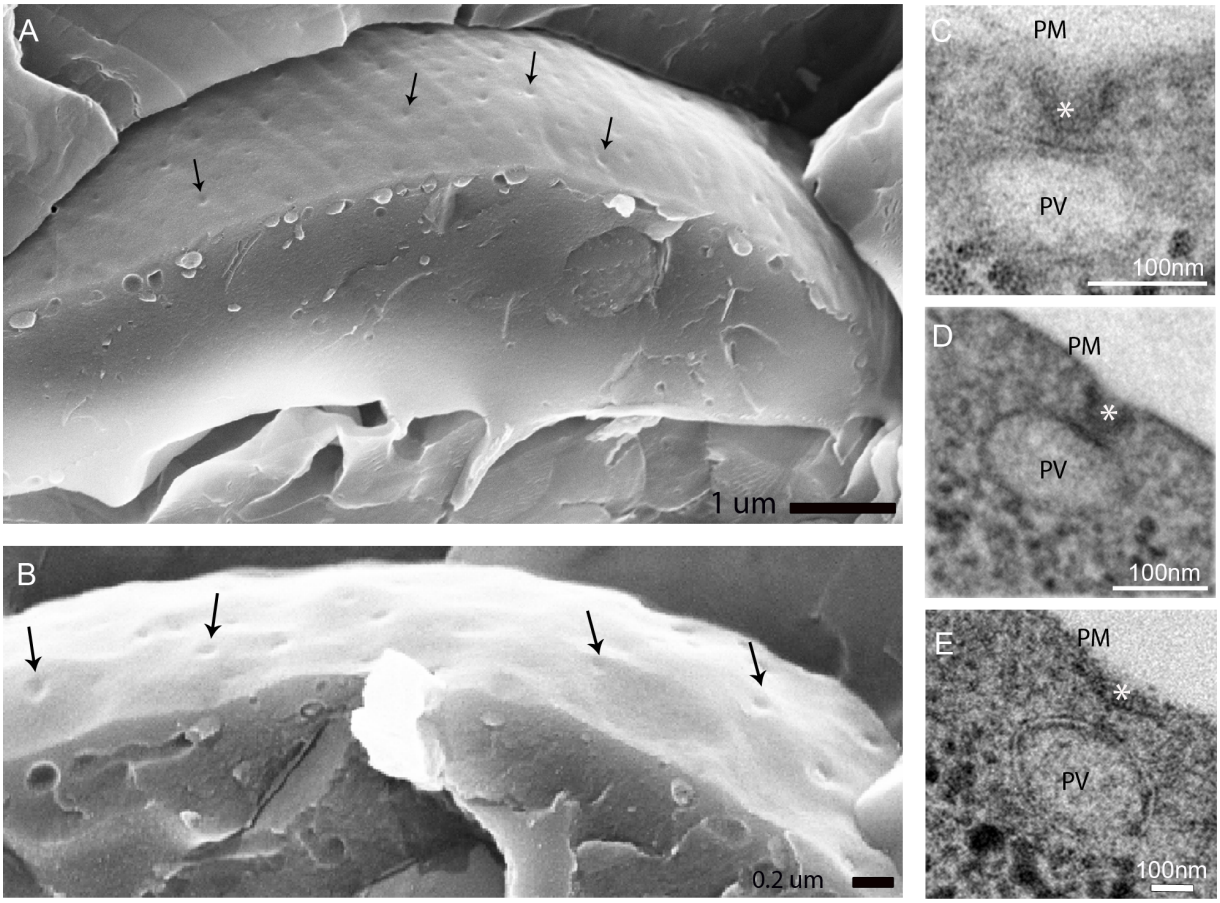

Fig.1: ***Scanning and transmission electron microscopy show PM-invaginations***

(A, B) SEM micrographs show dimples on the parasite surface (arrows). (C-E) tEM micrograph highlights of peripheral vacuole-associated plasma membrane-invaginations. PV: PV lumen; PM: plasma membrane; asterisks: invaginations.

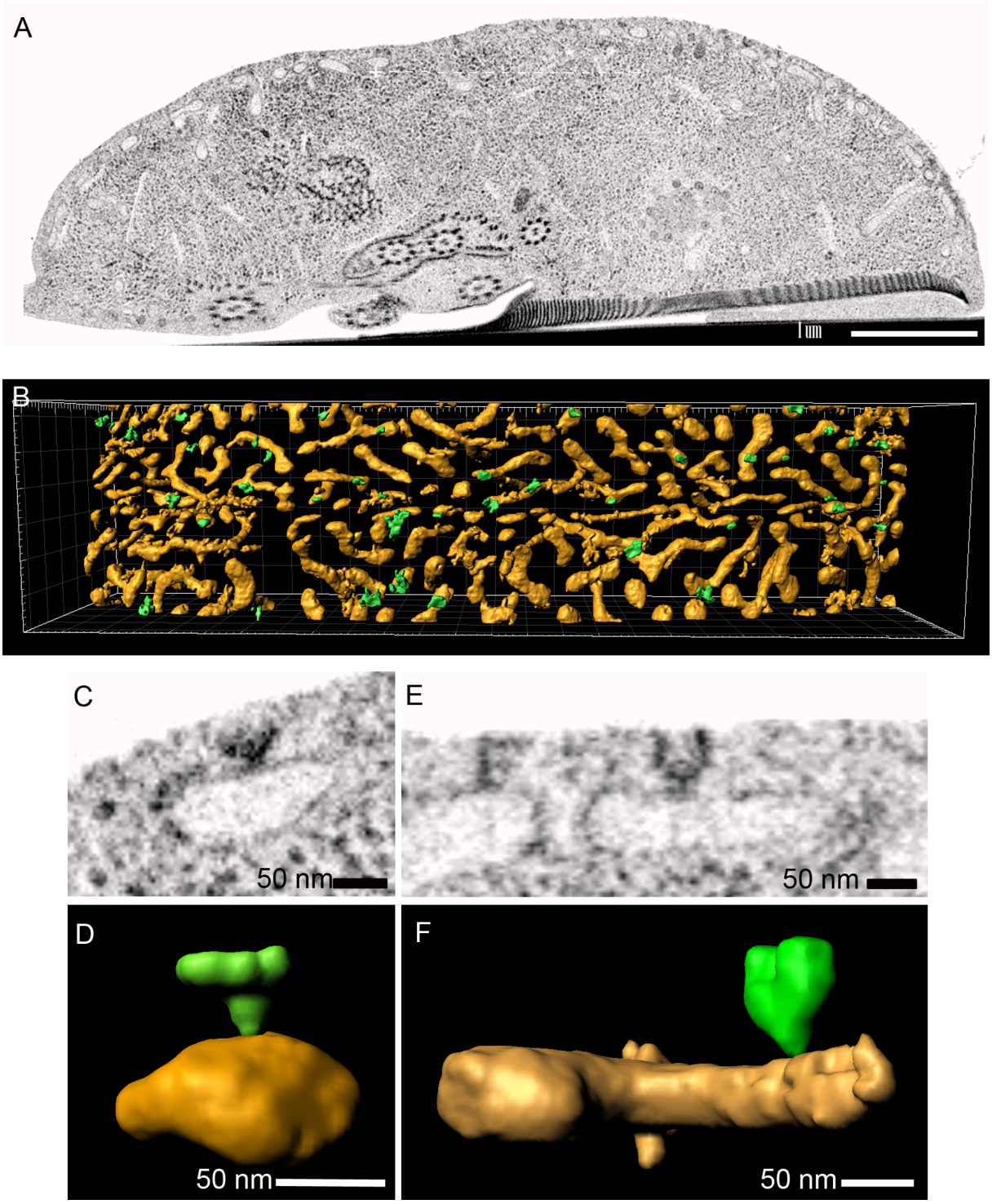

Fig.2: ***FIB-SEM based 3D rendering of PVs and PM-invaginations***

(A) Representative image of the FIB-SEM stack used for rendering in (B,D,F). (B) Dorsal view of the PV-network (yellow) with PM-associated invaginations (green). (D, F) Reconstruction of individual organelles with PM-associated invaginations as detected in FIB-SEM (C, E).

Giardia lamblia **clathrin heavy chain is organized in regularly distributed, focal assemblies at the PV-PM interface**

CCVs forming from coated pits at the PM are not detected in tEM images of *Giardia* trophozoites. Both the giardial clathrin heavy chain (*Gl*CHC) and the dynamin-related protein (*Gl*DRP) localize with significant signal overlap at punctate structures in the trophozoite cell cortex containing PVs by confocal fluorescence microscopy [3]. We investigated the nature of these small *Gl*CHC assemblies more precisely using gated STED super resolution confocal microscopy. *Gl*CHC-HA was detected in uniformly sized, small (<50nm) assemblies, which were regularly distributed in the cortical area of the cell (Fig. 3A,B). In line with the absence of CCVs in tEM, the small size and distribution of the CHC assemblies visualized by STED microscopy was not consistent with coated vesicles (average size 80-100nm [11, 39-41]). To analyze the *Gl*CHC distribution in relation to PV-organelles we imaged endocytosed dextran-TxR with *Gl*CHC::GFP in living cells using confocal microscopy. Single optical sections and three dimensional reconstructions of image stacks consistently showed localization of the *Gl*CHC::GFP signal distal to the endocytosed dextran-TxR at the PM-PV interface (PPI) (Fig. 3C-G). The localization of clathrin assemblies on a single organelle level was further specified by an ectopically expressed CHC construct tagged with APEX2, a genetically encoded enzymatic reporter for tEM [42, 43]. The *Gl*CHC::APEX2-2HA-specific signal obtained in tEM from three different labeling conditions consistently showed specific and focal localization of electron dense deposits at the PPI with each signal specifically correlated to a PV-organelle and increasing over time (Fig. 4A-C). Importantly, the experiment with the lowest exposure time (Fig. 4a) emphasized basket-like structures at the PPI, which completely bridged the ~70nm gap between the PM and the PV membranes and contacted both. Untransfected control cells exposed to the substrate for the maximal incubation time of 15 min (Fig. 4D) showed no APEX-specific labelling, only the previously observed increased electron-density at invaginated regions where the PM is in close approximation to the PV membrane (compare also with Fig. 1C-D and S3 Fig.). The subcellular distribution of the APEX2-tagged reporter in immunofluorescence assays using the anti-HA antibody was completely consistent with incorporation in clathrin assemblies (S4A-D Fig.). Taken together, the data provides evidence for the organization of CHC as distinctive assemblies that are associated with membrane invaginations akin to coated pits, but not transport vesicles. This fits with the absence of CCVs in the cell cortex by tEM, and suggests that CCVs do not occur in the giardial endocytic pathway.

Fig.3:

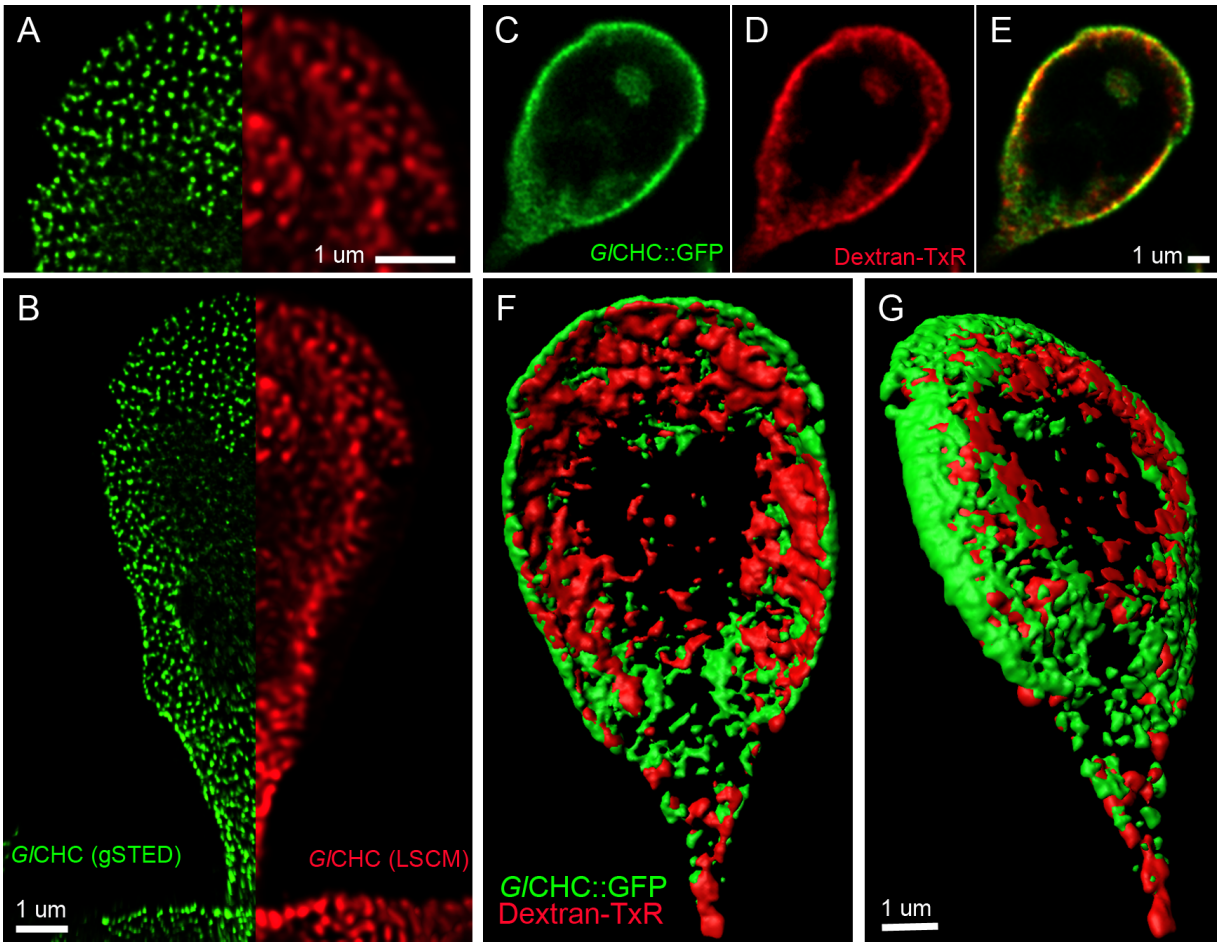
A
1 um
C
GlCHC::GFP
D
Dextran-TxR
E
1 um
B
GlCHC (gSTED)
GlCHC (LSCM)
1 um
F
GlCHC::GFP
Dextran-TxR
G
1 um

Fig.4:

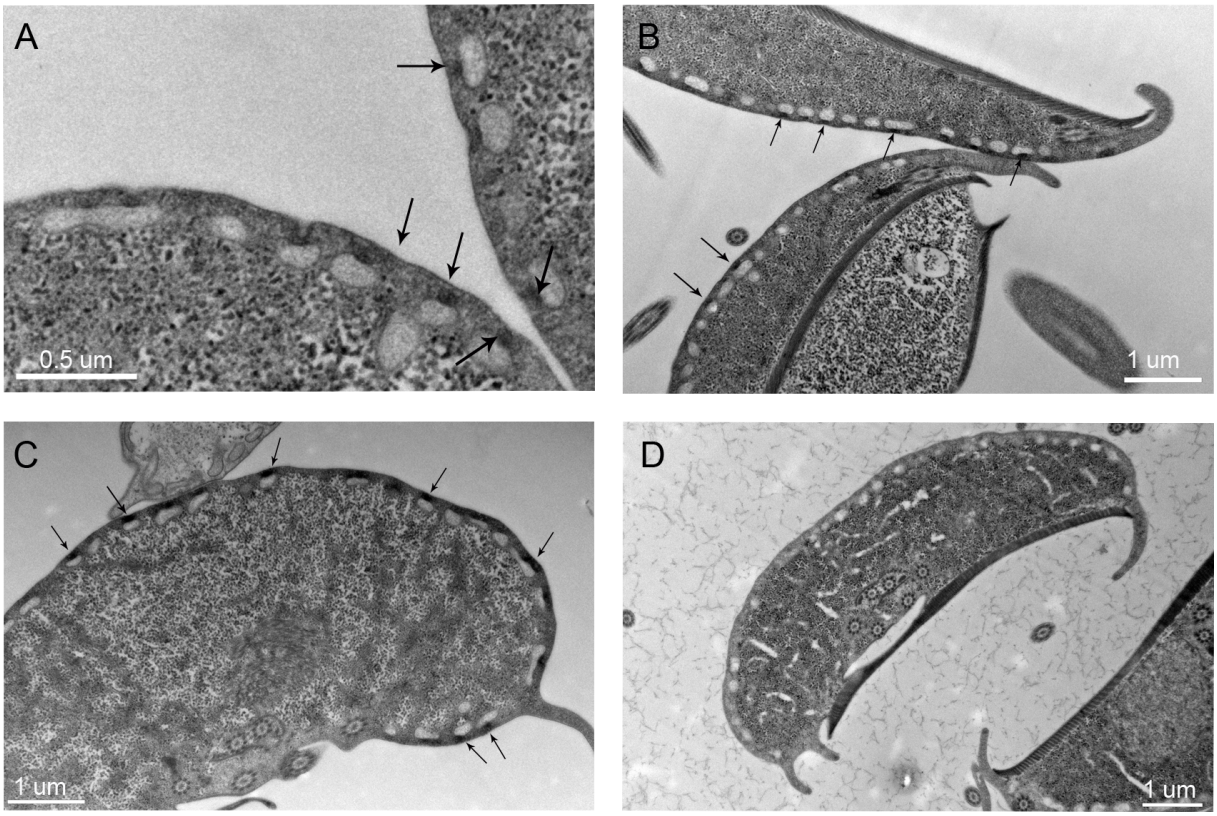
A
0.5 um
B
1 um
C
1 um
D
1 um

Fig.3: *GlCHC reporters as seen by gSTED microscopy, standard LSCM and co-labeled with dextran-TxR*

(A, B) The improved resolution of gSTED super resolution microscopy (green signal) compared to a standard LSCM signal (red signal) of the HA-tagged *Gl*CHC reporter in fixed cells indicates that *Gl*CHC assembly size is in the range of 50nm (A: inset of B). (C-E) Single optical sections of GFP-tagged *Gl*CHC-reporters (C) co-labeled with the fluid phase marker dextran-TxR (D) (E: merged images). (F, G) Surface rendering of optical sections from the cell shown in C-E shows that the *Gl*CHC-GFP reporter (green) localizes distal to the PV-marker dextran-TxR (F: ventral view, G: dorso-lateral view).

Fig.4: *Localization of the GlCHC APEX2-2HA reporter*

TEM images of *Gl*CHC-APEX2-2HA expressing cells after exposure to DAB for 1min (A), 5min (B) and 15min (C). In all conditions the signal specifically localizes to the PPI. Arrows indicate reporter-specific signals. (D) Non-transfected control cell exposed to DAB for 15min.

A *Gl*CHC reporter has no measurable turnover in focal assemblies

The absence of CCV formation at the PM suggested that *Gl*CHC assmblies might function to stabilize specialized regions of the PPI. Canonical CCVs have a lifetime of 45-80s (from emergence to fusion; [18]) and are highly dynamic, presenting constant exchange of CHC triskelia throughout all stages of CME [14]. Thus, rather than forming membrane vesicles for endocytic transport, giardial CHC assemblies might be more stable structures involved in membrane fusion events which physically connect the PV lumen to the extracellular environment, e.g. during fluid phase uptake. To address this, we quantified turnover of *Gl*CHC in assemblies at the PPI and measured the lifetime of assemblies in living cells.

We used FRAP and inverse FRAP (iFRAP) to quantify turnover of a constitutively expressed *Gl*CHC::GFP reporter which localized exclusively to clathrin assemblies in trophozoites. Selectively photo-bleached assemblies decorated with GFP in regions of interest (ROIs) did not recover any fluorescence after 220 seconds (Fig. 5A-D; ROIs 01-03). Further observations for > 10 min did not reveal any increase of the signal in the bleached area that would indicate turnover of the reporter (S4E Fig.). In line with this, iFRAP analysis of cells expressing *Gl*CHC::GFP demonstrated equal fluorescence loss over time as an unbleached control cell (Fig. 5A-D; ROIs 04 and 05).

Next, we analyzed the lifetime of individual *Gl*CHC-assemblies in cells expressing *Gl*CHC::GFP reporters by time-lapse microscopy. Resonance-scan live-cell microscopy (single focal plane imaging) was performed as 30min (60 frames) time lapse series. Statistical analysis of the spatio-temporal distribution of the *Gl*CHC::GFP signal (IMARIS spot tracking) showed that the labeled assemblies were spatially highly restricted, and that >90% had a lifetime that widely exceeded the maximal lifetime of

canonical CCVs (~3min) (Fig. 5E-H). Of note, 34 % of the GFP-labeled assemblies had a lifetime between 15 and ≥30 minutes which suggested a very high stability of the associated structures.

We asked if reduction of *Gl*CHC levels or interference with the composition of focal assemblies would alter their number or distribution. Although a single gene knockout (1 of 4 alleles) has been achieved as a proof of concept [44], *Giardia* is not amenable to complete knockouts and conditional complementation of essential genes. In addition, a *Gl*CHC knockdown using morpholinos [45] led to insufficient reduction of *Gl*CHC expression. As an alternative, we attempted to elicit a dominant-negative effect using a hub fragment (*Gl*CHC-hub, E1229 - H1871). Strong conditional over-expression of the CHC hub fragment in HeLa cells inhibits formation of coated pits and CCVs [46]. Conditional over-expression of *Gl*CHC-hub resulted in correct localization of the HA-tagged reporter to focal assemblies. However, using a specific antibody to *Gl*CHC, we could not detect any obvious changes in the number and distribution of *Gl*CHC assemblies in transgenic trophozoites (S4F Fig.)..

Taken together, the FRAP data showed no measurable turnover of the *Gl*CHC::GFP reporter in assemblies whilst fluorescence lifetime analysis demonstrated their highly static nature. This result is in line with the absence of CCVs and with a missing uncoating motif at the C-terminal end of the protein (S5 Fig.). The evidence presented so far supports a non-canonical role for *Gl*CHC in *G. lamblia*. The lack of measurable turnover in assemblies suggests a non-conventional system for recruitment of *Gl*CHC to membranes independent of endocytic stimuli.

Fig.5: ***Dynamic and lifetime analysis of the GlCHC:GFP reporter***

(A-D) FRAP and iFRAP analyses were done in the same field of view including an unbleached control cell (ROI05). FRAP analysis (ROI02, ROI03) shows no recovery whilst iFRAP analysis (ROI04) shows no loss of fluorescence after 225s, indicating no measurable turnover for the *Gl*CHC-GFP reporter. Pre-bleach (B), post-bleach t0 (C), post-bleach t220 (D). (E-H) Lifetime analysis of individual *Gl*CHC assemblies over 30min. The insets F and G show precise recognition of individual fluorescent events by the spot tracking tool in IMARIS. Clathrin assemblies are labelled in green whereas individual tracking spots are labelled in purple. (H) Analysis of 187 individual fluorescent events revealed lifetimes between 30-180s (9.65%), 210-900s (56.15) and 930-1800s (34.20%).

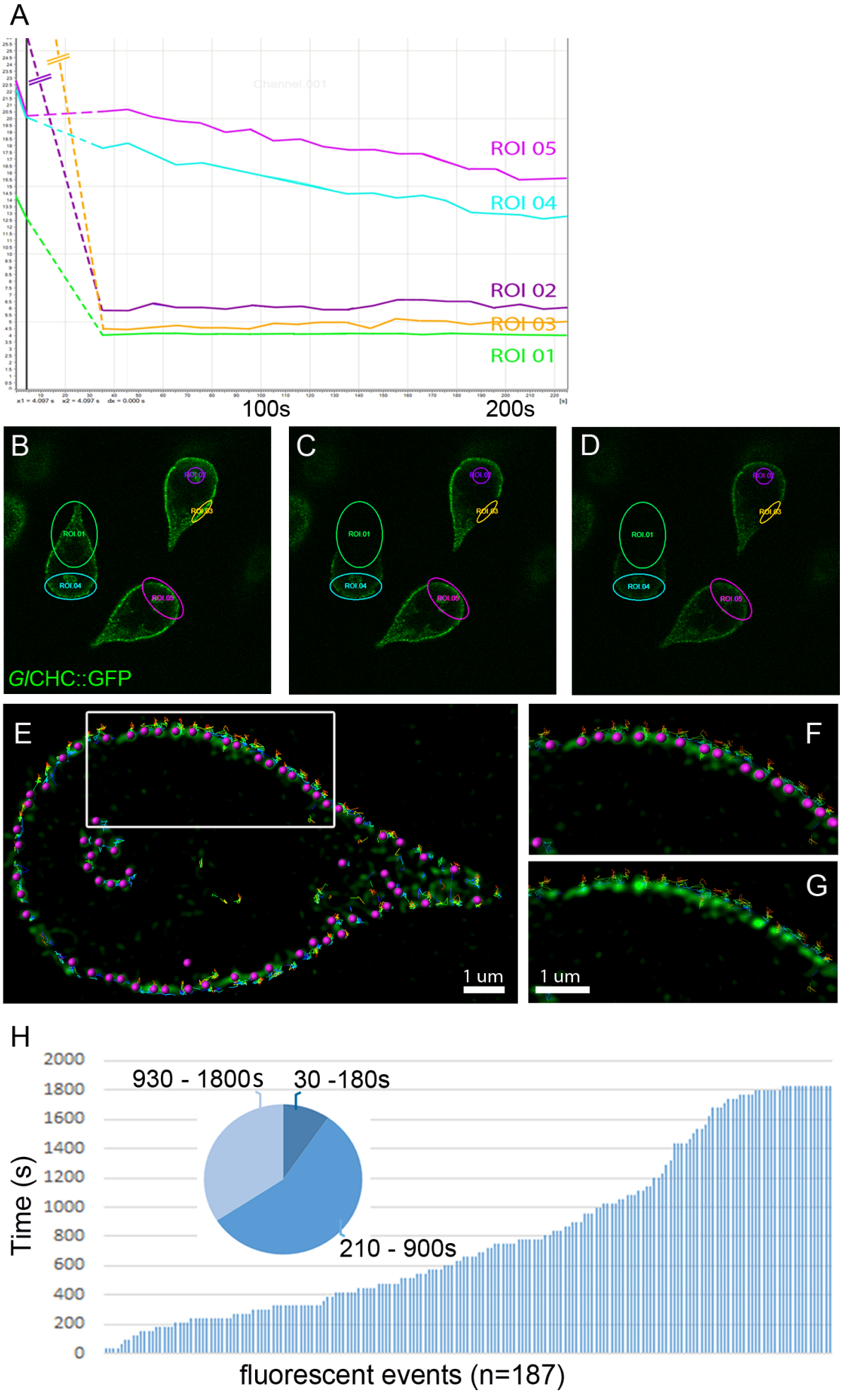
A
ROI 05
ROI 04
ROI 02
ROI 03
ROI 01
100s
200s
B
C
D
ROI.01
ROI.02
ROI.03
ROI.04
ROI.05
GlCHC::GFP
E
F
G
1 um
1 um
H
930 - 1800s
30 -180s
210 - 900s
Time (s)
2000
1800
1600
1400
1200
1000
800
600
400
200
0
fluorescent events (n=187)

Native co-IP detects a putative, highly diverged clathrin light chain

The unusual static nature of the small focal *Gl*CHC assemblies without a role in the formation of transport vesicles at the PM strongly suggest significant differences in their composition as well as in recruitment of CHC to the membrane, compared to canonical CME complexes. CCV cages or any other regular clathrin lattice structures were not observed despite extensive imaging and state-of-the-art sample preparation methods for tEM, SEM, and FIB-SEM. Consistent with the lack of turnover in assemblies (Fig. 5A-D), the *Gl*CHC C-terminus does not present the highly conserved QLMLT motif for HSC70-mediated coat disassembly (S5 Fig.) [47, 48]. The absence of a giardial HSC70 homolog and its cofactor auxillin in the genome underscore the scarcely dynamic nature of *Gl*CHC assemblies. However, genes coding for the heterotetrameric *Gl*AP2 complex and *Gl*DRP were identified in GiardiaDB (http://tinyurl.com/37z5zqp). Even taking into account the high degree of sequence divergence in *Giardia*, this is in marked contrast to other eukaryotes where 30-50 conserved proteins are involved in the formation of clathrin coats during CME [10, 11].

To dissect the composition of clathrin assemblies in trophozoites we implemented a co-IP strategy in two stages using a constitutively expressed *Gl*CHC-HA bait protein. Exclusive localization of *Gl*CHC-HA at assemblies was confirmed by IFA in transgenic trophozoites (Fig. 6A and S6 Fig.). Subcellular distribution of the reporter matched the distribution of endogenous *Gl*CHC as shown previously by us and others [3, 19, 38]. We generated LC-MS/MS datasets from co-IP experiments of a transgenic cell line expressing the *Gl*CHC-HA bait (*Gl*CHC co-IP) and an untransfected line (ctrl. co-IP) as a control for unspecific binding and physical trapping.

First, a native co-IP experiment was performed to identify the strongest *Gl*CHC interactors (Fig. 6B). We identified *Gl*4259, a protein of unknown function presenting no significant predictions for known functional domains, as the most prominent hit by far, and *Gl*5795, a protein containing a predicted leucine-rich domain. *Gl*4259's strong interaction with *Gl*CHC was reflected in matching subcellular distributions (Fig. 6C). Based on these data we hypothesized that *Gl*4259 was a highly diverged clathrin light chain (CLC). To investigate this further, we determined the subcellular localization of an epitope-tagged variant with respect to PVs. Fluorescence and electron microscopy analysis confirmed PPI-localization for HA-and APEX-tagged *Gl*4259 variants, respectively (fig. 6D-H and 6I). The combined data strongly suggested that *Gl*4259 is an integral part of *Gl*CHC assemblies. Furthermore, similar to *Gl*CHC::GFP, a *Gl*4259::GFP reporter lacks turnover in FRAP experiments (Fig. 6J-M).

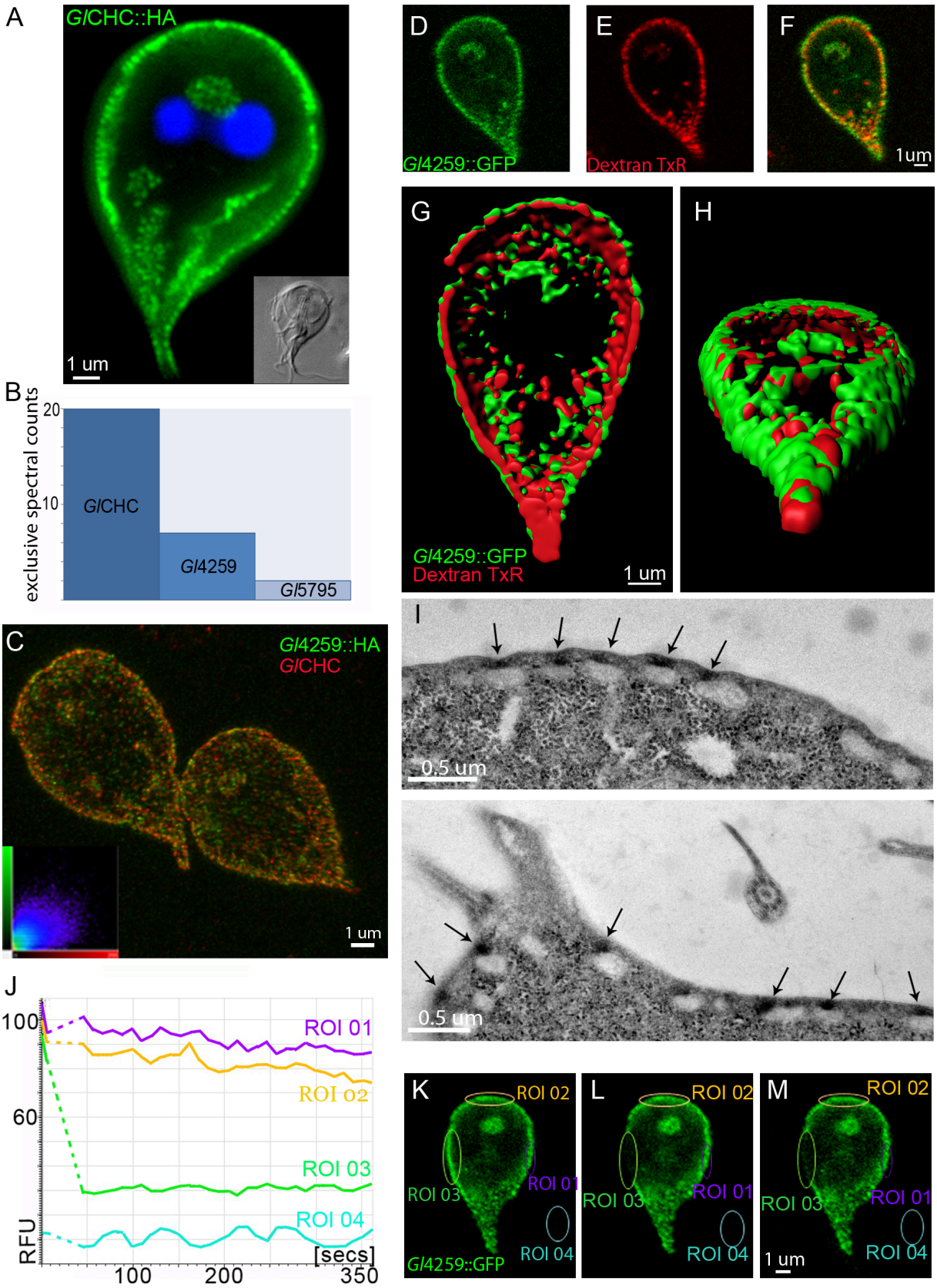
A
GlCHC::HA
1 um
B
exclusive spectral counts
20
10
GlCHC
Gl4259
Gl5795
C
Gl4259::HA
GlCHC
1 um
D
Gl4259::GFP
E
Dextran TxR
F
1um
G
Gl4259::GFP
Dextran TxR
1 um
H
I
0.5 um
0.5 um
J
100
60
RFU
100
200
350
[secs]
ROI 01
ROI 02
ROI 03
ROI 04
K
ROI 02
ROI 03
ROI 01
ROI 04
Gl4259::GFP
L
ROI 02
ROI 03
ROI 01
ROI 04
M
ROI 02
ROI 03
ROI 01
ROI 04
1 um

Fig.6: ***Proteomics and imaging-based analyses identify a putative clathrin light chain***

(A) Subcellular localization of the HA-epitope tagged *Gl*CHC reporter in the cell cortex. (B) Exclusive spectral counts for all proteins detected at high stringency parameters in a native co-IP using the *Gl*CHC-HA bait. (C) Co-labeling of HA-tagged *Gl*4259 and endogenous *Gl*CHC shows considerable signal overlap in three dimensional reconstructions of image stacks (inset: co-localization scatter plot). (D-F) Single optical sections of GFP-tagged *Gl*4259-reporters (D) co-labeled with the fluid phase marker dextran-TxR (E) (F: merge image). (G, H) Surface rendering of optical sections from the cell shown in D-F , shows a more peripheral localization of *Gl*4259-GFP (green) compared to the signal for the PV-marker dextran-TxR (red) (G: ventral view, H: caudo-dorsal view). (I) Localization of the *Gl*4259-APEX2-2HA reporter to the PPI in TEM micrographs after 5min exposure to DAB. (J-M) FRAP analysis shows no recovery in the bleached ROI03 over time indicating no measurable turnover for the *Gl*4259-GFP reporter. Pre-bleach (K), post-bleach t0 (L), post-bleach t350 (M). RFU: relative fluorescence units.

Because a solved structure of annotated full length CLC was not available, we used i-TASSER for protein structure prediction of *Gl*4259. To validate i-TASSER predictions for *Gl*4259, 9 additional annotated CLCs sequences were analyzed and compared with the models for *Gl*4259. i-TASSER provided 5 best-fit models for each sequence. For all modelled sequences, one out of five models showed protein folding into an elongated rod like structure (Fig.7A and S7 Fig.). This is in line with published structural predictions for annotated CLC [49, 50]. Additionally, we measured a considerable structural overlap (46.5% - 66.7.2%) for *Gl*4259 with the corresponding models of annotated CLC sequences (Fig. 7B, C and S7 Fig.). Functional analysis to determine if *Gl*4259 possessed CLC-like properties was based on several reports identifying either the C-terminus or a α-helical structure of the CLC middle domain to be responsible for CHC binding [50-53]. To test this we generated truncated versions of *Gl*4259 based on secondary structure analysis. A C-terminally truncated variant (L149 to K283) contained all predicted α-helices, while the N-terminally truncated variant (M1 to H148) contained none. Only the C-terminal fragment and the full-length control construct localized to CHC assemblies, whilst the N-terminal fragment was distributed throughout the cytoplasm (Fig. 7D-F). Additional analysis demonstrated protein-protein interactions between *Gl*CHC and the C-terminal fragment only (Fig. 7G). Taken together, our results demonstrate that *Gl*4259 is a very strong *Gl*CHC-interacting protein with matching localization and turnover dynamics. Together with structural and functional data this strongly supports the hypothesis that *Gl*4259 represents a highly diverged giardial CLC.

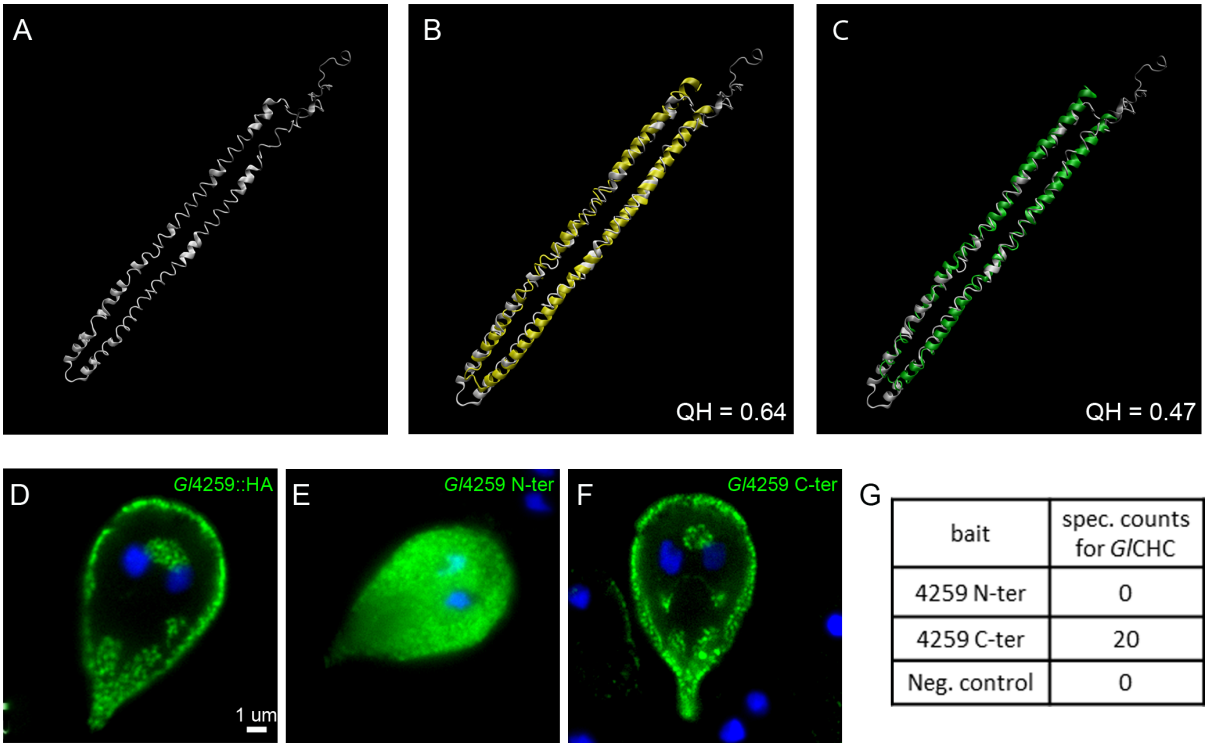

G

bait	spec. counts for *Gl*CHC
4259 N-ter	0
4259 C-ter	20
Neg. control	0

Fig.7: ***Functional and structural analysis of the putative clathrin light chain***

(A-C) iTASSER *de novo* structural predictions for *Gl*4259 (A) showing a 64% and 47% structural overlap with iTASSER predictions for *H. sapiens* (B) and *T. brucei* (C) annotated clathrin light chains, respectively. (D-F) Representative images for the subcellular distribution of epitope-tagged truncated versions of *Gl*4259. The full length HA-tagged construct for *Gl*4259 (D) distributes at the cell cortex, in contrast the N-terminally truncated variant (E) is mislocalized to the cytosol, whilst the C-terminally HA-tagged truncated variant (F) localizes similar to A. (G) Co-IP experiments using the truncated variants shown in (B) and (C) as baits reveal interaction with *Gl*CHC only for the C-terminally truncated variant.

Co-IP assays identify conserved and novel *Gl*CHC-associated proteins

*Gl*CHC and *Gl*4295 form highly stable interactions at the PPI and are likely the main structural components of clathrin focal assemblies. However, CME pathways in other eukaryotes are based on a network of weak protein-protein interactions which regulate the tightly-controlled assembly and disassembly of clathrin coat components [54]. To test whether additional proteins could be identified as components of *Gl*CHC assemblies, we used the *Gl*CHC-HA variant as bait in a co-IP protocol adapted to stabilize weak protein-protein interactions by including a chemical cross-linking step prior to cell disruption and bait pull-down [55-57]. For this study we titrated the reversible, cell-permeable, lysine-reactive crosslinker Dithiobis[succinimidyl propionate] (DSP, also known as Lamont's Reagent) to define optimal concentrations for limited cross-linking (S8 Fig.) [25-28].

Filtration of the co-IP and ctrl. co-IP datasets in Scaffold4 (http://www.proteomesoftware.com/products/) using high stringency parameters (95_2_95, FDR

0%) and manual curation revealed 36 hits exclusive to the *Gl*CHC co-IP dataset. 62 proteins were identified in both datasets, albeit with different abundance (Fig. 8A and S1 Table). We consistently detected *Gl*CHC in association to the three most important conserved endocytic factors, i.e. *Gl*DRP and the large α and β subunits of *Gl*AP2 (Fig. 8 B-K). The co-IP experiment also retrieved *Gl*4295 in addition to identifying five novel, previously non-annotated clathrin interactors. These 8 predicted interactors were epitope-tagged and IFA analysis unambiguously localized all 8 to PVs at the cell cortex (Fig. 8 B-I and S9 Fig.). To validate these protein-protein interactions (Fig. 8J) we performed reverse co-IP for each of the 8 candidate interaction partners. We defined the following stringent criteria for inclusion into the interactome model (Fig. 8K and Fig. 9M): i) exclusive detection with ≥3 spectral counts in bait-specific datasets or ii) an enrichment of peptide counts ≥3 with respect to the ctrl. co-IP dataset (S1 Table). Full lines in the interactomes represent detection with high stringency parameters (95_2_95, FDR 0% in Scaffold) and dashed lines show detection with slightly relaxed stringency (95_2_50, FDR 0 - 0.8% in Scaffold). The 8 reverse co-IP experiments confirmed strong interaction of endogenous *Gl*CHC with all other bait proteins (Fig. 8K) with the exception of *Gl*15411. This predicted metabolically inactive NEK kinase [58] appears to be associated only peripherally to assemblies and interacts with *Gl*CHC via the two large AP subunits. In contrast, α and β subunits of *Gl*AP2 are invariably associated to all other proteins in the interactome suggesting a key function in integrating the core *Gl*CHC assembly. From a phylogenetic point of view a central role for AP2 is not surprising given its hub function in clathrin networks in higher eukaryotes [54, 59]. The σ- and μ-adaptin subunits were not tagged for localization but were detected specifically in the co-IP datasets derived from *Gl*AP2 α and β subunits. This strongly suggests correct incorporation of the epitope-tagged large subunits into the heterotetrameric complex. Of note, 5 of the 8 validated *Gl*CHC-associated proteins harbor phosphoinositide-binding modules. The interaction of the AP2 protein complex with phosphatidylinositol 4,5-bisphosphate (PtdIns(4,5)P_2) at the PM is well established in many eukaryotes [54]. The novel *Gl*CHC assembly factor *Gl*16653 harbors a FYVE (Fab1, YOTB/ZK632.12, Vac1, and EEA1) domain predicted to bind to PtdIns(3)P, a membrane lipid enriched in early endosomes, on the internal vesicles of multivesicular bodies, and on the yeast vacuole [60, 61]. *Gl*16653 had been identified earlier by BLAST searches and was shown to specifically bind to PtdIns(3)P [62]. Two *Gl*CHC-interacting proteins, encoded by ORFs 7723 and 16595 contain a conserved Phox (PX) domain at the C-terminus. PX domains mediate membrane-specific targeting of more than 40 mammalian proteins including the endocytosis-associated sorting nexins (SNX) [63] and are highly specific for phosphoinositides. Consistent with the position of *Gl*CHC assemblies at the interface of PM and PV membranes and the absence of membrane interaction modules on *Gl*CHC, this data also revealed three novel proteins that potentially link *Gl*CHC to intracellular membranes in addition to *Gl*AP2.

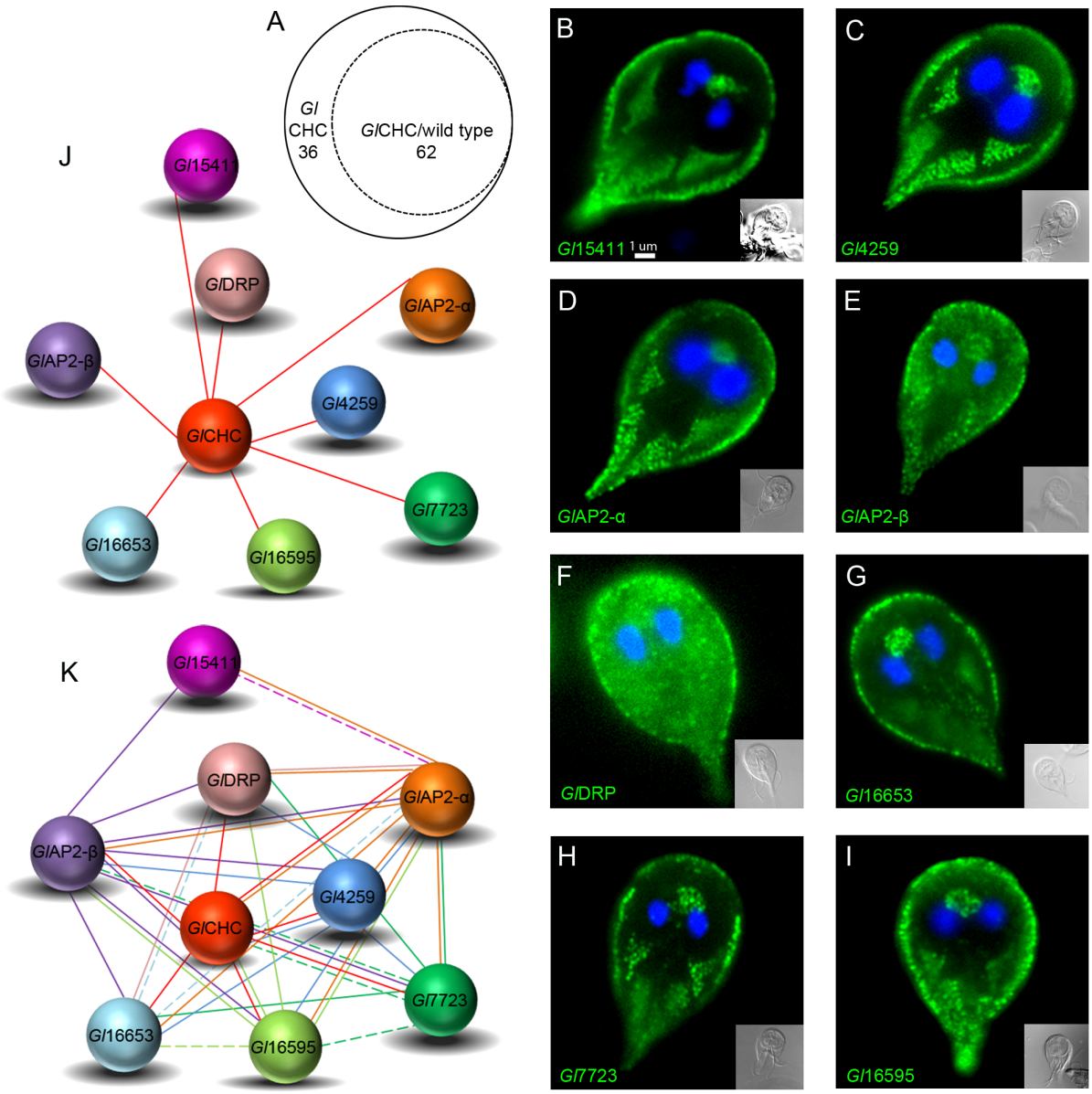

Fig.8: ***Proteomic and molecular analyses define GlCHC interacting proteins***

(A) Venn diagram indicating 36 specific hits for the *Gl*CHC derived co-IP and 62 hits present in both co-IP datasets. (B-I) IFA validation of HA-tagged candidate *Gl*CHC interacting partners: aside from *Gl*DRP (F), all proteins exhibit exclusive localization in the cell cortex. Cells were imaged at maximum width, where nuclei and the bare-zone are at maximum diameter. Representative images for HA-tagged *Gl*15411(B), *Gl*4259 (C), *Gl*α-adaptin(D), *Gl*β-adaptin(E), *Gl*16653(G), *Gl*7723(H) and *Gl*16595(I). (J) *Gl*CHC-coIP based interactome validated by subcellular localization of reporter constructs. Each *Gl*CHC-interacting protein depicted in (J) was used in reverse coIP analyses (K) to further validate the interactions. Full and dashed lines indicate high and low interaction stringency parameters, respectively.

The filtered and manually curated MS datasets from all 9 co-IPs were used to extend the *Gl*CHC interactome by detecting overlaps. The datasets of α- and β- *Gl*AP2 subunits alone yielded 12 additional proteins whose epitope tagged variants localized to the cell cortex in transgenic cells by IFA (Fig. 9 A-L). In total, the co-IP datasets yielded 32 candidate CHC assembly proteins of which 21 (65.62%) showed a corresponding subcellular distribution at the cell cortex (Fig. 6A, 8B-I, Fig. 9A-L, S1 Table). These results validate our experimental approach for detecting weak and transient protein interactions such as the ones occurring in canonical clathrin coat assemblies [54].

Taken together, data generated in a series of co-IP experiments reveal a small but highly interconnected protein network in *Gl*CHC assemblies with *Gl*AP2 subunits as central organizers and a highly stable *Gl*CHC-*Gl*4295 structural complex. Not surprisingly, α-adaptin shows the most extended interactome, compared to other tested bait proteins, as in the more complex endocytic systems of higher eukaryotes [64-67]. In addition to underscoring the central role of the conserved factors *Gl*CHC, *Gl*AP2, and *Gl*DRP within *Gl*CHC assemblies, this analysis demonstrates the presence of additional monomeric membrane adaptor proteins and interaction with potential cargo receptors.

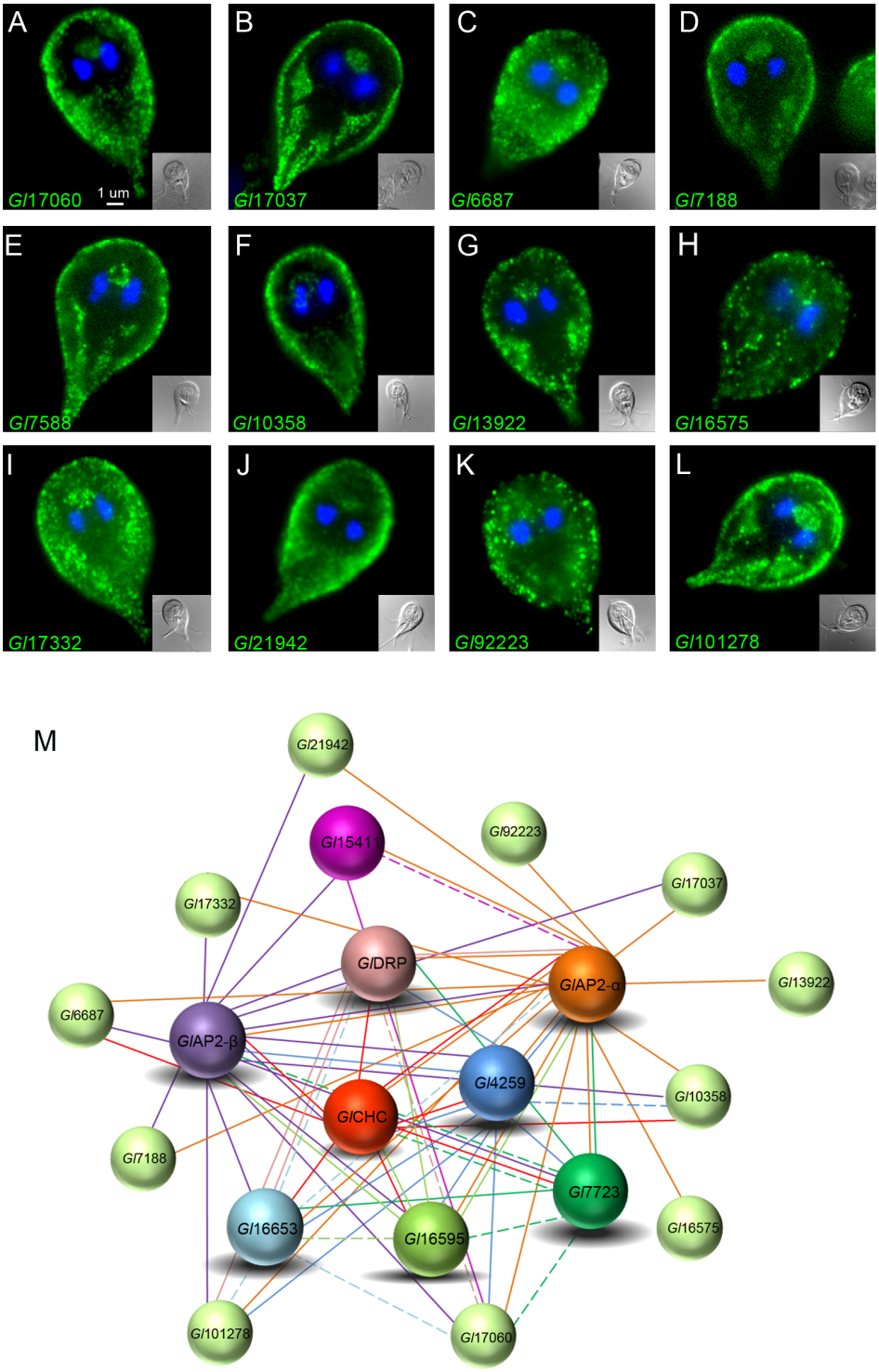

Fig.9: ***An expanded GlCHC-interactome***

(A-L) IFA validation of HA-tagged candidate proteins obtained by reverse coIP: All reporter constructs localize, in varying degrees, to the cell cortex. Aside from 9 H and K, all reporters show deposition at the barezone, an indicator of PV-associated localization. Cells were imaged at maximum width, where nuclei and the bare-zone are at maximum diameter. Representative images for HA-tagged *Gl*17060(A), *Gl*17037(B), *Gl*6687(C), *Gl*7188*(D), Gl*7588*(E), Gl*10358*(F), Gl*13922*(G), Gl*16575*(H), Gl*17332*(I), Gl*21942*(J), Gl*92223*(K) and, Gl*101278*(L). (M)* Expanded *Gl*CHC-interactome including IFA-validated HA-tagged proteins from A-L (spheres in light green). Full and dashed lines indicate high and low interaction stringency parameters, respectively.

Conserved endocytic factors *Gl*DRP and *Gl*AP2 have dynamic distributions

The static nature of giardial clathrin assemblies at the PPI is consistent with the lack of turnover of *Gl*CHC and *Gl*4295 at membranes (Fig. 5 and 6). In addition, the absence of motifs and machinery for disassembly of these structures points to an alternative, as yet unknown, mechanism for turning over of CHC assemblies. Nevertheless, the identification of the conserved components *Gl*AP2 and *Gl*DRP as interactors of *Gl*CHC and *Gl*4295 suggested that some factors of the CHC core interactome may have dynamic turnover, e.g. in a model where *Gl*CHC and *Gl*4295 constitute a static platform surrounded by mobile partners. To test this, we performed FRAP analysis of corresponding GFP fusions for both *Gl*AP2α and *Gl*DRP in transgenic cells. Identical conditions for live-cell confocal microscopy revealed rapid (≤150 sec) fluorescence recovery for both reporters (Fig.10A-H), in line with their dynamics in higher eukaryotes [64, 65]. Compared to data for *Gl*CHC and *Gl*4295 (Fig. 5a and Fig. 6h), the significant difference in turnover for GFP-tagged *Gl*AP2α and *Gl*DRP predicted a more peripheral distribution for these proteins at *Gl*CHC assemblies. Although the *Gl*DRP::APEX signal in tEM was strictly restricted to the region between the PM and the adjacent PV membrane it appeared more dispersed compared with APEX-tagged *Gl*CHC and *Gl*4295 variants (Fig.10I), which was consistent with transient recruitment of this large GTPase [64]. For as yet unknown reasons no signal for the *Gl*AP2::APEX reporter could be obtained, although this construct could be clearly detected in IFA by labelling of the HA epitope tag (S4D Fig.). However, the μ subunit of the *Gl*AP2 was previously localized at the PPI by immunoelectron microscopy [19]. Taken together, these data provide further evidence that both static and dynamic core interactome components of *Gl*CHC assemblies function in the narrow zone of the PPI.

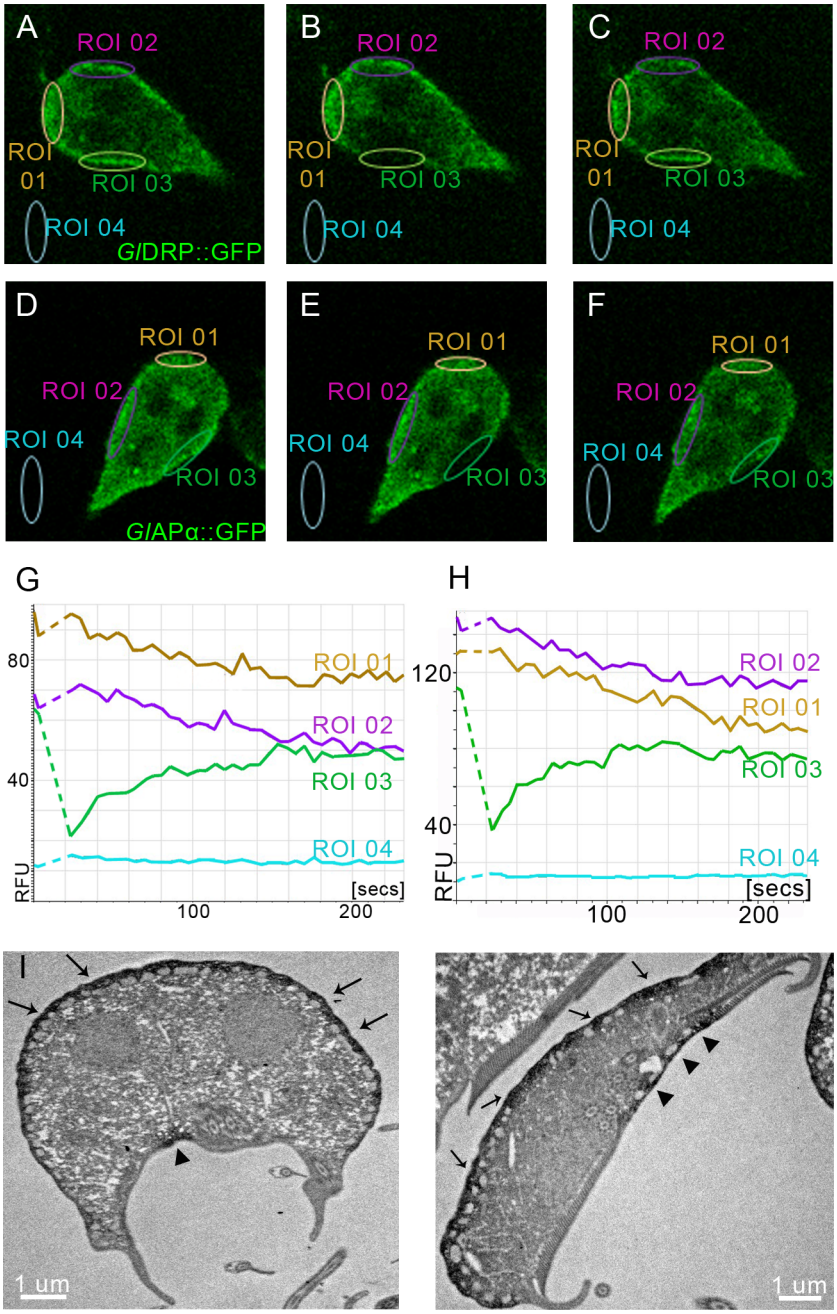

Fig.10: ***GFP-tagged GlDRP and GlAPα reporters show dynamic membrane association and the APEX2-2H-GlDRP reporter localizes in the cell cortex***

(A-C,G) FRAP analysis of *Gl*DRP::GFP shows complete recovery after 200s for the bleached ROI03. Pre-bleach (A), post-bleach t0 (B), post-bleach t220 (C). (D-F, H) FRAP analysis of a GFP-tagged reporter for *Gl*α-adaptin::GFP shows complete recovery after 200s for the bleached ROI03. Pre-bleach (D), post-bleach t0 (E), post-bleach t220 (F). RFU: relative fluorescence units. (I) Representative examples of tEM images of APEX2-2HA-*Gl*DRP expressing cells after exposure to DAB for 5min show reporter localization in the PPI (arrows and arrow-heads). Note the distinct signal in the PPI of the bare-zone (arrow-heads).

Discussion

Cell polarization and remodeling of giardial endocytic organelles

Giardia is the only diplomonad with an organelle that allows mechanical attachment to the host small intestinal epithelium to prevent expulsion by peristalsis [68]. Hence, the ventral disk with its complex cytoskeleton architecture is, in evolutionary terms, a new invention in this lineage, which resulted in a distinct dorso-ventral polarization of the parasite. Exposure of the dorsal PM to the gut lumen was likely the main driver of a subcellular reorganization of the endocytic system in close proximity with this membrane. Nevertheless, a population of PVs underlies the PM at the bare zone at the center of the ventral disk. *Spironucleus* spp., the closest relatives of *Giardia* [69], ingest fluid phase matter via a single cytostome into food vacuoles (S10 Fig.). This bulk endocytic system with a linearly organized digestive process is typical for ciliates but occurs also in other protozoa with completely different life styles (e.g. *Plasmodium*) [11, 70, 71]. Limiting endocytosis to a single protected site may be particularly advantageous for parasitic protozoa with dense surface coats that are permanently exposed to host immune effectors and/or deleterious substances. A case in point is the flagellar pocket of trypanosomes, an evolutionary adaptation that allows clathrin-mediated endocytosis in a hostile environment [72]. Although *Giardia* meets all those criteria, its endocytic organelle system is maximally dispersed, occupying all exposed sites at the PM of attached trophozoites. We hypothesized that this unique adaptive design entailed significant molecular changes in the endocytic transport machinery. Of particular interest was the function of clathrin given the extremely short distances between PVM and PM, and the absence of CCVs in tEM micrographs [73]. Consistent with this observation, the arrangement of PVs appears to be designed for rapid and efficient sampling of the extracellular space.

Giardial clathrin as a non-dynamic component of static focal assemblies

Continuous sampling of the environment by trophozoites was demonstrated previously in experiments with fluid-phase markers [3, 38]. The subcellular localization of PVs was fixed and EM micrographs consistently identified direct connections of PM and PV membranes (this study, [4]) as well as occasional direct links of both to the ER (S11 Fig.). This is consistent with previous reports of some fluid phase material being transported via PVs directly into the ER [38]. Taken together, this raises fundamental questions about the organization and molecular underpinnings of fluid phase and receptor-mediated endocytosis in *Giardia*. In the present study we focused on the function of *Gl*CHC and its interactions with other components of focal assemblies detected with a highly specific polyclonal antibody [3, 19, 38, 74]. Ectopically expressed, epitope- or GFP-tagged *Gl*CHC variants localized specifically to *Gl*CHC assemblies by fluorescence microscopy, with no indications of a

significant cytoplasmic pool. Imaging of *Gl*CHC assemblies by STED microscopy indicated a size consistent with focal assemblies (~50nm) rather than membrane coats or sheets associated with the PM or PV membranes. Typically, CCVs measure 80-150nm [11, 39-41] whereas flat clathrin sheets present on the cytosolic PM-leaflet in some mammalian cells are often >500nm in size [15, 16, 75-77]. In line with previous approaches to measure clathrin turnover during CCV formation, we quantified fluorescence recovery of photobleached *Gl*CHC::GFP or *Gl*4295::GFP reporters and measured the longevity of CHC assemblies. Membrane-associated triskelia show frequent exchange of CHC::GFP reporters in FRAP experiments with recovery times of <20s [78]. Unexpectedly, our data unequivocally showed that turnover of both reporters at assemblies in living cells was not measurable within a time frame of > 10min. Recruitment and assembly of CHC at membranes during canonical CME is highly dynamic and typical CCV lifetimes range between 30-60s [79]. FRAP based recovery values for fluorescently tagged clathrin light chains, a robust approach to study the dynamics of membrane-associated clathrin triskelia [80], are as fast as 5-10s [14] whilst the larger CHC plaques exhibit lifetimes sometimes exceeding 600s but with 50% reporter molecule turnover in in bleached areas after 115s [77]. FRAP analysis of *Gl*CHC::GFP and *Gl*4295::GFP dynamics in this study were in complete agreement and suggested high stability as well as extended lifetimes of *Gl*CHC assemblies. Taking into account that live-cell GFP-based imaging of assemblies is challenging in microaerophilic conditions, this exceeds the duration of complete CME events or the lifetimes of CHC plaques by far [77, 79, 80]. Of note, careful analysis of the tracking experiments provided no indication for a separate population of *Gl*CHC assemblies in the cytosol, e.g. coated vesicles derived from a *trans* Golgi compartment. This is consistent with the lack of a Golgi apparatus in proliferating trophozoites [8, 74] and the absence of any hits for AP1 subunits in *Gl*CHC co-IP datasets.

GFP is considerably larger than any epitope tag and may therefore affect functionality of its fusion partner(s) [81]. Transgenic *G. lamblia* cells constitutively expressing GFP fusions to *Gl*CHC, *Gl*4259, *Gl*DRP and *Gl*APα were indistinguishable from untransfected control cells and from transgenic cells expressing corresponding epitope-tagged variants (S4 A-D Fig., Figs. 5-8, 10,). Similarly, the subcellular distribution of all GFP fusion reporters was identical to the distribution of the corresponding HA-tagged variants. Specifically for *Gl*CHC, endogenous, HA and GFP -tagged variants were invariably detected in close proximity to PVs, with no indication of mislocalization for the recombinant variants. Although it is not currently feasible to test functionality by complementing *Gl*CHC knock-down (this work) or knock-out lines, these data strongly support the notion that GFP- and HA- tagged variants for *Gl*CHC, *Gl*4259, *Gl*DRP and *Gl*APα are correctly incorporated into clathrin assemblies and are likely functional.

Taken together, this is direct evidence for the highly stable nature of *Gl*CHC assemblies and strongly suggests that giardial clathrin, unlike other well-characterized homologues [72, 82-85], is not part of a dynamic process involving formation of short-lived membrane carriers for vesicular transport.

What drives and maintains clathrin recruitment to membranes in *G. lamblia*?

Formation of static focal assemblies by *Gl*CHC is in line with the observed lack of coated pits and CCVs in trophozoites. However, this raises the question how giardial clathrin is recruited to membranes. In well-described systems dynamic recruitment of clathrin triskelia to the cytoplasmic face of the PM is mediated by AP2. Specific domains of the two large subunits interact with transmembrane cargo proteins or phospholipid headgroups [86]. A recent single molecule study in BSC1 cells showed recruitment of one clathrin triskelion by 2 membrane bound AP2 complexes or 2 by 4, respectively, and demonstrated the importance of the triskelia to stabilize the initiating complexes allowing further progression of recruitment [87]. Furthermore, monomeric adapter-like stonins, GGAs or Dab2 increase the spectrum of cargo molecules that can be recognized and further stabilize association of clathrin to the PM [10]. However, with the exception of AP2, none of the common components associated with recruitment of clathrin to membranes are conserved in *Giardia*.

Interestingly, despite the longevity of *Gl*CHC assemblies, AP2α::GFP which localizes both to PM and PV membranes at PPIs (therefore to both poles of *Gl*CHC assemblies) [19] shows considerable turnover and recovery in ~160 seconds in FRAP experiments. Canonical AP2 is excluded from established membrane coats of coated pits, plaques and CCVs and acts only in zones of triskelion recruitment at the edges of clathrin coats [67, 88, 89]. Given the stability and longevity of assemblies built from tightly interconnected *Gl*CHC and *Gl*4259, the observation that these structures are not subject to ordered dismantling is contrasted by turnover of *Gl*AP2 in FRAP experiments. Taken together with the apparent lack of *Gl*CHC and *Gl*4259 cytoplasmic pools, the numerous interactions of *Gl*AP2 with other components of clathrin assemblies suggest that *Gl*AP2 acts at the edges of these long-lived structures. This hypothesis is also consistent with the identification of *Gl*AP2 and *Gl*DRP associated to *Gl*CHC only when co-IP experiments were performed in cross-linking conditions. In the absence of a recruitment and disassembly cycle we hypothesize that the role of *Gl*AP2 is geared towards stabilizing the connection between the rigid structure of the assembly proper and the flexible membranes at either end. Constant turnover of *Gl*AP2 at the edges of assemblies may contribute to mechanisms that keep these structures positioned at the PPI. Recent experiments in cell-free systems highlighted a switch function of *Gl*AP2 linked to interaction with PtdIns(4,5)P2 and transmembrane cargo proteins and the requirement for transmembrane proteins containing di-leucine ([DE]XXXL[LI]) [90] or tyrosine-based (YXXΦ) [91] endocytic motifs in their cytoplasmic C-

termini [92]. Indeed, co-IP experiments with *Gl*AP2 subunits (Fig.9) identified 2 related type Ia transmembrane proteins; ORFs *Gl*7188 (1103aa) and *Gl*13922 (1087aa), the first carrying a canonical YXXΦ motif (residues 1090-1093; Tyr-Leu-Arg-Val) in the predicted cytoplasmic tail. The presence of an endocytosis motif in *Gl*7188 suggests functional receptor-mediated endocytosis as previously demonstrated for the giardial protease ESCP [93]. However, in the absence of canonical CME in *Giardia* the exact mechanism for *Gl*7188 uptake into endocytic compartments requires further investigation. This putative receptor is part of the *Gl*AP2 interactome but is not pulled down by either *Gl*CHC or *Gl*DRP. Hence, *Gl*AP2 and associated proteins at the rims of *Gl*CHC assemblies are likely dynamic elements which recruit and organize transmembrane and cytoplasmic factors to stabilize the PPI as a whole. *Gl*AP2 cycles between a cytosolic and a membrane-bound state and likely undergoes the same conformational changes as canonical AP2 as it binds to endocytic motifs in C-termini of transmembrane proteins and to phospholipid headgroups [86]. However, maintaining the physical link between membranes and *Gl*CHC assemblies likely requires additional factors with lipid binding domains.

Phospholipid binding proteins in *Gl*CHC assemblies

Electron microscopy frequently shows deep invaginations of the PM towards PV membranes, with the membranes occasionally forming continuities. Although morphologically similar to canonical coated pits albeit smaller, these invaginations exhibit considerable membrane curvature. Interestingly, the *Gl*CHC core interactome revealed 3 proteins with predicted phosphatidylinositol binding domains. The single giardial FYVE domain protein (*Gl*16653) has confirmed PdtIns3P binding specificity [62]; two PX-domain proteins could act as monomeric adaptor proteins. However, the latter lack BAR domains and their involvement, if any, in generating membrane curvature cannot be predicted from sequence alone. In canonical systems PX-domain proteins such as sorting nexins form complexes with dynamin-2 and bind to PM-associated AP2 molecules lining developing coated pits [94]. Our data show robust interactions of these three phosphoinositide (PI)-binding proteins with the *Gl*CHC network. Further investigation is required to determine their possible involvement in selective recruitment of transmembrane proteins as shown in other systems [10, 95, 96] or a role in the morphogenesis and stabilization of *Gl*CHC assemblies. The giardial genome codes for 6 PX domain proteins. All members of this completely species-specific class of proteins localize to PVs and appear to contribute significantly to organizing PV membrane associated proteins, but only 2 are part of the extended *Gl*CHC interactome. In addition to their selective interaction with *Gl*CHC assemblies, the 6 members have PIs binding profiles with different specificities, and N-terminally tagged variants have distinct distributions at PV membranes (Zumthor, Cernikova & Hehl, in preparation).

Taken together, analysis of conserved and novel *Gl*CHC interacting partners reveals two functionally distinct groups with respect to dynamics of association with membranes: at least two highly static structural elements, *Gl*CHC and a putative light chain *Gl*4259, and dynamic components *Gl*AP2 [19] and *Gl*DRP [3] with turnovers at membranes similar to orthologues in coated pits of higher eukaryotes [64, 65]. Interestingly, the extended interactome accurately reflects this unique dichotomy and is conceptually in line with the absence of conserved disassembly factors HSC70 and auxillin [97] in *G. lamblia*. Such a striking divergence from canonical CME systems can also be appreciated in other parasitic protozoans such as *T. brucei*. CME in trypanosomes occurs in the absence of AP2 [98] and is mediated by a cohort of trypanosome-specific clathrin-associated proteins [99]. Similar to *Giardia*, trypanosomes employ a mixture of conserved and unique components to achieve a conserved function i.e. uptake from the extracellular space, using evolutionarily and molecularly distinct processes [100].

Our and previous data support a working model (Fig.11) for clathrin assemblies at the interface of PV-PM membranes, in which access to the fluid extracellular environment in the host's gut lumen, is achieved when the invaginated PM fuses with the PV. We have visualized this as replacement of fluid phase markers in the PV lumen by a combined endocytic/exocytic event [3]. Whether this phenomenon is always receptor-based and highly regulated or mainly spontaneous and stochastic remains an open question and probably depends on the nature of the cargo (membrane-associated *vs*. soluble). The most likely scenario calls for PM invaginations stabilized by *Gl*CHC-*Gl*4259 scaffolds. These are rimmed by dynamic *Gl*AP2 and linked to membranes by lipid binding proteins such as PX- and FYVE-domain proteins (akin to "frozen" clathrin coated pits). In canonical CME, coated pit formation can be driven by actin-mediated deformation of the plasma membrane [101]. Although previous reports established a link between actin and endocytosis in *Giardia* [102], our co-IP experiments did not detect any interaction between clathrin assemblies and actin.

Given the longevity of giardial clathrin assemblies we hypothesize that they are not formed *de novo* for each endocytic event but stabilize PM invaginations during multiple rounds. Successful uptake requires controlled membrane fusion at the interface of PM invaginations and PV membranes. The regulatory aspects of this process remain unclear. However, given its association to clathrin assemblies and its role in PV morphogenesis [3], the single dynamin in *Giardia* may be a key enzyme in membrane remodeling processes. Thus, the dispersion of the endocytic system with a large number of independently regulated points of entry allowing direct communication with the extracellular space may be an ideal strategy for *Giardia* trophozoites to thrive in the changing environment of the small intestine. The PV system under the protective layer of the giardial surface coat could act as a safety lock, allowing mostly unselective entry of fluid phase material for digestion and selective further endocytic transport to the ER lumen [38]. At the same time indigestible or

potentially harmful substances could be contained safely within PVs until elimination in the next round of “kiss and flush”.

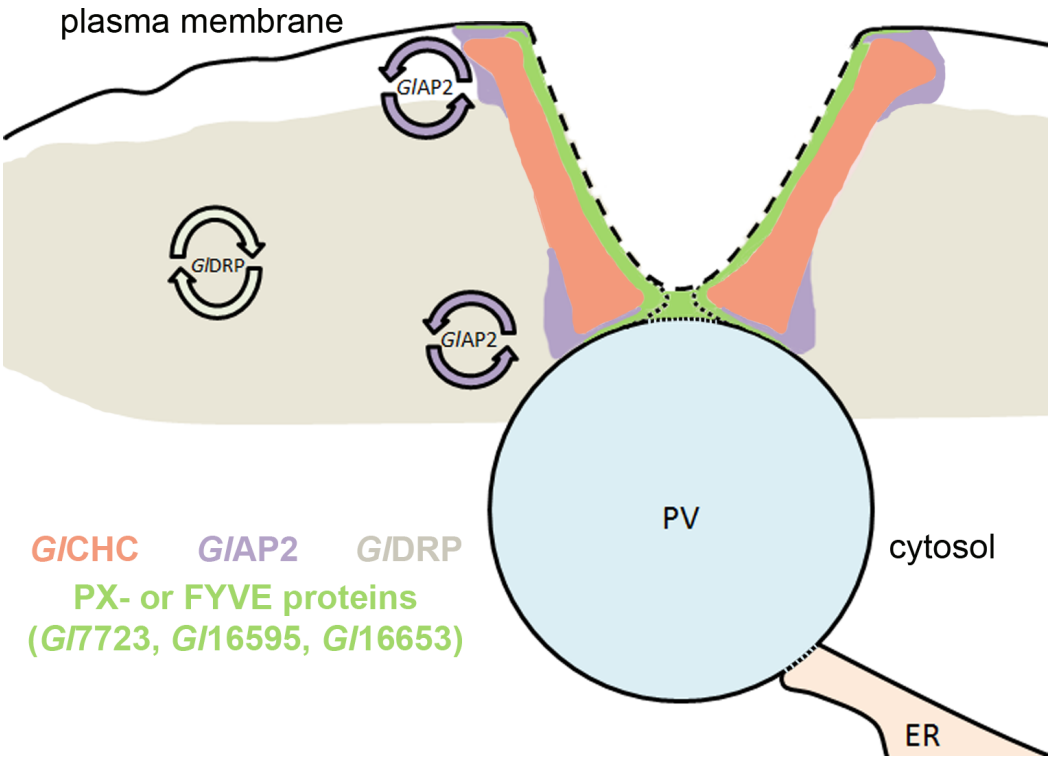

Fig.11: ***A working model for the organization of clathrin and associated proteins at the PPI***
The model shows a cross section through the PPI including a PV organelle and the PM. For endocytic uptake, PM invaginations fuse with PV membranes to create luminal continuity with the extracellular environment. This is the most likely explanation for bulk uptake of fluid phase markers and occasional direct transport to the ER [3, 38]. After uptake, membranes are separated whilst clathrin assemblies remain at the PPI. The distribution of relevant proteins is based on experimental data and functional properties [19]. Dashed lines indicate where membrane remodeling may occur. Circular arrows designate dynamic protein properties.

Acknowledgements

We thank Therese Michel for technical support. We also thank Drs Jana Döhner and Moritz Kirschmann of the Center for Microscopy and Image Analysis-Zürich and Dr. Peter Hunziker and his team at the Functional Genomics Center-Zürich. Dr. Alex Paredez is acknowledged for helpful discussions and technical support. Ásgeir Ástvaldsson and Prof. Staffan Svärd are acknowledged for helpful technical discussions and for sharing *S. vortens* cultures.

Bibliography

1. Heyworth, M.F., *Immunological aspects of Giardia infections.* Parasite, 2014. **21**: p. 55.

2. Tumova, P., J. Kulda, and E. Nohynkova, *Cell division of Giardia intestinalis: assembly and disassembly of the adhesive disc, and the cytokinesis.* Cell motility and the cytoskeleton, 2007. **64**(4): p. 288-98.
3. Gaechter, V., et al., *The single dynamin family protein in the primitive protozoan Giardia lamblia is essential for stage conversion and endocytic transport.* Traffic, 2008. **9**(1): p. 57-71.
4. Lanfredi-Rangel, A., et al., *The peripheral vesicles of trophozoites of the primitive protozoan Giardia lamblia may correspond to early and late endosomes and to lysosomes.* Journal of structural biology, 1998. **123**(3): p. 225-35.
5. Ringqvist, E., et al., *Release of metabolic enzymes by Giardia in response to interaction with intestinal epithelial cells.* Molecular and biochemical parasitology, 2008. **159**(2): p. 85-91.
6. McCaffery, J.M., G.M. Faubert, and F.D. Gillin, *Giardia lamblia: traffic of a trophozoite variant surface protein and a major cyst wall epitope during growth, encystation, and antigenic switching.* Experimental parasitology, 1994. **79**(3): p. 236-49.
7. Slavin, I., et al., *Dephosphorylation of cyst wall proteins by a secreted lysosomal acid phosphatase is essential for excystation of Giardia lamblia.* Molecular and biochemical parasitology, 2002. **122**(1): p. 95-8.
8. Marti, M., et al., *The secretory apparatus of an ancient eukaryote: protein sorting to separate export pathways occurs before formation of transient Golgi-like compartments.* Molecular biology of the cell, 2003. **14**(4): p. 1433-47.
9. Ward, W., et al., *A primitive enzyme for a primitive cell: the protease required for excystation of Giardia.* Cell, 1997. **89**(3): p. 437-44.
10. Robinson, M.S., *Forty Years of Clathrin-coated Vesicles.* Traffic, 2015. **16**(12): p. 1210-38.
11. McMahon, H.T. and E. Boucrot, *Molecular mechanism and physiological functions of clathrin-mediated endocytosis.* Nature reviews. Molecular cell biology, 2011. **12**(8): p. 517-33.
12. Heuser, J. and T. Kirchhausen, *Deep-etch views of clathrin assemblies.* Journal of ultrastructure research, 1985. **92**(1-2): p. 1-27.
13. Heymann, J.B., et al., *Visualization of the binding of Hsc70 ATPase to clathrin baskets: implications for an uncoating mechanism.* The Journal of biological chemistry, 2005. **280**(8): p. 7156-61.
14. Avinoam, O., et al., *ENDOCYTOSIS. Endocytic sites mature by continuous bending and remodeling of the clathrin coat.* Science, 2015. **348**(6241): p. 1369-72.
15. Heuser, J., *Three-dimensional visualization of coated vesicle formation in fibroblasts.* The Journal of cell biology, 1980. **84**(3): p. 560-83.
16. Sanan, D.A. and R.G. Anderson, *Simultaneous visualization of LDL receptor distribution and clathrin lattices on membranes torn from the upper surface of cultured cells.* The journal of

histochemistry and cytochemistry : official journal of the Histochemistry Society, 1991. **39**(8): p. 1017-24.

17. Aggeler, J. and Z. Werb, *Initial events during phagocytosis by macrophages viewed from outside and inside the cell: membrane-particle interactions and clathrin.* The Journal of cell biology, 1982. **94**(3): p. 613-23.
18. Kirchhausen, T., D. Owen, and S.C. Harrison, *Molecular structure, function, and dynamics of clathrin-mediated membrane traffic.* Cold Spring Harbor perspectives in biology, 2014. **6**(5): p. a016725.
19. Rivero, M.R., et al., *Adaptor protein 2 regulates receptor-mediated endocytosis and cyst formation in Giardia lamblia.* The Biochemical journal, 2010. **428**(1): p. 33-45.
20. Hehl, A.B., M. Marti, and P. Kohler, *Stage-specific expression and targeting of cyst wall protein-green fluorescent protein chimeras in Giardia.* Molecular biology of the cell, 2000. **11**(5): p. 1789-800.
21. Boucher, S.E. and F.D. Gillin, *Excystation of in vitro-derived Giardia lamblia cysts.* Infection and immunity, 1990. **58**(11): p. 3516-22.
22. Morf, L., et al., *The transcriptional response to encystation stimuli in Giardia lamblia is restricted to a small set of genes.* Eukaryotic cell, 2010. **9**(10): p. 1566-76.
23. Stefanic, S., et al., *Neogenesis and maturation of transient Golgi-like cisternae in a simple eukaryote.* Journal of cell science, 2009. **122**(Pt 16): p. 2846-56.
24. Jimenez-Garcia, L.F., et al., *Identification of nucleoli in the early branching protist Giardia duodenalis.* International journal for parasitology, 2008. **38**(11): p. 1297-304.
25. Zhang, L., et al., *Successful co-immunoprecipitation of Oct4 and Nanog using cross-linking.* Biochemical and biophysical research communications, 2007. **361**(3): p. 611-4.
26. Salazar, G., et al., *Hermansky-Pudlak syndrome protein complexes associate with phosphatidylinositol 4-kinase type II alpha in neuronal and non-neuronal cells.* The Journal of biological chemistry, 2009. **284**(3): p. 1790-802.
27. Humphries, J.D., et al., *Proteomic analysis of integrin-associated complexes identifies RCC2 as a dual regulator of Rac1 and Arf6.* Science signaling, 2009. **2**(87): p. ra51.
28. Smith, A.L., et al., *ReCLIP (reversible cross-link immuno-precipitation): an efficient method for interrogation of labile protein complexes.* PloS one, 2011. **6**(1): p. e16206.
29. Konrad, C., C. Spycher, and A.B. Hehl, *Selective condensation drives partitioning and sequential secretion of cyst wall proteins in differentiating Giardia lamblia.* PLoS pathogens, 2010. **6**(4): p. e1000835.
30. Vizcaino, J.A., et al., *2016 update of the PRIDE database and its related tools.* Nucleic Acids Res, 2016. **44**(D1): p. D447-56.

31. Stefanic, S., et al., *Glucosylceramide synthesis inhibition affects cell cycle progression, membrane trafficking, and stage differentiation in Giardia lamblia.* Journal of lipid research, 2010. **51**(9): p. 2527-45.

32. Sommer, C.S., C.; Koethe, U. & Fred, A. *Ilastik: Interactive Learning and Segmentation Toolkit.* 2011.

33. Roy, A., A. Kucukural, and Y. Zhang, *I-TASSER: a unified platform for automated protein structure and function prediction.* Nature protocols, 2010. **5**(4): p. 725-38.

34. Yang, J., et al., *The I-TASSER Suite: protein structure and function prediction.* Nature methods, 2015. **12**(1): p. 7-8.

35. Zhang, Y., *I-TASSER server for protein 3D structure prediction.* BMC bioinformatics, 2008. **9**: p. 40.

36. Jackson, A.P. and P. Parham, *Structure of human clathrin light chains. Conservation of light chain polymorphism in three mammalian species.* The Journal of biological chemistry, 1988. **263**(32): p. 16688-95.

37. Roberts, E., et al., *MultiSeq: unifying sequence and structure data for evolutionary analysis.* BMC Bioinformatics, 2006. **7**: p. 382.

38. Abodeely, M., et al., *A contiguous compartment functions as endoplasmic reticulum and endosome/lysosome in Giardia lamblia.* Eukaryotic cell, 2009. **8**(11): p. 1665-76.

39. Doray, B., et al., *Cooperation of GGAs and AP-1 in packaging MPRs at the trans-Golgi network.* Science, 2002. **297**(5587): p. 1700-3.

40. Geuze, H.J., et al., *Possible pathways for lysosomal enzyme delivery.* J Cell Biol, 1985. **101**(6): p. 2253-62.

41. Klumperman, J., et al., *Differences in the endosomal distributions of the two mannose 6-phosphate receptors.* J Cell Biol, 1993. **121**(5): p. 997-1010.

42. Martell, J.D., et al., *Engineered ascorbate peroxidase as a genetically encoded reporter for electron microscopy.* Nature biotechnology, 2012. **30**(11): p. 1143-8.

43. Lam, S.S., et al., *Directed evolution of APEX2 for electron microscopy and proximity labeling.* Nature methods, 2015. **12**(1): p. 51-4.

44. Wampfler, P.B., C. Faso, and A.B. Hehl, *The Cre/loxP system in Giardia lamblia: genetic manipulations in a binucleate tetraploid protozoan.* Int J Parasitol, 2014. **44**(8): p. 497-506.

45. Carpenter, M.L. and W.Z. Cande, *Using morpholinos for gene knockdown in Giardia intestinalis.* Eukaryot Cell, 2009. **8**(6): p. 916-9.

46. Liu, S.H., M.S. Marks, and F.M. Brodsky, *A dominant-negative clathrin mutant differentially affects trafficking of molecules with distinct sorting motifs in the class II major histocompatibility complex (MHC) pathway.* J Cell Biol, 1998. **140**(5): p. 1023-37.

47. Rapoport, I., et al., *A motif in the clathrin heavy chain required for the Hsc70/auxilin uncoating reaction.* Molecular biology of the cell, 2008. **19**(1): p. 405-13.

48. Bocking, T., et al., *Single-molecule analysis of a molecular disassemblase reveals the mechanism of Hsc70-driven clathrin uncoating.* Nature structural & molecular biology, 2011. **18**(3): p. 295-301.

49. Fotin, A., et al., *Molecular model for a complete clathrin lattice from electron cryomicroscopy.* Nature, 2004. **432**(7017): p. 573-9.

50. Chen, C.Y., et al., *Clathrin light and heavy chain interface: alpha-helix binding superhelix loops via critical tryptophans.* The EMBO journal, 2002. **21**(22): p. 6072-82.

51. Pishvaee, B., A. Munn, and G.S. Payne, *A novel structural model for regulation of clathrin function.* The EMBO journal, 1997. **16**(9): p. 2227-39.

52. Wang, J., Y. Wang, and T.J. O'Halloran, *Clathrin light chain: importance of the conserved carboxy terminal domain to function in living cells.* Traffic, 2006. **7**(7): p. 824-32.

53. Ybe, J.A., et al., *Contribution of cysteines to clathrin trimerization domain stability and mapping of light chain binding.* Traffic, 2003. **4**(12): p. 850-6.

54. Schmid, E.M. and H.T. McMahon, *Integrating molecular and network biology to decode endocytosis.* Nature, 2007. **448**(7156): p. 883-8.

55. Studdert, C.A. and J.S. Parkinson, *In vivo crosslinking methods for analyzing the assembly and architecture of chemoreceptor arrays.* Methods in enzymology, 2007. **423**: p. 414-31.

56. Vretou, E., et al., *Identification and characterization of Inc766, an inclusion membrane protein in Chlamydophila abortus-infected cells.* Microbial pathogenesis, 2008. **45**(4): p. 265-72.

57. Zhou, M., et al., *Real-time measurements of kinetics of EGF binding to soluble EGF receptor monomers and dimers support the dimerization model for receptor activation.* Biochemistry, 1993. **32**(32): p. 8193-8.

58. Manning, G., et al., *The minimal kinome of Giardia lamblia illuminates early kinase evolution and unique parasite biology.* Genome biology, 2011. **12**(7): p. R66.

59. Traub, L.M., *Tickets to ride: selecting cargo for clathrin-regulated internalization.* Nature reviews. Molecular cell biology, 2009. **10**(9): p. 583-96.

60. Gillooly, D.J., et al., *Localization of phosphatidylinositol 3-phosphate in yeast and mammalian cells.* The EMBO journal, 2000. **19**(17): p. 4577-88.

61. Stenmark, H. and R. Aasland, *FYVE-finger proteins--effectors of an inositol lipid.* Journal of cell science, 1999. **112 (Pt 23)**: p. 4175-83.

62. Sinha, A., et al., *Identification and characterization of a FYVE domain from the early diverging eukaryote Giardia lamblia.* Current microbiology, 2011. **62**(4): p. 1179-84.

63. Seet, L.F. and W. Hong, *The Phox (PX) domain proteins and membrane traffic.* Biochimica et biophysica acta, 2006. **1761**(8): p. 878-96.

64. Aguet, F., et al., *Advances in analysis of low signal-to-noise images link dynamin and AP2 to the functions of an endocytic checkpoint.* Developmental cell, 2013. **26**(3): p. 279-91.

65. Motley, A.M., et al., *Functional analysis of AP-2 alpha and mu2 subunits.* Molecular biology of the cell, 2006. **17**(12): p. 5298-308.

66. Mishra, S.K., et al., *Dual engagement regulation of protein interactions with the AP-2 adaptor alpha appendage.* The Journal of biological chemistry, 2004. **279**(44): p. 46191-203.

67. Praefcke, G.J., et al., *Evolving nature of the AP2 alpha-appendage hub during clathrin-coated vesicle endocytosis.* The EMBO journal, 2004. **23**(22): p. 4371-83.

68. Holberton, D.V., *Mechanism of attachment of Giardia to the wall of the small intestine.* Trans R Soc Trop Med Hyg, 1973. **67**(1): p. 29-30.

69. Xu, F., et al., *The genome of Spironucleus salmonicida highlights a fish pathogen adapted to fluctuating environments.* PLoS Genet, 2014. **10**(2): p. e1004053.

70. Elliott, D.A., et al., *Four distinct pathways of hemoglobin uptake in the malaria parasite Plasmodium falciparum.* Proceedings of the National Academy of Sciences of the United States of America, 2008. **105**(7): p. 2463-8.

71. Lazarus, M.D., T.G. Schneider, and T.F. Taraschi, *A new model for hemoglobin ingestion and transport by the human malaria parasite Plasmodium falciparum.* Journal of cell science, 2008. **121**(11): p. 1937-49.

72. Allen, C.L., D. Goulding, and M.C. Field, *Clathrin-mediated endocytosis is essential in Trypanosoma brucei.* The EMBO journal, 2003. **22**(19): p. 4991-5002.

73. Touz, M.C., et al., *Lysosomal protein trafficking in Giardia lamblia: common and distinct features.* Frontiers in bioscience, 2012. **4**: p. 1898-909.

74. Marti, M., et al., *An ancestral secretory apparatus in the protozoan parasite Giardia intestinalis.* The Journal of biological chemistry, 2003. **278**(27): p. 24837-48.

75. Maupin, P. and T.D. Pollard, *Improved preservation and staining of HeLa cell actin filaments, clathrin-coated membranes, and other cytoplasmic structures by tannic acid-glutaraldehyde-saponin fixation.* The Journal of cell biology, 1983. **96**(1): p. 51-62.

76. Miller, K., et al., *Transferrin receptors promote the formation of clathrin lattices.* Cell, 1991. **65**(4): p. 621-32.

77. Grove, J., et al., *Flat clathrin lattices: stable features of the plasma membrane.* Molecular biology of the cell, 2014. **25**(22): p. 3581-94.

78. Loerke, D., et al., *Differential control of clathrin subunit dynamics measured with EW-FRAP microscopy.* Traffic, 2005. **6**(10): p. 918-29.

79. Kirchhausen, T., *Imaging endocytic clathrin structures in living cells.* Trends in cell biology, 2009. **19**(11): p. 596-605.

80. Hoffmann, A., et al., *A comparison of GFP-tagged clathrin light chains with fluorochromated light chains in vivo and in vitro.* Traffic, 2010. **11**(9): p. 1129-40.

81. Rappoport, J.Z. and S.M. Simon, *A functional GFP fusion for imaging clathrin-mediated endocytosis.* Traffic, 2008. **9**(8): p. 1250-5.

82. Agarwal, S., et al., *Clathrin-mediated hemoglobin endocytosis is essential for survival of Leishmania.* Biochimica et biophysica acta, 2013. **1833**(5): p. 1065-77.

83. Elde, N.C., et al., *Elucidation of clathrin-mediated endocytosis in tetrahymena reveals an evolutionarily convergent recruitment of dynamin.* PLoS Genet, 2005. **1**(5): p. e52.

84. Kalb, L.C., et al., *Clathrin expression in Trypanosoma cruzi.* BMC Cell Biol, 2014. **15**: p. 23.

85. Corrêa, J.R., et al., *Clathrin in Trypanosoma cruzi: in silico gene identification, isolation, and localization of protein expression sites.* J Eukaryot Microbiol, 2007. **54**(3): p. 297-302.

86. Popova, N.V., I.E. Deyev, and A.G. Petrenko, *Clathrin-mediated endocytosis and adaptor proteins.* Acta Naturae, 2013. **5**(3): p. 62-73.

87. Cocucci, E., et al., *The first five seconds in the life of a clathrin-coated pit.* Cell, 2012. **150**(3): p. 495-507.

88. Saffarian, S. and T. Kirchhausen, *Differential evanescence nanometry: live-cell fluorescence measurements with 10-nm axial resolution on the plasma membrane.* Biophysical journal, 2008. **94**(6): p. 2333-42.

89. Cheng, Y., et al., *Cryo-electron tomography of clathrin-coated vesicles: structural implications for coat assembly.* Journal of molecular biology, 2007. **365**(3): p. 892-9.

90. Hofmann, M.W., et al., *The leucine-based sorting motifs in the cytoplasmic domain of the invariant chain are recognized by the clathrin adaptors AP1 and AP2 and their medium chains.* J Biol Chem, 1999. **274**(51): p. 36153-8.

91. Ohno, H., et al., *Interaction of tyrosine-based sorting signals with clathrin-associated proteins.* Science, 1995. **269**(5232): p. 1872-5.

92. Kelly, B.T., et al., *Clathrin adaptors. AP2 controls clathrin polymerization with a membrane-activated switch.* Science, 2014. **345**(6195): p. 459-63.

93. Touz, M.C., et al., *Sorting of encystation-specific cysteine protease to lysosome-like peripheral vacuoles in Giardia lamblia requires a conserved tyrosine-based motif.* The Journal of biological chemistry, 2003. **278**(8): p. 6420-6.

94. Rangarajan, E.S., et al., *Mechanism of aldolase control of sorting nexin 9 function in endocytosis.* J Biol Chem, 2010. **285**(16): p. 11983-90.

95. Mishra, S.K., et al., *Disabled-2 exhibits the properties of a cargo-selective endocytic clathrin adaptor.* The EMBO journal, 2002. **21**(18): p. 4915-26.

96. Mishra, S.K., S.C. Watkins, and L.M. Traub, *The autosomal recessive hypercholesterolemia (ARH) protein interfaces directly with the clathrin-coat machinery.* Proceedings of the National Academy of Sciences of the United States of America, 2002. **99**(25): p. 16099-104.

97. Saffarian, S., E. Cocucci, and T. Kirchhausen, *Distinct dynamics of endocytic clathrin-coated pits and coated plaques.* PLoS biology, 2009. **7**(9): p. e1000191.

98. Manna, P.T., S. Kelly, and M.C. Field, *Adaptin evolution in kinetoplastids and emergence of the variant surface glycoprotein coat in African trypanosomatids.* Mol Phylogenet Evol, 2013. **67**(1): p. 123-8.

99. Adung'a, V.O., C. Gadelha, and M.C. Field, *Proteomic analysis of clathrin interactions in trypanosomes reveals dynamic evolution of endocytosis.* Traffic, 2013. **14**(4): p. 440-57.

100. Wideman, J.G., et al., *The cell biology of the endocytic system from an evolutionary perspective.* Cold Spring Harbor perspectives in biology, 2014. **6**(4): p. a016998.

101. Mooren, O.L., B.J. Galletta, and J.A. Cooper, *Roles for actin assembly in endocytosis.* Annu Rev Biochem, 2012. **81**: p. 661-86.

102. Paredez, A.R., et al., *An actin cytoskeleton with evolutionarily conserved functions in the absence of canonical actin-binding proteins.* Proc Natl Acad Sci U S A, 2011. **108**(15): p. 6151-6.

Supporting Information

Tables S1 and S2 can be accessed online: http://journals.plos.org/plospathogens/

S1 Table: *Oligonucleotides used in the study*

S2 Table: *Overview of all analyzed open reading frames identified by co-IP*

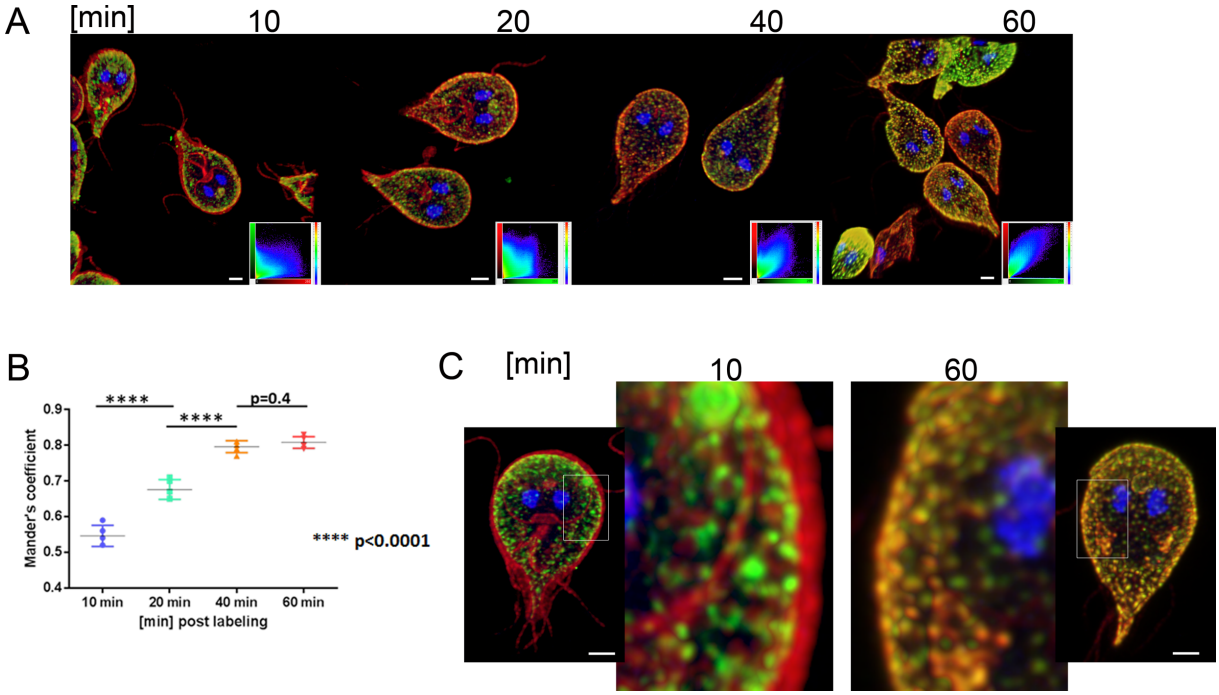

S1 Fig.: *Confocal microscopy and image analysis of cholera toxin endocytosis*

A) Representative volume images of cells (three dimensional reconstructions of image stacks) at 4 time points (10 – 60 min) post labeling with dextran-Oregon Green (fluid phase marker, green) and cholera toxin-AF594 (membrane marker, red). Nuclear DNA is labeled with DAPI (blue); scale bars: 2 µm. Insets : two dimensional scatter plots showing signal distribution (green, red) in voxels. B) Quantification of signal overlap: statistical analysis of Mander's coefficients from five image sets per time point (each set containing an average of 3 cells). C) Enlarged volume images showing typical signal distribution at 10 and 60 min post labeling. Enlarged areas are indicated; scale bars: 2 µm.

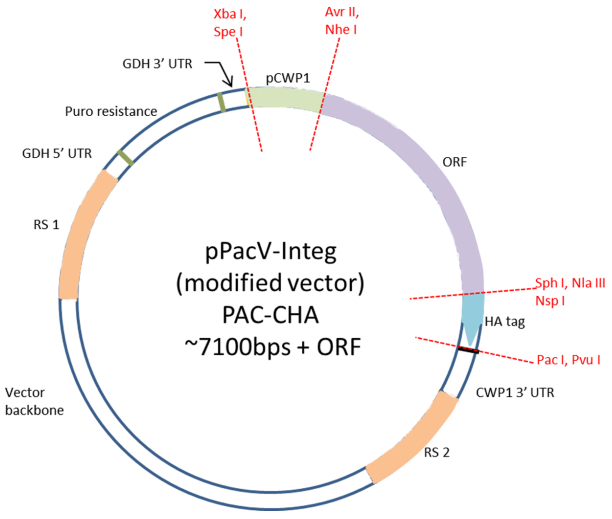

S2 Fig.: *Vector map for pPACV_Integ modified*

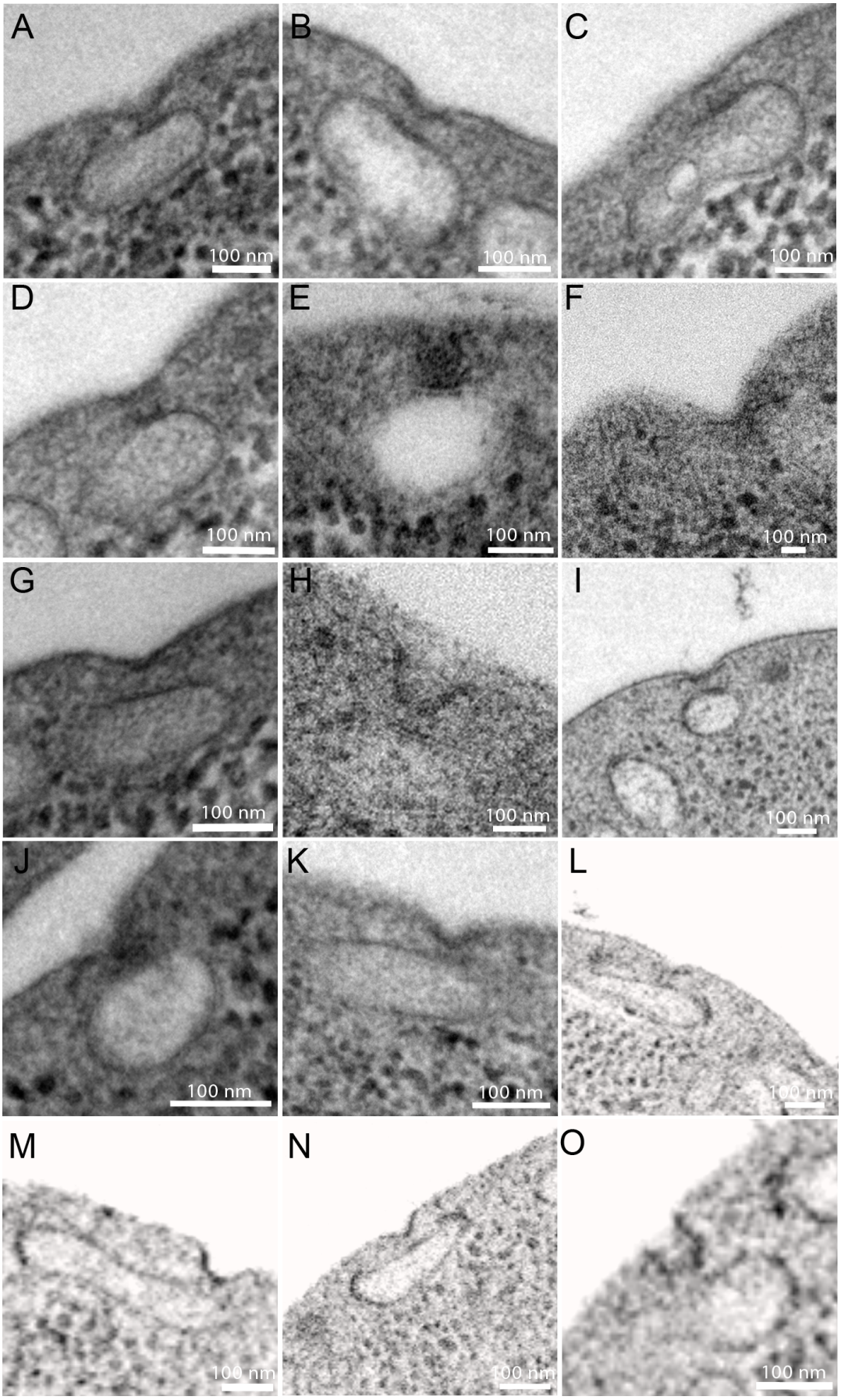

S3 Fig.: ***Compilation of electron micrographs showing PV-associated PM-invaginations***

(A-K) TEM images, (L-O) FIB-SEM images

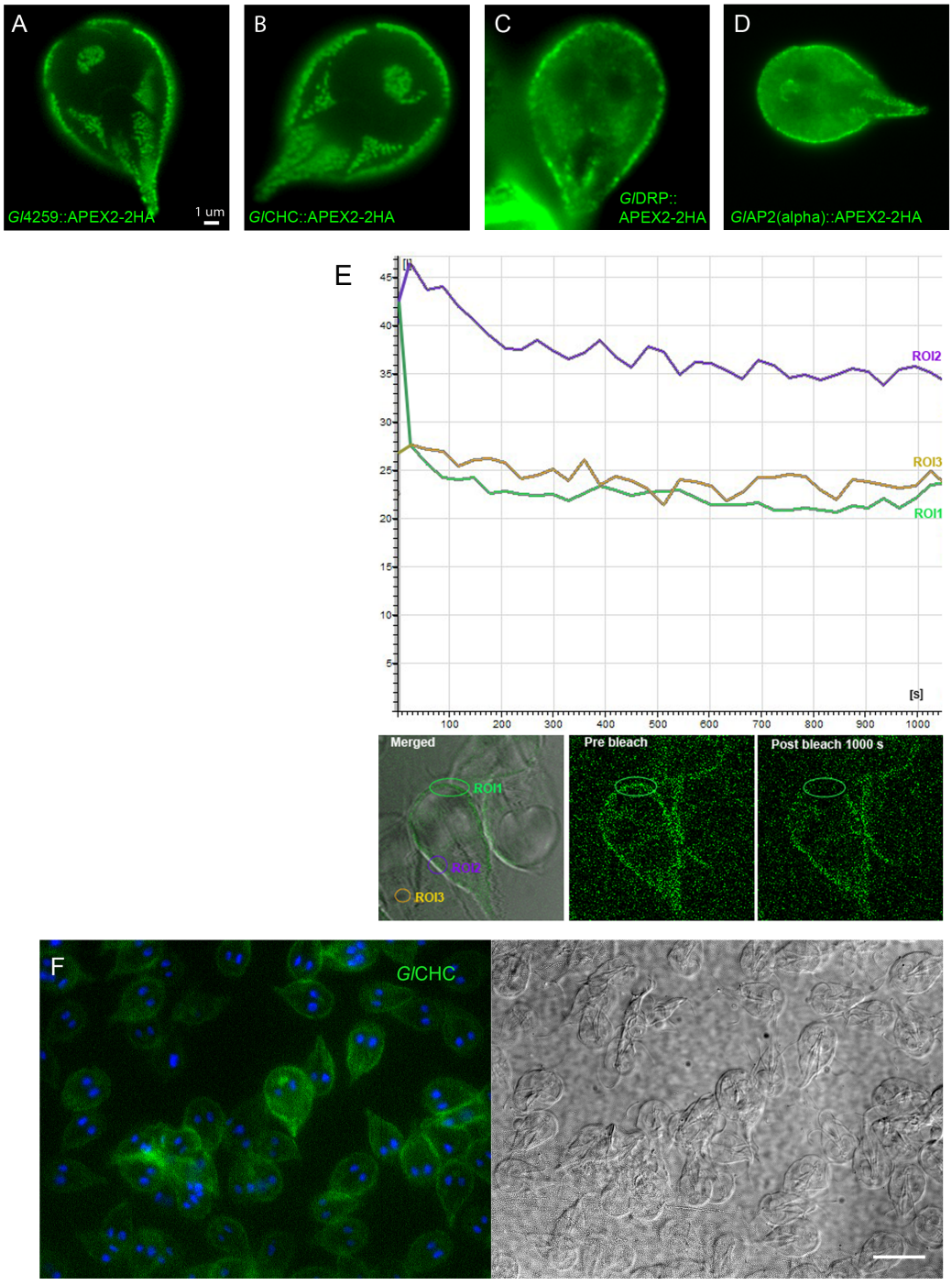

S4 Fig.: ***Localization and dynamics of GlCHC and interaction partners***

Confirmation of the cortical localization of the APEX2 variants used in TEM by IFAs directed against the double HA-tags of (A) *Gl*4259 (B) *Gl*CHC, (C) *Gl*DRP and (D) *Gl*AP2-alpha. (E) No recovery is measured after >15 mins imaging of photobleached areas (ROI 1) in cells expressing a *Gl*CHC-GFP reporter. (F) Distribution of *Gl*CHC in cells constitutively expressing a *Gl*CHC-hub fragment. Scale bar: 10 µm.

```
                    1861                                                                                                    193
H. sapiens          LFTCYDLLRPDVVLETAWRHNIMDFAMPYFIQVMKEYLTKVDKLDASESLRKEEEQATETQPIVYGQPQLMLTAG.PSVAVPPQAP.FGYGYTA.....PPYGQPQPGFGYS
M. mulatta          LFTCYDLLRPDVVLETAWRHNIMDFAMPYFIQVMKEYLTKVDKLDASESLRKEEEQATETQPIVYGQPQLMLTAG.PSVAVPPQAP.FGYGYTA.....PPYGQPQPGFGYS
P. troglodytes      LFTCYDLLRPDVVLETAWRHNIMDFAMPYFIQVMKEYLTKVDKLDASESLRKEEEQATETQPIVYGQPQLMLTAG.PSVAVPPQAP.FGYGYTA.....PPYGQPQPGFGYS
C. lupus            LFTCYDLLRPDVVLETAWRHNIMDFAMPYFIQVMKEYLTKVDKLDASESLRKEEEQATETQPIVYGQPQLMLTAG.PSVAVPPQAP.FGYGYTA.....PPYGQPQPGFGYS
B. taurus           LFTCYDLLRPDVVLETAWRHNIMDFAMPYFIQVMKEYLTKVDKLDASESLRKEEEQATETQPIVYGQPQLMLTAG.PSVAVPPQAP.FGYGYTA.....PPYGQPQPGFGYS
M. musculus         LFTCYDLLRPDVVLETAWRHNIMDFAMPYFIQVMKEYLTKVDKLDASESLRKEEEQATETQPIVYGQPQLMLTAG.PSVAVPPQAP.FGYGYTA.....PPYGQPQPGFGYS
R. norvegicus       LFTCYDLLRPDVVLETAWRHNIMDFAMPYFIQVMKEYLTKVDKLDASESLRKEEEQATETQPIVYGQPQLMLTAG.PSVAVPPQAP.FGYGYTA.....PPYGQPQPGFGYS
G. gallus           LFTCYDLLRPDVVLETAWRHNIMDFAMPYFIQVMKEYLTKVDKLDASESLRKEEEQATETQPIVYGQPQLMLTAG.PSVAVPPQAP.FGYGYTA.....PPYGQPQPGFGYS
D. rerio            LFTCYDLLRPDVVLETSWRNNIMDFAMPYFIQVMREYLSKVDKLETSESLRKEEEQATETQPIVYGTPQLMLTAG.PSVPVPPQQG.YGYGYTAAPGYPPQAPQAQPGFGYG
D. melanogaster     LYQCYDLLRPDVILELAWKHKIVDFAMPYLIQVLREYTTKVDKLELNEAQREKEDDSTEHKNIIQMEPQLMITAG.PAMGIP...PQYAQNYPPGAATVTAAGGRNMGYPYL
A. gambiae          LFQCYDLLRPDVILELAWRHNIMDFAMPYIIQVTREYTSKVDKLEASDAERQKEGESTEHKSIIMPEPQLMLTAG.PGIGIP...PQYAQNYPPGAATVTAAGGRNMGYPYL
C. elegans          LYHCYDLLHPDVIMELAWKHKIMDYAMPYMIQVMRDYQTRLEKLERSEHERKEEKAEQQQNNGMTMEPQLMLTYGAPAPQMPQYAPQYAGAYVPPQPNMPPYQYGGM.....
S. salmonicida      VSRCDTLAPVDVVMELGWRCGMSDYAMPYMISKMAMMTSIITDLQKKNKEEEVEKILAPEKE.EYQEFQEEEEQWAPADNW..............................
G. lamblia          LIRCGHCIRPDVVMELAWVNRMTDYMMPYMISTLQRYGSAVRTLAGSIAEA...RGMIPAQQ.APQQH.........................................
```

S5 Fig.: ***The giardial clathrin heavy chain lacks the QLMLT motif essential for uncoating***

ClustalW alignment of the C-terminal ends of clathrin heavy chains harboring conserved QLMLT motifs (red) with clathrin heavy chains from *G. lamblia* and its close relative *S. salmonicida*. Note how the giardial sequence ends just before the QLMLT motif. Conserved residues in green indicate robust sequence alignment upstream of the uncoating motif.

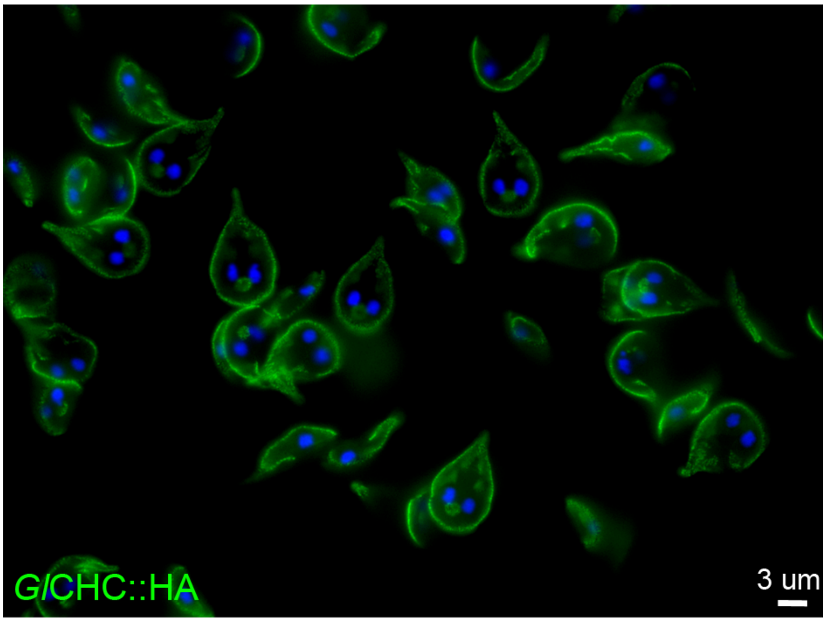

S6 Fig.: ***Subcellular distribution of the HA-tagged GlCHC variant in the cell line used for co-IP***

A representative wide-field microscopy image shows reproducible *Gl*CHC-HA signals in transgenic trophozoites.

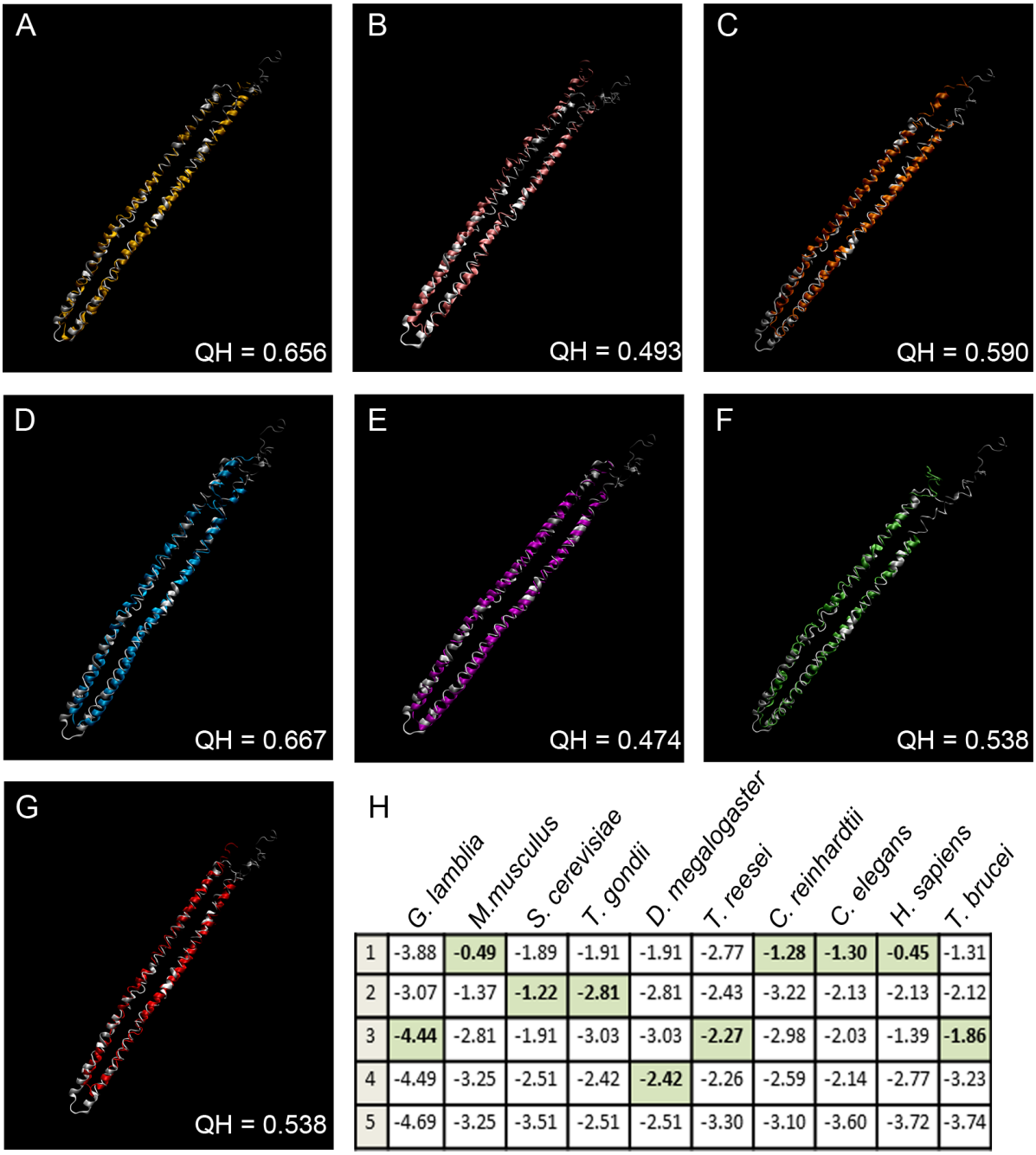

	G. lamblia	*M.musculus*	*S. cerevisiae*	*T. gondii*	*D. megalogaster*	*T. reesei*	*C. reinhardtii*	*C. elegans*	*H. sapiens*	*T. brucei*
1	-3.88	**-0.49**	-1.89	-1.91	-1.91	-2.77	**-1.28**	**-1.30**	**-0.45**	-1.31
2	-3.07	-1.37	**-1.22**	**-2.81**	-2.81	-2.43	-3.22	-2.13	-2.13	-2.12
3	**-4.44**	-2.81	-1.91	-3.03	-3.03	**-2.27**	-2.98	-2.03	-1.39	**-1.86**
4	-4.49	-3.25	-2.51	-2.42	**-2.42**	-2.26	-2.59	-2.14	-2.77	-3.23
5	-4.69	-3.25	-3.51	-2.51	-2.51	-3.30	-3.10	-3.60	-3.72	-3.74

S7 Fig.: ***Structural overlap of iTASSER de novo predictions for GI4259 and annotated clathrin light chains***

Overlap of predicted structures for *GI*4259 and annotated clathrin light chains from with (A) *T. reesei*, (B) *T. gondii*, (C) *S. cerevisiae*, (D) *M. musculus*, (E) *C. reinhardtii*, (F) *D. melanoogaster* and (G) *C. elegans*. (H) The table summarizes C-scores for all five iTASSER models predicted for each sequence. The models that were chosen for structural comparison are highlighted in green.

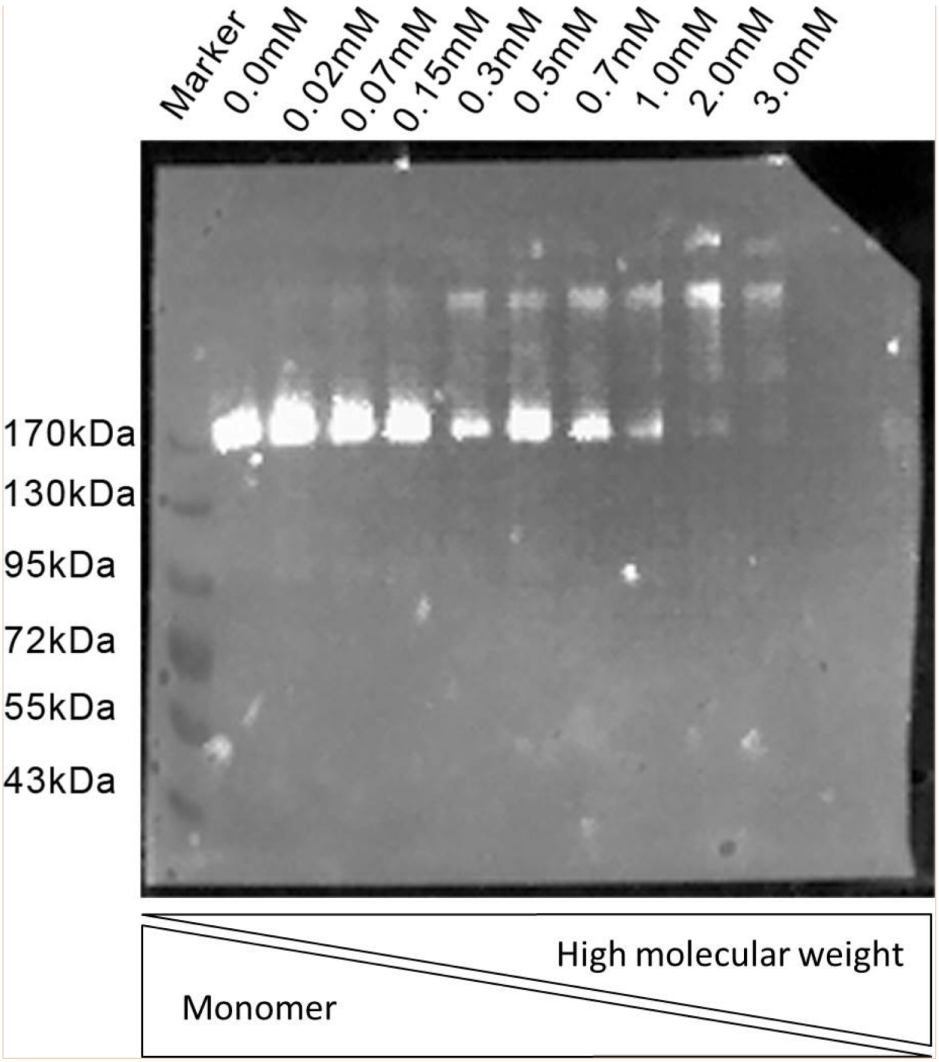

S8 Fig.: ***Titration of DSP used for co-IP assays with limited crosslinking***

Immuno-detection (Western blot) of the GlCHC-HA reporter presents a shift from the monomeric form to higher molecular weight complexes, with increasing concentrations of DSP (0-3 mM). Molecular size (kDa) marker bands are indicated on the left.

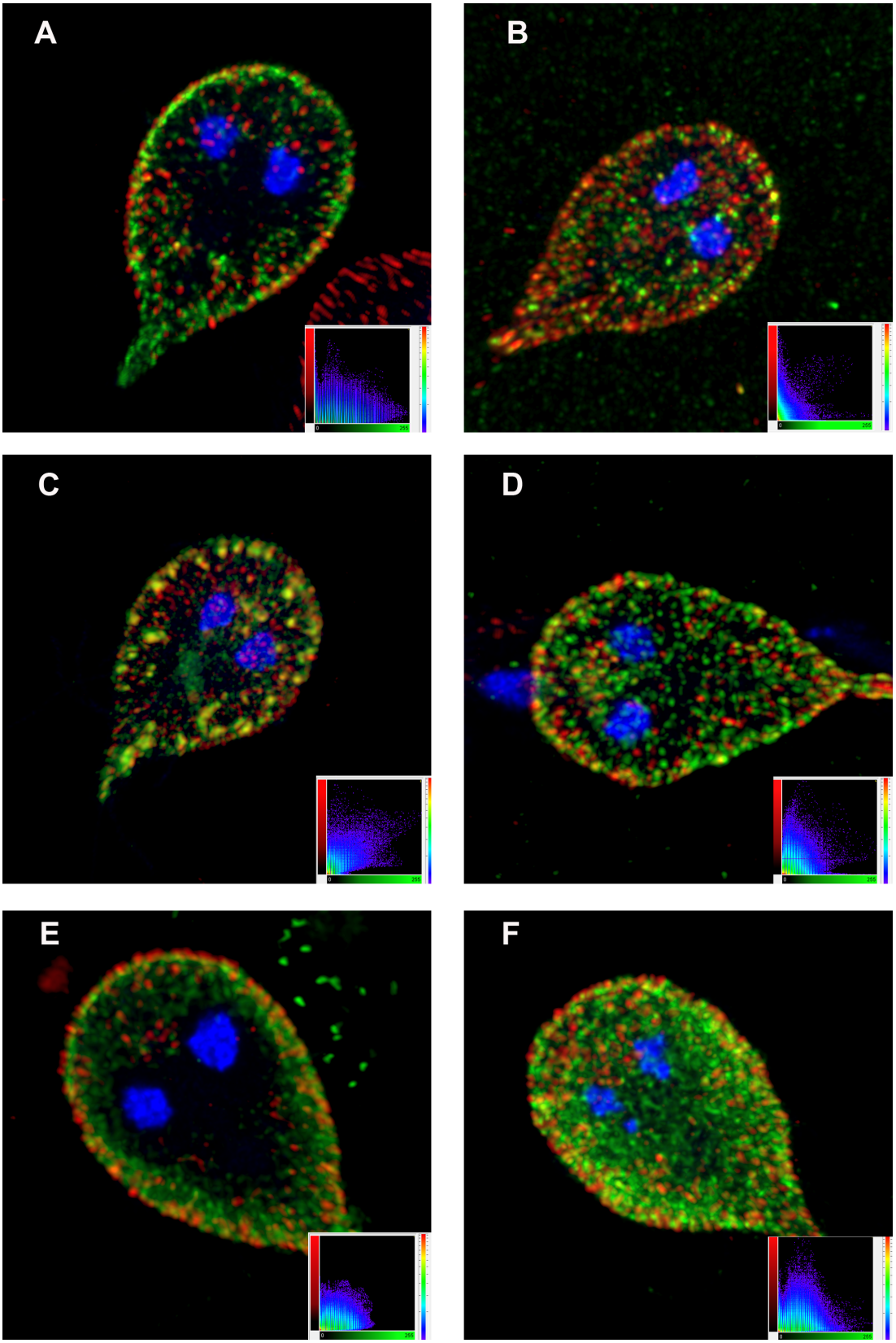

S9 Fig.: ***Confocal microscopy and signal overlap analysis of novel GICHC interacting partners and GICHC***

Immunofluorescence assays and confocal microscopy analysis of HA-tagged reporter lines for ORFs 15411, 7723, 16595, 16653, 10358, and 6687 (A - F), labeled for both the HA tag (green) and

endogenous *Gl*CHC (red). Insets: two dimensional scatter plots showing signal overlap (green, red) in voxels. Nuclei are labelled with DAPI (blue).

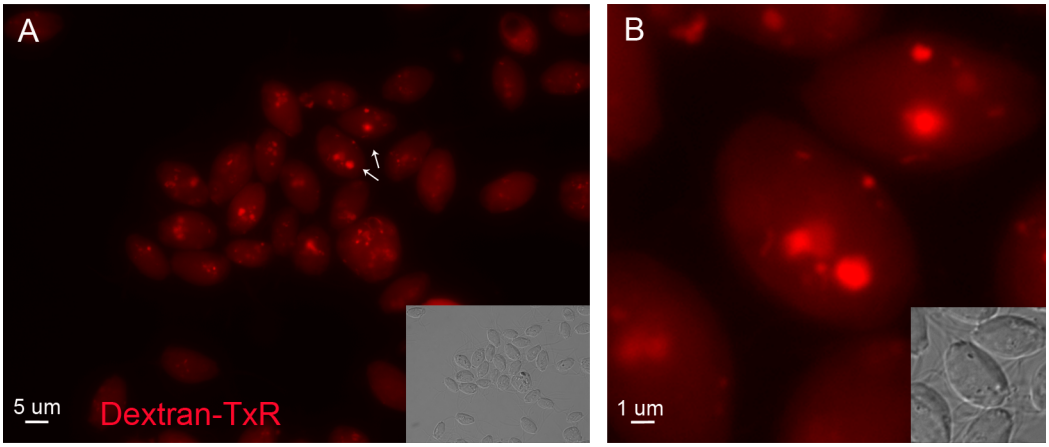

S10 Fig.: ***Dextran-TxR uptake in S. vortens***

(A) The fluid phase marker dextran-TxR is taken up into intracellular compartments of varying sizes. (B) Inset of (A) as indicated by the arrows. Insets: DIC images.

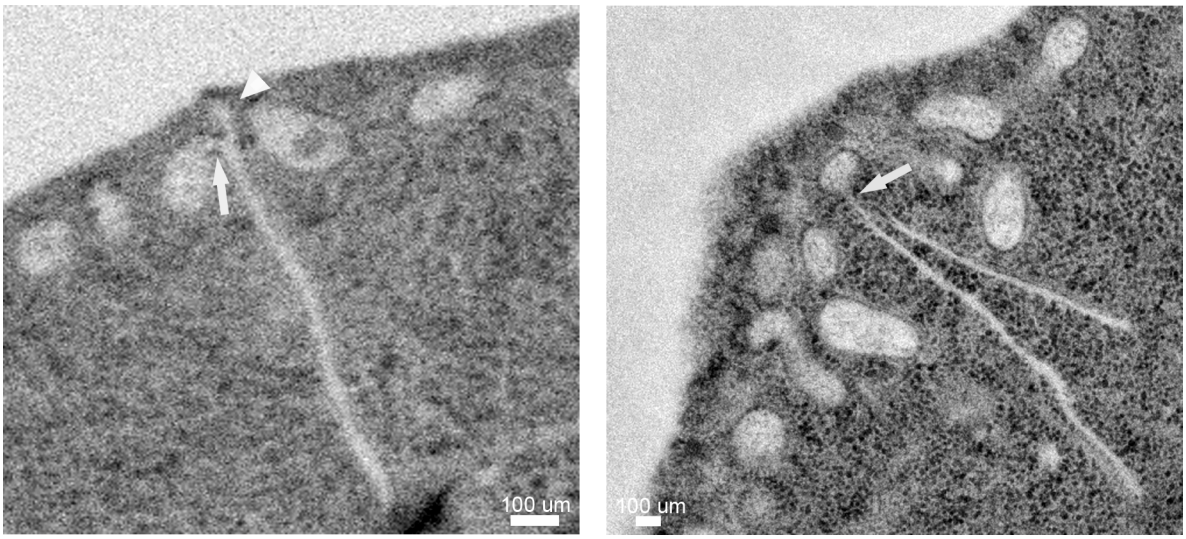

S11 Fig.: ***TEM micrographs of direct continuity of the ER with PVs (arrows) and the PM (arrow head)***

2. Manuscript II (Draft)

Characterization of the PXD protein family demonstrates differential lipid composition of individual organelles in the static endocytic system of *Giardia lamblia*

The work on the characterization of the family of PX domain-containing proteins in *Giardia* originated as a subproject from my main work. My contribution to this work includes cloning and expression of the GlPXDs, cloning and protein-expression of isolated PX domains with subsequent lipid binding analysis, confocal microscopy and image analysis, the development of the co-IP protocol, the writing of the manuscript draft and participation in the conceptual planning. Currently, a PhD student from my host laboratory (Ms. Lenka Cernikova) is completing all remaining relevant experiments for this project. I will therefore share the first authorship on the resulting publication with her. In the present thesis I provide a manuscript draft which includes preliminary data but is not yet ready for submission.

Manuscript status: *in preparation*

Research Article Draft

Characterization of the PXD protein family demonstrates differential lipid composition of individual organelles in the static endocytic system of Giardia lamblia

Jon Paulin Zumthor[1]*, Lenka Cernikova[1]*, Carmen Faso[1] and Adrian B. Hehl[1#]

[1] Institute of Parasitology, University of Zurich (ZH), Zurich, Switzerland

* Equally contributing

[#]To whom correspondence and requests for materials should be addressed:

Adrian B. Hehl; adrian.hehl@uzh.ch

Abstract

Phosphatidylinositols (PtdIns) are key signaling molecules in eukaryotic endocytic systems. Generation of phosphorylated PtdIns (PIs) is tightly controlled and leads to specific membrane identities in the endocytic pathway and governs the spatio-temporal membrane recruitment of effector proteins with an affinity to PIs. This process is key for the regulate progression of the endocytic pathway. The genome of the highly divergent protozoan parasite *Giardia lamblia* encodes all enzymes necessary for the generation of PIs and PI-binding proteins. The largest family of PI-binding proteins in *Giardia* comprises six proteins containing a PX-domain, which are among the most typical PI-binding domains associated to endocytic systems. An association to the giardial endocytic system has been described only for two of the six family members. Here we show diverse PI binding specificities for all six members of the PX-protein family in *Giardia* and that all six proteins localize to endocytic compartments with distinct sub-organellar distributions. Our results indicate a conserved role for PIs in the regulation of the endocytic process in this parasite and demonstrate differential distribution of PIs in the membrane of single endocytic organelles.

Introduction

The endocytic system of the parasitic protozoan *Giardia lamblia* is diverged with respect to canonical uptake mechanisms described in other eukaryotes. As a consequence of host-parasite co-evolution the endocytic system of *Giardia* is almost completely restricted to the dorsal domain of the plasma membrane (PM) and consists of an array of non-fusogenic and non-motile set of individual organelles termed peripheral vacuoles (PVs) [1, 2] (Zumthor et. al. 2016). These organelles underly the PM in close proximity and are thought to communicate with the host environment via direct

fusion to the PM. Morphological and spatiotemporal live cell analysis suggest that PVs are not subject to organelle maturation as is the case for endosomes in classical CME [1]. In conserved systems, endosomal maturation and organelle identity is governed by the accumulation, phosphorylation and de-phosphorylation of phosphatidylinositols (PtdIns); phosphorylated PtdIns are collectively referred to as phosphoinositides (PIs). PtdIns can be phosphorylated at position 3, 4, and 5 of their inositol ring as mono-,di- or triphosphates, giving rise to seven different phosphorylation states [3]. The interconvertibility of PIs is governed by the concerted action of PI-kinases and phosphatases. This allows rapid changes in membrane identities for the finely-regulated recruitment of distinct sets of proteins at the right time to the right place [4, 5]. This is exemplified in the endocytic pathway of many eukaryotic cells where PI conversion marks organelle maturation, starting with PI4,5P_2-positive PM-derived endocytic vesicles, fusing with PI3P positive early- and PI3,5P_2-positive late endosomes, respectively.

Despite the high degree of genome divergence observed in *Giardia lamblia*, functional phosphoinositide-kinases, -phosphatases and several of the corresponding downstream effectors (proteins containing the membrane recruitment modules of the PX-, FYVE- or ENTH-domain type) have been identified in this organism [6-10]. Most mammalian PX domain-containing proteins (at least 49) belong to the family of sorting nexins and constitute a protein family with diverse roles in membrane tracking, organelle motility, membrane remodeling and cell signaling. Even though most PX domains bind to PI3P, interactions with other PIs have been reported [11, 12]. FYVE domains are present in more than three hundred different proteins [13]. Typically, these proteins are found at membranes of the endocytic system such as endosomes, phagosomes or internal vesicles of multivesicular bodies (MVBs) [13]. One well characterized example is the FYVE domain-containing protein EEA1 (early endosomal antigen 1), that is recruited to early endosomes via Rab5 and binding of PI3P to regulate endosomal fusion and endocytic transport [14-18]. The ENTH domain mainly binds to PI4,5P_2 and is found in proteins functioning in clathrin mediated endocytosis [19, 20]. Whilst FYVE and ENTH domain containing proteins are present as single genes in *Giardia* [7, 9], the PX domain containing proteins (*Gl*PXD) constitute a protein family of six members. Moreover, two PX- and the single FYVE- domain containing proteins were shown to interact with clathrin assemblies at the PM-PV interface (PPI) in close proximity to PVs (Zumthor et. al. 2016). These specific associations are intriguing because they suggest that PI-dependent pathways may be involved in the correct functioning of the diverged endocytic system in *G. lamblia*.

Since only 2 out of 6 *Gl*PXD proteins were found complexed to *Gl*CHC assemblies, the question of where the other 4 are deposited within the cell and what they bind, in terms of both PI residues and protein partners, remained open. We hypothesized that *Gl*PXD protein family members bind with

varying affinities to PI residues that mark specific subcellular sites, in particular PVs. To test this, we analyzed the lipid binding affinities and subcellular distribution for all *Gl*PXD proteins. We found distinct lipid binding preferences across the protein family. This data was in line with tertiary structure modeling of all giardial PX domains, which demonstrated overall structural conservation and maintenance of key PI-binding residues. By combining fluorescence microscopy of epitope-tagged *Gl*PXD protein variants and proteomics-based methodologies, we could show distinct sub-organellar deposition patterns for individual *Gl*PXD family members at PVs. These data point towards an important role for *Gl*PXD proteins in defining PV microdomains likely based on their association to specific PI residues. This highlights how definition of endosome-related compartment identity using PI residues and associated proteins is a conserved feature of endocytic systems, however diverged they may be.

Materials and Methods

Homology modeling

For each giardial PX-domain containing protein a protein homolog with a percent sequence identity higher than 25% was identified by blasting the PDB protein database using Blosum45 and Position-Specific Iterated BLAST (PSI-BLAST) algorithms [21]. Three-dimensional template-based protein structure modelling was done using MODELLER 9.14. The template was built from the 5 best fit homologues in terms of sequence identity, query cover and e-value. The validation of the predicted three-dimensional structures was performed using DOPE (Discrete Optimized Protein Energy) [22] and the GA341 method [23]. PDB structures were visualized by VMD (Visual Molecular Dynamics) [24].

Giardia cell culture, induction of encystation and transfection

For culturing and harvesting of the *G. lamblia* WBC6 (ATCC catalog number 50803) trophozoites standard protocols were applied [25]. Encystation was induced by the two-step method as previously described [26, 27]. Genetically modified parasites were generated using established protocols for the electroporation of linearized pPacV-Integ-based plasmid vectors propagated in *E.coli* as described in [28]. After the selection of transgenic cells puromycin resistance, cells were cultured without antibiotics.

Oligonucleotides used in this study are listed below.

Table 1: Oligonucleotides used for the generation of epitope-tagged reporter constructs.

ORF number	Forward	Reverse
Gl50803_7723	5'GCCCTAGGGAGGAGTTTTTTGGGTTTTCAGAC	5'GCTTAATTAACTAGTGGCGATGCATCCCCT
7723-promoter	5'GCACTAGTTTTGGAGGCATATTGTGGAGAC	5'GCCCTAGGCGCGTAGTCTGGGACATCGTATGGGTACATGGCGATTGTTTTTAAAGTAAT
Gl50803_16595	5'GCGCGGCCGCAGAGGACATTGCCTACACCGAC	5'GCTTAATTAATCACCGGTGATATACAAGGATATCG
16595-promoter	5'GCCCTAGGAAAGAGACTAACCAAGTACCTGAC	5'GCGCGGCCGCCGCGTAGTCTGGGACATCGTATGGGTACATCCGTCAGACACTTTTTTTTAAG
Gl50803_42357	5'GCGCGCGGCCGCAGACGGTGATCAGGAGCAGG	5'GCTTAATTAATCAGCAGCGAGCTGCCTTTAAGAA
42357-promoter	5'GCTCTAGAGTCAATTCGGTCGTTAGCATACC	5'GCGCGGCCGCCGCGTAGTCTGGGACATCGTATGGGTACATTTTTTTAAGATACAGAGGCAAAAGGC
Gl50803_16596	5'GCCCTAGGTCTAATAGGTTTACCACCCAGACG	5'GCTTAATTAATCACTCTTTAAGAGCATAAGTGATCGGC
16596-promoter	5'GCTCTAGATTGCTTAGCGTTAAGCTACCGC	5'GCCCTAGGCGCGTAGTCTGGGACATCGTATGGGTACATAAAGTTTTACTTACATATTTAATCGAAC
Gl50803_24488	5'GCCCTAGGACGCACGTTGTTTCGACTGCAT	5'GCTTAATTAATCACCTCAAGGTGTAGCTCTC
24488-promoter	5'GCTCTAGACAGGAGGATGCTTAAATCCTTTATT	5'GCCCTAGGCGCGTAGTCTGGGACATCGTATGGGTACATCATTTTTAAATAGCTTCCCTGCGC
Gl50803_16548	5'GCCCTAGGATAAAAAACGTACTCATGTTTGCAGCAG	5'GCTTAATTAACTATGTGTATCCTTCCTCAATAGAAC
16548-promoter	5'GCTCTAGAAGTTGCTTCCATTAATAGCGAGT	5'GCCCTAGGCGCGTAGTCTGGGACATCGTATGGGTACATTCACACCAAGAAACCTAGACC

Construction of expression vectors

Sequences for all oligonucleotides used for cloning are listed in Table 1. All recombinant proteins in this manuscript were expressed from endogenous promoter-driven open reading frames (ORF). N-terminally hemagglutinin (HA)-tagged proteins were generated using a modified pPacV-Integ with additional restrictions sites (Zumthor et. al. 2016).

Co-immunoprecipitation with limited cross-linking

Co-immunoprecipitation was done as described in Zumthor et. al. 2016 (ref). Additionally protein input was standardized to 8oomg/ml by measuring input quantities by Bradford assay.

Protein analysis and sample preparation for mass spectrometry (MS)-based protein identification

Quality control and sample preparation for MS was done as described previously (Zumthor et. al. 2016).

Mass Spectrometry and protein identification

MS –based protein identification was performed as described in Zumthor et al. 2016 (ref).

Immunofluorescence analysis (IFA) and microscopy

Sample preparation for immunofluorescence-based widefield and laser-scanning confocal microscopy (LSCM) analysis of transgenic cell lines was done as described previously in [28, 29]. Nuclear DNA was labeled with 4',6-diamidino-2-phenylindole (DAPI). Huygens Professional (Scientific Volume Imaging) was used to deconvolve image stacks of optical sections. Three-dimensional reconstructions, isosurface models were performed using IMARIS x64 version 7.7.2 software suite (Bitplane AG).

Expression and Purification of Bacterial Fusion Proteins

The corresponding nucleotide stretches for amino acid residues 553-691 of *Gl*7723, 1665-1801 of *Gl*16595, 443-587 of *Gl*16596, 883-1023 of *Gl*42357, 90-233 of *Gl*16548 and 39-178 of *Gl*24488 were modified by including a HA-coding sequence at the ORF's 5' end and then subcloned into the pMal-2Cx expression vector (New England Biolabs). This gave rise to the corresponding recombinant variants MBP-HA-*Gl*7723, MBP-HA-*Gl*16595, MBP-HA-*Gl*16596, MBP-HA-*Gl*42357, MBP-HA-*Gl*16548 and MBP-HA-*Gl*24488 which were expressed and purified from *E.coli* was done as described previously [30].

Protein Lipid Overlay (PLO) assay

E. coli-extracted lyophilized proteins were reconstituted in 1x PBS, protein concentration was measured using a micro- spectrophotometer (NanoDrop ND-1000 Spectrophotometer, Thermo Scientific). PIP strips (PIP strips, Cat. Nr. P-6001, Echelon) were first floated on ultrapure water for 5 min before incubation in blocking buffer (1xPBS containing 0.1%v/v Tween-20 and 3% fatty-acid free BSA (Sigma A7030)) at RT for 1h. Thereafter 0.5ug/ml of protein in PBS containing 3% fatty acid free BSA were incubate for 1h at RT with gentle agitation. After washing with 1xPBS containing 0.1% v/v Tween-20, PIP–strips were incubated (1h, RT, agitated) with a monoclonal anti-HA antibody (clone 3F10, monoclonal antibody from Roche) at a dilution of 1:500 in blocking buffer. Subsequently strips were washed and incubated (1h, RT, agitated) with polyclonal anti-rat antibody conjugated to HRP at a dilution of 1:2000 in blocking buffer (Goat Anti-Rat IgG(H+L), Cat. Nr. 3050-05, SouthernBiotech). After further washing, strips were developed using a chemiluminescent substrate (WesternBright ECL HRP Substrate, Cat. Nr. K-12045-D50, advansta). Data collection was done as described previously [29].

Densitometry

To make the PLO-assay data comparable among individual lipid strips, each strip was subjected to densitometry analysis using imageJ [31]. Pixel values of single lipid spots were determined. Spots with no specific signal served as blank values or 0%. The spots with the highest pixel values defined 100%. All other spots were normalized against these two values. This procedure was applied to each strip. For visualization purposes each signal was assigned to one of the following categories of signal intestines: 0%, 1-49%, 50-75% and 76-100%.

Results

Tertiary structure modeling shows conservation of the PIP binding pocket

Currently, twenty different structures for PX-domains have been solved, three of them complexed to PtdIns(3)P [32]. This enabled identification of structural prerequisites and critical amino acid residues for substrate binding. Despite weak primary sequence identity, PX-domains are structurally conserved and characterized by a common PI binding pocket [11]. This pocket consists of an N-terminal three-stranded β-sheet and 3 α-helices forming a helical subdomain [11, 33, 34]. To test if PX domains of the *Gl*PXD protein family share these distinct structural characteristics, we used MODELLER [21] to perform a template-based prediction of tertiary protein structure. All six modelled giardial PX domains were predicted to contain the characteristic three stranded β-sheet and the helical subdomain (Fig.1B). Furthermore, a proline rich domain (PxxP) involved in membrane anchoring [11, 33, 34], and arginine residues that were shown to be essential for PI binding [33, 35] are fairly conserved in the giardial PX-domains (Fig.1A). Taken together, our *in-silico* analysis of the giardial PX domains showed overall structural as well as canonical residue conservation, leading us to hypothesize that 6 *Gl*PXD family members are functionally capable of PI-binding.

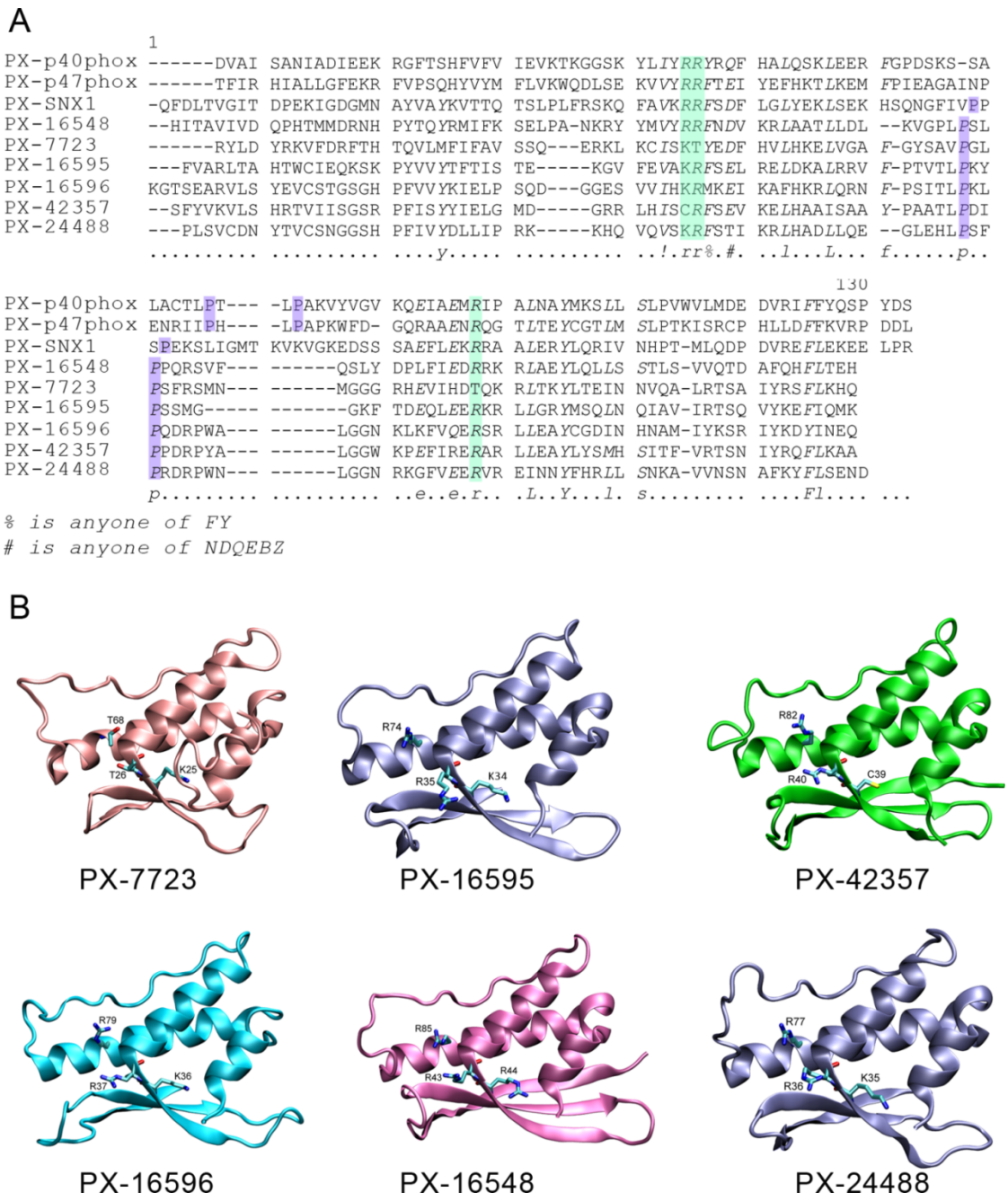

Fig. 1: Giardial PX domains are structural conserved and maintained canonical residues for PI binding
A: Alignment of the amino acid sequence of the giardial PX domains compared to PX domains of three human proteins. Conserved residues shown to be essential for PI binding are highlighted in light green. The PxxP domain is highlighted in purple. B: Three-dimensional structures for all six giardial PX domains. The indicated residues correspond to residues highlighted in light green in A.

PLO assays demonstrates functionality and PI binding preferences for all predicted giardial PX domains

PLOs are widely used to investigate protein lipid interactions, also in *G. lamblia* [7, 9, 33, 36]. Here, we applied this methodology using PIP strips to test whether giardial PX-domains are capable of binding PIs and to determine their individual binding specificities. To do so, isolated PX-domains of all 6 family members in *G. lamblia* were expressed as MBP HA-tagged fusion proteins in *E.coli*. The

relative lipid binding capacity of purified recombinant proteins was evaluated by densitometry (Fig.2). Giardial PX domains showed no specific signal for binding to any other class of lipids, other than to PI residues.

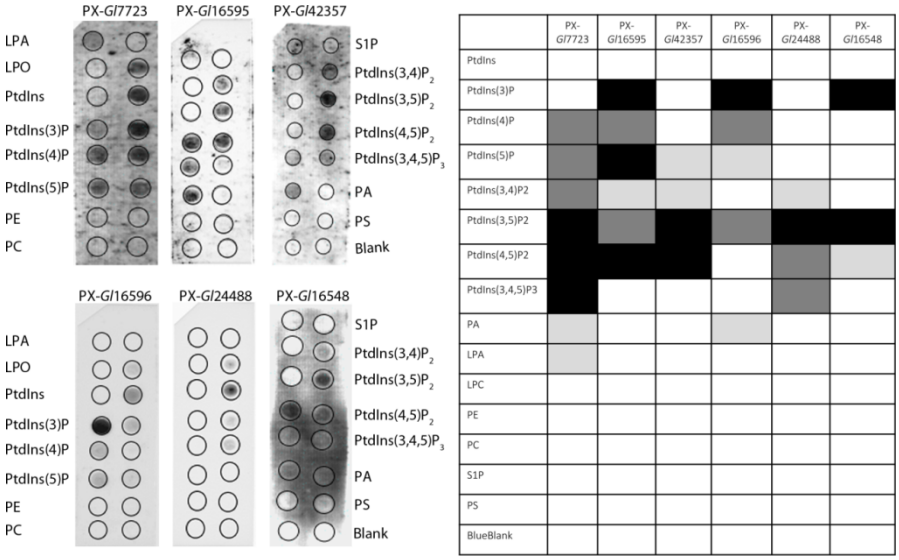

Fig. 2: Lipid binding preferecences of *Gl*PXDs
Left column: Binding preferences were determined by a protein:lipid overlay assay. Right column: The table visualizes the pixel intensities of each lipid spot normalized against the background. The strongest pixel intensity was set to a 100%, background was set to 0%. Black indicates values from 76-100%, dark gray from 50-75%, light gray from 1-50% and white indicates no binding.

PX-domains of ORFs Gl7723 and Gl16595

ORFs *Gl*7723 and *Gl*16595 were shown to interact with clathrin assemblies found at the PPI (Zumthor et. al.2016). In mammalian cells, PM domains singled out for clathrin-mediated endocytic events are marked by increased levels of PtdIns(4,5)P2 [37]. In line with these data, the PLO assay for the PX domains of ORFs *Gl*7723 (PX-7723) and *Gl*16595 (PX-16595) showed high binding affinity to PtdIns(4,5)P_2. At the same time, both PX-domains interacted specifically with PtdIns(3)P and PtdIns(3,5)P_2, PI residues typically found on early and or late endosomes [3, 11]. Additionally, PX-7723 showed strong interaction with PtdIns(3,4,5)P_3 (usually found at the PM [3]) while PX-16595 interacted with PI5P. PI5P is the least well described monophosphate derivative but there is substantial evidence that it is involved in the regulation of trafficking events between endosomes and lysosomes [38].

*PX-domains of ORFs Gl*16596, *Gl*16548, *Gl*24488 and *Gl*42357

These PX-domains presented the strongest interactions with PtdIns(3,5)P_2 and/or PtdIns(3)P, suggesting preferential interaction for these domains with membranes from the endocytic system rather than with the PM [3, 11]. PX-42357 showed similar PI binding affinity as PX-*Gl*7723 and PX-*Gl*16595 which interacted with PIs usually present at the PM (PtdIns(4,5)P2) and at endosomal membranes (PtdIns(3,5)P2),. In summary our data demonstrated differential lipid binding specificities among the *Gl*PXD protein family.

PX-domain containing proteins localize in the cell periphery by IFA

The data from the PLO assays indicated that *Gl*PXD proteins bind endocytosis-related PI residues with high affinity (Fig. 2). Combined with the fact that PX domain-containing proteins are usually associated with endocytic systems [3, 11], this prompted us to investigate localization of all *Gl*PXD members to see whether all would localize to the PV organelle system. To do this, each *Gl*PXD was epitope tagged at the N-terminus and expressed as a full length variant in native conditions. Indeed, IFA analysis of the epitope tagged variants unambiguously showed localization in the cortical area of the cell, consistent with PV and/or PM associated localization and in line with the data from PLO assays. However, given that PX domains showed defined PI residue binding preferences, this would suggest that, although all *Gl*PXD members localize similarly, their positioning could match a differential distribution of PIs on a sub-organellar level. This hypothesis is further supported by data showing how two of the six *Gl*pxdcp interact with clathrin assemblies that specifically sit at the PM-PV interface (PPI) (Zumthor et al. 2016).

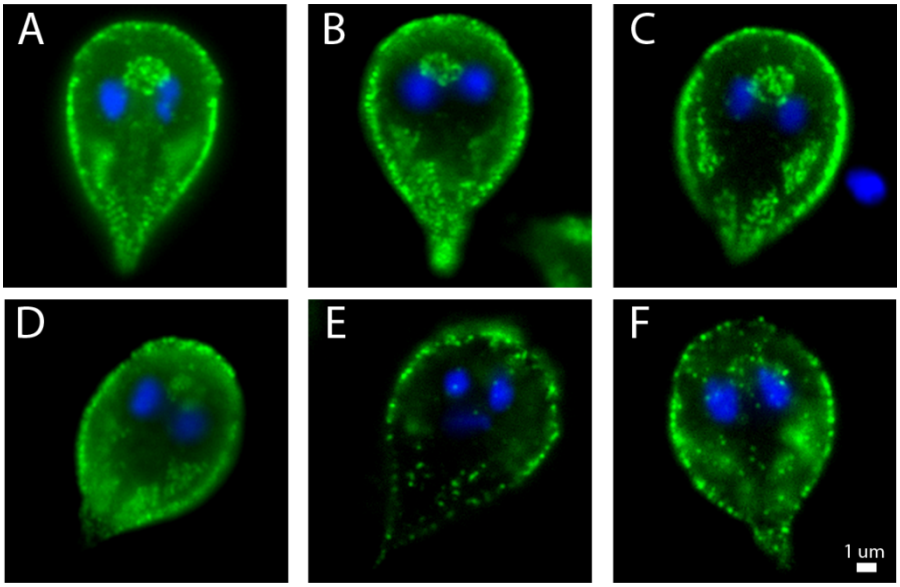

Fig.3: Subcellular localization of *Gl*PXD-reporters
Immunofluorescence assay detects all *Gl*PXD-reporters to localize in the cell cortex Representative images for HA-tagged *Gl*7723 (A), *Gl*16595 (B), *Gl*42357 (C), *Gl*16596 (D), *Gl*24488 (E), *Gl*16548 (F).

Confocal microscopy reveals PPI-localization for PX-7723, PX-16595 and PX-42357 but not for PX-16596

To investigate the subcellular distribution of the *Gl*PXD in relation to PVs we imaged HA-tagged variants expressing trophozoites saturated with the PV marker dextran-TxR by confocal microscopy. By performing 3D-reconstructions we were able to define the cortical localization for four out of six *Gl*PXD proteins (Fig. 3). Due to technical reasons this analysis was not completed for PX-16548 and PX-24488. In particular, limited cell-permeabilization necessary to maintain the distinct fluorescent signal of the PV-marker dextran prevented sufficient antibody-detection of the HA-tagged fusion

proteins in these two cell lines. Previous observations demonstrated interaction of *Gl*7723 and *Gl*16595 with clathrin assemblies that localize distinctly at the PPI (Zumthor et al., 2016). Similarly, our data indicated PPI localization for the reporters of HA-*Gl*7723 (Fig. 4A-C) and HA-*Gl*16595 (Fig. 4D-F). HA-tagged *Gl*42357 mainly distributed at the PPI (Fig. 4G-I). In contrast, HA-*Gl*16596 reporter molecules showed a localization lateral to PV organelles, in some cases encircling organelles completely (Fig. 4J-L). Moreover, HA-*Gl*16596 reporter molecules seem to be excluded from the distal and ventral domains of PVs. These preliminary microscopy data pointed towards heterogenous sub-organellar distributions for *Gl*PXD proteins, consistent with differential lipid binding affinities. Taken together these data suggest that differentially distributed lipids in the limiting PV membrane may define specific organelle subdomains marked by preferential binding of *Gl*PXD proteins.

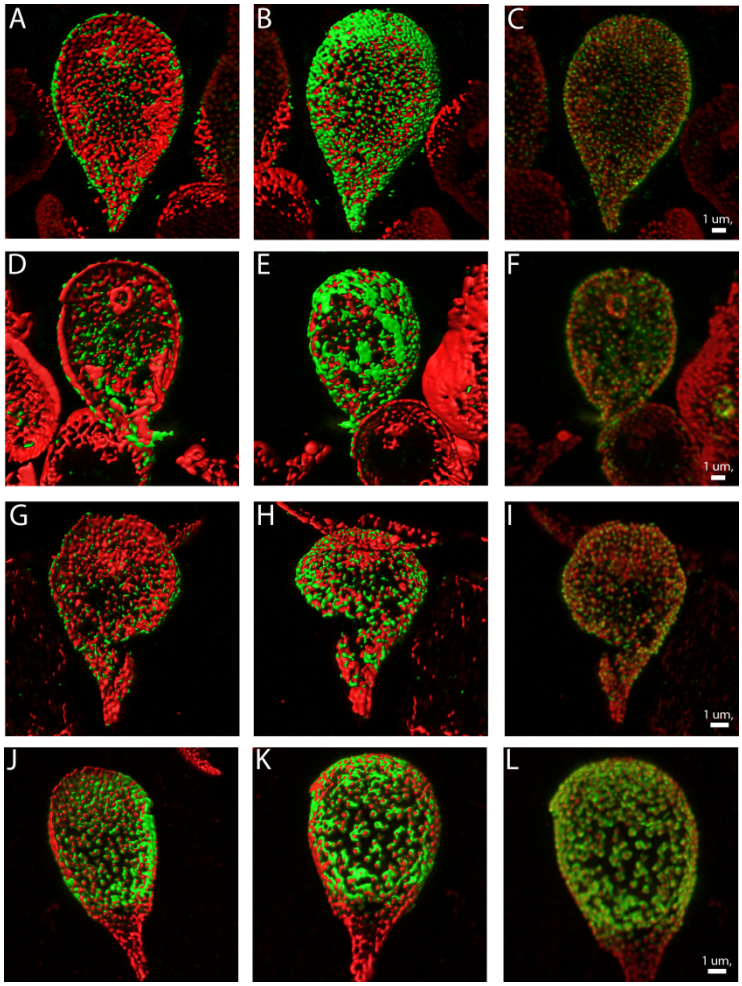

Fig. 4 Localizations of HA-tagged *Gl*PXD-reporters in context of PV organelles
*Gl*7723 (A-C), *Gl*16595 (D-F) and *Gl*42357 (J-L) localize distal to the PV-marker dextran-TxR i.e. at the PPI. *Gl*16596 localizes lateral to the PV-marker dextran-TxR but excludes the ventral and distal domains of PVs.
Left and middle column: Surface rendering of optical sections from the corresponding cells shown in the right column. Left column: ventral view. Middle column: dorsal view. Right column: merged fluorescent image total projections.

Preliminary co-immunoprecipitation (co-IP) data for five *Gl*PXDs

To analyze if the differential distribution of the *Gl*PXD is also reflected in the corresponding protein-protein interactions we aimed to perform a co-IP experiment and analysis for each *Gl*PXD protein. To date, we have performed five out of six co-IPs specific to HA-tagged variants of each *Gl*PXD protein, except for *Gl*16548 which is still pending. However, here we included a preliminary analysis of the available coIP data with a focus on validated core components for clathrin assemblies presented in Zumthor et al. 2016. The analysis based on the number of exclusive spectrum counts for clathrin-assembly core components (CAcC) as a read-out for strength of interaction and/or proximity. CAcCs were divided into two clusters, static (*Gl*CHC and *Gl*4259 i.e. putative clathrin light chain) and

dynamic (*Gl*DRP, *Gl*AP2). The exclusive spectrum counts in Table 2 suggested strong interactions for HA-*Gl*7723 and HA-*Gl*16595 with clathrin assemblies. In contrast, HA-*Gl*16596 appeared to be mostly associated to the dynamic CAcC clusters. For HA-*Gl*42357 and HA-*Gl*24488 fewer total spectral counts were obtained. Whilst HA-*Gl*42357 mainly interacted with the static clathrin cluster, HA-*Gl*24488, similar to HA-*Gl*16596, mostly interacted with the dynamic core components *Gl*DRP and *Gl*AP2.

Given these protein interaction data, we propose that HA-*Gl*7723, HA-*Gl*16595 and HA-*Gl*42357 are in closer proximity to clathrin assemblies (i.e. closer to the PM) than HA-*Gl*24488 and HA-*Gl*16596. This hypothesis is supported by the imaging data where the same clustering was obtained with respect to whether HA-tagged *Gl*PXD protein variants were more or less proximal to PVs.

	Cumulative exclusive spectral counts	
	*Gl*CHC&*Gl*4259	*Gl*AP2&*Gl*DRP
*Gl*7723	76	23
*Gl*16595	65	24
*Gl*42357	6	4
*Gl*16596	9	36
*Gl*24488	8	14

Tab. 2: Specturm counts for static and dynamic clusters of CAcC obtained in *Gl*PXD specific co-IPs
MS analysis of individual co-IPs shows a enrichment for spectrum counts of the static clathrin components when *Gl*7723 or *Gl*16595 were used as baits. For baits *Gl*16596 and *Gl*24488 spectrum counts were enriched for the dynamic components. Bait *Gl*42357 shows no enrichment for neither components.

Discussion

The latest count on mammalian proteins containing a predicted PX domain is 49 [12]. The majority of them belong to the sorting nexin family involved in membrane trafficking whilst others function in immune defense mechanisms [11]. The giardial family of PX domain containing proteins comprises six proteins. These proteins seem to be *G. lamblia* specific as HMMER searches against a representative eukaryotic dataset yielded no non-giardial homologues using a hidden markov model based on a multiple sequence alignment of all *Gl*PXD (Faso and Hehl, unpublished). Except for the C-terminally located PX-domain, suggesting association to endocytic membranes [39-41], *Gl*PXD family members share no detectable sequence similarities. Proteins *Gl*7723 and *Gl*16595 has been previously shown to interact with clathrin heavy chain and to localize in the vicinity of PVs, the endocytic organelles in *G. lamblia*. These data are consistent with the findings presented here, which lend further support to the hypothesis that, although *Giardia's* endocytic system is highly diverged, *Gl*PXD family members maintain association to PVs, this parasite's endo-lysosomal compartments.

Based on the conserved structural and sequence-based elements we could predict that each of the *Gl*PXDs would displayed selective and differential PI binding *in vitro.* In this study cortical localization for all six *Gl*PXDs was determined by IFA and further defined by LSCM for four of them. Similarly to

clathrin, HA-tagged variants for -*Gl*7723, -*Gl*16595 and -*Gl*42357 localized at the PPI although the latter was not found to interact with clathrin (Zumthor et. al 2016). A possible explanation for this is that, although *Gl*42537 is found at the PPI, it may associate to PV membrane subdomains that are distinct from the ones focal clathrin assemblies interact with. Distribution of *Gl*16596 is the most divergent, with HA-tagged reporters localizing laterally to PVs, in some cases completely surrounding the organelles without covering their "poles". These preliminary results on the sub-organellar distribution are in agreement with data from the PLO assays and the preliminary data from the coIPs in that:

i) only the 3 PPI-localized *Gl*PXD showed interaction with PM and endo-/lysosome associated phosphorylated derivatives of PtdIns. In contrast, *Gl*16596 specifically and solely interacts with PtdIns(3)P, typically present on endosomal membranes. ii) coIP data showed strong interaction of *Gl*7723 and *Gl*16595 with clathrin and specific deposition at the PPI (Zumthor et al. 2016). Although *Gl*42357 was also localized at the PPI, it is not comparable to *Gl*7723 and *Gl*16595 in terms of clathrin interaction. The few spectral counts we detected for clathrin assemblies in the *Gl*42357-specific co-IP dataset are likely due to protein proximity at the PPI and, in contrast to *Gl*7723 and *Gl*16595, do not reflect incorporation in the same complex. Despite their distinct binding affinities for PIs in vitro, all *Gl*PXD localize in the vicinity of PV organelles. This suggests that PV membranes are composed of subdomains enriched for different phosphorylated-derivatives of PtdIns that may act as "homing signals" for *Gl*PXDs. In turn, *Gl*PXDs may recruit clathrin assemblies and other currently unknown proteins to these specific membrane platforms.

PVs are the initial and only site for material uptake, act as digestive organelles and are thought to facilitate retrograde transport via transient ER connections [42]. The current view suggests that PVs maintain these diverse functions without undergoing a maturation cycle but fulfil endo-and lysosomal functions at once. Therefore specific membrane platforms defined by PIs may be crucial for these distinct functions to be established at the right place and time at these static and large endocytic organelles. The current work sets the basis for further investigations on these potential PV specific membrane microdomains. *Gl*PXDs and also the single giardial FYVE domain-containing protein could serve as PI-markers in cutting edge imaging techniques to determine exact PI distributions in endomembranes involved in endocytosis. Functional analysis (e.g. by the expression of dominate negative mutants, as shown for the PX domain-containing Protein AP180 [43]) of *Gl*PXDs is necessary to further characterize the role of PIs in *G. lamblia* endocytosis. Taken together, the data presented here indicate that the endocytic process in *G. lamblia* is subject to regulation by PIs, similar to observations made in other protozoan parasites like plasmodium or trypanosoma [39, 40].

1. Gaechter, V., et al., *The single dynamin family protein in the primitive protozoan Giardia lamblia is essential for stage conversion and endocytic transport.* Traffic, 2007. **9**(1): p. 57-71.
2. Touz, M.C., et al., *Lysosomal protein trafficking in Giardia lamblia: common and distinct features.* Frontiers in bioscience, 2011. **4**: p. 1898-909.
3. Di Paolo, G. and P. De Camilli, *Phosphoinositides in cell regulation and membrane dynamics.* Nature, 2006. **443**(7112): p. 651-7.
4. McCartney, A.J., Y. Zhang, and L.S. Weisman, *Phosphatidylinositol 3,5-bisphosphate: low abundance, high significance.* BioEssays : news and reviews in molecular, cellular and developmental biology, 2014. **36**(1): p. 52-64.
5. Sasaki, T., et al., *The physiology of phosphoinositides.* Biological & pharmaceutical bulletin, 2007. **30**(9): p. 1599-604.
6. Cox, S.S., et al., *Evidence from bioinformatics, expression and inhibition studies of phosphoinositide-3 kinase signalling in Giardia intestinalis.* BMC microbiology, 2006. **6**: p. 45.
7. Ebneter, J.A. and A.B. Hehl, *The single epsin homolog in Giardia lamblia localizes to the ventral disk of trophozoites and is not associated with clathrin membrane coats.* Molecular and biochemical parasitology, 2014. **197**(1-2): p. 24-7.
8. Hernandez, Y., et al., *Transcriptional analysis of three major putative phosphatidylinositol kinase genes in a parasitic protozoan, Giardia lamblia.* The Journal of eukaryotic microbiology, 2007. **54**(1): p. 29-32.
9. Sinha, A., et al., *Identification and characterization of a FYVE domain from the early diverging eukaryote Giardia lamblia.* Current microbiology, 2011. **62**(4): p. 1179-84.
10. Banerjee, S., S. Basu, and S. Sarkar, *Comparative genomics reveals selective distribution and domain organization of FYVE and PX domain proteins across eukaryotic lineages.* BMC genomics, 2010. **11**: p. 83.
11. Seet, L.F. and W. Hong, *The Phox (PX) domain proteins and membrane traffic.* Biochimica et biophysica acta, 2006. **1761**(8): p. 878-96.
12. Teasdale, R.D. and B.M. Collins, *Insights into the PX (phox-homology) domain and SNX (sorting nexin) protein families: structures, functions and roles in disease.* Biochem J, 2012. **441**(1): p. 39-59.
13. Kutateladze, T.G., *Phosphatidylinositol 3-phosphate recognition and membrane docking by the FYVE domain.* Biochim Biophys Acta, 2006. **1761**(8): p. 868-77.
14. Simonsen, A., et al., *EEA1 links PI(3)K function to Rab5 regulation of endosome fusion.* Nature, 1998. **394**(6692): p. 494-8.
15. Mills, I.G., A.T. Jones, and M.J. Clague, *Involvement of the endosomal autoantigen EEA1 in homotypic fusion of early endosomes.* Curr Biol, 1998. **8**(15): p. 881-4.
16. McBride, H.M., et al., *Oligomeric complexes link Rab5 effectors with NSF and drive membrane fusion via interactions between EEA1 and syntaxin 13.* Cell, 1999. **98**(3): p. 377-86.
17. Rubino, M., et al., *Selective membrane recruitment of EEA1 suggests a role in directional transport of clathrin-coated vesicles to early endosomes.* J Biol Chem, 2000. **275**(6): p. 3745-8.
18. Christoforidis, S., et al., *Phosphatidylinositol-3-OH kinases are Rab5 effectors.* Nat Cell Biol, 1999. **1**(4): p. 249-52.
19. Horvath, C.A., et al., *Epsin: inducing membrane curvature.* Int J Biochem Cell Biol, 2007. **39**(10): p. 1765-70.
20. Itoh, T., et al., *Role of the ENTH domain in phosphatidylinositol-4,5-bisphosphate binding and endocytosis.* Science, 2001. **291**(5506): p. 1047-51.
21. Sali, A. and T.L. Blundell, *Comparative protein modelling by satisfaction of spatial restraints.* Journal of molecular biology, 1993. **234**(3): p. 779-815.
22. John, B. and A. Sali, *Comparative protein structure modeling by iterative alignment, model building and model assessment.* Nucleic Acids Res, 2003. **31**(14): p. 3982-92.

23. Melo, F., R. Sánchez, and A. Sali, *Statistical potentials for fold assessment.* Protein Sci, 2002. **11**(2): p. 430-48.
24. Humphrey, W., A. Dalke, and K. Schulten, *VMD: visual molecular dynamics.* Journal of molecular graphics, 1996. **14**(1): p. 33-8, 27-8.
25. Hehl, A.B., M. Marti, and P. Kohler, *Stage-specific expression and targeting of cyst wall protein-green fluorescent protein chimeras in Giardia.* Molecular biology of the cell, 2000. **11**(5): p. 1789-800.
26. Boucher, S.E. and F.D. Gillin, *Excystation of in vitro-derived Giardia lamblia cysts.* Infection and immunity, 1990. **58**(11): p. 3516-22.
27. Morf, L., et al., *The transcriptional response to encystation stimuli in Giardia lamblia is restricted to a small set of genes.* Eukaryotic cell, 2010. **9**(10): p. 1566-76.
28. Stefanic, S., et al., *Neogenesis and maturation of transient Golgi-like cisternae in a simple eukaryote.* Journal of cell science, 2009. **122**(Pt 16): p. 2846-56.
29. Konrad, C., C. Spycher, and A.B. Hehl, *Selective condensation drives partitioning and sequential secretion of cyst wall proteins in differentiating Giardia lamblia.* PLoS pathogens, 2010. **6**(4): p. e1000835.
30. Marti, M., et al., *An ancestral secretory apparatus in the protozoan parasite Giardia intestinalis.* The Journal of biological chemistry, 2003. **278**(27): p. 24837-48.
31. Schneider, C.A., W.S. Rasband, and K.W. Eliceiri, *NIH Image to ImageJ: 25 years of image analysis.* Nat Methods, 2012. **9**(7): p. 671-5.
32. Jia, Z., et al., *The recognition of membrane-bound PtdIns3P by PX domains.* Proteins, 2014. **82**(10): p. 2332-42.
33. Kanai, F., et al., *The PX domains of p47phox and p40phox bind to lipid products of PI(3)K.* Nature cell biology, 2001. **3**(7): p. 675-8.
34. Shultis, D., G. Dodge, and Y. Zhang, *Crystal structure of designed PX domain from cytokine-independent survival kinase and implications on evolution-based protein engineering.* Journal of structural biology, 2015. **191**(2): p. 197-206.
35. Bravo, J., et al., *The crystal structure of the PX domain from p40(phox) bound to phosphatidylinositol 3-phosphate.* Molecular cell, 2001. **8**(4): p. 829-39.
36. Dowler, S., G. Kular, and D.R. Alessi, *Protein lipid overlay assay.* Science's STKE : signal transduction knowledge environment, 2002. **2002**(129): p. pl6.
37. Honing, S., et al., *Phosphatidylinositol-(4,5)-bisphosphate regulates sorting signal recognition by the clathrin-associated adaptor complex AP2.* Molecular cell, 2005. **18**(5): p. 519-31.
38. Viaud, J., et al., *Phosphatidylinositol 5-phosphate: a nuclear stress lipid and a tuner of membranes and cytoskeleton dynamics.* BioEssays : news and reviews in molecular, cellular and developmental biology, 2014. **36**(3): p. 260-72.
39. Hall, B.S., et al., *TbVps34, the trypanosome orthologue of Vps34, is required for Golgi complex segregation.* J Biol Chem, 2006. **281**(37): p. 27600-12.
40. Rodgers, M.J., J.P. Albanesi, and M.A. Phillips, *Phosphatidylinositol 4-kinase III-beta is required for Golgi maintenance and cytokinesis in Trypanosoma brucei.* Eukaryot Cell, 2007. **6**(7): p. 1108-18.
41. Daher, W., et al., *Lipid kinases are essential for apicoplast homeostasis in Toxoplasma gondii.* Cell Microbiol, 2015. **17**(4): p. 559-78.
42. Abodeely, M., et al., *A contiguous compartment functions as endoplasmic reticulum and endosome/lysosome in Giardia lamblia.* Eukaryotic cell, 2009. **8**(11): p. 1665-76.
43. Doherty, G.J. and H.T. McMahon, *Mechanisms of endocytosis.* Annu Rev Biochem, 2009. **78**: p. 857-902.

3. Manuscript III

A Tom40-centered membrane interactome of the highly diverged parasite Giardia lamblia reveals functional conservation of protein import and organelle morphogenesis machinery in mitosomes

As a co-author, I was involved in designing, developing and executing of the co-IP experiments.

Manuscript status: *submitted*

A Tom40-centered membrane interactome of the highly diverged parasite Giardia lamblia reveals functional conservation of protein import and organelle morphogenesis machinery in mitosomes

Samuel Rout[1], **Jon Paulin Zumthor**[1], Elisabeth M. Schraner[2], Carmen Faso* and Adrian B. Hehl[1]*

1 Institute of Parasitology, University of Zurich (ZH), Switzerland

2 Institute of Veterinary Anatomy, University of Zurich (ZH), Switzerland

*Corresponding authors

Email: adrian.hehl@access.uzh.ch (AH)

carmen.faso@access.uzh.ch (CF)

Abstract

Protozoan parasites of the genus Giardia are highly prevalent globally and infect a wide range of vertebrate hosts including humans, but proliferation and pathology is restricted to the small intestine. This narrow ecological specialization entailed extensive structural and functional adaptations during host-parasite co-evolution. G. lamblia mitochondria-related organelles (mitosomes) are at the farthest extreme on the spectrum of mitochondrial reductive evolution with iron-sulphur protein maturation as the only identifiable biochemical pathway. We describe construction of the extensively diverged mitosome-specific proteome based entirely on protein-protein interactions, using the only identifiable component of a predicted TOM/TIM protein import complex (Tom40) as a starting point. Using serial co-immunoprecipitation assays and validation steps we extended a robust Tom40 core interactome network outwards, revealing additional outer membrane proteins and candidate links to membranes of the endoplasmic reticulum (ER), as well as inwards, identifying many novel imported proteins in addition to the few annotated conserved metabolic factors and chaperones. Live cell imaging revealed that the 30-40 organelles in a cell are highly immobilized and do not form dynamic networks, which is also consistent with interactome data suggesting physical links with the cytoskeleton, in particular with the basal body complex. On the other hand, identification of small GTPases and factors with dual mitosome and ER localization in the interactome suggested intimate connections with the ER. Functional analysis of mitosomes showed conceptual conservation of protein import although the machinery for translocation is diverged beyond recognition, as well as association of the single G. lamblia dynamin-related protein with mitosomes and direct evidence for its involvement in organelle morphogenesis. This study underscores the potential of this strategy for identification of proteins and machinery ab initio in a highly diverged but clearly delimited organelle system.

Author Summary

Organelles with endosymbiotic origin are present in all extant eukaryotes and have undergone considerable remodeling during > 1 billion years of evolution. Highly diverged organelles such as mitosomes or plastids in some parasitic protozoa are the product of extensive secondary reduction. They are sufficiently unique to generate interest as targets for pharmacological intervention, in addition to providing a rich ground for evolutionary cell biologists. The so-called mitochondria-related organelles (MROs) comprise mitosomes and

hydrogenosomes, with the former having lost any role in energy metabolism along with the organelle genome. The mitosomes of the intestinal pathogen Giardia lamblia are the most highly reduced MROs known and have proven difficult to investigate because of their extreme divergence and their unique physical properties. Here, we implemented a novel strategy aimed at systematic analysis of the organelle proteome by iterative expansion of a protein-protein interaction network. We demonstrated the effectiveness of serial co-immunoprecipitations combined with mass spectrometry analysis and in vivo validation for generating an interactome network centered on a giardial Tom40 homolog. This iterative ab initio proteome reconstruction provided protein-protein interaction data in addition to identifying novel organelle proteins and functions. Building on this information we investigated mitosome morphogenesis and organelle dynamics in living cells, and showed that the single giardial dynamin plays a role in organelle replication.

Introduction

Since the single endosymbiotic event leading to establishment of mitochondria approximately 2 billion years ago [1,2,3] these organelles have undergone massive changes and have evolved into highly specialized and essential subcellular compartments in all eukaryotes [4,5]. These changes comprise a dramatic size reduction, nuclear transfer of organelle genomes, and a renewal of the proteome, which is synthesized almost entirely as precursor proteins on cytosolic ribosomes [6,7,8,9,10,11,12,13] and imported from the cytoplasm [14]. Mitochondria have been remodeled and/or restructured to very different degrees in different species. Mitochondria-related organelles (MROs), i.e. hydrogenosomes and mitosomes [15,16,17,18,19] in some protists lacking canonical mitochondria represent extreme forms of reduction and/or divergence. The potential of highly diverged organelle-specific pathways as targets for intervention has sparked research into the evolution of MROs in single-celled organisms of all five eukaryotic supergroups [20,21]. Notably, the microaerophilic protozoan pathogens Entamoeba histolytica [19], Giardia lamblia [22,23], Blastocystis hominis [24] as well as obligate intracellular parasites such as Cryptosporidium parvum [25] and Encephalitozoon cuniculi [26] harbor highly reduced mitosomes. Interestingly, recent investigation of MROs in Spironucleus salmonicida, a diplomonad and the closest relative of G. lamblia belonging to the Excavata super-group, revealed that these organelles are in fact hydrogenosomes [27]. Although it has been demonstrated that G. lamblia mitosomes don't produce hydrogen, this sheds a completely new light on the evolution of MRO's in diplomonads.

Proliferating G. lamblia trophozoites contain 20-50 double membrane-bounded 100 nm spherical mitosomes [22,23] devoid of an organellar genome [28,29,30,31]. Although not proven experimentally, G. lamblia mitosomes are likely essential due to a subset of conserved mitochondrial proteins required for iron- sulphur (Fe-S) protein maturation [22,32,33,34,35]. Yeast genetic experiments suggested that Fe-S protein maturation, the only function currently ascribable to G. lamblia mitosomes, is in fact the minimal essential function of mitochondria [36]. Hence, these organelles have also generated considerable interest as cell biological models to study extreme reductive evolution of MROs [22,37,38,39,40,41,42]. However, due to massive, albeit selective sequence divergence in G. lamblia, conventional strategies for identification of mitosome proteins based on homology-based in silico searches fall short [26,28,32,43,44,45,46,47]. Moreover, proteome analyses approaches have had very limited success due to the small size of the organelles and the omnipresence of contaminating endoplasmic reticulum (ER) and cytoskeleton elements in enriched mitosome fractions [33,48].

Nevertheless, there is unambiguous experimental evidence for the functional conservation of the mitosomal protein import machinery [19,22,23]. The small subset of structurally conserved mitosome proteins such as G. lamblia IscU, ferredoxin, Cpn60, IscS and mtHsp70 are imported by transit peptide-dependent and -independent mechanisms [22]. However, the predicted components of the TOM/TIM import apparatus are diverged beyond recognition by state-of-the-art homology search tools or have been lost. Only one subunit of

the translocon in the outer mitochondrial (TOM) complex, a highly diverged Tom40 homologue (GlTom40), has been identified [49].

Because most G. lamblia mitosome components have undergone extreme sequence divergence or have been lost altogether, the vast knowledge about the molecular biology and biochemistry of mitochondria cannot be directly applied to investigations into evolution, morphogenesis, and function of these organelles. Hence, exploration of the range of G. lamblia mitosome functions requires alternative strategies aimed at comprehensive identification of their proteome and of essential Giardia-specific factors. We hypothesized that the diminutive organelles harbored no more than 100-150 different proteins inside or associated with a clearly delineated cellular compartment. Thus, it should be possible to use a putative GlTOM40 [22,33] as a starting point for identifying a core membrane interactome and extend this in an iterative process to eventually encompass the whole organelle proteome. The rationale for using GlTom40 as a starting point is the fact that it is the only, albeit poorly, conserved outer membrane protein and plays a key role for the import of organelle proteins. Using a series of co-immunoprecipitation assays we obtained a robust GlTom40 interactome and extend this network in both directions, i.e. outwards onto the cytoplasmic face of mitosomes, including peripheral membrane proteins such as a diverged putative TOM receptor (GlTom40R), and inwards, encompassing the few known and many novel imported organelle proteins. We used this information to probe mitosome morphogenesis and function and to test constraints for import of nuclear encoded mitosome proteins.

Materials and Methods

Giardia cell culture, induction of encystation, pulse-empty chase set-up and transfection

G. lamblia WBC6 (ATCC catalog number 50803) trophozoites were grown and harvested using standard protocols [50]. Encystation was induced with the two-step method as described previously [40,51]. Transgenic parasites were generated according to established protocols by electroporation of linearized pPacV-Integ-based plasmid vectors prepared from E. coli as described in [42]. After selection for puromycin resistance, transgenic G. lamblia cell lines were cultured and analyzed without antibiotic.

Construction of expression vectors

All sequences of oligonucleotide primers for PCR used in this work are listed in S1 Table.

For cloning of C-terminally hemagglutinin (HA)-tagged proteins in Giardia, a vector PAC-CHA was designed on the basis of the previously described vector pPacV-Integ [42], where additional restriction sites were inserted. A detailed vector map can be found in S1 Fig.

A cyst wall protein 1 promoter (pCWP1)-driven G. lamblia ferredoxin (fd)-human dihydrofolate reductase (DHFR) chimeric gene was generated by fusing two genes by overlapping PCR: i) an intron-less fd mitosomal targeting signal (MTS) (MTSfdΔint) open reading frame (ORF) was generated using primer pair 33 (S1 Table) with G. lamblia cDNA as template, ii) a DHFR_HA minigene was generated using primer pair 34 (S1 Table) with a cloned human DHFR cDNA as template. The fused product was digested with SpeI and PacI and inserted in a PAC vector to yield construct pCWP1_MTSfdΔint-DHFR_HA.

A pCwp1_ MTSfdΔint-DHFR_Neomycin resistance construct (without HA tag) was generated for protein import block assays. Primer pair 35 (S1 Table) was used on pCwp1_ MTSfdΔint-DHFR_HA as a template. The amplified product was digested with NsiI and PacI and ligated into a vector containing a neomycin resistance cassette [52].

Co-immunoprecipitation with limited cross-linking

G. lamblia WBC6 and transgenic trophozoites expressing C-terminally HA tagged bait proteins were harvested and subjected to immunofluorescence assay to confirm correct subcellular distribution of bait proteins. Parasites were collected by centrifugation (900 x g, 10 minutes, 4 °C), washed in 50 ml of cold phosphate buffer saline solution (PBS) and adjusted to 2 *107 cells .ml-1 in PBS (VWR Prolabo). The appropriate formaldehyde concentration for cross-linking (2.25%) was determined by a titration assay (S2 Fig). For the co-immunoprecipitation (co-IP) assays, 109 parasites were resuspended in 10 ml 2.25% formaldehyde (in PBS) supplemented with 1 mM phenylmethylsulfonyl fluoride (PMSF; SIGMA, Cat. No. P7626) and incubated for 30 minutes at room temperature (RT). Cells were pelleted, washed once with 10 ml PBS, and quenched in 10 ml 100 mM glycine in PBS for 15 minutes at RT. The collected cells were then resuspended in 5 ml RIPA lysis buffer (50 mM Tris pH 7.4, 150 mM NaCl, 1% IGEPAL, 0.5% sodium deoxycholate, 0.1% SDS, 10 mM EDTA) supplemented with 2 mM PMSF and 1 x Protease Inhibitor cocktail (PIC, Cat. No. 539131, Calbiochem USA) and sonicated twice using a Branson Sonifier with microtip (Branson Sonifier 250, Branson Ultrasonics Corporation) with the following settings: 60 pulses, 2 output control, 30% duty cycle and 60 pulses, 4 output control, 40% duty cycle. The sonicate was incubated on a rotating wheel for 1 h at 4 °C, aliquoted into 1.5 ml tubes and centrifuged (14,000 x g, 10 minutes, 4 °C). The soluble protein fraction was mixed with an equal volume detergent-free RIPA lysis buffer supplemented with 2% TritonX (TX)-100 (Fluka Chemicals) and 40 µl anti-HA agarose bead slurry (Pierce, product # 26181). After binding of tagged proteins to the beads at 4 °C for 2 h on a rotating wheel, beads were pulse-centrifuged and washed 4 times with 3 ml Tris-Buffered Saline (TBS) supplemented with 0.1% TX-100 at 4 °C. After a final wash with 3 ml PBS the loaded beads were resuspended in 350 µl PBS, transferred to a spin column (Pierce spin column screw cap, product # 69705, Thermo Scientific) and centrifuged for 10 s at 4 °C. Elution was performed by resuspending beads in 30 µl of PBS. Dithiothreitol (DTT; 100mM; Thermo Scientific, Cat. # RO861) was added and samples were boiled for 5 min followed by centrifugation (14,000 x g, 10 minutes, RT).

Protein analysis and sample preparation for mass spectrometry-based protein identification

SDS-PAGE and immunoblotting analysis of input, flow-through, and eluate fractions was performed on 4%-12% polyacrylamide gels under reducing conditions, (molecular weight marker Cat. No. 26616, Thermo Scientific, Lithuania). Transfer to nitrocellulose membranes and antibody probing were done as described previously [53]. Gels for mass spectrometry (MS) analysis were stained using Instant blue (Expedeon, Prod. # ISB1L) and de-stained with sterile water.

Mass Spectrometry and protein identification

Stained gel lanes were cut into 8 equal sections. Each section was further diced into smaller pieces and washed twice with 100 µl of 100 mM ammonium bicarbonate/ 50 % acetonitrile for 15 min at 50 °C. The sections were dehydrated with 50 µl of acetonitrile. The gel pieces were rehydrated with 20 µl trypsin solution (5 ng/µl in 10 mM Tris-HCl/ 2 mM CaCl2 at pH 8.2) and 40 µl buffer (10 mM Tris-HCl/ 2 mM CaCl2 at pH 8.2). Microwave-assisted digestion was performed for 30 minutes at 60 °C with the microwave power set to 5 W (CEM Discover, CEM corp., USA). Supernatants were collected in fresh tubes and the gel pieces were extracted with 150 µl of 0.1% trifluoroacetic acid/ 50% acetonitrile. Supernatants were combined, dried, and the samples were dissolved in 20 µl 0.1% formic acid before being transferred to the autosampler vials for liquid chromatography-tandem MS (injection volume 7 to 9 µl). Samples were measured on a Q-exactive mass spectrometer (Thermo Scientific) equipped with a nanoAcquity UPLC (Waters Corporation). Peptides were trapped on a Symmetry C18, 5 µm, 180 µm x 20 mm column (Waters Corporation) and separated on a BEH300 C18, 1.7 um, 75 µm x 150 mm column (Waters Corporation) using a gradient formed between solvent A (0.1% formic acid in water) and solvent B (0.1% formic acid in acetonitrile). The gradient started at 1% solvent B and the concentration of solvent B was increased to 40% within 60 minutes. Following peptide data acquisition, database searches were performed using the MASCOT search program against the G. lamblia database

(http://tinyurl.com/37z5zqp) with a concatenated decoy database supplemented with commonly observed contaminants and the Swissprot database to increase database size. The identified hits were then loaded onto the Scaffold Viewer version 4 (Proteome Software, Portland, US) and filtered based on high stringency parameters (minimal mascot score of 95% for peptide probability, a protein probability of 95%, and a minimum of 2 unique peptides per protein). For a description of relaxed conditions see "Results".

In silico co-immunoprecipitation dataset analysis

Analysis of primary structure and domain architecture of putative mitosomal hypothetical proteins was performed using the following tools and databases: MITOPROT (http://ihg.gsf.de/ihg/mitoprot.html) and PSORTII (http://psort.hgc.jp/form2.html) for subcellular localization prediction, TMHMM (http://www.cbs.dtu.dk/services/TMHMM/) for transmembrane helix prediction, SMART (http://smart.embl-heidelberg.de/) for prediction of patterns and functional domains, pBLAST for protein homology detection (http://blast.ncbi.nlm.nih.gov/Blast.cgi?PAGE=Proteins), HHPred (http://toolkit.tuebingen.mpg.de/hhpred) for protein homology detection based on Hidden Markov Model (HMM-HMM) comparison, and the Giardia Genome Database (http://giardiadb.org/giardiadb/) to extract other/organism-specific information, e.g. expression levels of the protein, predicted molecular size and nucleotide/protein sequence. For functional domains predicted by SMART we used an e-value of 10e-5 as cutoff, and for protein homologies predicted by pBLAST we accepted alignment scores above 80. However, since G. lamblia homologs for eukaryotic proteins are highly diverged, we also considered functional domain predictions associated to a lower e-value. Alignment scores between 50 and 80 were accepted only when pBLAST predictions were consistent with HHPred output.

Immunofluorescence analysis (IFA) and microscopy

Preparation of chemically fixed cells for immunofluorescence and analysis of subcellular distribution of reporter proteins by wide-field and confocal microscopy were done as described previously [42,53]. Nuclear labelling was performed with 4',6-diamidino-2-phenylindole (DAPI).

Live-cell microscopy and fluorescence recovery after photobleaching (FRAP)

Transgenic G. lamblia trophozoites expressing GFP-GlTom40 or Gl29147-GFP were harvested and prepared for imaging in PBS supplemented with 5 mM glucose (Cat. No. 49139, Fluka), 5 mM L-cysteine (Cat. No. C6852, Sigma) and 0.1 mM ascorbic acid (Cat. No. 95209, Fluka) at pH 7.1. FRAP and time-lapse series were performed as described previously [53,54] .

Sample preparation for transmission electron microscopy

Transgenic trophozoites ectopically expressing wild type G. lamblia dynamin related protein (GlDRP) (ORF Gl50803_14373) or the constitutively active (GTP-locked) GlDRP-K43E variant under the control of the CWP1 promoter [54] were harvested 3 h post induction and analyzed by transmission electron microscopy (TEM) as described previously [54].

Sub-cellular fractionation analysis

For sub-cellular fraction experiments, 4.106 GlDRP-HA and GlDRP-K43E-HA- expressing transgenic cells were lysed by freeze-thawing and supernatant (soluble fraction) and pellet (membrane fraction) were prepared by centrifugation at 14'000 x g for 10 minutes at 4 °C. The HA-tagged proteins were detected by SDS-PAGE and Western blot using a rat anti-HA mAb (clone 3F10, Roche) as described previously [53].

DHFR-MTX protein import block assay

The MTSfdΔint-DHFR fusion (see also above under "Constructs") was expressed under the control of the inducible CWP1 promoter in a background transgenic line constitutively expressing HA- tagged 17030 (cell line

Cwp1_MTSfdΔint-DHFR/Gl17030HA). DHFR expression was induced using the 2-step method [40] for 4 h and "chased" for 24 h by placing the cells again in standard growth medium in the presence or absence of 1 μM methotrexate (MTX). Total cell lysates were separated by SDS-PAGE and Western blot to detect processed and unprocessed forms of the Gl17030HA reporter. Subcellular distribution was analyzed by immunofluorescence assay (IFA) using wide field microscopy.

Results

Co-IP with the G. lamblia Tom40 homolog identifies novel interacting proteins of the mitosome outer membrane

Despite efforts aimed at defining the protein content of mitosomes [49] in Giardia, the composition of this organelle's membrane proteome and specifically the predicted import machinery in the outer and inner membranes remained unknown, with the exception of a highly diverged putative Tom40 homologue (GlTom40; ORF Gl50803_17161) [49]. To generate the first mitosome outer membrane proteome we focused on GlTom40 as a point of origin and developed a customized co-IP protocol with an HA-tagged variant as "bait". A transgenic line GlTom40-HA constitutively expressing the epitope-tagged bait protein was generated; exclusive mitosome localization of the bait protein in transgenic cells was confirmed by IFA (Fig. 1A). However, a broad range of conditions and detergents that are standard for purifying mitochondrial membrane proteins [55] yielded not a single protein associated to the GlTom40-HA bait in initial co-IP experiments (data not shown). Because conditions necessary for solubilizing the strongly curved double membranes of these tiny organelles apparently also dispersed all GlTom40-interacting proteins, we used carefully titrated, formaldehyde-based cross-linking [56] to stabilize predicted protein-protein interactions for co-IP experiments (S2 Fig; see also in Materials and Methods). Co-IP and tandem MS analyses yielded a first Tom40 interactome dataset (GlTom40 co-IP); a control dataset obtained from un-transfected cells (ctrl co-IP) was generated under identical conditions for data filtration, i.e. identification and elimination of hits in GlTom40 co-IP generated by non-specific interactions (e.g. physical trapping). Data processing was done in Scaffold4 viewer (http://www.proteomesoftware.com/products/free-viewer/) initially with high stringency parameters (95_2_95), yielding a total of 78 hits with a false discovery rate (FDR) of 0% (S2 Table). Data filtering showed 46 hits exclusively in the GlTom40 co-IP dataset, whereas 31 proteins were identified in both datasets and 1 protein was exclusive to the ctrl co-IP dataset (Fig. 1B). The 46 GlTom40-

Fig. 1

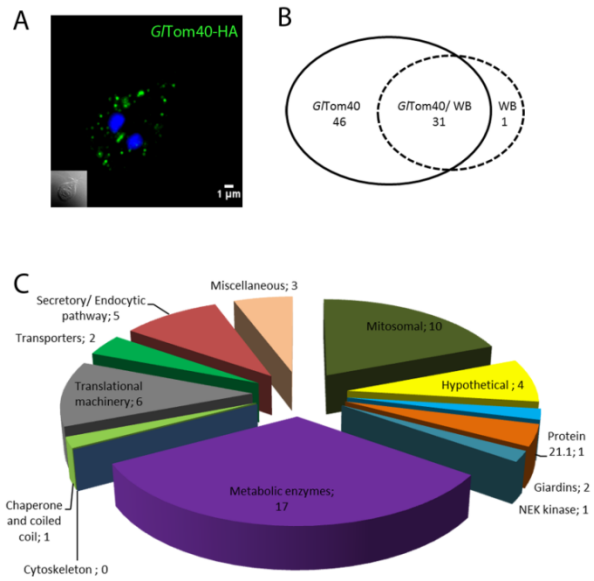

Fig 1. Co-IP with G. lamblia Tom40 yields numerous candidate interacting proteins.

(A) Immunofluorescence microscopy: C-terminally HA-tagged GlTom40 (GlTom40-HA) is an exclusive marker for mitosomes (green). Nuclear DNA is stained with DAPI (blue). Inset: DIC image. (B) Venn diagram indicating 46 GlTom40 specific hits. (C) Parsing of 46 GlTom40-specific proteins and an additional 6 candidates from the GlTom40/ctrl co-IP overlap that had peptide ratios >5 (metabolic and/or functional categories are indicated in the pie chart).

specific hits and an additional 6 candidates from the GlTom40/ctrl co-IP intersection that had peptide ratios >5 (S3 Table) were parsed and subdivided into different metabolic and/or functional categories (Fig. 1C). Four previously identified mitosome proteins were detected: mitochondrial HSP70 (ORF Gl50803_14581), oxidoreductase 1 (GlOR1; ORF Gl50803_91252) and hypothetical proteins Gl50803_9296 and Gl50803_14939 [33]. Based on the topology of GlTom40 in the outer membrane and the conditions used in these co-IP experiments, it was not surprising to find 20 hits for annotated metabolic enzymes and other cytosolic components which could be eliminated from the candidate pool. We extracted additional information from the GlTom40 co-IP data by relaxing stringency parameters to (95_1_95), obtaining a total of 150 proteins (FDR 3.4%; S4 Table). Of these, 109 hits were exclusive to the expanded GlTom40 co-IP dataset, whereas 40 proteins were identified in both datasets and 1 protein was exclusive to the ctrl co-IP dataset. Of note, the expanded dataset contained three additional annotated mitosome proteins namely, chaperonin 60 (Cpn60; ORF Gl50803_103891), GlQb-SNARE 3 (putative Sec20, ORF Gl50803_5161) and NifU-like protein (ORF Gl50803_15196). Pending validation of the remaining non-annotated hits strongly suggests that the expanded dataset contains additional as yet unidentified mitosome proteins.

Validation of the GlTom40 co-IP data

Because of the non-targeted nature of limited chemical cross-linking in co-IP assays we performed careful validation of the datasets generated in these experiments based on two criteria: i) subcellular localization of ectopically expressed, epitope-tagged candidates to mitosomes, and ii) successful retrieval of the endogenous protein previously used as bait in reverse co-IP experiments.

To test subcellular localization we selected 13 of the 109 candidate Tom40 interacting proteins based on MASCOT scores or protein domains identified in HHPred. The 9 hypothetical proteins with the highest MASCOT scores and four additional candidates with domains predicted to be involved in mitochondrial functions (S5 Table) were cloned as endogenous promoter-driven C-terminally HA-tagged variants into a G. lamblia expression vector and used to generate transgenic lines [57]. Using IFA of chemically fixed transgenic cells, we confirmed mitosomal localization for 8 out of 9 candidates (Figs. 2A-2N). This high proportion underscores the quality of the GlTom40 co-IP dataset. Interestingly, 4 proteins without annotation (ORFs Gl50803_ 21943, 22587, 5785 and 9503) presented dual localization (mitosome and ER) (Figs. 2F-2I). The cartoon in Fig. 2O shows a consolidated depiction of a first GlTom40 interactome, which includes the 8 proteins localized to mitosomes described above, as well as 4 previously identified matrix proteins and 3 newly validated hypothetical proteins comprised in the list of GlTom40 interacting proteins.

Fig. 2

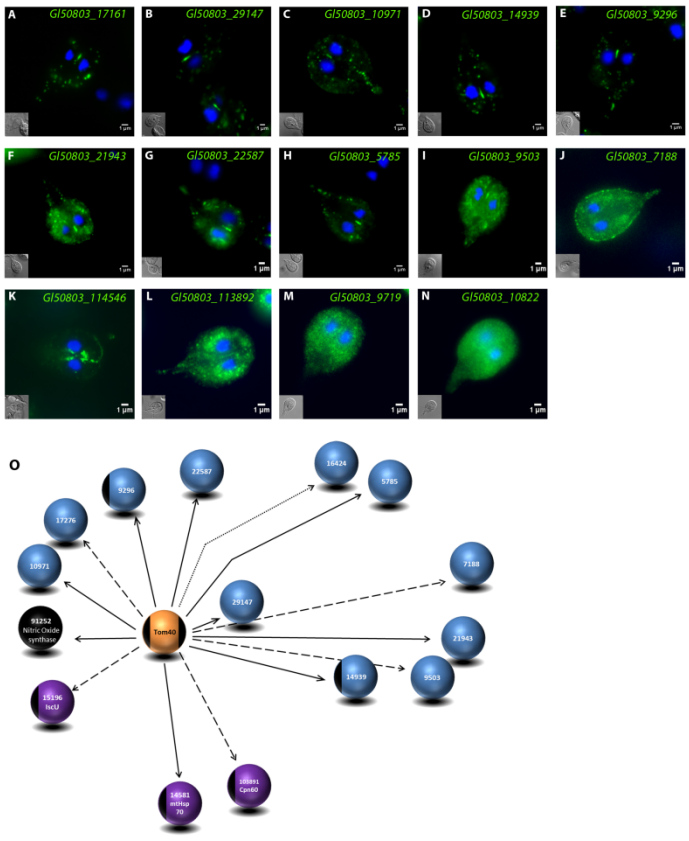

Fig 2. Subcellular localization of candidate GlTom40 interaction partners.
(A-N) Immunofluorescence microscopy: subcellular localization of C-terminally HA-tagged GlTom40 and 13 putative interaction partners (green) falls into 3 categories: Typical mitosome localization (A-E); dual localization to mitosomes and ER (F-I); no or ambiguous mitosome localization (J-N). Nuclear DNA is stained with DAPI (blue). Insets: DIC image. (O) Partially validated GlTom40 interactome showing the bait protein (orange sphere), matrix proteins (purple), previously identified and mitosome-localized proteins (black), and mitosome-localized hypothetical proteins (blue). The stringency parameters used for detection (high, medium, and relaxed) are represented by bold, dashed, and dotted arrows, respectively.

To test the second validation criterion, we performed reverse co-IP experiments, using the GlTom40 interaction partner with the highest MASCOT score (Gl50803_29147) as a first bait. The gene codes for a predicted single-pass transmembrane protein of 133 amino acids with mitosomal localization of an HA-tagged variant confirmed by fluorescence microscopy (Fig. 2B). Its domain structure is reminiscent of Tom40 receptors found in mitochondria of higher eukaryotes, i.e. a transmembrane helix in the N-terminal part of the protein followed by a cytoplasmically exposed C-terminal domain as predicted by TMHMM (http://www.cbs.dtu.dk/services/TMHMM/). Although experimental confirmation of a receptor function is pending, we henceforth refer to the Gl50803_29147 product as GlTom40R. A cell line, constitutively expressing HA-tagged GlTom40R as a mitosome-localized co-IP bait protein produced a dataset of 221 GlTom40R co-IP exclusive proteins after filtering and elimination of all hits intersecting with the ctrl co- IP fraction at high stringency parameters (Fig. 3A; S6 Table). Importantly, the GlTom40R-HA bait protein and endogenous GlTom40 were detected with high MASCOT values, confirming the GlTom40 – GlTom40R interaction. The 221 GlTom40R co-IP specific hits and an additional 20 candidates from the GlTom40R/ctrl co-IP intersection that had peptide ratios >5 were parsed according to different metabolic and/or functional categories (Fig. 3B; S7 Table). In addition to GlTom40, the dataset contained several known mitosomal proteins, including matrix proteins HSP70 and GiOR1, cysteine desulfurase (IscS; Gl50803_14519), Cpn60, [2Fe-2S] ferredoxin (Gl50803_27266) and NifU-like protein. Using high stringency criteria, we retrieved all 8 hypothetical proteins previously identified in the GlTom40 co-IP dataset and 4 additional non-annotated candidate mitosome proteins listed in S8 Table (Fig. 3C-3F). Taken together, combined subcellular localization experiments and a first reverse co-IP dataset using the single-pass transmembrane GlTom40-interacting protein GlTom40R provided robust validation of the experimental approach used to identify mitosome membrane proteins, and has expanded the predicted mitosomal membrane and import machinery interactome to 22 proteins (Fig. 3G). Interestingly, this dataset contained two axoneme-associated GASP-180 proteins (Gl50803_137716 and Gl50803_16745) [58]with high MASCOT scores.

The two high-stringency co-IP datasets suggests a strong interaction between GlTom40 and GlTom40R. Thus, hits appearing in the intersection of the two are considered to be particularly informative (Fig. 3H). The curated list of hits after elimination of obvious cytoplasmic contaminants (S9 Table) contains 27 candidates, 10 of which have now been confirmed as mitosome proteins.

Fig 3. Expansion and validation of the interactome by reverse co-IP with GlTom40R.
(A) Venn diagram showing GlTom40R-specific proteins identified after filtering the dataset. (B) Parsing of 221 bait-specific and an additional 20 candidates from the GlTom40R/ctrl co-IP overlap that had peptide ratios >5 (metabolic and/or functional categories are indicated in the pie chart). (C-F) Subcellular localization of selected C-terminally HA-tagged novel hypothetical proteins by IFA (green). Nuclear DNA is stained with DAPI (blue). Insets: DIC images. (G) Preliminary interactome of GlTom40 and GlTom40R showing validated hits. Bait proteins (orange spheres), matrix proteins (purple), previously identified and localized proteins (black), and localized hypothetical proteins (blue). The stringency parameters used for detection (high, medium, and relaxed) are represented by bold, dashed, and dotted arrows, respectively. (H)

Fig. 3

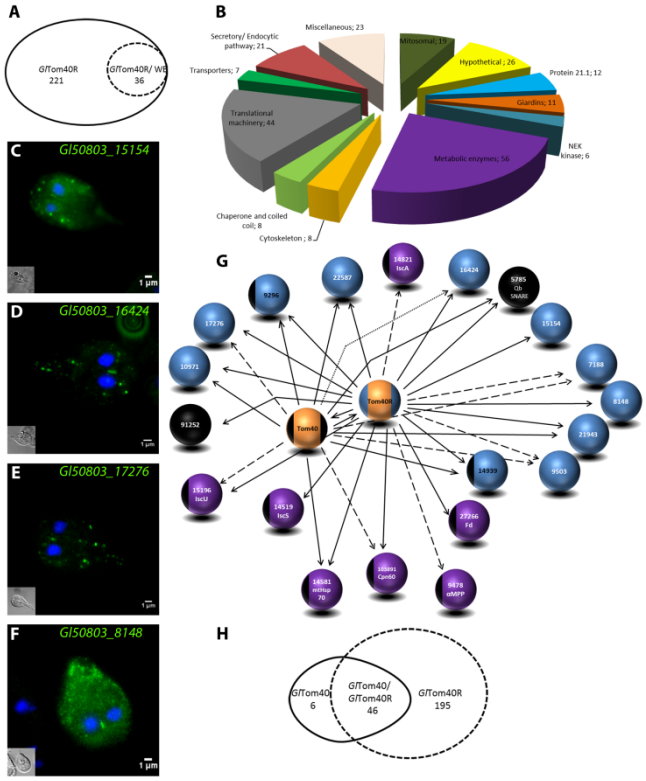

Co-IP experiments confirm GlTom40-specific protein-protein interactions and reveal strong links with four additional mitosome proteins

In the absence of an absolute measure for strength/affinity of the physical interaction between proteins in these interactomes we used MASCOT peptide scores as a non-exclusive qualitative criterion for "interaction" in a preliminary manner. To determine a robust GlTom40- and GlTom40R-centered core interactome consisting of the most frequently detected interaction partners and, more importantly, to explore the boundaries of the growing interaction network (Fig. 3G), we performed a series of additional co-IP experiments using HA-tagged Qb-SNARE 4 (Gl50803_5785), GlIscS, and hypothetical proteins Gl50803_9296 and Gl50803_14939 as baits. These proteins were chosen because they were identified, in some cases exclusively, in both the GlTom40- and GlTom40R co-IP datasets (S2 and S6 Tables), suggesting they may be most proximal to GlTom40. Furthermore, mitosomal localization of all four HA-tagged bait proteins was confirmed by IFA (Fig. 2). As was done previously, all bait-specific datasets were processed by filtering with a ctrl co-IP dataset generated from un-transfected trophozoites and analyzed in MASCOT using high stringency (95_2_95) and more relaxed (95_1_95) parameters.

Co-IP with the mitosome transmembrane protein Gl50803_14939

Gl50803_14939, which contains two transmembrane domains (TMD), was analyzed because of its potential role as a component of the import complex. Using high stringency parameters (95_2_95) 129 proteins with a FDR of 10% were detected with 93 candidates specific for the Gl14939 co-IP dataset (S10 Table). Both GlTom40 and G. lamblia oxidoreductase 1 (GiOR1; ORF Gl50803_91252) were detected with these parameters, in addition to several previously identified hypothetical mitosome proteins (e.g. GlTom40R, Gl50803_10971 and Gl50803_7188) (Fig. 4A). This further supports the idea that Gl50803_14939 is a significant interacting partner of GlTom40 and GlTom40R.

Fig 4. Validation of the GlTom40 interactome by reverse co-IP using four additional mitosome proteins as bait.
(A) Gl14939, (B) Gl5785, (C) GlIscS and (D) Gl9296 –derived interactomes. (E, F) Alternative depictions of the cumulative interactome of proteins localizing to mitosomes generated with 6 bait proteins. Note the tight association of GlTom40 with GlTom40R and Gl14939. (F) Matrix and soluble proteins are grouped at the bottom left, proteins with dual localization (ER and mitosomes) and possibly involved in inter-organelle communication are grouped at the top right. GlDRP is pulled down with all 6 bait proteins used in the co-IP assay and is also included (green sphere). Bait proteins (orange spheres), matrix proteins (purple), previously identified and localized proteins (black), and localized hypothetical proteins (blue). The stringency parameters used for detection (high, medium, and relaxed) are represented by bold, dashed, and dotted arrows, respectively.

Fig. 4

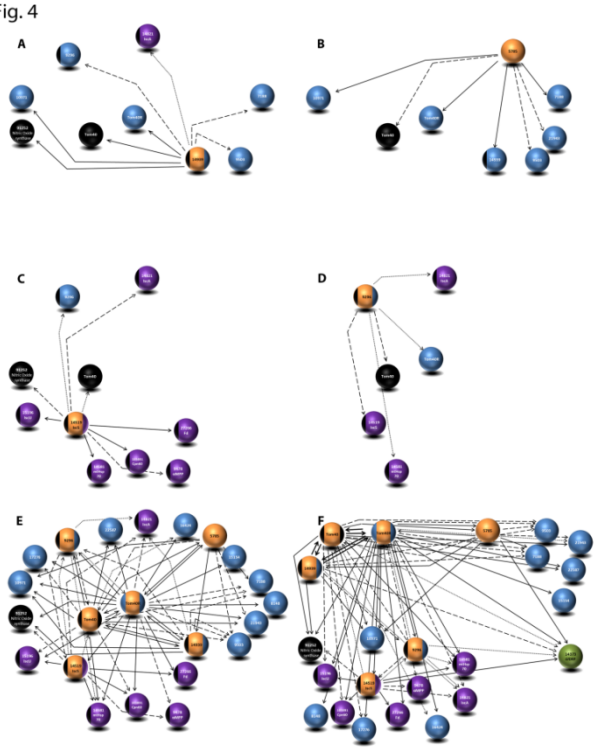

Co-IP with the predicted outer membrane protein Qb-SNARE 4 (Gl50803_5785)

Qb-SNARE 4 has dual localization, (mitosome and ER; Fig. 2H) and was identified in both the GlTom40 co-IP and the GlTom40R reverse co-IP datasets. This suggests that Qb-SNARE 4 may have a role in inter-organelle communication between mitosomes and the ER, and potentially in protein/lipid transport [59,60]. We reasoned that identifying interaction partners could shed light on the nature of physical contacts between mitosomes and other membrane-bounded compartments. MS analysis of the Gl5785 co-IP dataset with medium stringency parameters (95_1_95) yielded a total of 260 proteins with a FDR of 0% of which 157 were bait-specific after filtering with ctrl co-IP (S11 Table). The bait protein itself along with Gl14939 were the only 2 proteins detected with high MASCOT values (≥ 5 peptide score). Several non- annotated proteins, e.g., Gl50803_10971, GlTom40R, Gl50803_7188, GlTom40 as well as Type III DnaJ protein Gl50803_9751 were detected with lower MASCOT values (>1 but <5). Interestingly, another hypothetical protein in this dataset, Gl50803_9503, was also shown to have a dual localization (Fig. 2I). This protein was present in the GlTom40 co-IP and GlTom40R co-IP datasets with medium stringency parameters (95_1_95). Identification of Gl50803_9503 by the SNARE proteins and bait proteins harboring trans-membrane domains combined with dual localization to mitosomes and ER suggests that this protein might be involved in the organization of physical contact points, establishing direct links between mitosomes and ER. All known or previously identified proteins interacting with Gl5785 are depicted in Fig. 4B.

Co-IP with the matrix protein cysteine desulfurase (GlIscS)

Cysteine desulfurase (Gl50803_14519) is a mitosomal matrix protein and the central component of the Fe-S assembly machinery [61]. All mitosomal matrix proteins including GlIscS are translated in the cytoplasm and reach their final destination after unfolding and translocation across the mitosome double membrane. Thus, this trafficking route (cytoplasm – translocon – matrix) should be reflected in the protein-protein interactions of a co-IP dataset with Gl14519-HA as bait. The MS dataset contained a total of 208 proteins using high stringency parameters (95_2_95), with a FDR of 1.5%. After filtering with ctrl co-IP, 177 bait-specific hits remained (S12 Table). Among those, we identified 5 known matrix proteins namely, NifU-like protein, HSP70, [2Fe-2S] ferredoxin, Cpn60, and GiOR1. GlTom40 as the sentinel protein for the translocon was detected only with relaxed stringency (50_1_50, FDR of 30%). Seventy out of 177 hits were highly specific for GlIscS with ≥ 5 peptide counts. Eighteen of those (25%) belong to the Protein 21.1 family. The biological function of this cytoplasmic protein family in G. lamblia and the significant association to GlIscS is not known [62]. The frequency of hits for 21.1 family members in the dataset might be relevant in the context of stabilization of GlIscS in the cytoplasm before translocation and merits further investigation. No additional candidate components of the import machinery (i.e. novel proteins harboring TMDs) and/or novel or previously identified soluble proteins were identified using Gl14519 as bait protein. However, 43 additional hypothetical proteins still remain to be investigated for their localization and putative function. Fourteen out of 43 hypothetical proteins have high MASCOT values (peptide score of >5). Interestingly, MITOPROT analysis suggests that six out of these fourteen proteins harbor an identifiable MTS (S13 Table) and thus merit further investigation. All known/ previously identified proteins interacting with Gl5785 at varying stringency parameters are depicted in Fig. 4C.

Co-IP with a hypothetical imported mitosome protein Gl50803_9296

Gl50803_9296 is a predicted soluble protein of unknown function localizing exclusively to mitosomes (Fig. 2E). Despite this, MS data analysis performed at high stringency parameters (95_2_95) yielded only 22 proteins with a FDR of 0% with 12 bait-specific hits. The bait protein itself was by far the most significant hit in the dataset and under stringent analysis conditions the dataset contained no known mitosome proteins. Analysis with more relaxed stringency parameters (90_1_90) yielded 85 proteins with a FDR of 6.2% with 47 bait-specific identifications (S14 Table). Aside from the bait, 2 known mitosome proteins namely, GlIscS and GlTom40 were identified. Taken together, the Gl9296 co-IP dataset suggests that this mitosome protein doesn't have an interactome enriched in matrix or membrane proteins despite its clear-cut localization and considerable expression levels judged by the signal obtained in Fig. 2E. Its localization might be in the intermembrane space, but remains to be determined. The fact that the putative GlTom40R was identified once with a very low stringency of 20_1_20 with a FDR of 51% suggested that Gl9296 and GlTom40R don't interact directly, but could be connected via bridging proteins. All identified Gl9296-interacting proteins are depicted in Fig. 4D.

In summary, we have generated an extensive protein interaction network (Fig. 4E) from 6 independent co-IP assays using GlTom40 and 5 interaction partners (GlTom40R, Gl50803_14939, Gl50803_5785, Gl50803_14519 and Gl50803_9296) selected as baits based on i) number of peptide hits in the GlTom40 co-IP dataset and ii) confirmed localization of epitope-tagged variants to mitosomes by IFA. Pending final validation of the >200 novel candidate matrix-, outer membrane, and membrane-associated mitosome components, the validated information from this series of co-IP experiments will be instrumental to refine and complete the current map of the mitosome protein repertoire shown in (Fig. 4E and 4F).

Pharmacological induction of a mitosome matrix-targeted DHFR complex generates a protein import block and inhibits processing of an endogenous reporter in mitosomes

The highly diverged GlTom40 orthologue in the G. lamblia genome is considered the translocase across the outer mitosomal membrane. However, there are currently no reports on the organelle-specific effects of interference on protein import into mitosomes. We tested to what degree mitosome protein import is functionally conserved with respect to the corresponding process in bona fide mitochondria by adapting the DHFR-folate analogue system [63] to G. lamblia. Pre-sequence directed DHFR is a classical substrate used in protein translocation studies due to its ability to fold irreversibly upon binding a folate analog, e.g. MTX. Complexed with MTX, DHFR becomes unsuitable as a substrate for import and blocks translocons, which results in a general blockage of organelle protein import [63]. Transfection of MTSfdΔint-DHFR into a Gl17030-HA background, i.e. a line expressing a HA-tagged MTS-directed mitosomal reporter, allowed testing of the general effects of MTX-induced import block. Importantly, G. lamblia lacks a DHFR homologue, and heterologous over-expression of human DHFR did not result in any detectable phenotypic aberration or change in growth rate (data not shown). We reasoned that the presence of MTX in MTSfdΔint-DHFR expressing cells would lead to an import block with cytosolic accumulation of the unprocessed form of Gl17030-HA due to jamming of the translocase. IFA indeed showed an increased cytosolic Gl17030-HA signal after addition of 1 μM MTX (Fig. 5B) compared to parasites exposed to the solvent alone (Fig. 5A). To test whether this was due to a generalized import block we measured the ratio of the slightly larger Gl17030-HA reporter precursor protein (+MTS) and the imported and therefore processed form (-MTS) by SDS-PAGE and Western blot using anti-HA antibodies. We detected accumulation of unprocessed Gl17030-HA in the MTX treated sample, whilst in the absence of MTX, only the processed form was present (Fig. 5C). Taken together the data strongly supported functional conservation of the structurally highly diverged protein import machinery of G. lamblia mitosomes.

Fig. 5

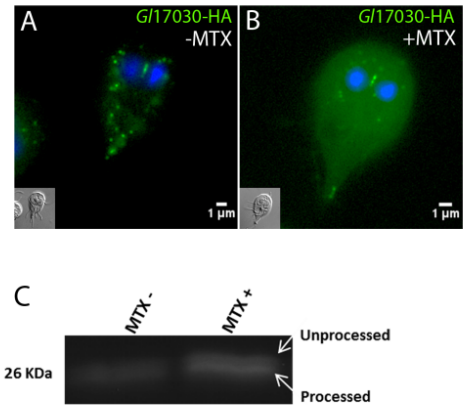

Fig 5. Mitosome-targeted DHFR protein blocks import and processing of a reporter in transgenic cells treated with MTX.

Subcellular distribution of a matrix targeted reporter (Gl17030-HA) without MTX (A) or after addition of 1µM MTX for 24 h (B) in transgenic cells expressing mitosome-targeted DHFR. Note the accumulation of HA-signal in the cytoplasm. Nuclear DNA is stained with DAPI (blue). Insets: DIC images. (C) Immunoblot analysis detects accumulation of unprocessed Gl17030-HA in the presence of MTX.

Conditional ectopic expression of a dominant-negative GTP-locked DRP variant elicits a mitosome morphogenesis phenotype

Despite intensive research in the field of MROs, little is known regarding factors required for their division. Dynamin-related proteins (DRPs) are implicated in mitochondrial and hydrogenosome division in higher eukaryotes and in protozoa such as Trypanosoma brucei [64,65] and Trichomonas vaginalis [66]. G. lamblia harbors a single DRP (ORF Gl50803_14373) [54] with a previously documented role in trafficking of cyst wall material, and endocytic and exocytic organelle homeostasis [54]. Interestingly, GlDRP was strongly overrepresented in 3 high-stringency co-IP datasets where mitosome membrane proteins were used as bait. Moreover, with relaxed stringency parameters GlDRP was detected in all 6 co-IP datasets (Fig. 6H). To test for a hitherto unrecognized role of GlDRP in determining mitosome morphology and/number, we used a dual cassette expression vector [53] to express constitutive C-terminally myc-tagged GlTom40 and inducible C-terminally HA-tagged wild-type (GlDRP) or GTP-locked (GlDRP-K43E) variants in trophozoites. IFA analyses (Fig. 6A- 6F) demonstrate how the subcellular distribution for GlTom40-myc changed from “dispersed” in cells expressing GlDRP-HA (Fig. 6A-6C) to “clustered” (Fig. 6D-6F), indicative of enlarged organelles in cells expressing GlDRP-K43E-HA. Consistent with this phenotype and in line with previous reports [54], the subcellular distribution of HA-tagged GlDRP remained mostly cytosolic (Fig. 6B). Conversely, GlDRP-K43E-HA showed a punctate distribution (Fig. 6E) and significant signal overlap with GlTom40-myc (Fig. 6F), suggesting selective accumulation of GlDRP-K43E-HA on mitosome membranes. We tested whether this marked association of ectopically expressed GlDRP-K43E with organelle membranes compared to the wild type DRP variant in IFA could be corroborated in cell fractionation experiments. Separation by SDS-PAGE and immunoblot analysis revealed that epitope-tagged GlDRP-HA was almost equally distributed between the “cytosolic” and “membrane” fraction, whereas the mutated variant GlDRP-K43E-HA was detected only in the “membrane” fraction (Fig. 6G). This data was consistent with the microscopical analysis in Fig. 6E and a strongly increased association with organelle membranes compared to wild-type GlDRP-HA. To characterize the nature of the GlDRP-K43E phenotype in more detail, we performed transmission electron microscopy of induced transgenic cells. Cells expressing the GTP-locked GlDRP-K43E-HA variant frequently presented elongated and tubular mitosome structures (Fig. 6J and 6K) compared to cells expressing wild type GlDRP (Fig. 6I). This was consistent with IFA data in Fig. 6D and 6A and suggestive of an organelle morphogenesis phenotype. Taken together, these data provide an explanation for the frequent detection of GlDRP in co-IP datasets and strongly support a transient association of GlDRP to these organelles. The phenotype elicited by expression of GTP-locked GlDRP-K43E-HA suggests a previously unappreciated role for this GTPase in the maintenance of mitosome integrity and organelle morphogenesis.

Fig. 6

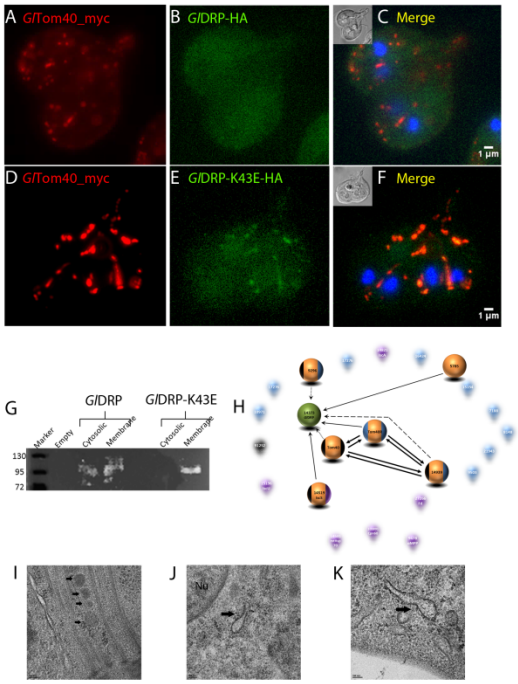

Fig 6. Conditional expression of GlDRP-K43E elicits a mitosome morphogenesis phenotype.
(A-C) Subcellular localization of a C-myc tagged GlTom40 (red) by IFA in cells induced to express a wild type GlDRP (green) or GlDRP-K43E (D-F). Note the altered size and distribution of organelles labeled with Tom40-myc in GlDRP-K43E expressing lines. Nuclear DNA is stained with DAPI (blue). Insets: DIC images (G) -Cell fractionation experiments confirm fixed membrane localization of GlDRP-K43E. (H) GlDRP (green) is associated to 6 bait proteins and identified at different stringency parameters as depicted in the GlTom40-centered interactome. Bait proteins (orange spheres), matrix proteins (purple), previously identified proteins (black), and localized hypothetical proteins (blue). The stringency parameters used for detection (high, medium, and relaxed) are represented by bold, dashed, and dotted arrows, respectively. (I) TEM: normal morphology of mitosomes (black arrows) in the CMC in cells expressing wild type GlDRP whilst cells expressing GlDRP-K43E show enlarged dumbbell-shaped mitosomes (black arrow in J, K) indicative of defective organelle division. Nu: nucleus. Scale bars: 100 nm.

G. lamblia mitosomes are immobilized and do not form dynamic networks

Mitochondria in higher eukaryotes are highly dynamic organelle networks that move in the cell via microtubules and microfilaments and undergo constant fission and fusion to meet the energy requirements of the cell [67,68]. IFA and TEM analyses suggest that G. lamblia mitosomes are very small spherical organelles with no evidence of network formation. In addition, the mitosome population in each cell can be divided into peripheral mitosomes (PM) distributed randomly in the cytoplasm and what has been dubbed the central mitosome complex (CMC) [22]. The latter appear to form a grape-like cluster of individual organelles of the size and shape of peripheral mitosomes that is closely and permanently associated to the basal body complex between the two nuclei [22]. Interestingly, these organelles remain separate despite their close proximity. The motility of this central cluster is restricted to segregation with the duplicated basal body complex during cell division [22]. However, no information is available on the spatial dynamics of peripheral mitosomes in the cytoplasm. We investigated organelle dynamics in living cells by performing time lapse microscopy of cells expressing GFP-tagged mitosome reporters. Conditional expression of N-terminally GFP-tagged GlTom40 with 3 h of induction followed by “chasing” newly-synthesized GFP-Tom40 into mitosomes over 2-3 h in normal conditions can be used to label organelles for imaging (Fig. 7A and 7B). Tracking of individual organelles over a period of >30 min showed no significant cytoplasmic movement or changes in morphology (Fig. 7C), suggesting that organelles neither move randomly nor are they transported directionally in the cytoplasm along cytoskeleton structures. This is consistent with the lack of motor proteins in any of the interactomes, suggesting that peripheral organelles do not undergo frequent fusion and fission and may have lost the ability for fusion altogether. To test whether mitosome outer membrane proteins are exchanged between organelles we performed FRAP experiments on cells conditionally expressing GlTom40-GFP. Since GlTom40-GFP is membrane-anchored, FRAP addresses the question how isolated mitosome organelles are and whether they form membrane continuities. No recovery of fluorescence in bleached CMC or PM organelles was detected (Fig. 7D- 7G), even when re-imaging bleached areas after 20 min. Identical outcomes were observed in cells constitutively expressing GFP-tagged GlTom40R (data not shown). GFP-tagged GlTom40R was expressed constitutively from episomal (circular) expression vectors. The reporter localized exclusively to mitosome organelles in all cases, but many cells showed a mitosome morphology dubbed “string” phenotype suggestive of extensive elongation of organelles to large tubules (Fig. 7H). In many cases, virtually all PMs had been replaced by a single long organelle with a diameter that corresponded to that of an individual mitosome. FRAP

analysis confirmed that these tubular mitosomes were made from a single contiguous membrane (data not shown). Although the "string" mitosome phenotype was compatible with survival of the parasites, many trophozoites appeared to be delayed or even arrested in cytokinesis and had a typical heart-shaped appearance (Fig. 7I) previously observed in cells which cannot complete cytokinesis [69]. Because the tubular organelles ran through the non-divided part connecting both daughter cells, we postulated that inability to divide mitosomes impairs completion of cytokinesis.

Fig. 7

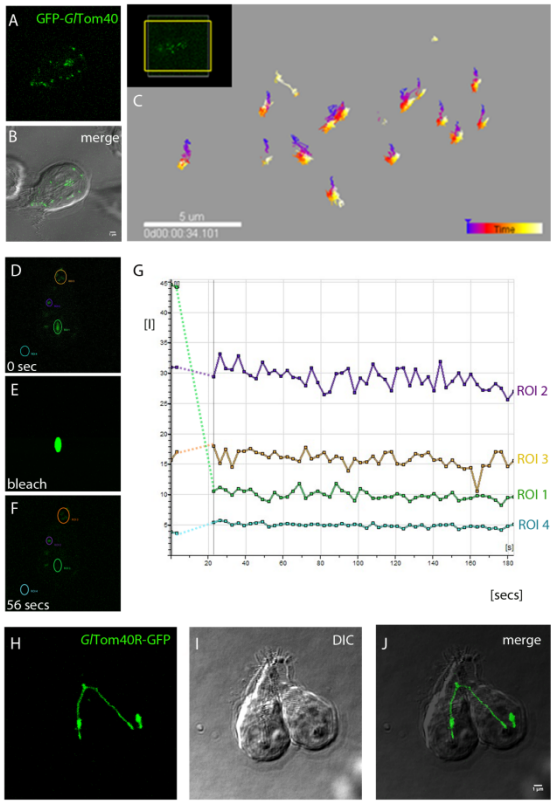

Fig 7. G. lamblia mitosomes are immobilized and do not form dynamic networks

(A-B) Detection of typical organelle distribution of GFP-tagged GlTom40 (green) in time-lapse microscopy. (B) Overlay showing the CMC in between the two nuclei and PMs dispersed throughout the cell. (C) Tracking of organelles during a period of 30 min shows no significant movement of mitosomes in the cytosol. (D-G) FRAP experiments performed on cells conditionally expressing GFP-tagged GlTom40 suggest that outer membrane proteins are not able to move amongst/in between organelles. (E) Photobleaching of a single mitosome (region of interest 1 (ROI 1)) in a living cell is shown. (F-G) Fluorescence in a bleached organelle (green line in the graph) does not recover even after several minutes (>20 min). Purple and brown lines in the graph represent fluorescence in unbleached areas (ROIs 2 and 3). (G) Fluorescence micrographs from the image series at the start (0 sec) of the experiment, during bleaching, and at the beginning of the recovery phase (20 sec). Arbitrary units of fluorescence are indicated [I]. Broken lines connect pre- and post-bleaching values in the graph. (H-J) "String" mitosome phenotype observed upon constitutive expression of GFP-tagged GI50803_29147 (GlTom40R- GFP). (H) GlTom40R-GFP localized exclusively to mitosomes and in some cases virtually all of the peripheral organelles have been replaced by a single long tubular mitosome spanning both daughter cells length-wise. (I) DIC image. (J) Overlay of the two channels. Scale bar: 1 µM.

Discussion

Eukaryotes that were previously considered to be amitochondriate are now known to contain MROs such as hydrogenosomes and mitosomes [70,71]. Although there is a consensus that MROs are evolutionarily derived from mitochondria, there is extensive structural and functional divergence among organelles in different species. Bioinformatics analyses show clearly that constraints for sequence divergence vary greatly, i.e. components of the universal enzymatic machinery for the Fe-S protein maturation in MROs can be detected in the nuclear genome using straightforward homology searches, whereas most MRO membrane proteins have diverged beyond recognition if they were not lost altogether. Three groups of membrane proteins are of particular interest in terms of organelle function and propagation: the TOM/TIM complex and other protein import machinery, factors that mediate interaction with the ER and the cytoskeleton, and transporters for ADP/ATP and other building blocks. Attempts to discern the contribution of MROs to the cell's metabolism and catabolism and to understand why these organelles have been preserved even after they lost their role in energy metabolism are confronted with two obstacles. Firstly, extensive sequence divergence prevents identification of organelle proteins via homology-based searches and secondly, the function of candidate factors identified by other means and localized to organelle membranes can usually not be deduced based on existing structural information from well-characterized mitochondrial homologs. In addition, the divergence between orthologues of MRO proteins even in closely related species is very high. A case in point is GlTOM40

whose sequence degeneration is so extensive that the identification of orthologues in Giardia, Entamoeba or Spironucleus remains tentative despite the constraints imposed by the beta barrel structure of these mitochondrial porins [44]. Unambiguous identification is even more difficult for highly diverged proteins that lack clearly identifiable structural domains (e.g. a putative GlTim44 homolog, a component of the TIM complex) [72].

G. lamblia mitosomes remain the smallest known and least characterized MROs. Systematic identification of protein components using proteome analysis of enriched mitosome preparations has proven challenging primarily due to extensive contamination and difficulty to isolate organelles in sufficient amounts [33,48]

Here, we accounted for the paucity of data which may inform strategies for the systematic identification of Giardia mitosome proteins by implementing an approach based on MS analysis of chemically stabilized protein-protein interactions. Our starting premise was that the diminutive mitosomes harbored no more than 100-150 different proteins inside or associated with a clearly delineated cellular compartment. Using a putative GlTOM40 [22,33] as a starting point, this study focused on organelle membrane components, in particular the mitosome protein import machinery whose function has been demonstrated but whose composition remains unknown.

With only six bait proteins, the strategy based on iterative co-IP experiments allowed for building a core membrane interactome and a complex interactome network extending inwards to the organelle matrix as well as outwards to components of the ER membrane, the axoneme cytoskeleton and the cytoplasm. The rationale is that with sufficient numbers of reverse co-IP experiments using validated organelle proteins as baits, a comprehensive organelle proteome can be built.

Co-IP with GlTom40 as bait and reverse co-IP performed with 5 subsequent new bait proteins resulted in identification of 22 mitosomal proteins (annotated and hypothetical) out of which 16 proteins were localized to mitosomes; 5 proteins displayed dual localization to mitosomes and ER and one protein (Gl7188) showed a ER and PV pattern even though it was pulled down exclusively with mitosome-localized bait proteins harboring TMDs. Based on their localization pattern, we grouped these mitosome proteins into 2 categories (Fig. 4F). The group at the bottom left with GlIscS at the center depict proteins with exclusive mitosome localization suggesting that these proteins are mitosome residents (soluble or membrane-anchored) whereas the group at the top right (Fig. 4F) includes all proteins with dual localization, suggesting they might be at the junction between ER and mitosomes with a potential role in establishing inter-organelle communication, e.g. for lipid transport.

GlTom40 and interaction partners GlTom40R and Gl14939: a minimized mitosome protein import apparatus?

Following its identification as a prominent GlTom40 interaction partner, the single pass membrane protein GlTom40R was the first bait protein selected for reverse co-IP in order to validate the experimental procedure and to expand the GlTom40 interactome. Importantly, the protein has a predicted N-terminal TMD similar to mitochondrial Tom40 receptors (Tom20 and Tom70) in Saccharomyces cerevisiae. Furthermore, this TMD is preceded by a short N-terminal region and followed by a large C-terminal stretch. Ectopic expression of the C-terminal portion of GlTom40R alone showed a distinct cytosolic localization by IFA (data not shown), without a detectable phenotype. However, several in silico analysis tools failed to predict a MTS at the protein's N-terminus. Nevertheless, a C-terminally GFP-tagged full-length variant determines the specific topology of this protein. We have shown previously that GFP only fluoresces if exposed to the cytoplasm and never after import into mitosomes ([22] and unpublished data). Therefore, the brightly fluorescing and mitosome-localized GlTom40R-GFP fusion provided conclusive data and is a direct proof for the proposed topology of GlTom40R. This transgenic line also provided an additional tool for time lapse microscopy of mitosomes in trophozoites.

Reverse co-IP using GlTom40R as bait pulled down GlTom40 with the most abundant peptide counts and 220 additional specific proteins (annotated and hypothetical). So far 20 proteins have been validated by localization to mitosomes, allowing for a significant expansion of the GlTom40/GlTom40R interactome. The topology of GlTom40R, its exclusive mitosomal localization, and the repertoire of pulled down proteins further supports that GlTom40R is a Tom40 accessory protein with a potential receptor function for protein import. Specifically, the long cytoplasmically exposed C-terminal stretch interacts with several imported matrix proteins independently of the presence of a predicted transit peptide (S6 Table). To test this idea, we performed co-IP using the HA-tagged C-terminal part of GlTom40R (amino acid 31-133), which has a cytoplasmic localization, under non-crosslinking conditions. The resulting data is difficult to interpret, given that out of a total of 232 proteins detected at high stringency (95_2_95), 171 were specific to the C-terminal GlTom40R with none of the previously known mitosomal resident proteins in the dataset. However, upon analysis with medium stringency parameters (95_1_95), we identified only 2 novel hypothetical mitosomal proteins (Gl16424, Gl9503) in the C-terminal GlTom40R specific dataset. This suggests that the cytoplasmic GlTom40R fragment does not recapitulate the interaction properties of the full-length membrane anchored variant. Taken together, the co-IP data suggest that i) capture of imported matrix proteins is context-dependent, i.e. likely requires incorporation of the receptor domain into a TOM complex, and ii) interaction with GlTom40 requires the domains on either side of the membrane anchor and possibly additional accessory membrane proteins. Hence, the hypothesis of a receptor function for GlTom40R remains to be tested directly to evaluate its exact role in proteins import. Interestingly, although BLASTp yielded no strong homologs for GlTom40R, profile sequence comparisons with HHpred showed homology to a “high potential iron sulfur protein” (p-value 0.007). “High potential iron sulfur protein” in higher eukaryotes, also known as mitoNEET, is an integral membrane protein localized at the outer membrane of mitochondria and is responsible for transport of iron into mitochondria [73]. If we consider that Fe-S protein maturation is the only metabolic pathway currently associated to G. lamblia mitosomes, GlTom40R might also function as a mitoNEET homolog in G. lamblia.

Another GlTom40 interaction partner of special interest is Gl14939. This protein was exclusively identified in the GlTom40 and the GlTom40R co-IP datasets, suggesting that Gl14939 and GlTom40R may function as part of a complex. TMHMM predicts two TMDs at its N-terminus, followed by a large C-terminal domain in Gl14939. Powerful HMMER-based searches across several eukaryotic lineages, including the closely related diplomonad Spironucleus salmonicida [74], yielded no orthologues for this protein (data not shown). To date, there is no further information available indicating a function for Gl14939. However, a recent study showed that Gl14939 (dubbed GiMOMP35) localizes at the outer mitosome membrane with its C- terminus in the cytosol [72]. Nonetheless, given that GlTom40 (the translocon), GlTom40R, and Gl14939 (putative accessory protein) are outer membrane-associated proteins and part of the same interactome, the data is consistent with a minimized import apparatus whose core import machinery is composed of only these three proteins. Likewise, a function in protein import of several other novel hypothetical proteins without TMD, e.g. Gl10971, Gl9296, Gl8148, Gl17276, and Gl16424, remains to be elucidated. Reverse co-IP using Gl9296 as bait protein pulled down GlIscS, GlIscA, GlHsp70, and outer membrane proteins including GlTom40 and GlTom40R, indicating close association to the import machinery and imported matrix proteins. Furthermore, Gl9296 has a predicted MTS but protein sequence analysis using the SMART prediction tool identified no functional domain of significance. Similarly, Gl9296 appears specific to the Giardia lineage. Given its interaction profile, predicted import signal, and lack of homology to metabolic enzymes, we hypothesize that Gl9296 is a matrix protein interacting with the import pore in mitosomes. Recent developments in gene knockout strategies in G. lamblia [75] will facilitate the definition of the role of these novel hypothetical proteins.

All 24 localized mitosome proteins (previously known and newly identified hypotheticals) were parsed according to molecular function and biological process (S3A and S3B Figs) using Blast2go (https://www.blast2go.com/). Metal ion, Fe-S, ATP, and protein binding were the major molecular functions associated with these proteins. Interestingly, other biological processes involving response to lipid and transmembrane transport were also identified with significant p-values. An additional 93 candidates annotated as hypothetical proteins (from all the 6 co-IP assays) were analyzed using Blast2go (S4A and S4B Figs). Binding

and catalytic activities were the 2 major GO terms associated to this group. Their potential involvement in binding of lipids, flavin mono-nucleotide co-factor, metal ion, Fe-S cluster, calcium ion, nucleotide, Fe and protein kinase will have to be tested experimentally. The number of combined candidate mitosome proteins after elimination of obvious contaminants such as cytoplasmic proteins is sufficiently large to suggest that mitosomes may have a role beyond Fe-S protein maturation. Only recently the major function of E. histolytica mitosomes was shown to be sulfate activation, and not Fe-S protein maturation as previously thought [44]. Although genes involved in this pathway are missing in other MRO-containing organisms such as G. lamblia, T. vaginalis, and C. parvum, the Entamoeba example points to a wider range of functions ascribable to mitosomes. This may even include general functions in stage-differentiation as recently shown in E. histolytica whose mitosomes are essential for the encystation process [76].

Mitosome-ER contact sites

Co-IP data identified proteins with dual localization at mitosomes and ER. Contact between these organelles mediates at least two major functions, i.e. replication of mitosomes and transport associated to lipid biosynthesis. Thus far, we have identified five mitosome proteins with dual localization potentially involved in inter-organelle communication (Fig. 4F). One of them is a transmembrane Qb-SNARE 4 (Gl50803_5785) [77] identified in GlTom40 and GlTom40R co-IP datasets. IFA analysis localized a tagged variant to mitosomes and parts of the ER.

For their biogenesis, mitochondria and MROs rely on lipid transfer from the ER, the central site for phospholipid synthesis in the cell [78,79]. SNAREs are best known for mediating membrane fusion in vesicular transport [80] In the context of mitochondria and the ER, they function as components of so called ER-mitochondria encounter structures (ERMES). In addition to being associated to mitochondrial protein import [81,82], ERMES fulfills an essential function in inter-organelle lipid transport [81]. Phosphatidylserine is shuttled from the ER to mitochondria through the ERMES complex where it is converted to phosphatidylethanolamine (PE) by a decarboxylation reaction that generates most if not all PE in mitochondria [81,83]. Whether this function is preserved in Giardia mitosomes is not known, however, organelle biogenesis necessarily depends on ER-derived lipids which are transported to mitosomes either by carrier proteins or via membrane contact sites. The latter requires a tethering complex to facilitate phospholipid exchange between the two organelles. We explored the idea that Qb-SNARE 4 is part of a larger complex mediating ER-mitosome interaction by generating co-IP data. Indeed, in addition to outer membrane proteins such as GlTom40, GlTom40R and Gl14939, 3 hypothetical proteins were identified in the dataset, two of which, Gl9503 (3 TMDs) and Gl21943 (soluble), localized both to the ER and to mitosomes. In addition, data mining identified a domain in Gl9503 with similarity to a yeast “Maintenance of mitochondrial morphology” protein 1 (Mmm1) of the ERMES complex as well as a predicted anhydrolase domain involved in lipid synthesis. HHpred analysis revealed a link between Gl21943 and a beta barrel lipid binding protein MLN64 (e-value 0.0006) in H. sapiens which facilitates cholesterol transport to mitochondria [84]. This preliminary data points to an outer mitosomal membrane-associated complex in G. lamblia mitosomes involved in generating ER-mitosome membrane contact sites analogous to ERMES. However, unlike in the hydrogenosome-containing T. vaginalis [85], ERMES homologs have not been identified in G. lamblia possibly due to extensive sequence divergence. Further experiments are necessary to test whether the dually-localized proteins Gl21943, Gl22587, Gl5785, Gl9503 and Gl15154 (Figs. 2F-2I and Fig. 3C) are indeed components of bona fide ER-mitosome membrane contact sites.

Functional analysis of protein import into the mitosome matrix

Using transgenic lines co-expressing MTSfdΔint-DHFR and Gl17030-HA we induced a protein import block by addition of the folate analog MTX. Accumulation of the reporter in the cytoplasm upon MTX treatment shown in IFA (Fig. 5A and 5B) suggested blocked import of the reporter presumably as a result of clogging of the import pore. Consistent with this, cells exposed to MTX presented accumulation of the unprocessed form of

the reporter Gl17030-HA in a Western blot analysis (Fig. 5C). Based on the interaction of MTX with the mitosome targeted DHFR this is evidence for a blockage of the import pore analogous to established assays in bona fide mitochondria [63]. The data also confirms the previously tested notion that membrane translocation requires pre-proteins to remain in an unfolded state [72]. Furthermore, it provides direct experimental evidence for the functional conservation of the mitosome protein import pathway and the presence of a canonical general insertion pore (GIP)/translocon in G. lamblia mitosomes. Given that GlTom40 localizes exclusively to mitosomes and is the only predicted beta barrel protein in G. lamblia, this highly diverged protein is currently the only candidate for the mitosomal translocon. Interestingly, recent reports on mitochondrial protein import in T. brucei (Excavata super-group) identified an archaic TOM (ATOM) as the functional translocase at the outer mitochondrial membrane [86]. ATOM is not phylogenetically related to canonical Tom40 proteins, suggesting there is more than one kind of eukaryotic translocase that can function as an import pore. Whether this is also the case in G. lamblia remains to be investigated.

Mitosome dynamics and a novel role for GlDRP in mitosome morphogenesis

We had previously shown that replication and inheritance of the CMC is coordinated in a cell cycle-dependent manner, whereas PMs divided stochastically [22]. The lack of a system to track organelles in living trophozoites precluded addressing the question whether mitosomes were motile and constituted a dynamic network of organelles. Development of two GFP-tagged reporters GFP-GlTom40 and GlTom40R-GFP (this study) allowed for time-lapse experiments to follow individual organelles in a cell. However, we found no evidence for motility of organelles, neither in the CMC nor in PMs, even after prolonged observation (1.5 h). Moreover, FRAP experiments revealed no exchange of GFP-tagged membrane proteins between organelles during the period of observation (Fig. 7F and 7G), which further corroborated the relative isolation of mitosomes within the cytosol. The lack of motility, inter-organelle contact and -interaction in Giardia mitosomes complicates investigation of their replication and morphogenesis. The two most plausible scenarios for this are currently the following: i) PMs are released from the CMC, which continuously produces new organelles by elongation and fission to maintain a constant number of organelles in a cell-cycle independent manner; ii) PMs and the CMC organelles replicate independently in a cell-cycle independent and -dependent manner, respectively [22]. Although time-lapse microscopy experiments did not provide evidence for either scenario, conditional expression of a dominant-negative, constitutively active GlDRP-K43E revealed a distinct morphogenesis phenotype (see also below) indicative of an organelle replication defect. Moreover, the distinctive “string” mitosome phenotype in cells expressing GlTom40R-GFP clearly demonstrated that mitosomes can assume an elongated, tubular morphology, which is a prerequisite for organelle division and replication. The implication is that G. lamblia mitosomes retain at least the machinery for fission in which the mechanoenzyme DRP plays a central role. Without the capability for fusion, this organelle “network” remains in a maximally fragmented state. The “string” mitosome phenotype therefore reflects a lack of fission, for example because the presence of the GFP-tagged protein on the surface interferes with recruitment of DRP to the mitosome membrane.

As one of the key players in the regulation of mitochondrial fission, dynamin related protein (DRP) is a mechanoenzyme conserved from yeast to vertebrates [87,88,89,90]. G. lamblia harbors a single dynamin homologue (GlDRP) encoded by ORF Gl50803_14373; this protein has been shown to play a major role in this parasite’s endocytic pathway and stage conversion [54,91,92]. Transgenic parasites expressing the mutant GlDRP-K43E protein exhibited larger and fewer mitosomes, compared to cells overexpressing wild type GlDRP (Fig. 6). This is in line with the dominant-negative effect on mitochondrial fission elicited by the corresponding mutation in DRPs in other organisms. To our knowledge, this is the first report on the involvement of GlDRP in mitosome homeostasis, supporting the (at least partial) functional conservation of mitochondrial and MRO fission [93,94,95,96]. The notion that G. lamblia mitosome fission is functionally conserved is further substantiated by the identification of ORF Gl22587 in the mitosome-specific co-IP datasets. This protein presents dual localization to mitosomes and the ER. Interestingly, HMMER-based predictions relate Gl22587 to human mitochondrial fission protein (Fis1, e-value 6.3E-05) which, along with mitochondrial fission factor (Mff) and mitochondrial dynamics proteins (MiD 49 and MiD51), acts as a receptor to recruit dynamin-related

protein 1 (Drp1) to the mitochondrial surface [97,98]. The isolation of GlI22587-interaction partners might lead to the identification of regulators and recruiting factors for GlDRP, thereby shedding light on the composition of the mitosome fission machinery and replication mechanism in Giardia.

Conclusion

Starting from the premise that mitosomes represent distinct cellular compartments with a very limited number of components in close physical proximity, we used an iterative approach based on co-IP experiments to generate a GlTom40-centered interactome network. The ultimate purpose of this strategy is to build a full proteome, which delineates the full complement of organelle proteins, peripherally associated factors, as well as interfaces with the ER and the cytoskeleton. Although this strategy requires numerous rounds of sequential co-IP and validation, it is highly informative because it produces interaction data in addition to identifying novel proteins. Combined with testing of epitope-tagged variants of candidate proteins for organelle localization as a straightforward validation criterion, serial co-IPs allow unambiguous definition of the organelle-specific proteome, as well as interfaces with other cellular structures. A case in point is the complete lack of false-negative hits in the GlIscS co-IP dataset, which contained all previously identified factors in addition to numerous novel candidate matrix and inner membrane proteins. Due to the extreme sequence divergence in nuclear-encoded genes for mitosome proteins, functional models for most components and pathways cannot simply be replicated based on a mitochondrial blueprint, but require almost complete ab initio (re)construction. Consequently, an exact and comprehensive delineation of the organelle proteome is an indispensable prerequisite for any attempt at defining the functional range of mitosome metabolism, as well as the organelle's machinery for replication and morphogenesis.

Acknowledgements

We thank Therese Michel for technical assistance. Dr. Peter Hunziker and his team at the proteomics service facility of the Functional Genomics Center-Zürich are gratefully acknowledged for their support in tandem mass spectrometry performance and analysis. Prof. Robert Sinden at Imperial College, London (UK) is gratefully acknowledged for providing the human DHFR-encoding plasmid. Dr. Chandra Ramakrishnan is gratefully acknowledged for critical revision of the manuscript.

References

1. Gray MW, Burger G, Lang BF (1999) Mitochondrial evolution. Science 283: 1476-1481.
2. Hedges SB, Blair JE, Venturi ML, Shoe JL (2004) A molecular timescale of eukaryote evolution and the rise of complex multicellular life. BMC Evol Biol 4: 2.
3. Yang D, Oyaizu Y, Oyaizu H, Olsen GJ, Woese CR (1985) Mitochondrial origins. Proc Natl Acad Sci U S A 82: 4443-4447.
4. Olsen GJ, Woese CR, Overbeek R (1994) The winds of (evolutionary) change: breathing new life into microbiology. J Bacteriol 176: 1-6.
5. Viale AM, Arakaki AK (1994) The chaperone connection to the origins of the eukaryotic organelles. FEBS Lett 341: 146-151.
6. Bauer MF, Hofmann S, Neupert W, Brunner M (2000) Protein translocation into mitochondria: the role of TIM complexes. Trends Cell Biol 10: 25-31.
7. Jensen RE, Johnson AE (2001) Opening the door to mitochondrial protein import. Nat Struct Biol 8: 1008-1010.
8. Koehler CM, Merchant S, Schatz G (1999) How membrane proteins travel across the mitochondrial intermembrane space. Trends Biochem Sci 24: 428-432.
9. Matouschek A, Pfanner N, Voos W (2000) Protein unfolding by mitochondria. The Hsp70 import motor. EMBO Rep 1: 404-410.

10. Prokisch H, Scharfe C, Camp DG, 2nd, Xiao W, David L, et al. (2004) Integrative analysis of the mitochondrial proteome in yeast. PLoS Biol 2: e160.
11. Reinders J, Zahedi RP, Pfanner N, Meisinger C, Sickmann A (2006) Toward the complete yeast mitochondrial proteome: multidimensional separation techniques for mitochondrial proteomics. J Proteome Res 5: 1543-1554.
12. Sickmann A, Reinders J, Wagner Y, Joppich C, Zahedi R, et al. (2003) The proteome of Saccharomyces cerevisiae mitochondria. Proc Natl Acad Sci U S A 100: 13207-13212.
13. Pfanner N, Truscott KN (2002) Powering mitochondrial protein import. Nat Struct Biol 9: 234-236.
14. Gabaldon T, Huynen MA (2004) Shaping the mitochondrial proteome. Biochim Biophys Acta 1659: 212-220.
15. Cerkasovová A, Lukasová G, Cerkasòv J, J K (1973) Biochemical characterization of large granule fraction of Tritrichomonas foetus (strain KV1). Journal of Protozoology 20.
16. Lindmark DG, Muller M (1973) Hydrogenosome, a cytoplasmic organelle of the anaerobic flagellate Tritrichomonas foetus, and its role in pyruvate metabolism. J Biol Chem 248: 7724-7728.
17. Mai Z, Ghosh S, Frisardi M, Rosenthal B, Rogers R, et al. (1999) Hsp60 is targeted to a cryptic mitochondrion-derived organelle ("crypton") in the microaerophilic protozoan parasite Entamoeba histolytica. Mol Cell Biol 19: 2198-2205.
18. Muller M (1993) The hydrogenosome. J Gen Microbiol 139: 2879-2889.
19. Tovar J, Fischer A, Clark CG (1999) The mitosome, a novel organelle related to mitochondria in the amitochondrial parasite Entamoeba histolytica. Mol Microbiol 32: 1013-1021.
20. Shiflett AM, Johnson PJ (2010) Mitochondrion-related organelles in eukaryotic protists. Annu Rev Microbiol 64: 409-429.
21. Adl SM, Simpson AG, Lane CE, Lukes J, Bass D, et al. (2012) The revised classification of eukaryotes. J Eukaryot Microbiol 59: 429-493.
22. Regoes A, Zourmpanou D, Leon-Avila G, van der Giezen M, Tovar J, et al. (2005) Protein import, replication, and inheritance of a vestigial mitochondrion. J Biol Chem 280: 30557-30563.
23. Tovar J, Leon-Avila G, Sanchez LB, Sutak R, Tachezy J, et al. (2003) Mitochondrial remnant organelles of Giardia function in iron-sulphur protein maturation. Nature 426: 172-176.
24. Makiuchi T, Nozaki T (2014) Highly divergent mitochondrion-related organelles in anaerobic parasitic protozoa. Biochimie 100: 3-17.
25. Riordan CE, Ault JG, Langreth SG, Keithly JS (2003) Cryptosporidium parvum Cpn60 targets a relict organelle. Curr Genet 44: 138-147.
26. Katinka MD, Duprat S, Cornillot E, Metenier G, Thomarat F, et al. (2001) Genome sequence and gene compaction of the eukaryote parasite Encephalitozoon cuniculi. Nature 414: 450-453.
27. Jerlstrom-Hultqvist J, Einarsson E, Xu F, Hjort K, Ek B, et al. (2013) Hydrogenosomes in the diplomonad Spironucleus salmonicida. Nature communications 4: 2493.
28. Abrahamsen MS, Templeton TJ, Enomoto S, Abrahante JE, Zhu G, et al. (2004) Complete genome sequence of the apicomplexan, Cryptosporidium parvum. Science 304: 441-445.
29. Leon-Avila G, Tovar J (2004) Mitosomes of Entamoeba histolytica are abundant mitochondrion-related remnant organelles that lack a detectable organellar genome. Microbiology 150: 1245-1250.
30. Turner G, Muller M (1983) Failure to detect extranuclear DNA in Trichomonas vaginalis and Tritrichomonas foetus. J Parasitol 69: 234-236.
31. van der Giezen M, Sjollema KA, Artz RR, Alkema W, Prins RA (1997) Hydrogenosomes in the anaerobic fungus Neocallimastix frontalis have a double membrane but lack an associated organelle genome. FEBS Lett 408: 147-150.
32. Dolezal P, Smid O, Rada P, Zubacova Z, Bursac D, et al. (2005) Giardia mitosomes and trichomonad hydrogenosomes share a common mode of protein targeting. Proc Natl Acad Sci U S A 102: 10924-10929.
33. Jedelsky PL, Dolezal P, Rada P, Pyrih J, Smid O, et al. (2011) The minimal proteome in the reduced mitochondrion of the parasitic protist Giardia intestinalis. PLoS One 6: e17285.
34. Lill R (2009) Function and biogenesis of iron-sulphur proteins. Nature 460: 831-838.
35. Craig EA, Voisine C, Schilke B (1999) Mitochondrial iron metabolism in the yeast Saccharomyces cerevisiae. Biol Chem 380: 1167-1173.
36. Schilke B, Voisine C, Beinert H, Craig E (1999) Evidence for a conserved system for iron metabolism in the mitochondria of Saccharomyces cerevisiae. Proc Natl Acad Sci U S A 96: 10206-10211.
37. Ankarklev J, Jerlstrom-Hultqvist J, Ringqvist E, Troell K, Svard SG (2010) Behind the smile: cell biology and disease mechanisms of Giardia species. Nat Rev Microbiol 8: 413-422.
38. Morrison HG, McArthur AG, Gillin FD, Aley SB, Adam RD, et al. (2007) Genomic minimalism in the early diverging intestinal parasite Giardia lamblia. Science 317: 1921-1926.

39. Davis-Hayman SR, Nash TE (2002) Genetic manipulation of Giardia lamblia. Molecular and biochemical parasitology 122: 1-7.
40. Boucher SE, Gillin FD (1990) Excystation of in vitro-derived Giardia lamblia cysts. Infect Immun 58: 3516-3522.
41. Abodeely M, DuBois KN, Hehl A, Stefanic S, Sajid M, et al. (2009) A contiguous compartment functions as endoplasmic reticulum and endosome/lysosome in Giardia lamblia. Eukaryot Cell 8: 1665-1676.
42. Stefanic S, Morf L, Kulangara C, Regos A, Sonda S, et al. (2009) Neogenesis and maturation of transient Golgi-like cisternae in a simple eukaryote. J Cell Sci 122: 2846-2856.
43. Goldberg AV, Molik S, Tsaousis AD, Neumann K, Kuhnke G, et al. (2008) Localization and functionality of microsporidian iron-sulphur cluster assembly proteins. Nature 452: 624-628.
44. Mi-ichi F, Abu Yousuf M, Nakada-Tsukui K, Nozaki T (2009) Mitosomes in Entamoeba histolytica contain a sulfate activation pathway. Proc Natl Acad Sci U S A 106: 21731-21736.
45. Putignani L, Tait A, Smith HV, Horner D, Tovar J, et al. (2004) Characterization of a mitochondrion-like organelle in Cryptosporidium parvum. Parasitology 129: 1-18.
46. Sanderson SJ, Xia D, Prieto H, Yates J, Heiges M, et al. (2008) Determining the protein repertoire of Cryptosporidium parvum sporozoites. Proteomics 8: 1398-1414.
47. Tsaousis AD, Kunji ER, Goldberg AV, Lucocq JM, Hirt RP, et al. (2008) A novel route for ATP acquisition by the remnant mitochondria of Encephalitozoon cuniculi. Nature 453: 553-556.
48. Wampfler PB, Tosevski V, Nanni P, Spycher C, Hehl AB (2014) Proteomics of secretory and endocytic organelles in Giardia lamblia. PLoS One 9: e94089.
49. Dagley MJ, Dolezal P, Likic VA, Smid O, Purcell AW, et al. (2009) The protein import channel in the outer mitosomal membrane of Giardia intestinalis. Mol Biol Evol 26: 1941-1947.
50. Hehl AB, Marti M, Kohler P (2000) Stage-specific expression and targeting of cyst wall protein-green fluorescent protein chimeras in Giardia. Mol Biol Cell 11: 1789-1800.
51. Morf L, Spycher C, Rehrauer H, Fournier CA, Morrison HG, et al. (2010) The transcriptional response to encystation stimuli in Giardia lamblia is restricted to a small set of genes. Eukaryot Cell 9: 1566-1576.
52. Hehl AB, Marti M, Kohler P (2000) Stage-specific expression and targeting of cyst wall protein-green fluorescent protein chimeras in Giardia. Molecular biology of the cell 11: 1789-1800.
53. Konrad C, Spycher C, Hehl AB (2010) Selective condensation drives partitioning and sequential secretion of cyst wall proteins in differentiating Giardia lamblia. PLoS Pathog 6: e1000835.
54. Gaechter V, Schraner E, Wild P, Hehl AB (2008) The single dynamin family protein in the primitive protozoan Giardia lamblia is essential for stage conversion and endocytic transport. Traffic 9: 57-71.
55. Pusnik M, Mani J, Schmidt O, Niemann M, Oeljeklaus S, et al. (2012) An essential novel component of the noncanonical mitochondrial outer membrane protein import system of trypanosomatids. Molecular biology of the cell 23: 3420-3428.
56. Rajala N, Hensen F, Wessels HJ, Ives D, Gloerich J, et al. (2015) Whole cell formaldehyde cross-linking simplifies purification of mitochondrial nucleoids and associated proteins involved in mitochondrial gene expression. PLoS One 10: e0116726.
57. Jimenez-Garcia LF, Zavala G, Chavez-Munguia B, Ramos-Godinez Mdel P, Lopez-Velazquez G, et al. (2008) Identification of nucleoli in the early branching protist Giardia duodenalis. International journal for parasitology 38: 1297-1304.
58. Elmendorf HG, Rohrer SC, Khoury RS, Bouttenot RE, Nash TE (2005) Examination of a novel head-stalk protein family in Giardia lamblia characterised by the pairing of ankyrin repeats and coiled-coil domains. International journal for parasitology 35: 1001-1011.
59. Isenmann S, Khew-Goodall Y, Gamble J, Vadas M, Wattenberg BW (1998) A splice-isoform of vesicle-associated membrane protein-1 (VAMP-1) contains a mitochondrial targeting signal. Mol Biol Cell 9: 1649-1660.
60. Duman JG, Forte JG (2003) What is the role of SNARE proteins in membrane fusion? Am J Physiol Cell Physiol 285: C237-249.
61. Bandyopadhyay S, Chandramouli K, Johnson MK (2008) Iron-sulfur cluster biosynthesis. Biochemical Society transactions 36: 1112-1119.
62. Manning G, Reiner DS, Lauwaet T, Dacre M, Smith A, et al. (2011) The minimal kinome of Giardia lamblia illuminates early kinase evolution and unique parasite biology. Genome biology 12: R66.
63. Eilers M, Schatz G (1986) Binding of a specific ligand inhibits import of a purified precursor protein into mitochondria. Nature 322: 228-232.
64. Morgan GW, Goulding D, Field MC (2004) The single dynamin-like protein of Trypanosoma brucei regulates mitochondrial division and is not required for endocytosis. J Biol Chem 279: 10692-10701.

65. Chanez AL, Hehl AB, Engstler M, Schneider A (2006) Ablation of the single dynamin of T. brucei blocks mitochondrial fission and endocytosis and leads to a precise cytokinesis arrest. Journal of cell science 119: 2968-2974.
66. Wexler-Cohen Y, Stevens GC, Barnoy E, van der Bliek AM, Johnson PJ (2014) A dynamin-related protein contributes to Trichomonas vaginalis hydrogenosomal fission. Faseb J 28: 1113-1121.
67. Chan DC (2006) Mitochondria: dynamic organelles in disease, aging, and development. Cell 125: 1241-1252.
68. Chen H, Chan DC (2009) Mitochondrial dynamics--fusion, fission, movement, and mitophagy--in neurodegenerative diseases. Human molecular genetics 18: R169-176.
69. Sonda S, Stefanic S, Hehl AB (2008) A sphingolipid inhibitor induces a cytokinesis arrest and blocks stage differentiation in Giardia lamblia. Antimicrobial agents and chemotherapy 52: 563-569.
70. van der Giezen M (2009) Hydrogenosomes and mitosomes: conservation and evolution of functions. J Eukaryot Microbiol 56: 221-231.
71. Aguilera P, Barry T, Tovar J (2008) Entamoeba histolytica mitosomes: organelles in search of a function. Experimental parasitology 118: 10-16.
72. Martincova E, Voleman L, Pyrih J, Zarsky V, Vondrackova P, et al. (2015) Probing the biology of Giardia intestinalis mitosomes using in vivo enzymatic tagging. Mol Cell Biol.
73. Paddock ML, Wiley SE, Axelrod HL, Cohen AE, Roy M, et al. (2007) MitoNEET is a uniquely folded 2Fe 2S outer mitochondrial membrane protein stabilized by pioglitazone. Proc Natl Acad Sci U S A 104: 14342-14347.
74. Xu F, Jerlstrom-Hultqvist J, Einarsson E, Astvaldsson A, Svard SG, et al. (2014) The genome of Spironucleus salmonicida highlights a fish pathogen adapted to fluctuating environments. PLoS genetics 10: e1004053.
75. Wampfler PB, Faso C, Hehl AB (2014) The Cre/loxP system in Giardia lamblia: genetic manipulations in a binucleate tetraploid protozoan. International journal for parasitology 44: 497-506.
76. Mi-Ichi F, Miyamoto T, Takao S, Jeelani G, Hashimoto T, et al. (2015) Entamoeba mitosomes play an important role in encystation by association with cholesteryl sulfate synthesis. Proc Natl Acad Sci U S A.
77. Elias EV, Quiroga R, Gottig N, Nakanishi H, Nash TE, et al. (2008) Characterization of SNAREs determines the absence of a typical Golgi apparatus in the ancient eukaryote Giardia lamblia. J Biol Chem 283: 35996-36010.
78. de Kroon AI, Dolis D, Mayer A, Lill R, de Kruijff B (1997) Phospholipid composition of highly purified mitochondrial outer membranes of rat liver and Neurospora crassa. Is cardiolipin present in the mitochondrial outer membrane? Biochim Biophys Acta 1325: 108-116.
79. Zinser E, Sperka-Gottlieb CD, Fasch EV, Kohlwein SD, Paltauf F, et al. (1991) Phospholipid synthesis and lipid composition of subcellular membranes in the unicellular eukaryote Saccharomyces cerevisiae. J Bacteriol 173: 2026-2034.
80. Kumar P, Guha S, Diederichsen U (2015) SNARE protein analog-mediated membrane fusion. Journal of peptide science : an official publication of the European Peptide Society 21: 621-629.
81. Tamura Y, Sesaki H, Endo T (2014) Phospholipid transport via mitochondria. Traffic 15: 933-945.
82. Yamano K, Tanaka-Yamano S, Endo T (2010) Tom7 regulates Mdm10-mediated assembly of the mitochondrial import channel protein Tom40. J Biol Chem 285: 41222-41231.
83. Tatsuta T, Scharwey M, Langer T (2014) Mitochondrial lipid trafficking. Trends Cell Biol 24: 44-52.
84. Rigotti A, Cohen DE, Zanlungo S (2010) STARTing to understand MLN64 function in cholesterol transport. Journal of lipid research 51: 2015-2017.
85. Wideman JG, Gawryluk RM, Gray MW, Dacks JB (2013) The ancient and widespread nature of the ER-mitochondria encounter structure. Mol Biol Evol 30: 2044-2049.
86. Mani J, Desy S, Niemann M, Chanfon A, Oeljeklaus S, et al. (2015) Mitochondrial protein import receptors in Kinetoplastids reveal convergent evolution over large phylogenetic distances. Nature communications 6: 6646.
87. Zhao J, Lendahl U, Nister M (2013) Regulation of mitochondrial dynamics: convergences and divergences between yeast and vertebrates. Cell Mol Life Sci 70: 951-976.
88. van der Bliek AM, Shen Q, Kawajiri S (2013) Mechanisms of mitochondrial fission and fusion. Cold Spring Harb Perspect Biol 5.
89. Okamoto K, Shaw JM (2005) Mitochondrial morphology and dynamics in yeast and multicellular eukaryotes. Annu Rev Genet 39: 503-536.
90. Elgass K, Pakay J, Ryan MT, Palmer CS (2013) Recent advances into the understanding of mitochondrial fission. Biochim Biophys Acta 1833: 150-161.
91. Marti M, Li Y, Schraner EM, Wild P, Kohler P, et al. (2003) The secretory apparatus of an ancient eukaryote: protein sorting to separate export pathways occurs before formation of transient Golgi-like compartments. Mol Biol Cell 14: 1433-1447.
92. McArthur AG, Morrison HG, Nixon JE, Passamaneck NQ, Kim U, et al. (2000) The Giardia genome project database. FEMS Microbiol Lett 189: 271-273.

93. Smirnova E, Shurland DL, Ryazantsev SN, van der Bliek AM (1998) A human dynamin-related protein controls the distribution of mitochondria. The Journal of cell biology 143: 351-358.
94. Miyagishima SY, Nishida K, Mori T, Matsuzaki M, Higashiyama T, et al. (2003) A plant-specific dynamin-related protein forms a ring at the chloroplast division site. Plant Cell 15: 655-665.
95. Nishida K, Takahara M, Miyagishima SY, Kuroiwa H, Matsuzaki M, et al. (2003) Dynamic recruitment of dynamin for final mitochondrial severance in a primitive red alga. Proc Natl Acad Sci U S A 100: 2146-2151.
96. Pan R, Hu J (2011) The conserved fission complex on peroxisomes and mitochondria. Plant Signal Behav 6: 870-872.
97. Otera H, Mihara K (2011) Discovery of the membrane receptor for mitochondrial fission GTPase Drp1. Small GTPases 2: 167-172.
98. Lee H, Yoon Y (2014) Mitochondrial fission: regulation and ER connection. Molecules and cells 37: 89-94.

PART V Discussion and future directions

1. Discussion

1.1. General

During infection most *G. lamblia* trophozoites are attached to the intestinal epithelium of their host. To cope with the changing environment in the intestine and to initiate encystation under inappropriate conditions for proliferation, trophozoites require constant sampling of the extracellular space. To date, the main route for host-parasite communication identified in this parasite occurs through the endocytic system, which has also been implicated in protein secretion. Consequently, peripheral vacuoles (PVs), the only known endocytic compartments in *Giardia*, are thought to function at the crossroads of endo- and exocytic protein transport. The non-fusogenic PVs distribute in fixed position at the cell cortex and combine endo- and lysosomal properties i.e. there is no distinction of different endocytic compartments as in higher eukaryotes. Even though conserved homologues of eukaryotic clathrin mediated endocytosis (CME), namely clathrin heavy chain (*Gl*CHC), adaptor protein complex 2 (*Gl*AP2) and dynamin related protein (*Gl*DRP), are found in close proximity to PVs in immuno-fluorescence assays (IFA), no vesicular transport in the form of clathrin coated vesicles (CVVs) has been observed. The current data rather suggest a mechanism that involves direct fusion of the plasma membrane (PM) and PV membrane (PVM) to govern endocytic uptake. However, several aspects of the endocytic system such as the mode of uptake and the function of the *Gl*CHC in the absence of CCVs remain unknown. Here, we implemented an array of state-of-the-art imaging techniques and developed a customized co-immuno precipitation (co-IP) protocol to test our premise that the minimal distance between PM and PVMs and the presence of a uptake mechanism that creates luminal continuity with the extracellular space via direct fusion of the PM with the PVM has made CCVs obsolete. In turn, this may have caused cooption of *Gl*CHC towards a structural role in the endocytic pathway of *G. lamblia*.

Our global aims were to i) characterize *Gl*CHC concerning the exact subcellular localization, its molecular function and interacting proteins, ii) investigate the morphological aspects for material uptake occurring between PVM and PM to iii) understand how this parasite specific endocytic pathway functions and how it has evolved in *G. lamblia* in the course of reductive evolution.

To investigate the morphological aspect of the endocytic mechanism in *Giardia* we used several electron microscopy (EM) techniques by which we showed that PVs consist of an array of elongated/tubular organelles that contact the PM via PM invaginations. Combining different approaches in fluorescence and electron microscopy we showed that *Gl*CHC localizes as small, focal

and static assemblies at the PM-PVM interface (PPI) i.e. at the most distal position of PV membranes. We further defined a *Gl*CHC interactome comprising of 21 mostly lineage specific proteins that, aside from two conserved CME factors (*Gl*AP2 and *Gl*DRP), included a putative clathrin light chain and several proteins capable of lipid binding.

Our work provided evidence that reorganization of the giardial endocytic apparatus in the course of reductive evolution has resulted in a system which functions in the absence of membrane derived transport intermediates. Importantly, this system relies on a new, static, and most likely structural role for the *Gl*CHC in association with several lineage specific and very few conserved interaction partners. Our conclusions will be discussed in detail hereinafter.

1.2. Redistribution of PVs in the course of reductive evolution favors endocytic communication via the shortest and most direct route

In the course of reductive evolution, which is the current and best fit theory to explain the minimization seen in all cell biological aspects of *G. lamblia*, the giardial endocytic system has undergone remarkable morphological and molecular changes. We hypothesized, that the invention of the ventral disc for epithelial attachment was the driving force for the strong cell polarization observed in giardial trophozoites. We further proposed that this process also includes the redistribution of the endocytic compartments in close proximity with the dorsal PM facing the intestinal lumen. Such a high degree of morphological adaptation is also seen in the endocytic system of several other parasitic protozoans. *Plasmodium* spp. internalize material via a cytostome [3], which is a single PM invagination with an interruption of the inner membrane complex that penetrates a few micrometers into the cytoplasm [4-7], and is also found in the closest *Giardia* relative *Spironucleus spp.* (Faso and Hehl, unpublished). In African trypanosomes and in *Leishmania* all endocytosis occurs through the flagellar pocket [3], which is a small invagination of the membrane where the flagellum exits and many cellular processes occur, including endo- and exocytosis [8]. Although these parasites are highly adapted to their host environments and the corresponding endocytic systems utilize conserved short lived transport intermediates formed in association with clathrin [9-12]. In contrast and despite the presence of *Gl*CHC, such transport vesicles have never been observed in *Giardia* [13]. Therefore we propose that the minimal distance between PVM and PM made CCVs obsolete and that this maximally dispersed endocytic system has, in contrast to the single site of uptake through a cytostome or flagellar pocket, evolved towards fast and efficient sampling of the constantly changing intestinal environment through multiple sites of endocytic uptake.

1.3. Cooption of giardial clathrin - from dynamic to static

The subcellular localization of *Gl*CHC in close vicinity to PVs has been known for more than a decade [14]. However, the exact localization of *Gl*CHC has not yet been determined. We and others have unsuccessfully attempted to answer this question using cryo-immuno electron microscopy of epitope-tagged reporters for *Gl*CHC (Zumthor and Hehl, unpublished data). Here, we used electron, fluorescence super resolution and confocal microscopy to show that *Gl*CHC localizes as small (~50nm) and defined assemblies at the PPI. Unlike *Gl*CHC, canonical endocytic clathrin is organized in CCVs that typically measure 80-150nm [15-18] and distributes as membrane coats around entire vesicles [19, 20]. Furthermore classical CCVs are of a temporary nature with fast dynamics. The usual lifetimes of clathrin coats at vesicles ranges between 30-60s from assembly until disassembly [21] and individual clathrin molecules are exchange throughout this process, suggesting high protein turnover [22]. In fluorescence recovery after photobleaching (FRAP), inverse (i)FRAP and fluorescence lifetime analysis, *Gl*CHC appears to be static in all terms. The longevity of most *Gl*CHC assemblies measured in this study even exceed the lifetimes measured for long-lived clathrin plaques (lifetimes ~600s), sometimes found at the cytosolic leaflet of mammalian PMs [23]. The static behavior the *Gl*CHC::GFP reporters are in line with the absence of the QLMLT (Gln-Leu-Met-Leu-Thr) uncoating motif in the *Gl*CHC protein sequence (this thesis). This motif was found to be essential for heat shock cognate protein 70 (HSC70) dependent clathrin coat disassembly in many systems with dynamic clathrin molecules [24, 25]. A homologue of the ATPase HSC70 is also found in the dynamic clathrin mediated endocytic system of *Trypanosoma brucei* and this otherwise highly divergent parasite further contains a recognizable QLMLT motif in the clathrin heavy chain protein sequence [26]. In addition to the absent QLMLT motif, the ATPase HSC70 appears to have no homologues in *Giardia* as it was not identified in either our co-IP data or in a genomic survey (this thesis).

Membrane deformations observed during CCV formation in classical systems are thought, at least in part, to be driven by clathrin [22]. One proposition suggests that the reorganization of clathrin lattices consisting mostly of hexagons to a mixture of pentagons and hexagons supports membrane deformation, which is in line with the constant exchange of individual clathrin molecules observed during the CCV generation [27]. Given the measurements for *Gl*CHC protein turnover and *Gl*CHC assembly lifetimes, it is unlikely that *Gl*CHC actively participates in formation of the observed PM invaginations found in *Giardia* [28] (this thesis). Moreover, there are no indications that actin, which plays a role in membrane deformation in some canonical systems [19], is involved in giardial endocytosis as no actin or actin binding proteins could be identified in our co-IP datasets. Taken together, our results provide direct evidence for the highly stable nature of *Gl*CHC assemblies and strongly suggests that *Gl*CHC, unlike other well-characterized protozoan clathrin homologues [9, 11,

29-31], is not part of a dynamic process involving formation of short-lived membrane carriers for vesicular transport.

1.4. Does GFP alter *Gl*CHC behavior?

The discovery and scientific use of GFP has revolutionized live cell imaging and the three responsible scientists were awarded with the 2008 Nobel Prize in Chemistry [32]. However, GFP has a molecular weight of *ca*. 30kDa which is a considerable size for a protein marker. In comparison, a commonly used epitope tag such as the HA tag is predicted to weigh only 1.1Da. Consequently, it is possible that a GFP reporter for any given protein of interest may be impaired in its functional properties, a scenario that is also known in endocytic pathways [33]. Further it has been shown that the overexpression of proteins, in particular in the CME pathway, can lead to severe alterations of the system [34]. The gold standard to investigate CME dynamics in live cell imaging is to fuse clathrin light chains (CLC) with GFP as reporter molecules [35]. At the beginning of the present study however, no putative giardial clathrin light chain (*Gl*CLC) could be identified to act as reporter for clathrin protein dynamics. We were therefore constrained to use *Gl*CHC for our initial study on clathrin dynamics. Currently, complementation tests based on rescuing a knockout/down phenotype are not yet feasible in *Giardia*. However, we found that constitutive expression *Gl*CHC::GFP in *Giardia* trophozoites has no influence in terms of cell growth, motility and fluid phase uptake capacity. Similarly, the subcellular distribution of *Gl*CHC::GFP reporters was identical to the distribution of endogenous *Gl*CHC and to the corresponding HA-tagged variants**.** Fortunately, we were able to repeat the live cell microscopy analysis on the newly identified and putative *Gl*CLC and showed that *Gl*CHC and *Gl*CLC showed identical dynamic behavior. In addition, FRAP analyses of *Gl*AP2 and *Gl*DRP revealed fast reporter molecule turnover. Hence, GFP reporter analysis in *Giardia* allowed for the documentation of dynamic and static reporter behavior. Therefore, despite the limited toolkit for functional characterization of (fusion-) proteins in *Giardia*, all obtained data point towards full compliance of the GFP fusions used in this study.

1.5. *Gl*DRP performs a conserved role in membrane fission events

The single *Gl*DRP possesses all necessary domains that define the minimal architecture of dynamin related proteins (DRPs) [36]. Nonetheless, domain organization shows some unusual features. On one hand, it misses the pleckstrin homology domain (PHD) while on the other hand it possess the equivalent of a proline/arginine rich domain (PRD) [36].Both these domains are usually found in endocytosis associated classical dynamins but are absent in dynamin related proteins (DRPs), that mainly function in mitochondrial homeostasis [37]. The PRD and PHD are both involved in targeting dynamin to the endocytic sites at the PM [38]. The PHD binds to phosphatidyl-4,5-bisphosphate ($PI4,5P_2$), the same lipid preferred by AP2 [39, 40], and mediates the interaction between dynamin

and membranes [41]. Prior to this, unassembled dynamin is correctly targeted to clathrin coated pits (CCPs) by the PRD domain that interacts with a multitude of endocytic accessory factors [42] For *Gl*DRP however, the species specific domain architecture features a mixture of classical dynamins and DRPs [36]. This is reflected in its association with the giardial endocytic system [36] and in the possible fulfillment of its the archetypal function at mitosomes (Rout et. al. 2016, submitted). This dual function may explain the loss of the PHD. A functional PHD could lead to a default recruitment to $PI4,5P_2$ enriched membranes which could in turn prevent targeting of the single *Gl*DRP to mitosomes. A possible scenario for a single protein that functions at different compartments, such as *Gl*DRP, is that correct recruitment to distinct sites of action depends on accessory factors. One of these could be a very recently detected PHD-containing protein that could govern *Gl*DRP membrane recruitment during endocytosis (Zumthor, Cernikova, et. al. in preparation; draft manuscript in this thesis). On one hand we showed that, consistent with classical dynamins [43], *Gl*DRP undergoes measurable protein turnover at the cell cortex and on the other hand previous reports show how the overexpression of a dominant negative-effect variant of the giardial dynamin caused an enlargement of PV organelles compared to a wild type control [36]. This phenotype is line with a deficiency for the dynamin mutant to separate the membrane fusions that were observed between PM and PVM (this study). Moreover, no other giardial protein with membrane scission properties is known. Taken together, all available experimental data on *Gl*DRP suggest a conserved role for this large GTPase in membrane scission events but question about targeting of dynamin to distinct sites of action remains to be elucidated.

1.6. *Gl*AP2 functions – some conserved, some not

The heterotetramer AP2 is a key player and the most abundant non-clathrin component in canonical CME [44]. Hence its function is very well described in many aspects. AP2 acts as the main adapter that recruits clathrin to endocytic nucleation sites and links it to the PM. AP2 in turn recognizes these nucleation sites by its affinity for $PI4,5P_2$ and its binding to the endocytic motif of membrane receptors [44-46]. The four subunits of AP2 are fairly conserved in the *Giardia* genome [13]. In the present study we showed that *Gl*AP2 is a core component of a *Gl*CHC centered endocytic interactome and it was the factor for which most interactions with other proteins were found. Furthermore FRAP analysis of the large α-subunit suggested that *Gl*AP2 is of a dynamic nature (this thesis). The multitude of interactions and the dynamic behavior is also seen for AP2 in canonical systems and suggests a high degree of functional conservation for *Gl*AP2 in the giardial endocytic system. Considering the dynamic nature of *Gl*AP2, its role in recruiting *Gl*CHC to static assemblies is unlikely. However, given its conserved sequence and its proposed role in giardial receptor mediated endocytosis [2] it is possible that *Gl*AP2 maintained its capability to bind endocytic motifs in the cytoplasmic tail of membrane receptors. This assumption yields support from the detection of two

type-1A transmembrane proteins in *Gl*AP2 specific co-IPs datasets, both of which harbor endocytic motifs in their short cytoplasmic domains. Following the premise that clathrin assemblies remain static at the PPI one could hypothesize that *Gl*AP2 senses the endocytic trigger by an enrichment for $PI4,5P_2$ and internalization motifs of membrane receptors, a combined binding stimulus that was shown to be essential for correct AP2 assembly [47]. AP2 subsequently participates in the recruitment of dynamic factors (e.g. involved in membrane deformation) to nucleation sites for further progression of the endocytic process. Given *Gl*AP2s high turnover compared to *Gl*CHC, its role as a clathrin adaptor in *Giardia* is unlikely. Considering that clathrin per se has no intrinsic membrane binding tendency, this raises the question as to how static clathrin assemblies are kept in association with the endocytic membranes at the PPI.

1.7. How is *Gl*CHC linked to the endocytic membranes?

Clathrin is the prototype of membrane coat scaffolds and, in line with other coat scaffolds such as the Sec31p-Sec13p complex in COPII coats [48], is unable to interact with membrane lipids directly [20]. In standard endocytic systems AP2 and monomeric adaptors link lipids and cargo to clathrin in emerging CCVs [49]. In *Giardia* however it is unlikely that *Gl*AP2 is functioning as a bona fide clathrin adaptor given the opposed dynamics of *Gl*AP2 and *Gl*CHC presented herein. Importantly, the co-IP assay using *Gl*CHC as bait identified three interacting proteins harboring lipid binding domains usually found in proteins that associate to endocytic membranes in higher eukaryotes. The single FYVE (Fab1, YOTB/ZK632.12, Vac1, and EEA1) domain containing protein *Gl*16653 and the two Phox (PX) domain containing proteins *Gl*7723 and *Gl*16595 could act as monomeric adaptors for clathrin (putative clathrin adaptors). For all three proteins the functionality of the predicted PX domain in terms of endocytic PI binding has been proven [50] (Zumthor, Cernikova et. al., in preparation). Furthermore, results from our laboratory showed that the predicted effector domains of *Gl*7723 and *Gl*16595 (i.e. HA-tagged fusion variants short of the PX domain) are correctly targeted to clathrin assemblies at the PPI (Zumthor and Cernikova et. al. in preparation). This suggests strong interactions with components of clathrin assemblies and includes the possibility that these proteins mediate *Gl*CHC-assembly binding to membranes. The engagement of binding partners other than PIs (e.g. clathrin) is a feature commonly observed in PI binding proteins [47]. At the same time the recruitment of the isolated effector domains to clathrin assemblies suggest that these two proteins are not the driving forces for clathrin recruitment, at least not as individual effectors. Taken together, the PI binding proteins found in the giardial clathrin interactome could be responsible for holding clathrin static assemblies in place at the membrane. However, the factors that determine initial *Gl*CHC targeting remain unknown.

1.8. A customized co-IP protocol involving limited crosslinking enables the detection of protein interactions in the giardial clathrin protein network

The identification of *Gl*CHC interacting proteins such as the putative light chain or the lipid binding proteins was achieved through the development of a co-IP protocol that was customized to *Giardia* trophozoites and to the characteristics of our bait protein clathrin. In a first MS analysis of an eluted fraction a total of three proteins were detected; the bait *Gl*CHC, the putative light chain and *Gl*5795, an abundant ER resident protein identified as a non-specific contaminant. Given the identification of only one specific *Gl*CHC interactor, we hypothesize that most *Gl*CHC specific interactions are of weak or transient nature and were probably disrupted during the experimental procedure. Our assumption gained support from the literature describing the clathrin interactome, aside from clathrin light chains [35], as networks of weak protein-protein interactions [45]. To overcome this, we adapted the concept of reversible crosslinking using Dithiobis Succinimidyl Propionate (DSP), a protocol suited for the detection of weak interactions [51]. The introduction of a chemical crosslinker in co-IP protocols to stabilize weak protein interactions is a known concept [52] but comes at the cost of an increased number of false positives in MS-analysis which require careful manual post-acquisition filtering. To account for this and to optimize our "signal-to-noise" ratio, we defined three strategies:

i) we titrated the crosslinker to define the minimal necessary amount of DSP to reduce precipitation of excessive false positive interactome elements. To do this, we monitored the ratio of high molecular weight complexes to the monomeric bait with increasing amounts of DSP (up to 3 mM) (Fig.1); this was used as a read-out for the stabilization of some protein interactions with *Gl*CHC. The defined optimal concentration for DSP was between 0.3 and 0.5 mM, corresponding to a range where high molecular weight and monomeric species co-existed in comparable amounts (Fig.1).

ii) the stabilization of weak and transient protein interactions by crosslinking allowed the implementation of more stringent washing procedures which aimed to reduce unspecifically bound or physically trapped proteins [53].

iii) to each co-IP dataset we applied subtractive hybridization with co-IP data obtained from untransfected wild type cells. This approached aimed to further reduce abundant false positive proteins present in both the bait specific and wild type sets.

Taken together, the establishment of this co-IP protocol tailored to the membrane associated, cytosolic protein *Gl*CHC in *Giardia* using a limited crosslinking approach was successful as it identified PV resident proteins such as *Gl*AP2 and *Gl*DRP, previously unrecognized clathrin interacting proteins and a putative *Gl*CLC. In total, >60% of the validated proteins displayed subcellular localizations similar to *Gl*CLC, supporting their association to clathrin assemblies.

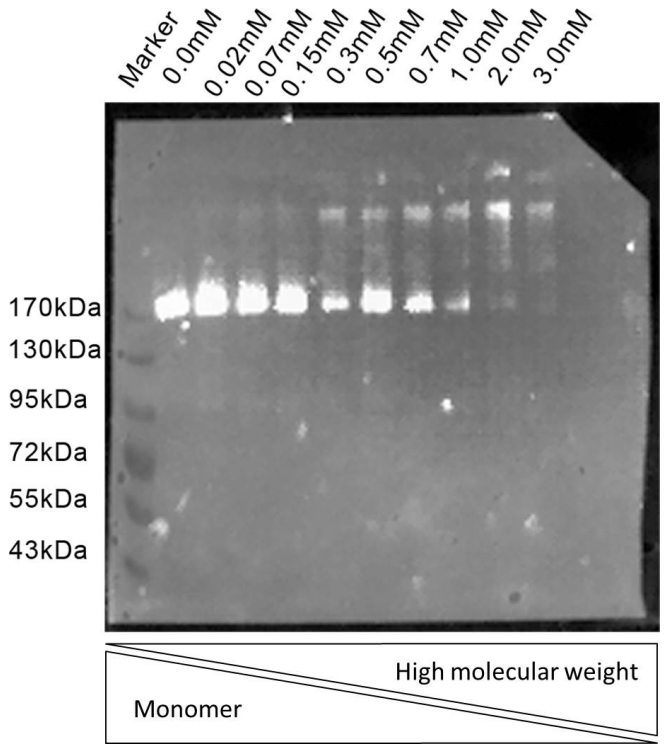

Fig. 1: ***DSP titration experiment***

Prior to cell lysis, trophozoites expressing an HA-tagged variant of *Gl*CHC were incubated with 0-3mM DSP. The western blot signal detected for *Gl*CHC::HA is shifted from a monomeric state (0mM DSP) to a state where clathrin is mainly present in higher molecular complexes (3mM DSP). For the "limited crosslinking" approach in this study, 0.4mM DSP were applied prior to co-IP..

1.9. Conclusions

In Fig. 2 we developed a working model that takes all available data into account. *Gl*CHC assembles at the PPI through which the fluid extracellular environment in the host's intestinal lumen is accessed when PM invaginations fuse with the PVMs. The exchange of fluid phase material was visualized by fluorescence microscopy showing the replacement of luminal PV contents in a cycle of endo- and exo- cytic events [54]. Currently, there is no data that allows the distinction between receptor based and fluid phase based endocytic processes and all traceable cargo molecules used so far end up in PVs ([28, 54, 55]. Hence, the initiation/regulation of the giardial endocytic process, whether it is highly regulated or mainly spontaneous and stochastic or if it depends on stimuli of receptor/ligand complexes, remains to be elucidated. Our data support a scenario where endocytic membrane deformation is not initiated but stabilized by *Gl*CHC-*Gl*CLC scaffolds linked to membranes by potential monomeric clathrin adaptors such as PX- and FYVE- domain proteins. Given the longevity of giardial clathrin assemblies, the absence of CVVs and conserved uncoating mechanisms we suggest that clathrin assemblies are not formed *de novo* for each endocytic event but stabilize PM invaginations during multiple rounds. The fusion and scission of membranes is a prerequisite for all endocytic processes. Although the exact regulation for this is not known in *Giardia, Gl*DRP appears to be the best candidate to play an essential role in the recurring membrane remodeling events, given its association to clathrin assemblies and its role in PV homeostasis [54]. The endocytic system in

Giardia is maximally dispersed as PVs distribute in the entire cell cortex and each organelle marks a point of entry. This system appears to be specifically adapted to the host and allows fast and efficient communication with the extracellular space to thrive in the changing environment of the small intestine.

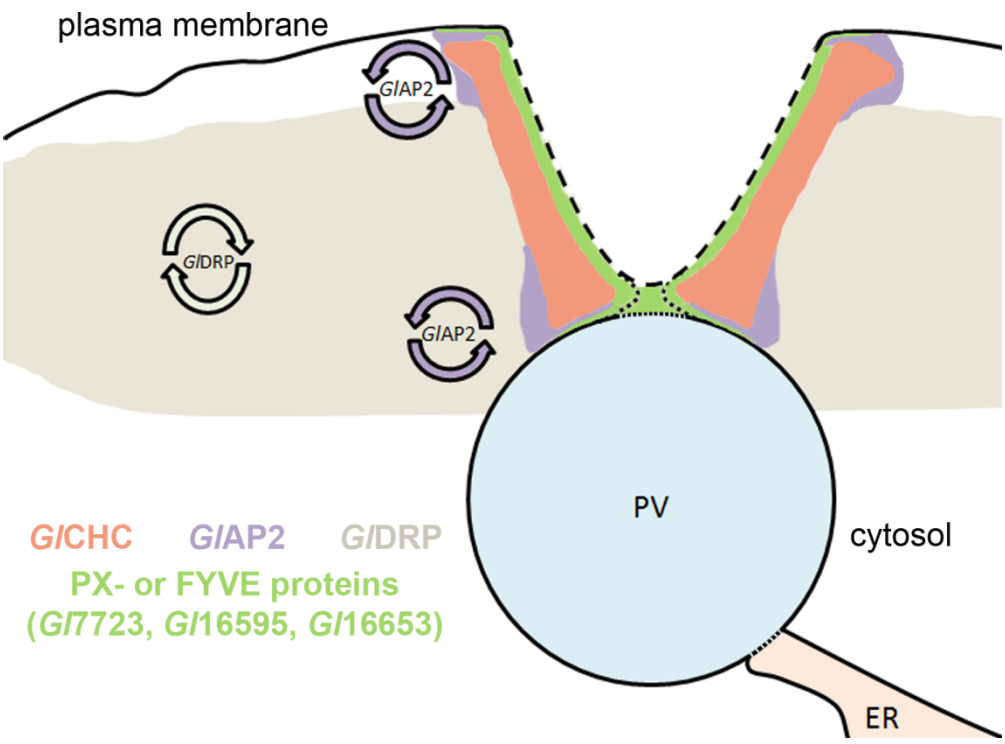

Fig. 2: ***A working model for the organization of clathrin and associated proteins at the PPI***

The model shows a cross section through the PPI including a PV organelle and the PM. For endocytic uptake, PM invaginations fuse with PV membranes to create luminal continuity with the extracellular environment. This is the most likely explanation for bulk uptake of fluid phase markers and occasional direct transport to the ER [1]. After uptake, membranes are separated whilst clathrin assemblies remain at the PPI. The distribution of relevant proteins is based on experimental data and functional properties [2]. Dashed lines indicate where membrane remodeling may occur. Circular arrows designate dynamic protein properties.

The observation that some material is further transported towards the cell interior and some is expelled in the next round of "kiss and flush" [1] suggests that a sorting step occurs and that the PV organelles could act as a safety lock for the distinction of useful from harmful material.

T.brucei presents another example of a highly specialized/adapted endocytic system that functions in the absence of AP2 but nonetheless depends on the formation of dynamic CCVs [26]. In this system, AP2 as a sensor for endocytic nucleation sites may have become dispensable as endocytosis only occurs at the one distinct position of the PM, the flagellar pocket, where the endocytic machinery can be concentrated. Although highly adapted, *T. brucei* endocytosis is not considered simplified but rather to comprise a cohort of pan-eukaryotic proteins combined with a lineage specific group [26].

In *Giardia*, we hypothesize that cell polarization entailed the redistribution of the endocytic vacuoles, in such close association to the PM that dynamic transport, including the machinery for clathrin disassembly, was lost. In contrast to *T.brucei*, the giardial system appears molecularly and conceptually more simplified and reflects another example of how host adaptation drives sculpting of an endomembrane system that was already present in the latest common eukaryotic ancestor [56].

2. Future directions

2.1. Static *Gl*CHC is not involved in transient membrane coat formation but its function remains elusive – suggestions to functionally analysis *Gl*CHC

The question about the exact molecular role for *Gl*CHC is essential to unravel the molecular underpinnings of giardial endocytosis. We attempted to disrupt giardial endocytosis by overexpressing clathrin-hub, a well established clathrin truncated variant which interferes with correct CME. However, accumulation of clathrin-hub elicited no discernible effect on fluid-phase uptake in PVs (Zumthor and Hehl, unpublished). The hub mutant interferes with the closed polyhedron of a CCV by assembling in an open ended lattice which is abortive to CCV formation [57]. Given that CCVs are not present in *Giardia*, this may explain the lack of phenotypic aberrations upon clathrin-hub overexpression. Despite the challenges of performing functional characterizations in *Giardia*, some experimental approaches may be implemented to understand *Gl*CHCs role more precisely:

- Given the level of conservation and the general nature of clathrin homologues, we hypothesized that giardial clathrin assembles into periodic, lattice like structures. Classical clathrin coats can be imaged using quick-freeze deep-etch electron microscopy [58]. Our attempts to adapt this technique to image giardial clathrin assemblies did not lead to the observation of any periodic structure reminiscent of clathrin lattices. I therefore suggest expression and purification of *Gl*CHC in insect cells to subsequently test *Gl*CHC ability for *in vitro* assembly using cage assembly buffer [59] similar to experiments performed earlier [24]. This would allow answering the question if the static giardial clathrin has maintained the basic property of self-assembly common to all scaffolding proteins.

- The PX domain-containing proteins fulfil the basic properties (i.e. interaction with *Gl*CHC and binding to PIs) to function as potential *Gl*CHC adaptors. To further elucidate the roles of these proteins I suggest two experiments:

- i) One prerequisite of *Gl*CHC adaptor proteins is a similar protein turnover compared to *Gl*CHC itself. This can be tested by FRAP and iFRAP experiments in cells expressing the corresponding GFP fusion proteins;

  ii) The ability of proteins to link clathrin to lipid layers can be tested in an *in vitro* experimental setup where lipid monolayers or liposomes are either incubated with *Gl*CHC alone or together with potential adaptors amenable to electron microscopy readout [60].

- In classical CME the monomeric clathrin adaptor AP180/CALM binds $PI4,5P_2$ and clathrin at the same time [60] and matches therewith the basic properties of the potential clathrin adaptors found in *Giardia.* The overexpression of a AP180 truncated mutant variant consisting of the binding domain for clathrin without the membrane anchor results in inhibition of CME [61]. However, due to the longevity of *Gl*CHC assemblies we hypothesized they do not disassemble during the endocytic cycle. In this case, they only occasion to influence and/or observe clathrin targeting as a result of the overexpression of truncated adaptors to PVs would be during cell division, when PV organelles are duplicated. Cell cycle synchronization is possible in *Giardia* [62] and could be used to analyze the putative giardial clathrin adaptors and their role as adaptors or recruitment factors for *Gl*CHC and their potential for eliciting dominant negative effects on giardial endocytosis.

- Recently Pitstop 1 and 2, selective inhibitors of CME became commercially available. Pitstop 1 and 2 inhibit ligand association with clathrin's terminal domain e.g. binding of amphiphysin to clathrin [63]. These membrane permeable small molecule inhibitors may elicit an effect in *Giardia*. It is important to note however, that the transfer of molecular tools established in canonical eukaryotic systems to *Giardia* research has proven to be challenging and, in many cases, simply inapplicable.

-

2.2. Testing the conserved membrane severing function of *Gl*DRP

In classical systems the expression of a dynamin protein containing a single amino acid mutation is an established tool to block CME [64]. In *Giardia* however, fluid phase uptake into PVs is unaffected by the expression of the corresponding mutant variant of *Gl*DRP (*Gl*DRP_K443E). This result is consistent with the hypothesis that *Gl*DRP severs the fusion between the PM and PVMs. In this scenario the force driving membrane fusion necessary for material uptake is not influenced by a mutant *Gl*DRP and fluid phase markers are taken up normally. But with progression of the endocytic cycle,

membrane scission is hampered and the connection between PV lumen and extracellular space remains open and leads to uncontrolled loss of PV contents. This hypothesis is testable using focused ion beam electron microscopy to compare the number of PM invaginations connected to PVM in wild type cells and cells expressing the *Gl*DRP mutant.

The major obstacle for functional protein analysis in *G. lamblia* is the lack of reliable molecular tools for protein knockdown/knockout. In 2014 our laboratory published a proof of concept study that the sequential knock out of four alleles in *Giardia* is made possible by the recycling of selection markers using the Cre/loxP system [65]. Since then, the approached has been develop further and has resulted in the first knock out cell line generated in *Giardia* (Faso, Ebneter et. al. in preparation). This strategy is likely to be feasible only for non-essential genes or for genes with stage regulated expression patterns (e.g. genes induced during encystation). Conditional knockouts of essential genes will require complementation controlled by an on/off system. Such systems, e.g. the Tet-Off and Tet-On systems, have been used in *Giardia* [66] but present some "leakiness" in the Off-status (Hehl, unpublished). However, sequential knocking out using the Cre/loxP system allows the generation of 1-,2-,3- or 4n- knockout lines. The resulting decrease in gene expression may be enough to elicit a phenotype for some protein targets and in my opinion represents the most controllable and most promising approach to unravel the function of clathrin in *Giardia lamblia.*

3. Bibliography

1. Abodeely M, DuBois KN, Hehl A, Stefanic S, Sajid M, DeSouza W, et al. A contiguous compartment functions as endoplasmic reticulum and endosome/lysosome in Giardia lamblia. Eukaryotic cell. 2009;8(11):1665-76. Epub 09/15. doi: 10.1128/EC.00123-09. PubMed PMID: 19749174.
2. Rivero MR, Vranych CV, Bisbal M, Maletto BA, Ropolo AS, Touz MC. Adaptor protein 2 regulates receptor-mediated endocytosis and cyst formation in Giardia lamblia. The Biochemical journal. 2010;428(1):33-45. Epub 03/05. doi: 10.1042/BJ20100096

10.1042/BJ20100096. PubMed PMID: 20199400.
3. de Souza W, Sant'Anna C, Cunha-e-Silva NL. Electron microscopy and cytochemistry analysis of the endocytic pathway of pathogenic protozoa. Prog Histochem Cytochem. 2009;44(2):67-124. doi: 10.1016/j.proghi.2009.01.001. PubMed PMID: 19410686.
4. Aikawa M, Hepler PK, Huff CG, Sprinz H. The feeding mechanism of avian malarial parasites. J Cell Biol. 1966;28(2):355-73. PubMed PMID: 5914696; PubMed Central PMCID: PMCPMC2106916.
5. Langreth SG, Jensen JB, Reese RT, Trager W. Fine structure of human malaria in vitro. J Protozool. 1978;25(4):443-52. PubMed PMID: 105129.
6. Olliaro P, Castelli F, Milano F, Filice G, Carosi G. Ultrastructure of Plasmodium falciparum "in vitro". I. Base-line for drug effects evaluation. Microbiologica. 1989;12(1):7-14. PubMed PMID: 2654573.
7. Rudzinska MA, Trager W, Bray RS. Pinocytotic uptake and the digestion of hemoglobin in malaria parasites. J Protozool. 1965;12(4):563-76. PubMed PMID: 5860234.
8. Field MC, Carrington M. The trypanosome flagellar pocket. Nat Rev Microbiol. 2009;7(11):775-86. doi: 10.1038/nrmicro2221. PubMed PMID: 19806154.

9. Agarwal S, Rastogi R, Gupta D, Patel N, Raje M, Mukhopadhyay A. Clathrin-mediated hemoglobin endocytosis is essential for survival of Leishmania. Biochimica et biophysica acta. 2013;1833(5):1065-77. Epub 01/19. doi: 10.1016/j.bbamcr.2013.01.006

10.1016/j.bbamcr.2013.01.006. Epub 2013 Jan 14. PubMed PMID: 23328080.
10. López-Soto F, González-Robles A, Salazar-Villatoro L, León-Sicairos N, Piña-Vázquez C, Salazar EP, et al. Entamoeba histolytica uses ferritin as an iron source and internalises this protein by means of clathrin-coated vesicles. Int J Parasitol. 2009;39(4):417-26. doi: 10.1016/j.ijpara.2008.08.010. PubMed PMID: 18848948.
11. Allen CL, Goulding D, Field MC. Clathrin-mediated endocytosis is essential in Trypanosoma brucei. The EMBO journal. 2003;22(19):4991-5002. Epub 10/01. doi: 10.1093/emboj/cdg481. PubMed PMID: 14517238.
12. Grünfelder CG, Engstler M, Weise F, Schwarz H, Stierhof YD, Morgan GW, et al. Endocytosis of a glycosylphosphatidylinositol-anchored protein via clathrin-coated vesicles, sorting by default in endosomes, and exocytosis via RAB11-positive carriers. Mol Biol Cell. 2003;14(5):2029-40. doi: 10.1091/mbc.E02-10-0640. PubMed PMID: 12802073; PubMed Central PMCID: PMCPMC165095.
13. Touz MC, Rivero MR, Miras SL, Bonifacino JS. Lysosomal protein trafficking in Giardia lamblia: common and distinct features. Frontiers in bioscience. 2011;4:1898-909. Epub 12/29. PubMed PMID: 22202006.
14. Hehl AB, Marti M. Secretory protein trafficking in Giardia intestinalis. Mol Microbiol. 2004;53(1):19-28. doi: 10.1111/j.1365-2958.2004.04115.x. PubMed PMID: 15225300.
15. McMahon HT, Boucrot E. Molecular mechanism and physiological functions of clathrin-mediated endocytosis. Nature reviews Molecular cell biology. 2011;12(8):517-33. Epub 07/23. doi: 10.1038/nrm3151

10.1038/nrm3151. PubMed PMID: 21779028.
16. Doray B, Ghosh P, Griffith J, Geuze HJ, Kornfeld S. Cooperation of GGAs and AP-1 in packaging MPRs at the trans-Golgi network. Science. 2002;297(5587):1700-3. doi: 10.1126/science.1075327. PubMed PMID: 12215646.
17. Geuze HJ, Slot JW, Strous GJ, Hasilik A, von Figura K. Possible pathways for lysosomal enzyme delivery. J Cell Biol. 1985;101(6):2253-62. PubMed PMID: 2933416; PubMed Central PMCID: PMCPMC2114005.
18. Klumperman J, Hille A, Veenendaal T, Oorschot V, Stoorvogel W, von Figura K, et al. Differences in the endosomal distributions of the two mannose 6-phosphate receptors. J Cell Biol. 1993;121(5):997-1010. PubMed PMID: 8099077; PubMed Central PMCID: PMCPMC2119677.
19. McMahon HT, Mills IG. COP and clathrin-coated vesicle budding: different pathways, common approaches. Curr Opin Cell Biol. 2004;16(4):379-91. doi: 10.1016/j.ceb.2004.06.009. PubMed PMID: 15261670.
20. Robinson MS. Forty Years of Clathrin-coated Vesicles. Traffic. 2015;16(12):1210-38. doi: 10.1111/tra.12335. PubMed PMID: 26403691.
21. Kirchhausen T. Imaging endocytic clathrin structures in living cells. Trends in cell biology. 2009;19(11):596-605. Epub 10/20. doi: 10.1016/j.tcb.2009.09.002

10.1016/j.tcb.2009.09.002. PubMed PMID: 19836955.
22. Wu X, Zhao X, Baylor L, Kaushal S, Eisenberg E, Greene LE. Clathrin exchange during clathrin-mediated endocytosis. The Journal of cell biology. 2001;155(2):291-300. Epub 10/18. doi: 10.1083/jcb.200104085. PubMed PMID: 11604424.
23. Grove J, Metcalf DJ, Knight AE, Wavre-Shapton ST, Sun T, Protonotarios ED, et al. Flat clathrin lattices: stable features of the plasma membrane. Molecular biology of the cell. 2014;25(22):3581-94. Epub 08/29. doi: 10.1091/mbc.E14-06-1154

10.1091/mbc.E14-06-1154. Epub 2014 Aug 27. PubMed PMID: 25165141.

24. Rapoport I, Boll W, Yu A, Bocking T, Kirchhausen T. A motif in the clathrin heavy chain required for the Hsc70/auxilin uncoating reaction. Molecular biology of the cell. 2007;19(1):405-13. Epub 11/06. doi: 10.1091/mbc.E07-09-0870. PubMed PMID: 17978091.
25. Heuser JE, Anderson RG. Hypertonic media inhibit receptor-mediated endocytosis by blocking clathrin-coated pit formation. J Cell Biol. 1989;108(2):389-400. PubMed PMID: 2563728; PubMed Central PMCID: PMCPMC2115439.
26. Adung'a VO, Gadelha C, Field MC. Proteomic analysis of clathrin interactions in trypanosomes reveals dynamic evolution of endocytosis. Traffic. 2013;14(4):440-57. Epub 01/12. doi: 10.1111/tra.12040

10.1111/tra.12040. Epub 2013 Feb 5. PubMed PMID: 23305527.
27. Jin AJ, Nossal R. Topological mechanisms involved in the formation of clathrin-coated vesicles. Biophys J. 1993;65(4):1523-37. doi: 10.1016/S0006-3495(93)81189-5. PubMed PMID: 8274646; PubMed Central PMCID: PMCPMC1225879.
28. Lanfredi-Rangel A, Attias M, de Carvalho TM, Kattenbach WM, De Souza W. The peripheral vesicles of trophozoites of the primitive protozoan Giardia lamblia may correspond to early and late endosomes and to lysosomes. Journal of structural biology. 1999;123(3):225-35. Epub 01/08. doi: 10.1006/jsbi.1998.4035. PubMed PMID: 9878577.
29. Elde NC, Morgan G, Winey M, Sperling L, Turkewitz AP. Elucidation of clathrin-mediated endocytosis in tetrahymena reveals an evolutionarily convergent recruitment of dynamin. PLoS Genet. 2005;1(5):e52. doi: 10.1371/journal.pgen.0010052. PubMed PMID: 16276403; PubMed Central PMCID: PMCPMC1277907.
30. Kalb LC, Frederico YC, Batista CM, Eger I, Fragoso SP, Soares MJ. Clathrin expression in Trypanosoma cruzi. BMC Cell Biol. 2014;15:23. doi: 10.1186/1471-2121-15-23. PubMed PMID: 24947310; PubMed Central PMCID: PMCPMC4073184.
31. Corrêa JR, Atella GC, Menna-Barreto RS, Soares MJ. Clathrin in Trypanosoma cruzi: in silico gene identification, isolation, and localization of protein expression sites. J Eukaryot Microbiol. 2007;54(3):297-302. doi: 10.1111/j.1550-7408.2007.00258.x. PubMed PMID: 17552985.
32. Zimmer M. GFP: from jellyfish to the Nobel prize and beyond. Chem Soc Rev. 2009;38(10):2823-32. doi: 10.1039/b904023d. PubMed PMID: 19771329.
33. Rappoport JZ, Simon SM. A functional GFP fusion for imaging clathrin-mediated endocytosis. Traffic. 2008;9(8):1250-5. doi: 10.1111/j.1600-0854.2008.00770.x. PubMed PMID: 18498437; PubMed Central PMCID: PMCPMC2761611.
34. Doyon JB, Zeitler B, Cheng J, Cheng AT, Cherone JM, Santiago Y, et al. Rapid and efficient clathrin-mediated endocytosis revealed in genome-edited mammalian cells. Nat Cell Biol. 2011;13(3):331-7. doi: 10.1038/ncb2175. PubMed PMID: 21297641; PubMed Central PMCID: PMCPMC4113319.
35. Hoffmann A, Dannhauser PN, Groos S, Hinrichsen L, Curth U, Ungewickell EJ. A comparison of GFP-tagged clathrin light chains with fluorochromated light chains in vivo and in vitro. Traffic. 2010;11(9):1129-40. Epub 06/16. doi: 10.1111/j.1600-0854.2010.01084.x

10.1111/j.1600-0854.2010.01084.x. Epub 2010 Jun 2. PubMed PMID: 20545906.
36. Gaechter V, Schraner E, Wild P, Hehl AB. The single dynamin family protein in the primitive protozoan Giardia lamblia is essential for stage conversion and endocytic transport. Traffic. 2007;9(1):57-71. Epub 09/26. doi: 10.1111/j.1600-0854.2007.00657.x. PubMed PMID: 17892527.
37. Miyagishima SY, Kuwayama H, Urushihara H, Nakanishi H. Evolutionary linkage between eukaryotic cytokinesis and chloroplast division by dynamin proteins. Proc Natl Acad Sci U S A. 2008;105(39):15202-7. doi: 10.1073/pnas.0802412105. PubMed PMID: 18809930; PubMed Central PMCID: PMCPMC2567515.
38. Liu YW, Su AI, Schmid SL. The evolution of dynamin to regulate clathrin-mediated endocytosis: speculations on the evolutionarily late appearance of dynamin relative to clathrin-mediated endocytosis. Bioessays. 2012;34(8):643-7. doi: 10.1002/bies.201200033. PubMed PMID: 22592980.

39. Gaidarov I, Keen JH. Phosphoinositide-AP-2 interactions required for targeting to plasma membrane clathrin-coated pits. J Cell Biol. 1999;146(4):755-64. PubMed PMID: 10459011; PubMed Central PMCID: PMCPMC2156139.
40. Chang MP, Mallet WG, Mostov KE, Brodsky FM. Adaptor self-aggregation, adaptor-receptor recognition and binding of alpha-adaptin subunits to the plasma membrane contribute to recruitment of adaptor (AP2) components of clathrin-coated pits. EMBO J. 1993;12(5):2169-80. PubMed PMID: 8491205; PubMed Central PMCID: PMCPMC413438.
41. Lee A, Frank DW, Marks MS, Lemmon MA. Dominant-negative inhibition of receptor-mediated endocytosis by a dynamin-1 mutant with a defective pleckstrin homology domain. Curr Biol. 1999;9(5):261-4. PubMed PMID: 10074457.
42. Okamoto PM, Herskovits JS, Vallee RB. Role of the basic, proline-rich region of dynamin in Src homology 3 domain binding and endocytosis. J Biol Chem. 1997;272(17):11629-35. PubMed PMID: 9111080.
43. Taylor MJ, Lampe M, Merrifield CJ. A feedback loop between dynamin and actin recruitment during clathrin-mediated endocytosis. PLoS Biol. 2012;10(4):e1001302. doi: 10.1371/journal.pbio.1001302. PubMed PMID: 22505844; PubMed Central PMCID: PMCPMC3323523.
44. Praefcke GJ, Ford MG, Schmid EM, Olesen LE, Gallop JL, Peak-Chew SY, et al. Evolving nature of the AP2 alpha-appendage hub during clathrin-coated vesicle endocytosis. The EMBO journal. 2004;23(22):4371-83. Epub 10/22. doi: 10.1038/sj.emboj.7600445. PubMed PMID: 15496985.
45. Schmid EM, McMahon HT. Integrating molecular and network biology to decode endocytosis. Nature. 2007;448(7156):883-8. Epub 08/24. doi: 10.1038/nature06031. PubMed PMID: 17713526.
46. Brodsky FM, Chen CY, Knuehl C, Towler MC, Wakeham DE. Biological basket weaving: formation and function of clathrin-coated vesicles. Annual review of cell and developmental biology. 2001;17:517-68. Epub 11/01. doi: 10.1146/annurev.cellbio.17.1.517. PubMed PMID: 11687498.
47. Carlton JG, Cullen PJ. Coincidence detection in phosphoinositide signaling. Trends Cell Biol. 2005;15(10):540-7. doi: 10.1016/j.tcb.2005.08.005. PubMed PMID: 16139503; PubMed Central PMCID: PMCPMC1904488.
48. Lederkremer GZ, Cheng Y, Petre BM, Vogan E, Springer S, Schekman R, et al. Structure of the Sec23p/24p and Sec13p/31p complexes of COPII. Proc Natl Acad Sci U S A. 2001;98(19):10704-9. doi: 10.1073/pnas.191359398. PubMed PMID: 11535824; PubMed Central PMCID: PMCPMC58530.
49. Popova NV, Deyev IE, Petrenko AG. Clathrin-mediated endocytosis and adaptor proteins. Acta Naturae. 2013;5(3):62-73. PubMed PMID: 24307937; PubMed Central PMCID: PMCPMC3848845.
50. Sinha A, Mandal S, Banerjee S, Ghosh A, Ganguly S, Sil AK, et al. Identification and characterization of a FYVE domain from the early diverging eukaryote Giardia lamblia. Current microbiology. 2010;62(4):1179-84. Epub 12/18. doi: 10.1007/s00284-010-9845-5

10.1007/s00284-010-9845-5. Epub 2010 Dec 17. PubMed PMID: 21165741.
51. Smith AL, Friedman DB, Yu H, Carnahan RH, Reynolds AB. ReCLIP (reversible cross-link immuno-precipitation): an efficient method for interrogation of labile protein complexes. PloS one. 2011;6(1):e16206. Epub 02/02. doi: 10.1371/journal.pone.0016206

10.1371/journal.pone.0016206. PubMed PMID: 21283770.
52. Chelsky D, Dahlquist FW. Chemotaxis in Escherichia coli: associations of protein components. Biochemistry. 1980;19(20):4633-9. PubMed PMID: 6448631.
53. Salas PJ. Insoluble gamma-tubulin-containing structures are anchored to the apical network of intermediate filaments in polarized CACO-2 epithelial cells. J Cell Biol. 1999;146(3):645-58. PubMed PMID: 10444072; PubMed Central PMCID: PMCPMC2150552.
54. Gaechter V, Schraner E, Wild P, Hehl AB. The single dynamin family protein in the primitive protozoan Giardia lamblia is essential for stage conversion and endocytic transport. Traffic. 2008;9(1):57-71. Epub 2007/09/26. doi: 10.1111/j.1600-0854.2007.00657.x. PubMed PMID: 17892527.

55. Rivero MR, Miras SL, Quiroga R, Ropolo AS, Touz MC. Giardia lamblia low-density lipoprotein receptor-related protein is involved in selective lipoprotein endocytosis and parasite replication. Molecular microbiology. 2011;79(5):1204-19. Epub 01/06. doi: 10.1111/j.1365-2958.2010.07512.x

10.1111/j.1365-2958.2010.07512.x. Epub 2011 Jan 5. PubMed PMID: 21205007.
56. Wideman JG, Leung KF, Field MC, Dacks JB. The cell biology of the endocytic system from an evolutionary perspective. Cold Spring Harbor perspectives in biology. 2014;6(4):a016998. Epub 01/31. doi: 10.1101/cshperspect.a016998

10.1101/cshperspect.a016998. PubMed PMID: 24478384.
57. Liu SH, Marks MS, Brodsky FM. A dominant-negative clathrin mutant differentially affects trafficking of molecules with distinct sorting motifs in the class II major histocompatibility complex (MHC) pathway. J Cell Biol. 1998;140(5):1023-37. PubMed PMID: 9490717; PubMed Central PMCID: PMCPMC2132696.
58. Heuser J, Kirchhausen T. Deep-etch views of clathrin assemblies. Journal of ultrastructure research. 1985;92(1-2):1-27. Epub 07/01. PubMed PMID: 2870198.
59. Kirchhausen T, Harrison SC. Protein organization in clathrin trimers. Cell. 1981;23(3):755-61. PubMed PMID: 7226229.
60. Ford MG, Pearse BM, Higgins MK, Vallis Y, Owen DJ, Gibson A, et al. Simultaneous binding of PtdIns(4,5)P2 and clathrin by AP180 in the nucleation of clathrin lattices on membranes. Science. 2001;291(5506):1051-5. doi: 10.1126/science.291.5506.1051. PubMed PMID: 11161218.
61. Doherty GJ, McMahon HT. Mechanisms of endocytosis. Annu Rev Biochem. 2009;78:857-902. doi: 10.1146/annurev.biochem.78.081307.110540. PubMed PMID: 19317650.
62. Svärd S, Troell K. Synchronization of pathogenic protozoans. Methods Mol Biol. 2011;761:201-10. doi: 10.1007/978-1-61779-182-6_13. PubMed PMID: 21755450.
63. von Kleist L, Stahlschmidt W, Bulut H, Gromova K, Puchkov D, Robertson MJ, et al. Role of the clathrin terminal domain in regulating coated pit dynamics revealed by small molecule inhibition. Cell. 2011;146(3):471-84. doi: 10.1016/j.cell.2011.06.025. PubMed PMID: 21816279.
64. van der Bliek AM, Redelmeier TE, Damke H, Tisdale EJ, Meyerowitz EM, Schmid SL. Mutations in human dynamin block an intermediate stage in coated vesicle formation. J Cell Biol. 1993;122(3):553-63. PubMed PMID: 8101525; PubMed Central PMCID: PMCPMC2119674.
65. Wampfler PB, Faso C, Hehl AB. The Cre/loxP system in Giardia lamblia: genetic manipulations in a binucleate tetraploid protozoan. Int J Parasitol. 2014;44(8):497-506. doi: 10.1016/j.ijpara.2014.03.008. PubMed PMID: 24747534.
66. Sun CH, Tai JH. Development of a tetracycline controlled gene expression system in the parasitic protozoan Giardia lamblia. Mol Biochem Parasitol. 2000;105(1):51-60. PubMed PMID: 10613698.

Acknowledgements

With Prof. Adrian Hehl I had a great supervisor. His advice helped me to solve scientific problems on many occasions. However, his helpfulness was not restricted to science. I experienced his support in many other aspects and he even taught me how to change the tires of my car. Thank you very much Adrian for giving me the opportunity to be part of your group in which I not only grew scientifically and but also as a person.

Special thanks go to Dr. Carmen Faso aka DocF. I cannot imaagine a better “daily scientific advisor”, teacher or just friend to cope with the daily lab-challenges. I do not remember a single occasion where she had refused to help me or any other PhD student in our group. My successors are very lucky having you Carmen in the team!

Also I want to thank Dr. Cornelia Spycher who introduced me to the basic lab techniques. It was a lot of fun to work with you Cornelia!

No doubt, the Hehl-group is a great team. I had the honor to share office space for most of my PhD with the “krassischti Inder vu dr Welt” Dr. Samuel Rout. For the last months Lenka Cernikova moved into my small office. This was not only perfect because you are a great person, Lenka, but also because you took over my unfinished projects and which I know are in good hands now. I was pleased to work with Dr. Petra Wampfler, Dr. Chandra Ramakrishnan, Jacqueline Ebneter, Therese Michel Müller, Rahel Winiger, Rui Ramos Santos, Dr. Ramon Eichenberger, Dr. Saša Štefanić and Sally Heusser. My PhD included tough times and many frustrating moments, but looking back, with all of you guys, my PhD has just become an unforgettable time!

Another special thanks goes to Prof. Dr. Alexander Mathis. Since the day of his unfriendly takeover of my initial office space at the institute, I visited him almost every morning for a brief chat to start the day. We also spend some time on the tennis court for some epic battles that he, regardless of his age, mostly won.

I thank Prof. Dr. Peter Deplazes, the Institute’s Director. I contacted him after my studies in 2010, and it was him who supported me during the first year to get my PhD started. Thank you very much for this Peter!

Fortunately, it is not only the Hehl group members that created such a lively and nice working environment. All employees of the Institute of Parasitology such as the members from the other research groups, Felix’s team in diagnostics, Karin’s administrative team and the virologist made me feel welcome from day one. Thank you all for making this temporary building such a good place to work in!

Many thanks go to my committee members, Prof. Dr. Urs Greber and Prof. Dr. Lloyd Vaughan for supervising my thesis.

Heartfelt thanks to my parents who support during all steps of my education. It made me happy when Peter, my dad, got fascinated when I described certain aspects of biology, even though he likes to imagine the inside of his body as an empty space with only his soul levitating. My mama never stopped asking me about my thesis, even when talking became extremely exhausting for her. You are the best parents ever!

Through all these years my wonderful wife Nina supported me ceaselessly. Nothing could make me happier than knowing that you, Nina, are there, and as this was not enough, you made me the best present ever: two healthy children, Marlina and Johan, the best kids I could wish for! The four of us being a family is the greatest thing I have achieved in my life! Thank you so much!

Publications

Evolution of attachment to host epithelia drives cell polarization, remodeling of the endocytic system, and reassignment of clathrin function in the intestinal parasite *Giardia lamblia*.

Zumthor JP, Cernikova L, Rout S, Kaech A, Faso C, Hehl AB

(Under review in PloS Pathogens, Feb. 2016)

Characterization of the PXD protein family demonstrates differential lipid composition of individual organelles in the static endocytic system of *Giardia lamblia.*

Zumthor JP and Cernikova L, Faso C, Hehl AB

(In preparation)

A Tom40-centered membrane interactome of the highly diverged parasite *Giardia lamblia* reveals functional conservation of protein import and organelle morphogenesis machinery in mitosomes. Rout S, **Zumthor JP**, Schraner EM, Faso C, Hehl AB

(**Submitted**)

Awards and Funding

2013	**Forschungskredit UZH, Universität Zürich (CHF 50'000)** Project: "The Function of Clathrin Heavy Chain in the Highly Evolved Endocytic System of *Giardia lamblia*"
2012	**Forschungskredit UZH, Universität Zürich (CHF 50'000)** Project: "Unusual Clathrin Coats in the Endocytic System of *Giardia lamblia*: Exaptation or Minimized Function?"
2012	**Best Talk Award, MD-PhD Retreat**, **Richisau** Title: "Unusual Clathrin Coats in *Giardia lamblia*"